Chemical biology of glucosylceramide metabolism fundamental studies and applications for Gaucher disease

Oussoren, S.V.; Oussoren S.V.

Citation

Oussoren, S. V. (2017, September 28). *Chemical biology of glucosylceramide metabolism fundamental studies and applications for Gaucher disease*. Retrieved from https://hdl.handle.net/1887/55842

Version:	Not Applicable (or Unknown)
License:	[Licence agreement concerning inclusion of doctoral thesis in the Institutional Repository of the University of Leiden](https://hdl.handle.net/1887/55842)
Downloaded from:	https://hdl.handle.net/1887/55842

Note: To cite this publication please use the final published version (if applicable).

Cover Page

Universiteit Leiden

The handle http://hdl.handle.net/1887/55842 holds various files of this Leiden University dissertation

Author: Oussoren, Saskia
Title: Chemical biology of glucosylceramide metabolism : fundamental studies and applications for Gaucher disease
Date: 2017-09-28

Chemical Biology of Glucosylceramide metabolism

Fundamental studies and applications for Gaucher Disease

PROEFSCHRIFT

Ter verkrijging van

de graad van Doctor aan de Universiteit Leiden,

op gezag van Rector Magnificus prof. mr. C.J.J.M. Stolker

volgens het besluit van het College voor Promoties

Te verdedigen op donderdag 28 september 2017

Klokke 11:15 uur

door

Saskia Victoria Oussoren

Geboren te Koog aan de Zaan, Nederland

in 1988

Promotiecommissie

Promotor	Prof. dr. J.M.F.G. Aerts
Co-Promotor	Dr. R.G. Boot
Overige leden	Prof. dr. M.H.M. Noteborn
	Prof. dr. A.H. Meijer
	Prof. dr. T.M. Cox, Universiteit van Cambridge
	Prof. dr. E. Lutgens, Universiteit van Amsterdam

Table of contents

General Introduction

General Introduction

The human body produces various classes of complex glycoconjugates with very diverse functions, including glycolipids, glycoproteins, glycosaminoglycans, mucopolysaccharides and glycogen (Figure 1). Like other macromolecules, complex glycoconjugates are subject to recycling. Through autophagy or endocytotic pathways, complex glycoconjugates ultimately end up in lysosomes, the perinuclear acid compartments of cells specialized in degradation of macromolecules[1,2]. Lysosomes equipped with a broad range of glycosidases efficiently fragment glycoconjugates to release individual monosaccharides. A set of specialized transporter proteins in the lysosomal membrane facilitates the export of the simple sugars to the cytosol where further metabolism proceeds[3,4]. The release of nutrients by lysosomes, in particular amino acids, is sensed by lysosome-associated mTORC1 and linked to TFEB-regulated expression of genes coding for proteins required for lysosome biogenesis and autophagy[5–7]. Genetic defects in the intralysosomal turnover of glycoconjugates lead to a number of inherited lysosomal storage diseases, collectively a significant proportion of the inborn errors of metabolism in man[8–10].

Proteins involved in lysosomal glycoconjugates turnover.

The turnover of glycoconjugates in lysosomes requires a machinery of specialized proteins[8–10]. Table 1 provides an overview of the presently known lysosomal glycosidases and monosaccharide transport proteins. A considerable number of inborn errors of metabolism are due to primary defects in one of these proteins (see Table 1). For example, one inherited metabolic disorder, Salla disease, is due to primary defects in the lysosomal membrane protein mediating export of sialic acid. Defects in the accessory GM2 activator protein cause GM2 gangliosidosis, a neurodegenerative disease. Mutations in the prosaposin gene, affecting one or several of its intralysosomally generated accessory proteins (saposins A, B, C and D) cause impairments in degradation of glycolipids and associated disease manifestations. The majority of the inborn errors in lysosomal glycoconjugate degradation are caused by genetic defects in specific lysosomal glycosidases. Deficiency of almost every known lysosomal glycosidase has meanwhile been linked to an inherited metabolic disease with characteristic clinical presentation. This observation illustrates the great substrate specificity of each of the glycosidases and the apparent absence of functional redundancy.
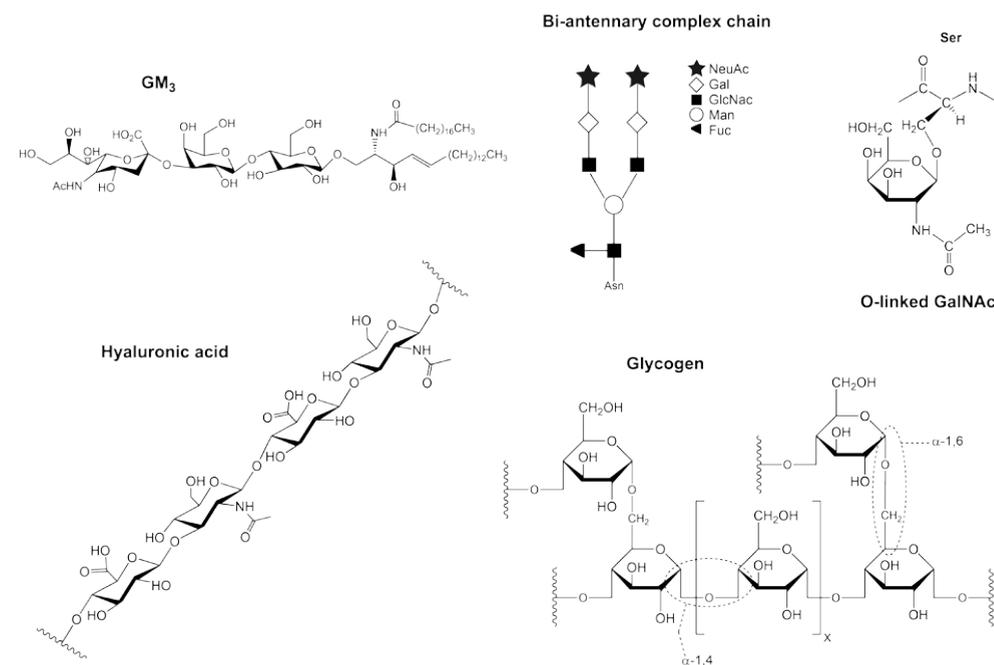

Figure 1. Examples of complex glycoconjugates in man. Upper row, left to right: glycolipid (example GM3), glycoprotein N-linked glycan (example bi-antennary complex chain), glycosaminoglycans (example O-linked saccharide). Lower row, left to right: mucopolysaccharides (example hyaluronic acid), glycogen (example branched structure with alpha-1,4 and alpha-1,6 linkages).

Classification of glycosidases.

Glycosidases (*a.k.a.* glycohydrolases), present in all forms of life, are often classified as either *retaining* or *inverting* enzymes according to the stereochemical outcome of the hydrolysis reaction[11]. Glycosidases are also grouped as *exo* or *endo* enzymes, dependent upon their ability to cleave at the, usually the non-reducing, end or in the middle of a saccharide chain. More recently sequence-based classifications of glycosidases have become popular[12]. The CAZy (CArbohydrate-Active EnZymes) classification (data base at CAZy Family Glycoside Hydrolase web site) distinguishes about 100 distinct (GH) protein families[13–15]. It offers predictions of retaining *versus* inverting mechanism, active site residues and possible substrates and it is supported by CAZypedia, an online encyclopedia of carbohydrate active enzymes. Based on three-dimensional structural similarities, sequence-based families have been classified into 'clans' of related structure and even an extended hierarchical classification of glycosidases has been proposed[16].

Table 1. Lysosomal proteins mediating glycoconjugate turnover and associated inherited diseases. Sources: OMIM, Expasy, Genetics home reference, Uniprot

Protein	Gene	Function	Substrate	Inherited disease
Acid β-Galactosidase	GLB1	Hydrolysis of terminal non-reducing β-D-galactose residues in β-D-galactosides	GM1 ganglioside	GM1 gangliosidosis
β-Hexosaminidase α subunit	HEXA	Hydrolysis of terminal non-reducing N-acetyl-D-hexosamine residues in N-acetyl-β-D-hexosaminides	GM2 ganglioside	GM2 gangliosidosis (Tay-Sachs)
β-Hexosaminidase β subunit	HEXB	Hydrolysis of terminal non-reducing N-acetyl-D-hexosamine residues in N-acetyl-β-D-hexosaminides	GM2 ganglioside	GM2 gangliosidosis (Sandhoff)
Sialidase/Neuraminidase	NEU1	Cleave terminal sialic acid residues	GM3 ganglioside	Sialidosis
α-Galactosidase A	GLA	Hydrolysis of terminal, non-reducing α-D-galactose residues in α-D-galactosides	Globotriaosylceramide (Gb3)	Fabry
Glucocerebrosidase	GBA	Catalyzes the breakdown of the glycolipid glucosylceramide (GlcCer) to ceramide and glucose	Glucosylceramide (GlcCer)	Gaucher
Galactosylceramidase	GALC	Catalyzes the breakdown of the glycolipid galactosylceramide (GalCer) to ceramide and galactose	Galactosylceramide (GalCer)	Krabbe
Acid α-Glucosidase	GAA	Catalyzes the breakdown of glycogen into glucose	Glycogen	Glycogen Storage Disease type II (Pompe)
α-L-Iduronidase	IDUA	Catalyses the hydrolysis of unsulfated α-L-iduronosidic linkages in dermatan sulfate	Glycosaminoglycans/ mucopolysaccharides	Mucopolysaccharidosis MPS I (Hurler/Scheie)
α-Mannosidase	MAN2B1	Catabolism of N-linked carbohydrates released during glycoprotein turnover	Non-reducing α-D-mannose residues in α-D-mannosides	α-Mannosidosis
β-Mannosidase	MANBA	Cleaves the single β-linked mannose residue from the non-reducing end of all N-linked glycoprotein oligosaccharides	Terminal, non-reducing beta-D-mannose residues in β-D-mannosides	β-Mannosidosis

Catalytic mechanisms.

The catalytic reaction of inverting and retaining glycosidases is fundamentally different[17,18]. Inverting glycosidases utilize two catalytic amino acid residues, typically carboxylate residues, that act as acid and base respectively and no covalent glycosyl-enzyme intermediate is generated during the reaction (Figure 2). In contrast, retaining glycosidases utilize a two-step mechanism in which each step results in inversion, leading to net retention of stereochemistry. Again two residues are involved, usually carboxylates. One acts as nucleophile and the other as acid/base. In the first step the nucleophile attacks the anomeric center, resulting in the release of the aglycon and formation of a covalent glycosyl enzyme intermediate, assisted by the protonated carboxylate of the acid/base residue. Next, the now deprotonated carboxylate acts as a base and assists a nucleophilic water to hydrolyze the

glycosyl enzyme intermediate, releasing the saccharide (Figure 2)[19]. An exception is formed by classes of chitinases (families GH18 and GH20) where the enzymes employ so-called substrate-assisted catalysis (Figure 2). These retaining chitinases use a single glutamate as catalytic residue. This glutamate in their catalytic $(\beta\alpha)_8$-barrel domain acts in concert with the carbonyl oxygen atom of the substrate's C2 *N*-acetyl group that functions as the nucleophile[20]. This mechanism is used by the human chitinase CHIT1, named chitotriosidase[21–24], as well as by the homologous AMCase (acidic mammalian chitinase; CHIT2) arisen by gene duplication[25,26].
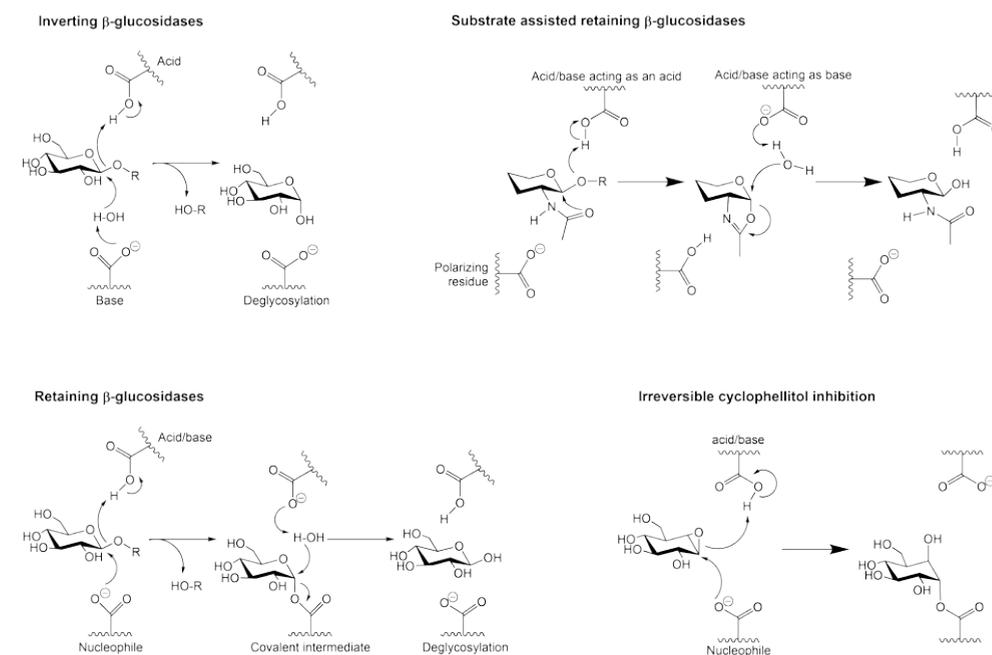

Figure 2. Catalytic mechanisms of glycosidases. Upper left: Inverting mechanism. Lower left: Retaining mechanism. Upper right: Substrate-assisted retaining mechanism. Lower right: Irreversible inhibition by cyclophellitol. Upper left, lower left and lower right figures adapted from WW Kallemeijn, upper right figure adapted from Gloster and Davies, 2009.

Glycosphingolipids: synthesis and lysosomal degradation.

Glycosphingolipids (GSLs), firstly identified by Johannes Thudichum at the end of the nineteenth century[27], are structural components of membranes. The outer leaflet of the plasma membrane bilayer is particularly rich in GSL. Their generic structure comprises a lipid moiety, being an N-acylated sphingosine named ceramide (Cer). Attached to the C1-hydroxyl of Cer is a monosaccharide (glucose or galactose) to which further sugars may be added[28]. Through van der Waals interactions GSLs form transient semi-ordered domains with

cholesterol molecules in membranes. Specific proteins preferentially reside in these so-called 'lipid rafts' and mediate signaling events there [29–31]. During their life cycle GSLs travel through various subcellular compartments (Figure 3). GSLs are synthesized at the endoplasmic reticulum (ER) as started by the enzyme serine palmitoyltransferase (SPT) generating a keto-sphinganine structure by the condensation of serine and fatty acyl-CoA, usually palmitoyl-CoA[32]. Next, keto-sphinganine is transformed to sphinganine by a reductase. A set of ceramide synthases (CerS 1-6)[33], each enzyme with acyl-CoA length preference, catalyze the N-acylation of sphinganine. Generated dihydroceramides are rapidly converted to ceramides by the action of dihydroceramide desaturase (DES)[34,35]. Subsequently, part of the newly formed Cer gets galactosylated inside the ER to galactosylceramide (GalCer), a reaction catalyzed by galactosylceramide synthase using UDP-galactose as sugar donor[36]. Alternatively, Cer molecules are transported by the protein CERT to the cytosolic leaflet of membranes of the cis-Golgi apparatus[37]. There, the enzyme glucosylceramide synthase (GCS) transfers glucose from UDP-glucose to Cer, generating β-glucosylceramide (glucocerebroside; GlcCer)[38]. Part of the formed GlcCer is immediately translocated to the luminal leaflet of the Golgi membrane via an unknown mechanism[39]. Inside the Golgi apparatus, GlcCer is next modified by stepwise addition of further sugars catalyzed by glycosyltransferases, yielding a broad spectrum of complex GSLs such as gangliosides and globosides[28,40]. Sulfation of specific lipids by sulfotransferases may also take place, adding to the structural diversity of GSLs[40,41]. After the modifications in the Golgi apparatus, GSLs reach the outer leaflet of the plasma membrane via membrane flow to play their various roles in interactions with the outside world.

Export of GSLs from cells may occur via nascent HDL particles, however most GSLs molecules remain in the plasma membrane. Ultimately, GSLs are internalized via endocytosis, ending up in multi-vesicular bodies within late endosomes destined for degradation inside lysosomes. Likewise, exogenous GSLs, for example components of endocytosed lipoproteins or phagocytosed cell debris and senescent cells, undergo lysosomal degradation. This is a coordinated process in which terminal sugar moieties are removed from GSLs in a stepwise manner by sequential action of glycosidases, assisted by specific accessory proteins (GM2 activator protein and saposins A-D)[42]. The degradation pathways of the most simple ganglioside GM3 and globoside Gb3 are depicted in Figure 4. The sphingolipid Cer is ultimately formed, either from GalCer by galactocerebrosidase (GALC) or GlcCer by glucocerebrosidase (GBA). Lysosomal acid ceramidase (AC) splits ceramide to free fatty acid and sphingosine that are subsequently exported. In the cytosol sphingosine can be re-used by CerS enzymes in the so-called salvage pathway to generate ceramide molecules[43]. Alternatively, sphingosine can be modified to sphingosine-1-phosphate (S1P) via sphingosine kinases (SK1 and SK2), whereafter S1P lysase (SPL) degrades it to phosphatidylethanolamine and 2-trans-hexadecenal[44,45].
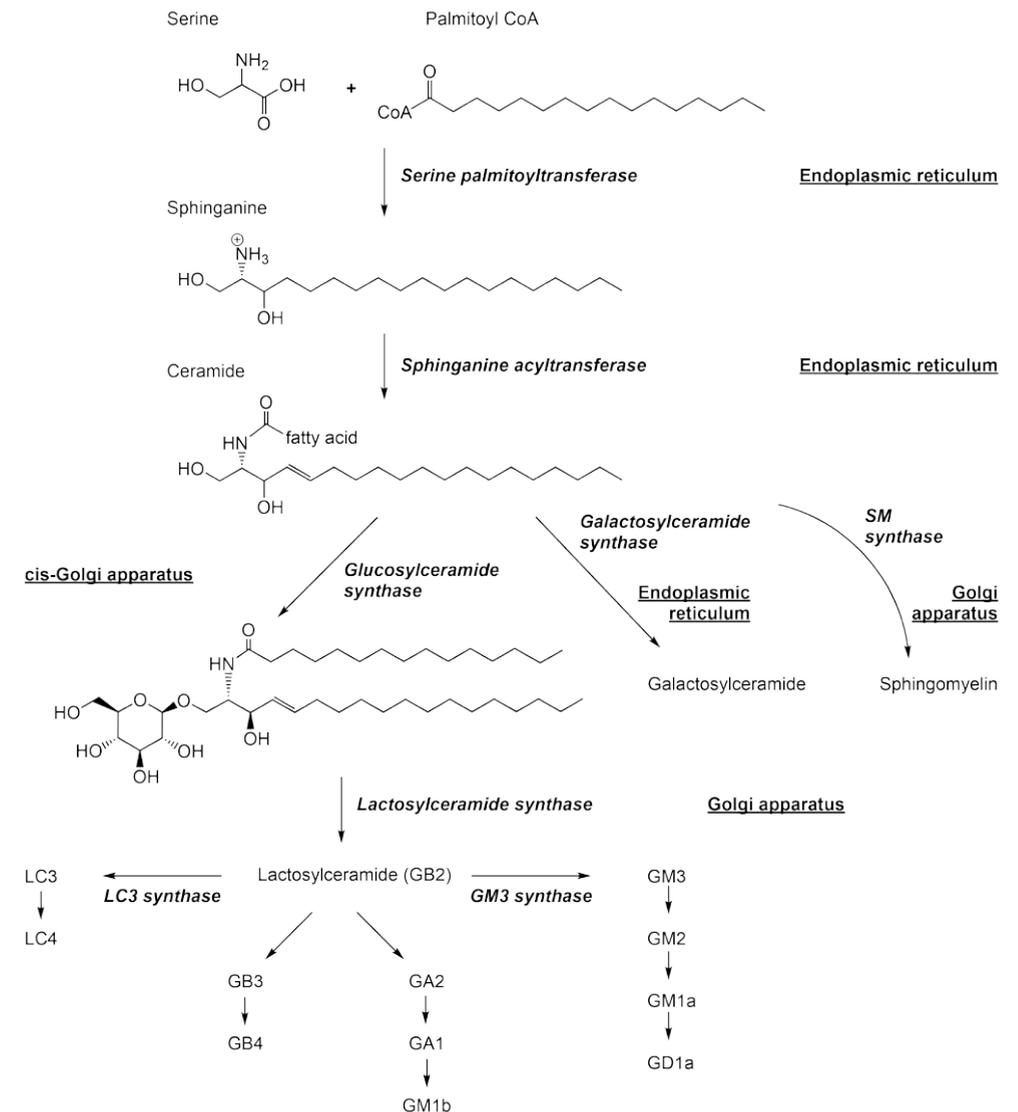

Figure 3. Schematic overview of GSL synthesis: enzymes and topology. Enzymes are indicated in bold and italic, topology is underlined and bold.
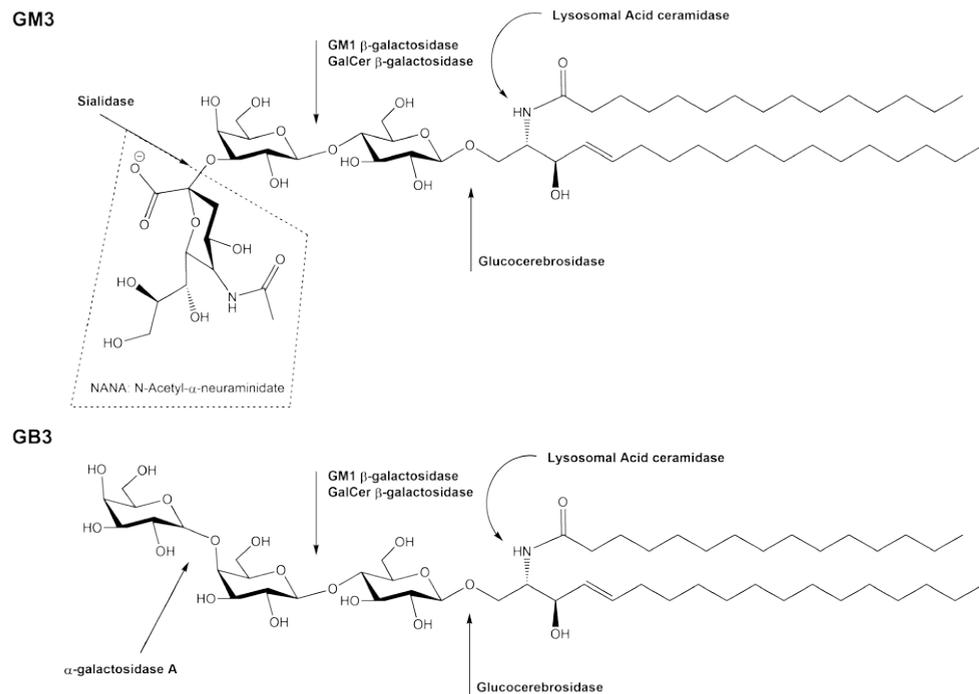
Figure 4. Overview of lysosomal degradation of ganglioside GM3 and globoside Gb3. Top: GM3 degradation in lysosomes. Bottom: Gb3 degradation in lysosomes. Involved enzymes are designated in **bold**.

Glucocerebrosidase: glucosylceramide hydrolase.

Glucocerebrosidase (GBA) is a retaining β-glucosidase, encoded by the *Gba1* gene at locus q21 of chromosome 1[46]. It is synthesized as 497 amino acid polypeptide at ER-associated ribosomes with a regular N-terminal signal sequence allowing co-translational translocation to the lumen of the ER[47]. Inside the ER, the signal peptide is removed and glycans are attached to the amino acids N19, N59, N146 and N270 of the nascent GBA, an essential modification for correct folding of the protein[48,49]. Next, within one hour of their synthesis, folded GBA molecules bind to the triple helical structure in the apical region of integral membrane protein LIMP-2 (lysosomes integral membrane protein 2, encoded by the *Scarb2* gene) containing trafficking information in its cytoplasmic tail[50,51]. Incorrectly folded GBA molecules failing to associate with LIMP-2 are removed from the ER and degraded in proteasomes[52]. Of note, GBA is not synthesized as inactive precursor but as active glycosidase, contrary to some other lysosomal hydrolases like α-glucosidase, acid ceramidase and cathepsins that require proteolytic processing to active enzyme[53]. Again in sharp contrast to most other lysosomal hydrolases, GBA does not acquire mannose-6-phosphate recognition moieties mediating mannose-6-phosphate receptor-mediated sorting to lysosomes[54]. Instead, the complex of GBA/LIMP-2 traverses the Golgi apparatus where most N-glycans in GBA are modified from high mannose-type to complex type-structures[53]. The precise manner in which the complex GBA/LIMP-2 is routed to lysosomes is unknown, but physically distinct vesicles from those containing mannose-6-phosphate receptors with their lysosomal hydrolase cargo are involved[55]. The travel of newly formed GBA from the ER to lysosomes is surprisingly slow in some cultured cells, taking several hours[53]. The survival of GBA in lysosomes is limited to 24-36 hours, at least as suggested by observations with cultured cells. Its proteolytic breakdown in cultured cells can be largely inhibited by leupeptin and E64, inhibitors of cysteine proteases[56,57]. Table 2 presents an overview of lysosomal proteases with corresponding inherited diseases in man.

Table 2. Lysosomal proteases and associated inherited diseases.
Sources: OMIM, Expasy, Genetics home reference, Uniprot

Protein	Gene	Type	Disease
Cathepsin A	CTSA	Serine	Galactosialidosis and Glycoproteinosis
Cathepsin C	CTSC	Cysteine	Papillon-Levèfre syndrome
Cathepsin D	CTSD	Aspartyl	Neuronal Ceroid Lipofuscinosis (CLN10)
Cathepsin F	CTSF	Cysteine	Kufs disease
Cathepsin K	CTSK	Cysteine	Pycnodysostosis (PKND)

After reaching acid late endosomes/lysosomes, GBA dissociates from LIMP-2, presumably due to the protonation of a specific histidine in LIMP-2's triple helical structure[58]. In lysosomes the enzyme GBA meets at acidic pH optimal for catalytic activity with saposin C, an 80 amino acid protein generated from 70 kDa prosaposin[59]. Saposin C stimulates enzymatic activity of GBA towards glucosylceramide, presumably by facilitating entry of lipophilic substrate in the catalytic pocket[42]. During catalysis GBA utilizes the double-displacement mechanism like most other retaining glucosidases. The key catalytic residues in GBA are the nucleophile glutamate 340 and acid/base glutamate 325[60]. As reaction intermediate the glucose of the GlcCer substrate becomes covalently linked to E340 and is released by subsequent attack of a nucleophilic water molecule assisted by E235. By the same mechanism, cyclophellitol and conduritol B-epoxide (CBE) irreversibly inhibit GBA. Cyclophellitol and CBE both form a permanent conjugate with the nucleophile E340 of GBA (Figure 2)[61]. Cyclophellitol scaffolds have been successfully used to design functionalized activity-based probes allowing *in situ* visualization of GBA[62,63] (see also section below). The 3D structure of GBA has been solved by X-ray diffraction crystal analysis, indicating a typical (β/α)8 TIM barrel catalytic core domain III, a three-strand antiparallel β-sheet flanked by a loop and a perpendicular strand (domain I) and an Ig-like fold formed by two β-sheets (domain II)[64,65]. A molecular dynamics model of

GBA has also been generated[66]. GBA has not yet been co-crystalized with saposin C and interaction of the two proteins has only been modelled *in silico*[67,68]. The part of saposin C essential for interacting with GBA has been determined with NMR and by site-directed mutagenesis[67,69,70]. How saposin C exactly stimulates enzymatic activity of GBA is still enigmatic. Saposin C is thought to perturb phospholipid-containing membranes at acid pH and thus offer better access for GBA to its lipid substrate[71]. However, saposin C also promotes activity of GBA towards water soluble artificial β-glucoside substrates[72]. It seems likely that binding of saposin C to GBA affects the enzyme's conformation. This is suggested by the observation that saposin C protects against inhibitory binding of α-synuclein to the enzyme[73]. Furthermore, saposin C influences resistance against degradation by lysosomal cysteine-proteases[74,75]. It has recently been shown that a LIMP-2 helix 5-derived peptide binds directly to GBA *in vitro*[51]. The helix 5 peptide fused to a cell-penetrating peptide was found to activate endogenous lysosomal GBA[51]. Beneficial transient interactions of LIMP-2 with GBA in lysosomes can at present not be excluded (see also chapter 3 of this thesis).

Figure 5. Glucocerebrosidase: a graphical narrative of composition, life cycle and interactors.
a) Schematic overview of *Gba1* gene. Source: ENSEMBL; b) 3D structure of GBA showing various domains and 4 N-linked glycans, adopted from Pol-Fachin et al. 2016; c) Schematic life cycle of GBA from ER via Golgi apparatus to lysosome: molecular mass maturation by glycan modifications made by WW Kallemeijn; symbols: ■=*N*-acetyl-*D*-glycosamine, ○=*D*-mannose, ●=*D*-mannose-6-phosphate, Δ=*L*-Fucose, ◆ =*D*-galactose, ◯=*N*-acetyl-*D*-neuraminic acid. d) LIMP-2 as transporter of GBA, model adopted from Zunke et al. 2016; e) Lysosomal interaction of saposin C with GBA, model adopted from Atrian et al. 2008. SapC docked onto GBA with GlcCer molecule visible in catalytic pocket.

Impaired lysosomal GlcCer degradation: molecular causes of disease.

Defects in GBA cause intralysosomal accumulation of GlcCer in characteristic tubular structures[76]. Inherited mutations in the *Gba1* gene constitute the molecular basis for the relatively common lysosomal storage disorder named Gaucher disease (GD). A patient suffering from GD was firstly described in 1882 by the French dermatologist Philippe E.C. Gaucher[77]. His thesis at the University of Paris consisted of a case report describing a young woman with unexplained massive splenomegaly. Soon it was realized that this patient represented a distinct disease entity that was subsequently referred to as Gaucher's disease. The chemical nature of the accumulating lipid in GD tissues was first correctly elucidated by Aghion in 1934[78]. Only 50 years ago, deficiency of glucocerebrosidase (acid β-glucosidase) was identified as the cause of GD, independently by Patrick, Brady and co-workers [79,80]. At present more than 200 mutations in the *Gba1* gene have been linked with GD[81]. Next to truncations and splicing defects, several hundred amino acid substitutions in GBA have been shown to cause GD. The position of amino acid substitutions in the protein, in the catalytic or another domain, proves to poorly predict the clinical severity of GD patients[82]. Some substitutions in the folding domain that are positioned far away from the catalytic pocket have nevertheless major negative consequences. For instance, the substitution L444P in GBA causes faulty folding of most enzyme molecules in the ER and subsequent proteasome mediated degradation[53]. Homozygosity for L444P GBA nearly always leads to a severe neuronopathic course of GD, albeit with great individual variability in onset and progression[76]. Premature degradation may also occur with mutations in the catalytic domain. In fact, quite many of the documented mutations in GBA lead to defective folding and reduced transport to lysosomes[83]. An exception is the N370S GBA substitution, the prevalent *Gba1* mutation among Caucasians GD patients. The amino acid substitution is in a loop close to the catalytic pocket and it was found to affect pH optimum and kinetic parameters such as affinity for substrate[57,84,85]. There are controversial reports regarding the impact of the N370S substitution in GBA on initial folding of the enzyme in the ER, claimed to be impaired as well as normal[86,87]. Certainly, the intralysosomal stability of N370S GBA is markedly reduced[56,88]. Hetero- and homo-allelic presence of the *Gba1* gene coding for N370S GBA is associated with a non-neuronopathic type 1 course of disease[76,89]. Otherwise, *Gba1* genotype – GD phenotype correlations are relatively poor, illustrated most explicit by the occurrence of phenotypically discordant monozygotic twins[90,91].
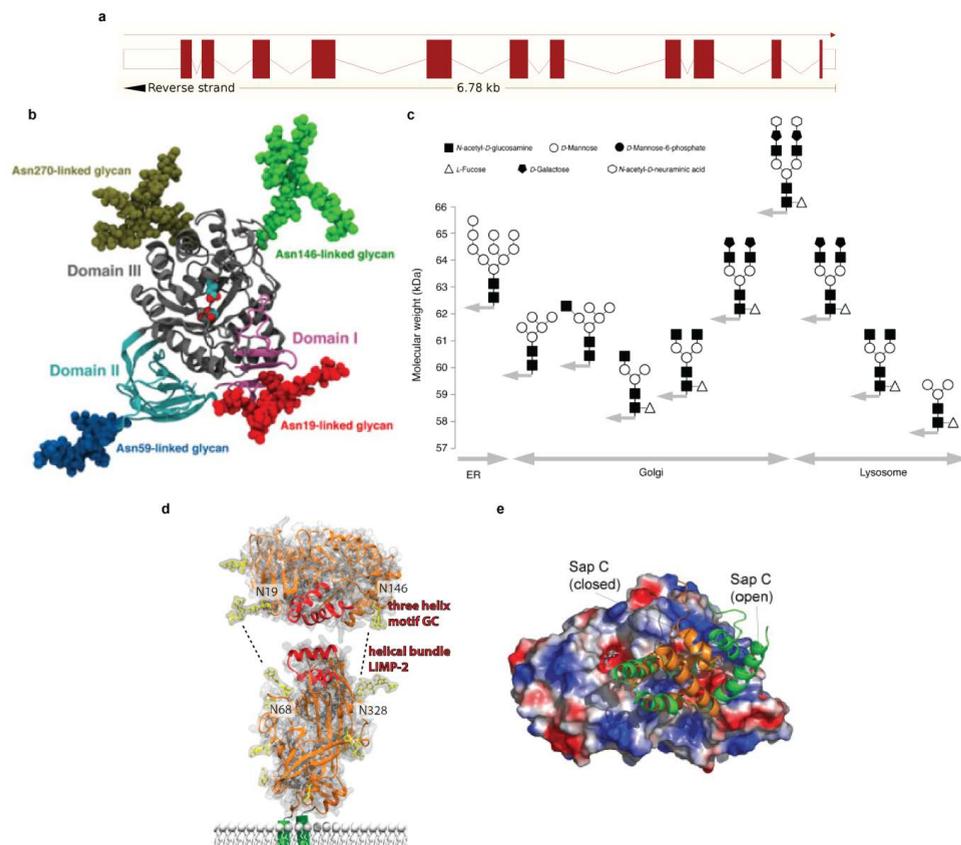
Gaucher disease: clinical manifestation and biomarkers.

The clinical presentation of GD is remarkably heterogeneous, ranging from fatal skin defects to an almost asymptomatic course of disease[76]. The most common phenotype of among Caucasian GD patients is referred to as type 1 or non-neuronopathic GD. Prominent in these patients is the ongoing storage of GlcCer in lysosomes of tissue macrophages, transforming into the characteristic enlarged lipid-laden Gaucher cells[92,93]. Progressive accumulation of these alternatively activated lipid-laden macrophages in tissues of GD patients is supposed to underlie the development of symptoms like splenomegaly and hepatomegaly[76]. Massive accumulation of Gaucher cells in the bone marrow is thought to contribute to hematological abnormalities, such as anemia and the commonly encountered thrombocytopenia. Other, highly variable, signs and complications associated with GD are skeletal deterioration, neuropathology including oculomotor apraxia and peripheral neuropathy as well as polyclonal and monoclonal gammopathies[76]. GD patients developing lethal complications in the central nervous system are classified as type 2 GD (infantile onset) and type 3 GD (late infantile/juvenile onset). Complete deficiency of GBA activity results in pre-natal/neo-natal phenotypes characterized by lethally aberrant permeability of the skin (so-called collodion baby showing severe ichthyosis)[94–96].

Major symptoms	Classification
Enlarged liver	Type 1, 2 & 3
Enlarged spleen	Type 1, 2 & 3
Bone disease	Type 1, 2 & 3
Bone marrow infiltration	Type 1, 2 & 3
Anemia	Type 1, 2 & 3
Thrombocytopenia	Type 1, 2 & 3
Pulmonary disease	Type 1, 2 & 3
Gammopathies	Type 1, 2 & 3
Cancer risk	Type 1, 2 & 3
Cholesterol choletithiasis	Type 1, 2 & 3
Neurodegeneration	Type 2 & 3
Epilepsy	Type 2 & 3
Eye movement disturbances	Type 3
Skin permeability	Lethal
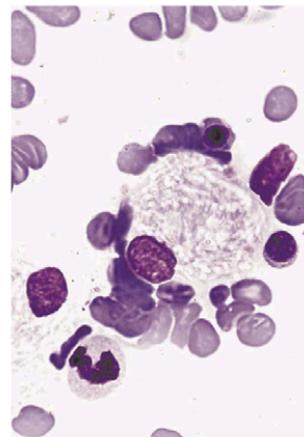
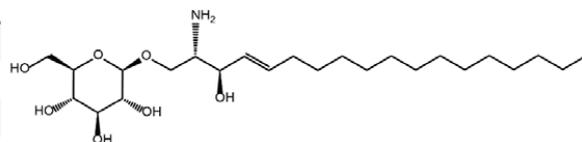| Protein Biomarkers |
|---|
| PARC/ CCL18 |
| Chitotriosidase |
| S-gpNMB |
| MIP-1α and MIP-1β |

Figure 6. Gaucher disease; a graphical narrative of clinical heterogeneity, Gaucher cells and biomarkers. Top left: Major symptoms and phenotype classification. Top right: Gaucher cell picture adopted from Aerts et al. 2003. Bottom left: Protein biomarkers of Gaucher cells. Bottom right: Glucosylsphingosine.

Carriers of mutant *Gba1* alleles do not develop Gaucher cells and characteristic GD symptoms, intriguingly however they, like patients, are at significantly increased risk for α-synucleinopathies such as Parkinsonism and Lewy-body dementia[97–99]. Given the poor prognostic value of *Gba1* genotype, early demonstration of onset of disease in individuals with aberrant GBA is essential. Several sensitive plasma biomarkers for the presence of Gaucher cells in the body have been identified, being proteins produced and secreted by lipid-laden macrophages, such as the chitinase chitotriosidase and the chemokine CCL18[21,93,100]. Gaucher cells also release soluble fragments of the membrane-proteins CD163 and gpNMB into the circulation, leading to markedly elevated plasma concentrations[101,102]. In addition, glucosylsphingosine (GlcSph), deacylated GlcCer, is several hundred-fold increased in plasma of symptomatic GD patients and may serve as biomarker[103,104]. These surrogate markers of disease in plasma are increasingly used as guidance in clinical management, especially after the availability of therapies for type 1 GD (see section below)[105,106]. Defects in saposin C impairing GBA activity lead to clinical symptoms similar to those presented by GD patients[107]. Mutations in the *Scarb2* gene causing deficiency of LIMP-2 result in markedly reduced GBA levels in many cell types in man and mice[108–110]. However, the corresponding human disease, action myoclonus renal failure syndrome (AMRF), is clinically very different from GD[111,112]. In LIMP-2 deficient mice relatively little GlcCer accumulates in tissues, a phenomenon explained by the ability of most cells to efficiently convert accumulating GlcCer in lysosomes to GlcSph by the action of lysosomal acid ceramidase[113,114]. White blood cells of AMRF patients and LIMP-2 deficient mice have a surprisingly high residual GBA content, possibly due to re-uptake of faulty secreted GBA. This considerable residual enzyme activity in macrophages seems sufficient to prevent formation of Gaucher cells and associated symptoms as occurring in GD patients. In line with this, AMRF patients do not show elevated plasma levels of Gaucher cell markers such as chitotriosidase, CCL18 and gpNMB, but plasma glucosylsphingosine is increased although far less spectacularly than in GD patients[112]. Plasma glucosylsphingosine abnormalities in type 1 GD patients have been found to be corrected upon various therapeutic interventions similar to the validated Gaucher cell biomarker chitotriosidase, indicating that most of the excessive plasma glucosylsphingosine in type 1 GD patients stems from their Gaucher cells[114].

Pathophysiology of Gaucher disease.

The most poorly understood aspects of GD are the pathophysiological mechanisms underlying the complex clinical picture of the disorder. A closer inspection of patients shows that numerous cell types and tissues can become affected. Ichtyotic skin disease is observed only in GD patients without virtual GBA activity. The ratio of glucosylceramide to ceramide in the

stratum corneum, determined by GBA, seems critical for correct barrier function of the skin[94]. Clinical symptoms related to the central nervous system such as epilepsy, apraxia and scoliosis are usually observed only in GD patients with markedly reduced GBA activity, but on the other hand even GD carriers show an increased risk for Parkinsonism[97]. Peripheral neuropathy also occurs in GD patients with an otherwise relative mild disease course and with significant residual GBA activity[115]. Growth retardation and signs of insulin resistance point to hormone disturbances, again also occurring in milder affected type 1 GD patients[116]. Some of the liver-related symptoms like hepatomegaly and gallstones occur frequently in GD patients; however, cirrhosis is more rare and associated with a more severe disease course in general[76]. Cardiac valve calcification is a symptom specifically occurring in GD patients with D409H mutated GBA, suggesting a very specific, but still enigmatic, mechanism[76,117–120]. Splenomegaly is again a very common sign of disease and associated with accumulation of Gaucher cells in the organ. Frequent in GD patients is polyclonal gammopathy, and quite often this evolves into monoclonal gammopathy[121]. Ultimately this can even lead to the development of multiple myeloma and amyloidosis[122–124]. Bone marrow filtration is another regular sign in GD patients and likely contributes besides splenomegaly to the common thrombocytopenia and anemia, albeit the latter generally develops only in more severely affected patients[76]. The skeletal disease and bone remodelling in GD patients is heterogeneous and focal of nature[76]. It seems not to correlate well with other disease manifestations and circulating biomarkers of Gaucher cells[125]. Osteoporosis is often encountered in GD patients, potentially linked to impaired osteoblasts rather than increased osteoclast activity[125,126]. It is unclear whether the presence of Gaucher cells in tissues explains the entire spectrum of symptoms and signs in GD patients. Indeed, the lipid-laden macrophages are viable cells able to secrete various proteins promoting the influx of further monocytes to disease loci and stimulating ongoing inflammation and tissue remodeling[92,93]. As discussed in more detail in chapter 6 of the thesis, it is conceivable that secondary abnormalities in GD patients stemming from adaptations to the primary lysosomal GlcCer accumulation contribute to specific symptoms. Briefly, compensatory increased metabolism of GlcCer by the cytosolic β-glucosidase GBA2[127–130] might promote loss of motor coordination by Purkinje cell loss[131]. It might also lead to excessive formation of potential toxic metabolites such as ceramide and glucosylated compounds, e.g. cholesterolglucoside[131,132]. Another adaptation in GBA deficient cells, the intralysosomal formation of GlcSph from accumulating GlcCer, may even be pathogenic as such. Excessive GlcSph has been linked to B-cell lymphoma[133–135]. It has very recently been reported that glucosylsphingosine in GD patients acts as auto-antigen driving B-cell proliferation and it is proposed to directly promote the development of multiple myeloma[133]. Of note, deacylation of accumulating storage GSLs to corresponding glycosphingoid bases is not unique for GD and AMRF, but also occurs in Fabry disease and Krabbe disease[136–138]. Again, toxicity of the generated glycosphingoid bases is considered: excessive galactosylsphingosine is thought to be neurotoxic in Krabbe disease patients[139,140] and excessive globotriaosylsphingosine (lysoGb3) is claimed to be toxic for nociceptive peripheral neurons and podocytes in Fabry disease patients[141,142].

Therapies for Gaucher disease.

Based on seminal studies by Brady and collaborators at the National Institutes of Health in Bethesda, U.S.A. half a century ago[143], the first effective treatment for GD was introduced, so-called enzyme replacement therapy (ERT)[144,145]. This treatment is based on two-weekly intravenous administration of glycan modified human recombinant GBA to supplement macrophages with enzyme. Initially GBA was isolated from human placenta and its N-glycans were enzymatically modified *in vitro* to expose terminal mannose residues favoring endocytotic uptake of enzyme via the mannose receptor, a lectin receptor present on tissue macrophages[146]. An effective ERT enzyme preparation was commercially developed by Genzyme (Boston, U.S.A.), involving large scale isolation of enzyme from placental extracts[143]. A few years later the placental enzyme preparation was replaced by a recombinant GBA produced in Chinese hamster ovary cells. Now several GBA preparations are in use for ERT of type 1 GD, all leading to reversal of organomegaly and hematological complications, stabilization of skeletal disease and markedly increased quality of life[147–151]. Clinical improvement is accompanied by corrections in plasma biomarkers of Gaucher cells and glucosylsphingosine. The quantification of plasma chitotriosidase is widely applied to monitor disease progression and response to therapy. Corrections in plasma chitotriosidase of GD patients have been found to correlate with corrections in organomegaly and to be associated with improvements in hematological abnormalities. Moreover, the extent of correction in chitotriosidase correlates with the incidence of long term complications such as pulmonary hypertension, multiple myeloma and Parkinsonism[106]. It soon became apparent that neurological manifestations in more severely affected GD patients are not prevented by ERT because the therapeutic enzyme fails to pass the blood-brain barrier[147]. An alternative treatment of type 1 GD is offered by so-called substrate reduction therapy (SRT)[152–155]. Here, three times daily GD patients take a small compound inhibitor of GCS orally, the key enzyme in glucosylceramide and subsequent glycosphingolipid biosynthesis. Two drugs (*Miglustat* and *Eliglustat,* Figure 7) are registered for treatment of type 1 GD patients. *Miglustat* (N-butyl-deoxynojirimycin), already registered in 2001, is a relative weak and non-specific inhibitor of GCS. Lately the far more potent and specific GCS inhibitor *Eliglustat* (*N*-[(1*R*,2*R*)-1-(2,3-dihydro-1,4-benzodioxin-6-yl)-1-hydroxy-3-(1-pyrrolidinyl)-2-propanyl] octanamide) has also been registered for SRT of type 1 GD patients[156–158]. The latter drug does not penetrate the brain well and is not considered suitable to treat neuronopathic variants of GD. The design of brain-permeable specific inhibitors of GCS is actively pursued by pharmaceutical industry and academic researchers. Brain-permeable N-(5'-adamantane-1'-yl-methoxy)-pentyl-1-deoxynojirimycin (AMP-DNM)[159] has earlier been identified as high nanomolar GCS inhibitor. It was observed that ido-variants of AMP-DNM inhibit GCS with the same efficacy but with much less affinity for GBA. Based on these compounds, a new generation of deoxynojirimycin type GCS inhibitors with IC_{50} values in the very low nanomolar range has been recently developed[160].

Table 3. Therapy approaches for Gaucher disease. ERT: Enzyme Replacement Therapy; SRT: Substrate Reduction Therapy; CT: Chaperone Therapy; LST: Lysosomal Stabilization Therapy; GT: Gene Therapy.

Therapy	Agent	Mode of action	Target	Status	Limitation	References
ERT	Recombinant GBA1	Enzyme supplementation	Macrophages	Registered	Costly, only for GD1	Barton 1990 & 1991
SRT	GCS inhibitor	Substrate reduction	Viscera	Registered	Costly, only for GD1	Platt 2001, Aerts 2006, Cox 2000, Elstein 2004
CT	GBA1 chaperone	Folding promotion	Total body	Experimental	Also inhibits enzyme	Boyd 2013, Fan 2003, Benito 2011, Jung 2016, Chang 2006, Yu 2007, Steet 2007, Tropak 2008, Lieberman 2009, Khanna 2010, Babajani 2012, Zimran 2013, Bendikov-Bar 2013
LST	Arimoclomol, others	Enzyme stabilization	Total body	Experimental	No known adverse effects	Kirkegaard 2016
GT	DNA construct	cDNA/gene correction	Stem cells	Experimental	Safety, Immune response	Dahl 2015

There is active research on additional treatments of GD, particularly for the non-neuronopathic variants for which there remains an unmet clinical need. Chemical chaperones of GBA might offer a novel additional treatment avenue. With this approach, small compounds interacting with the catalytic site of the enzyme should chaperone folding of (mutant) GBA in the ER, resulting in increased transport of enzyme to the lysosome[161–164]. In essence, chemical chaperones promoting correct conformation of GBA might also stabilize the enzyme intralysosomally. Whether the latter could offer clinical benefit is debated: chemical chaperones interacting with the active site of lysosomal GBA intrinsically also inhibit its enzymatic activity. As many GD patients produce mutant forms of GBA that are impaired in folding and/or lysosomal stability, these might profit from chaperone-based therapies. There is an explosive increase in reports on the design and synthesis of potential chemical chaperones for GBA. Recent reviews elegantly cover some of the glycomimetics classes currently under investigation as chaperones[165,166]. Many are reversible competitive, or mixed-type, inhibitors of GBA. The most extensively studied small compound so far has been isofagomine (IFG, Figure 7), which was the subject of several pre-clinical studies as well as a clinical study that did not meet the full expectations[167–176]. IFG is a potent competitive GBA inhibitor with an IC_{50} of approximately 30 nM at pH 5.2 and 5 nM at pH 7.0[177]. Compounds like IFG will only exert a beneficial effect on GBA in a delicate concentration window that is likely difficult to reach concomitantly in various tissues of GD patients. The effects of oral administration of *Ambroxol* (Figure 7), a weak mixed-type inhibitor of GBA have been investigated in studies with cells and small numbers of type 1 GD patients[177–180]. Impressive reductions in spleen and liver volumes of *Ambroxol*-treated type 1 GD patients have been documented, as well as reductions the GD biomarker chitotriosidase.
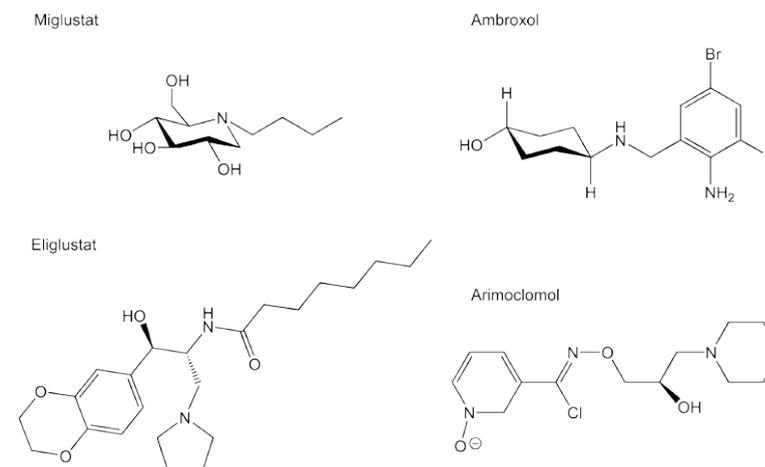

Figure 7. Small compound therapeutics for Gaucher disease. Top left: Miglustat. Lower left: Eliglustat. Top right: Ambroxol. Lower right: Arimoclomol.

N370S GBA is the prevalent mutant enzyme among Caucasian type 1 GD patients[76]. For example, almost every Dutch type 1 GD patient was found to possess at least one *Gba1* allele coding for N370S enzyme[89]. Significant amounts of N370S GBA molecules reach lysosomes[56,88], their intralysosomal stability is however reduced. Fibroblasts homozygous for N370S GBA show a marked increase in enzyme activity when cultured in the presence of leupeptin inhibiting lysosomal proteolysis[56]. Given this observation, a potential alternative treatment for such individuals could be lysosomal stabilization therapy (LST), in which agents promoting intralysosomal survival of GBA would be administered. Several approaches to be considered in this direction are the use of selected lysosomal protease inhibitors and glyco-mimetics acting as stabilizing chemical chaperone. Since GBA also exerts β-xylosidase activity (Chapter 7 of this thesis), xylo-mimetics might also be worthwhile to test as potential stabilizers. Little consideration as potential beneficial stabilizers has so far been given to agents binding to the aglycon site of GBA. An approach proposed for treatment of Niemann Pick disease types B and C is the administration of *Arimoclomol* (Figure 7)[181], a small compound boosting formation of endogenous Hsp70, a protein that assists (re)folding of unfolded mutant enzymes, even in the lysosome[182]. *Arimoclomol* is hoped to also exert positive effects in GD patients. Finally, targeting of (fragments of) saposin C or LIMP-2 to lysosomes might offer other ways to stabilize GBA *in situ* and augment GlcCer degradative capacity.

During a discussion of future GD treatments, gene therapy has to be mentioned[183]. Given the positive outcome of bone marrow transplantation in type 1 GD patients, genetic modification of hematopoietic stem cells has been, and still is, seriously considered as therapeutic avenue. Pioneering trials with retroviral vectors to introduce *Gba1* cDNA in hematopoietic stem cells of GD patients did not result in permanent correction of white blood cells[184], however in recent times encouraging data have been obtained with lentiviral gene therapy in type 1 GD mice[185]. Moreover, the exciting new possibilities for gene corrections using CRISPR-CAS technology may further promote a revival in research on gene therapy as therapeutic modality for GD[186].

Chemical biology tools: activity-based probes, isotope encoded and clickable GSLs, fluorogenic caged substrates.

Diagnosis of GD and fundamental research on the disorder were accelerated with the availability of an antibody toolbox. Polyclonal and monoclonal antibodies directed to GBA quickly found valuable applications in fundamental studies on the life cycle and subcellular localization of GBA, the diagnosis of GD patients and even the purification of therapeutic enzyme[187–189]. In recent times novel chemical biology tools have been designed allowing investigations on GBA and *in vivo* GlcCer metabolism in an unprecedented manner.

One recent breakthrough is the development of activity-based probes (ABPs) for GBA. The irreversible inhibition of GBA by cyclophellitol (see section above and Figure 2) was exploited for the design of ABPs for the enzyme[62,63]. Initially, β-glucopyranosyl-configured cyclophellitol-epoxides modified at C6 (glucopyranose numbering) with a fluorescent BODIPY (Figure 8) were synthesized as mechanism-based probes for GBA[62]. These ABPs bind covalently and with high specificity in a mechanism-based manner, to the catalytic nucleophile residue E340 of GBA[62]. *In situ* labeling of active GBA with the ABPs in intact cells is feasible, visualizing the intralysosomal location of the enzyme. Intravenous infusion of mice with these ABPs results in specific labeling of GBA in various tissues, except brain and eye[63]. Intracerebroventricular administration of the ABPs to mice allows visualization of active GBA in brain with high spatial resolution[190]. Reductions in active GBA molecules can be detected after the exposure of cultured GD fibroblasts to ABP and subsequent analysis of ABP-labeled protein by gel electrophoresis and quantitative fluorescence scanning[62]. The successful approach for design of GBA directed ABPs was successfully reproduced for the lysosomal β-galactosylceramidase (galactocerebrosidase, GALC), deficient in Krabbe disease[191]. Next, a broad spectrum ABP was generated by the design of β-glucopyranosyl-configured cyclophellitol-aziridines with a fluorophore modification (Figure 8)[63]. In these probes the fluorophore is positioned more closely to the position of the aglycon in substrates of β-glucosidases. Therefore, these ABPs covalently label a broad class of human β-glucosidases, including GBA, GBA2, GBA3 and lactase-phloridzin hydrolase[57]. Meanwhile, cyclophellitol-type ABPs with distinct sugar configuration have been developed as ABPs for α-glucosidases, α-fucosidase, α-mannosidases, α-iduronidase, α-galactosidases, β-galactosidases, β-

mannosidases and β-glucuronidases[192–195], (unpublished data: Artola, Jiang, Beenakker and Kuo).

The ABPs can be conceived to find application in the diagnosis of lysosomal storage diseases as well in fundamental research. Of note, the ABPs can be applied cross species given the conserved catalytic pockets of glycosidases. They can be also equipped with biotin instead of fluorophores, allowing convenient purification by means of streptavidin-based pull down and subsequent identification of proteins by proteomics[195,196]. This procedure should also allow identification of interacting proteins with the ABP-targeted enzyme. The GBA ABPs can be further optimized to monitor the precise localization of enzyme in life cells, by super-resolution microscopy as well as by correlative light and electron microscopy. For this cyclophellitol derivatives can be fitted out with a norbonene at C8 (cyclophellitol numbering) to generate a mechanism-based inhibitor projected to be (due to the bulk at this position) selective for GBA. Pulse labeling of tissue culture and washing away unbound probe can be followed by treatment with fluorogenic tetrazine. Only after inverse-electron demand Diels Alder the dye becomes fluorescent, thus limiting background labeling[197].
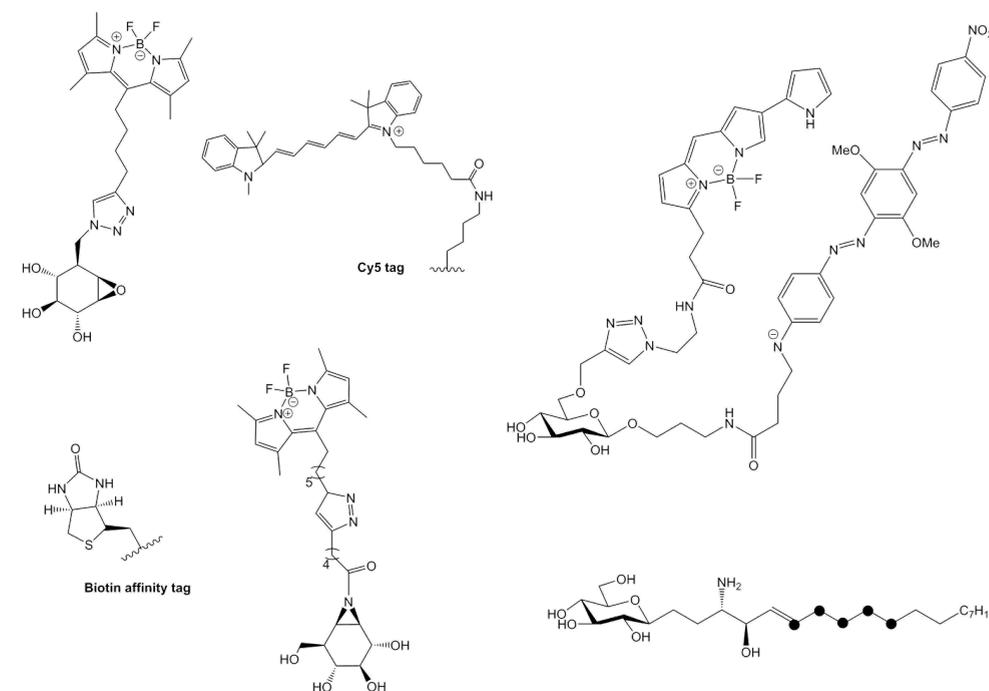

Figure 8. Chemical biology tools: ABPs, isotope and di-azirine-GSLs, and caged GBA substrate. Upper left panel: Cyclophellitol-epoxide with BODIPY and Cy5 fluorophore; Lower left panel: Cyclophellitol-aziridine with BODIPY and biotin; Upper right panel: Caged fluorogenic substrate for GBA[198]; Lower right panel: Isotope labeled glucosylsphingosine.

Other important chemical research tools developed in the last decades are reversible and irreversible inhibitors targeting various enzymes (GBA, GBA2 and GCS) involved in glucosylceramide metabolism[62,199]. Vocadlo and co-workers recently reported the design of a caged fluorogenic substrate specific for GBA (Figure 8)[198]. This substrate, suited for activity measurements in living cells, should find broad application. Ideally however, *in situ* activity of GBA towards natural substrates is detected. New tools for this are glycosphingolipids and glycosphingoid bases encoded with ^{13}C atoms. These isotope labeled lipids synthesized at the Leiden Institute of Chemistry can be used as internal standards in LC-MS/MS quantification of lipids[200,201]. Moreover, they can be used in the analysis of enzymatic activity towards natural substrates in cultured cells[113]. Particularly, feeding of cells with isotope (glyco)sphingoid bases offers a convenient way to monitor *in situ* lipid metabolism over time. A similar approach can be employed with mice to which isotope labeled lipids are intravenously administered. Recently photoactivatable lipid analogs have been developed that can be activated by UV light to form a covalent linkage to their protein-binding partners[202,203]. There now are commercial diazirine-functionalized and clickable lipids like pacFA, pacSph and pacGlcCer. As demonstrated in this thesis, pacGlcCer is very suitable to study *in vitro* features of the catalytic pocket of GBA.

Transglycosylation.

Several retaining glycosidases have been found to also efficiently transglycosylate, i.e. to transfer the released sugar from substrate to another acceptor than a water molecule. A thorough historical account of the realization that glycosidases may transglycosylate is provided by the review of Hehre on the topic[204]. Acceptors in transglycosylation reactions can be sugars, as is the case with chitinases such as chitotriosidase[205]. Other glycosidases like GBA may transglucosylate sugar to other structures such as for example retinol and sterol. Glew and co-workers were the first to demonstrate that GBA catalyzes the transfer of glucose from 4-methylumbelliferyl-β-glucoside to retinol and other alcohols[206]. Akiyama and colleagues more recently reported that *in vitro* GBA generates 25-NBD-cholesterol-glucoside through transglucosylation from GlcCer and 25-NBD-cholesterol[207]. This finding was recently recapitulated by Marques *et al.* showing GBA mediated transglucosylation of natural cholesterol with GlcCer as donor[132]. Importantly, it was demonstrated that also the cytosolic β-glucosidase GBA2 generates GlcChol through transglucosylation, again using GlcCer as donor. A sensitive quantitative detection of GlcChol by LC-MS/MS using [13]C$_5$-isotope labeled GlcChol as internal standard enabled the detection of the glucosylated sterol in human plasma and cultured cells[132]. Analysis of mouse organs revealed that GlcChol is present in almost all tissues, with relative high amounts in the thymus, of interest in view of the noted abnormalities in NKT and B-cells in GD patients[208–210]. It has been speculated by Mistry and colleagues that elevated GlcCer or GlcSph via binding to CD1 may be causing this phenomenon[208]. GlcChol should also be considered a serious candidate in this respect.

Interestingly, GlcChol is not directly formed by GCS by transfer of glucose from UDP-glucose to ceramide[132]. GBA2 is found to be largely responsible for biosynthesis of GlcChol using GlcCer as glucose donor. Whilst GBA seems to normally degrade GlcChol, high intralysosomal cholesterol concentrations as in Niemann Pick type C disease favor formation of GlcChol by GBA. Induction of lysosomal cholesterol accumulation in cells with U18666A causes a rapid increase in GlcChol, which is abolished by selective inactivation of GBA[132]. Pharmacological inhibition of GBA2 leads to reduction of GlcChol in cultured cells, plasma of mice and plasma of GD patients. The same is observed upon lowering of GlcCer by inhibition of GCS, further indicating that the availability of GlcCer is an important driver in formation of GlcChol through transglucosylation[132].

The recent discovery of additional metabolites linked to GlcCer seems highly relevant for a better understanding of the complex clinical picture of GD. The finding suggests that GBA may be responsible for metabolism of multiple glucosylated metabolites and not only GlcCer. Hypothetically, other metabolites than GlcCer might more directly underlie some disease manifestations of GD patients. The realization that GlcCer acts as intermediary metabolite donating glucose to other metabolites may help to understand better in the future the complex and highly variable clinical outcome of inherited disturbances in GlcCer metabolism such as GD.

References

1. Novikoff, A. B., Beaufay, H. & De Duve, C. Electron microscopy of lysosomen rich fractions from rat liver. *J. Biophys. Biochem. Cytol.* **2,** 179–84 (1956).
2. de Duve, C. The lysosome turns fifty. *Nat. Cell Biol.* **7,** 847–9 (2005).
3. Schwake, M., Schröder, B. & Saftig, P. Lysosomal Membrane Proteins and Their Central Role in Physiology. *Traffic* **14,** 739–748 (2013).
4. Settembre, C. & Ballabio, A. Lysosome: regulator of lipid degradation pathways. *Trends Cell Biol.* **24,** 743–750 (2014).
5. Settembre, C., Fraldi, A., Medina, D. L. & Ballabio, A. Signals from the lysosome: a control centre for cellular clearance and energy metabolism. *Nat. Rev. Mol. Cell Biol.* **14,** 283–96 (2013).
6. Efeyan, A., Zoncu, R. & Sabatini, D. M. Amino acids and mTORC1: from lysosomes to disease. *Trends Mol. Med.* **18,** 524–533 (2012).
7. Bar-Peled, L. & Sabatini, D. M. Regulation of mTORC1 by amino acids. *Trends Cell Biol.* **24,** 400–406 (2014).
8. Neufeld, E. F. Lysosomal storage diseases. *Annu. Rev. Biochem.* **60,** 257–80 (1991).
9. Platt, F. M. Sphingolipid lysosomal storage disorders. *Nature* **510,** 68–75 (2014).
10. Schulze, H. & Sandhoff, K. Sphingolipids and lysosomal pathologies. *Biochim. Biophys. Acta* **1841,** 799–810 (2014).
11. Sinnott, M. Catalytic mechanism of enzymic glycosyl transfer. *Chem. Rev.* (1990).
12. Henrissat, B. *et al.* Conserved catalytic machinery and the prediction of a common fold for several families of glycosyl hydrolases. *Proc. Natl. Acad. Sci. U. S. A.* **92,** 7090–4 (1995).
13. Davies, G. & Henrissat, B. Structures and mechanisms of glycosyl hydrolases. *Structure*

3, 853–859 (1995).

14. Bairoch, A. Classification of glycosyl hydrolase families and index of glycosyl hydrolase entries in SWISS-PROT. (1999).

15. Naumoff, D. G. DEVELOPMENT OF A HIERARCHICAL CLASSIFICATION OF THE TIM-BARREL TYPE GLYCOSIDE HYDROLASES. in *Proceedings of the Fifth International Conference on Bioinformatics of Genome Regulation and Structure* (eds. Kolchanov, N. & Hofestädt, R.) 294–298 (RUSSIAN ACADEMY OF SCIENCES SIBERIAN BRANCH INSTITUTE OF CYTOLOGY AND GENETICS , 2006).

16. Naumoff, D. G. Hierarchical classification of glycoside hydrolases. *Biochem.* **76,** 622–635 (2011).

17. Davies, G. J. & Williams, S. J. Carbohydrate-active enzymes: sequences, shapes, contortions and cells. *Biochem. Soc. Trans.* **44,** 79–87 (2016).

18. Kallemeijn, W. W., Witte, M. D., Wennekes, T. & Aerts, J. M. F. G. Mechanism-based inhibitors of glycosidases: design and applications. *Adv. Carbohydr. Chem. Biochem.* **71,** 297–338 (2014).

19. Vocadlo, D. J., Davies, G. J., Laine, R. & Withers, S. G. Catalysis by hen egg-white lysozyme proceeds via a covalent intermediate. *Nature* **412,** 835–838 (2001).

20. Ivo Tews, †, Anke C. Terwisscha van Scheltinga, ‡, Anastassis Perrakis, §, Keith S. Wilson, ‖ and & Bauke W. Dijkstra*, ‡. Substrate-Assisted Catalysis Unifies Two Families of Chitinolytic Enzymes. (1997). doi:10.1021/JA970674I

21. Hollak, C. E., van Weely, S., van Oers, M. H. & Aerts, J. M. Marked elevation of plasma chitotriosidase activity. A novel hallmark of Gaucher disease. *J. Clin. Invest.* **93,** 1288–1292 (1994).

22. Boot, R. G., Renkema, G. H., Strijland, A., van Zonneveld, A. J. & Aerts, J. M. Cloning of a cDNA encoding chitotriosidase, a human chitinase produced by macrophages. *J. Biol. Chem.* **270,** 26252–6 (1995).

23. Fusetti, F. *et al.* Structure of human chitotriosidase. Implications for specific inhibitor design and function of mammalian chitinase-like lectins. *J. Biol. Chem.* **277,** 25537–44 (2002).

24. Rao, F. V *et al.* Crystal structures of allosamidin derivatives in complex with human macrophage chitinase. *J. Biol. Chem.* **278,** 20110–6 (2003).

25. Boot, R. G. *et al.* Identification of a novel acidic mammalian chitinase distinct from chitotriosidase. *J. Biol. Chem.* **276,** 6770–8 (2001).

26. Bussink, A. P., Speijer, D., Aerts, J. M. F. G. & Boot, R. G. Evolution of mammalian chitinase(-like) members of family 18 glycosyl hydrolases. *Genetics* **177,** 959–70 (2007).

27. Thudichum, J. *A treatise on the chemical constitution of the brain*. (Bailliere Tindall and Cox, 1884).

28. Wennekes, T. *et al.* Glycosphingolipids--nature, function, and pharmacological modulation. *Angew. Chem. Int. Ed. Engl.* **48,** 8848–69 (2009).

29. Hancock, J. F. Lipid rafts: contentious only from simplistic standpoints. *Nat. Rev. Mol. Cell Biol.* **7,** 456–462 (2006).

30. Sonnino, S. & Prinetti, A. Membrane domains and the 'lipid raft' concept. *Curr. Med. Chem.* (2012).

31. Lingwood, D. & Simons, K. Lipid rafts as a membrane-organizing principle. *Science (80-.).* **327,** 46–50 (2010).

32. Merrill, A. H. Sphingolipid and Glycosphingolipid Metabolic Pathways in the Era of Sphingolipidomics. *Chem. Rev.* **111,** 6387–6422 (2011).

33. Tidhar, R. & Futerman, A. H. The complexity of sphingolipid biosynthesis in the endoplasmic reticulum. *Biochim. Biophys. Acta - Mol. Cell Res.* **1833,** 2511–2518 (2013).

34. Fabrias, G. *et al.* Dihydroceramide desaturase and dihydrosphingolipids: Debutant players in the sphingolipid arena. *Prog. Lipid Res.* **51,** 82–94 (2012).

35. Rodriguez-Cuenca, S., Barbarroja, N. & Vidal-Puig, A. Dihydroceramide desaturase 1, the gatekeeper of ceramide induced lipotoxicity. *Biochim. Biophys. Acta - Mol. Cell Biol. Lipids* **1851,** 40–50 (2015).

36. Gault, C. R., Obeid, L. M. & Hannun, Y. A. An overview of sphingolipid metabolism: from synthesis to breakdown. *Adv. Exp. Med. Biol.* **688,** 1–23 (2010).

37. Hanada, K. *et al.* Molecular machinery for non-vesicular trafficking of ceramide. *Nature* **426,** 803–9 (2003).

38. Ichikawa, S., Sakiyama, H., Suzuki, G., Hidari, K. I. & Hirabayashi, Y. Expression cloning of a cDNA for human ceramide glucosyltransferase that catalyzes the first glycosylation step of glycosphingolipid synthesis. *Proc. Natl. Acad. Sci. U. S. A.* **93,** 12654 (1996).

39. van Meer, G., Wolthoorn, J. & Degroote, S. The fate and function of glycosphingolipid glucosylceramide. *Philos. Trans. R. Soc. Lond. B. Biol. Sci.* **358,** 869–73 (2003).

40. Merrill, A. H., Wang, M. D., Park, M. & Sullards, M. C. (Glyco)sphingolipidology: an amazing challenge and opportunity for systems biology. *Trends Biochem. Sci.* **32,** 457–468 (2007).

41. D'Angelo, G., Capasso, S., Sticco, L. & Russo, D. Glycosphingolipids: synthesis and functions. *FEBS J.* **280,** 6338–6353 (2013).

42. Kolter, T. & Sandhoff, K. Lysosomal degradation of membrane lipids. *FEBS Lett.* **584,** 1700–1712 (2010).

43. Chigorno, V. *et al.* Metabolic processing of gangliosides by human fibroblasts in culture--formation and recycling of separate pools of sphingosine. *Eur. J. Biochem.* **250,** 661–9 (1997).

44. Pyne, S., Adams, D. R. & Pyne, N. J. Sphingosine 1-phosphate and sphingosine kinases in health and disease: Recent advances. *Prog. Lipid Res.* **62,** 93–106 (2016).

45. Serra, M. & Saba, J. D. Sphingosine 1-phosphate lyase, a key regulator of sphingosine 1-phosphate signaling and function. *Adv. Enzyme Regul.* **50,** 349–62 (2010).

46. Horowitz, M. *et al.* The human glucocerebrosidase gene and pseudogene: structure and evolution. *Genomics* **4,** 87–96 (1989).

47. Erickson, A. H., Ginns, E. I. & Barranger, J. A. Biosynthesis of the lysosomal enzyme glucocerebrosidase. *J. Biol. Chem.* **260,** 14319–24 (1985).

48. Takasaki, S. *et al.* Structure of the N-asparagine-linked oligosaccharide units of human placental beta-glucocerebrosidase. *J. Biol. Chem.* **259,** 10112–7 (1984).

49. Berg-Fussman, A., Grace, M. E., Ioannou, Y. & Grabowski, G. A. Human acid beta-glucosidase. N-glycosylation site occupancy and the effect of glycosylation on enzymatic activity. *J. Biol. Chem.* **268,** 14861–6 (1993).

50. Reczek, D. *et al.* LIMP-2 Is a Receptor for Lysosomal Mannose-6-Phosphate-Independent Targeting of β-Glucocerebrosidase. *Cell* **131,** 770–783 (2007).

51. Zunke, F. *et al.* Characterization of the complex formed by β-glucocerebrosidase and the lysosomal integral membrane protein type-2. *Proc. Natl. Acad. Sci.* **113,** 3791–3796 (2016).

52. Ron, I. & Horowitz, M. ER retention and degradation as the molecular basis underlying Gaucher disease heterogeneity. *Hum. Mol. Genet.* **14,** 2387–2398 (2005).

53. Aerts, J. M., Hollak, C., Boot, R. & Groener, A. Biochemistry of glycosphingolipid storage disorders: implications for therapeutic intervention. *Philos. Trans. R. Soc. Lond. B. Biol. Sci.* **358,** 905–14 (2003).

54. Aerts, J. M. *et al.* Glucocerebrosidase, a lysosomal enzyme that does not undergo oligosaccharide phosphorylation. *Biochim. Biophys. Acta* **964,** 303–8 (1988).

55. Saftig, P. & Klumperman, J. Lysosome biogenesis and lysosomal membrane proteins: trafficking meets function. *Nat. Rev. Mol. Cell Biol.* **10,** 623–635 (2009).

56. Jonsson, L. M. V *et al.* Biosynthesis and maturation of glucocerebrosidase in Gaucher fibroblasts. *Eur. J. Biochem.* **164,** 171–179 (1987).

57. Grace, M. E., Graves, P. N., Smith, F. I. & Grabowski, G. A. Analyses of catalytic activity and inhibitor binding of human acid beta-glucosidase by site-directed mutagenesis. Identification of residues critical to catalysis and evidence for causality of two Ashkenazi Jewish Gaucher disease type 1 mutations. *J. Biol. Chem.* **265,** 6827–35 (1990).

58. Zachos, C., Blanz, J., Saftig, P. & Schwake, M. A Critical Histidine Residue Within LIMP-2 Mediates pH Sensitive Binding to Its Ligand β-Glucocerebrosidase. *Traffic* **13,** 1113–1123 (2012).

59. Morimoto, S. *et al.* Interaction of saposins, acidic lipids, and glucosylceramidase. *J. Biol. Chem.* **265,** 1933–7 (1990).

60. Kallemeijn, W. W. *et al.* A Sensitive Gel-based Method Combining Distinct Cyclophellitol-based Probes for the Identification of Acid/Base Residues in Human Retaining -Glucosidases. *J. Biol. Chem.* **289,** 35351–35362 (2014).

61. Witte, M. D., van der Marel, G. a, Aerts, J. M. F. G. & Overkleeft, H. S. Irreversible inhibitors and activity-based probes as research tools in chemical glycobiology. *Org. Biomol. Chem.* **9,** 5908–5926 (2011).

62. Witte, M. D. *et al.* Ultrasensitive in situ visualization of active glucocerebrosidase molecules. *Nat. Chem. Biol.* **6,** 907–913 (2010).

63. Kallemeijn, W. W. *et al.* Novel activity-based probes for broad-spectrum profiling of retaining β-exoglucosidases in situ and in vivo. *Angew. Chemie - Int. Ed.* **51,** 12529–12533 (2012).

64. Dvir, H. *et al.* X-ray structure of human acid-β-glucosidase, the defective enzyme in Gaucher disease. *EMBO Rep.* **4,** 704–709 (2003).

65. Brumshtein, B. *et al.* Cyclodextrin-mediated crystallization of acid β-glucosidase in complex with amphiphilic bicyclic nojirimycin analogues. *Org. Biomol. Chem.* **9,** 4160 (2011).

66. Offman, M. N. *et al.* Comparison of a molecular dynamics model with the X-ray structure of the N370S acid- -glucosidase mutant that causes Gaucher disease. *Protein Eng. Des. Sel.* **24,** 773–775 (2011).

67. Gruschus, J. M. *et al.* Dissociation of glucocerebrosidase dimer in solution by its co-factor, saposin C. *Biochem. Biophys. Res. Commun.* **457,** 561–6 (2015).

68. Atrian, S. *et al.* An evolutionary and structure-based docking model for glucocerebrosidase-saposin C and glucocerebrosidase-substrate interactions - relevance for Gaucher disease. *Proteins* **70,** 882–91 (2008).

69. Weiler, S., Kishimoto, Y., O'Brien, J. S., Barranger, J. A. & Tomich, J. M. Identification of the binding and activating sites of the sphingolipid activator protein, saposin C, with

70. Qi, X., Qin, W., Sun, Y., Kondoh, K. & Grabowski, G. A. Functional organization of saposin C. Definition of the neurotrophic and acid beta-glucosidase activation regions. *J. Biol. Chem.* **271,** 6874–80 (1996).

71. Vaccaro, A. M. *et al.* Saposin C mutations in Gaucher disease patients resulting in lysosomal lipid accumulation, saposin C deficiency, but normal prosaposin processing and sorting. *Hum. Mol. Genet.* **19,** 2987–2997 (2010).

72. Aerts, J. M. *et al.* Conditions affecting the activity of glucocerebrosidase purified from spleens of control subjects and patients with type 1 Gaucher disease. *Biochim. Biophys. Acta* **1041,** 55–63 (1990).

73. Yap, T. L., Gruschus, J. M., Velayati, A., Sidransky, E. & Lee, J. C. Saposin C protects glucocerebrosidase against α-synuclein inhibition. *Biochemistry* **52,** 7161–3 (2013).

74. Sun, Y., Qi, X. & Grabowski, G. A. Saposin C is required for normal resistance of acid beta-glucosidase to proteolytic degradation. *J. Biol. Chem.* **278,** 31918–23 (2003).

75. Salvioli, R. *et al.* Glucosylceramidase mass and subcellular localization are modulated by cholesterol in Niemann-Pick disease type C. *J. Biol. Chem.* **279,** 17674–80 (2004).

76. E. Beutler, G. A. G. in *C.R. Scriver,W.S. Sly, D. Valle (Eds.), The Metabolic and Molecular Bases of Inherited Disease, 8th ed.* 3635–3668 (McGraw-Hill, New York, 2001).

77. GAUCHER, P. C. E. De l'épithélioma primitif de la rate. Hypertrophie idiopathique de la rate sans leucémie. (1882).

78. Aghion, H. La Maladie de Gaucher dans l'enfance. (These de Paris, 1934).

79. Brady, R. O., Kanfer, J. N., Bradley, R. M. & Shapiro, D. Demonstration of a deficiency of glucocerebroside-cleaving enzyme in Gaucher's disease. *J. Clin. Invest.* **45,** 1112–1115 (1966).

80. Patrick, A. A deficiency of glucocerebrosidase in Gaucher's disease. *Biochem J.* **97,** 17C–18C (1965).

81. Hruska, K. S., LaMarca, M. E., Scott, C. R. & Sidransky, E. Gaucher disease: mutation and polymorphism spectrum in the glucocerebrosidase gene (GBA). *Hum. Mutat.* **29,** 567–583 (2008).

82. Ferraz, M. J. *et al.* Gaucher disease and Fabry disease: New markers and insights in pathophysiology for two distinct glycosphingolipidoses. *Biochim. Biophys. Acta - Mol. Cell Biol. Lipids* **1841,** 811–825 (2014).

83. Schmitz, M., Alfalah, M., Aerts, J. M. F. G., Naim, H. Y. & Zimmer, K.-P. Impaired trafficking of mutants of lysosomal glucocerebrosidase in Gaucher's disease. *Int. J. Biochem. Cell Biol.* **37,** 2310–20 (2005).

84. Gatt, S., Dinur, T., Osiecki, K., Desnick, R. J. & Grabowski, G. A. Use of activators and inhibitors to define the properties of the active site of normal and Gaucher disease lysosomal beta-glucosidase. *Enzyme* **33,** 109–19 (1985).

85. van Weely, S. *et al.* Role of pH in determining the cell-type-specific residual activity of glucocerebrosidase in type 1 Gaucher disease. *J. Clin. Invest.* **91,** 1167–75 (1993).

86. Wei, R. R. *et al.* X-ray and Biochemical Analysis of N370S Mutant Human Acid - Glucosidase. *J. Biol. Chem.* **286,** 299–308 (2011).

87. Sawkar, A. R. *et al.* Chemical chaperones increase the cellular activity of N370S beta - glucosidase: a therapeutic strategy for Gaucher disease. *Proc. Natl. Acad. Sci. U. S. A.* **99,** 15428–33 (2002).

88. Ohashi, T. *et al.* Characterization of human glucocerebrosidase from different mutant alleles. *J. Biol. Chem.* **266,** 3661–7 (1991).

89. Boot, R. G. *et al.* Glucocerebrosidase genotype of Gaucher patients in The Netherlands: limitations in prognostic value. *Hum. Mutat.* **10,** 348–58 (1997).

90. Lachmann, R. H., Grant, I. R., Halsall, D. & Cox, T. M. Twin pairs showing discordance of phenotype in adult Gaucher's disease. *QJM* **97,** 199–204 (2004).

91. Biegstraaten, M. *et al.* A monozygotic twin pair with highly discordant Gaucher phenotypes. *Blood Cells. Mol. Dis.* **46,** 39–41 (2011).

92. Bussink, A. P., van Eijk, M., Renkema, G. H., Aerts, J. M & Boot, R. G. The biology of the Gaucher cell: the cradle of human chitinases. *Int. Rev. Cytol.* **252,** 71–128 (2006).

93. Boot, R. G. *et al.* Marked elevation of the chemokine CCL18/PARC in Gaucher disease: a novel surrogate marker for assessing therapeutic intervention. *Blood* **103,** 33–9 (2004).

94. Holleran, W. M., Takagi, Y. & Uchida, Y. Epidermal sphingolipids: Metabolism, function, and roles in skin disorders. *FEBS Lett.* **580,** 5456–5466 (2006).

95. Staretz-Chacham, O., Lang, T. C., LaMarca, M. E., Krasnewich, D. & Sidransky, E. Lysosomal storage disorders in the newborn. *Pediatrics* **123,** 1191–207 (2009).

96. Sidransky, E., Sherer, D. M. & Ginns, E. I. Gaucher disease in the neonate: a distinct Gaucher phenotype is analogous to a mouse model created by targeted disruption of the glucocerebrosidase gene. *Pediatr. Res.* **32,** 494–8 (1992).

97. Siebert, M., Sidransky, E. & Westbroek, W. Glucocerebrosidase is shaking up the synucleinopathies. *Brain* **137,** 1304–1322 (2014).

98. Blanz, J. & Saftig, P. Parkinson's disease: acid-glucocerebrosidase activity and alpha-synuclein clearance. *J. Neurochem.* **139,** 198–215 (2016).

99. Rothaug, M. *et al.* LIMP-2 expression is critical for -glucocerebrosidase activity and -synuclein clearance. *Proc. Natl. Acad. Sci.* **111,** 15573–15578 (2014).

100. Aerts, J. M. & Hollak, C. E. Plasma and metabolic abnormalities in Gaucher's disease. *Baillieres. Clin. Haematol.* **10,** 691–709 (1997).

101. Kramer, G. *et al.* Elevation of glycoprotein nonmetastatic melanoma protein B in type 1 Gaucher disease patients and mouse models. *FEBS Open Bio* **6,** 902–913 (2016).

102. Møller, H. J., de Fost, M., Aerts, H., Hollak, C. & Moestrup, S. K. Plasma level of the macrophage-derived soluble CD163 is increased and positively correlates with severity in Gaucher's disease. *Eur. J. Haematol.* **72,** 135–9 (2004).

103. Dekker, N. *et al.* Elevated plasma glucosylsphingosine in Gaucher disease: relation to phenotype, storage cell markers, and therapeutic response. *Blood* **118,** e118–e127 (2011).

104. Mirzaian, M. *et al.* Mass spectrometric quantification of glucosylsphingosine in plasma and urine of type 1 Gaucher patients using an isotope standard. *Blood Cells, Mol. Dis.* **54,** 307–314 (2015).

105. Deegan, P. B. *et al.* Clinical evaluation of chemokine and enzymatic biomarkers of Gaucher disease. *Blood Cells. Mol. Dis.* **35,** 259–67 (2005).

106. van Dussen, L. *et al.* Value of plasma chitotriosidase to assess non-neuronopathic Gaucher disease severity and progression in the era of enzyme replacement therapy. *J. Inherit. Metab. Dis.* **37,** 991–1001 (2014).

107. Tylki-Szymańska, A. *et al.* Gaucher disease due to saposin C deficiency, previously described as non-neuronopathic form — No positive effects after 2-years of miglustat therapy. *Mol. Genet. Metab.* **104,** 627–630 (2011).

108. Berkovic, S. F. *et al.* Array-Based Gene Discovery with Three Unrelated Subjects Shows SCARB2/LIMP-2 Deficiency Causes Myoclonus Epilepsy and Glomerulosclerosis. *Am. J. Hum. Genet.* **82,** 673–684 (2008).

109. Badhwar, A. *et al.* Action myoclonus-renal failure syndrome: characterization of a unique cerebro-renal disorder. *Brain* **127,** 2173–2182 (2004).

110. Gamp, A.-C. *et al.* LIMP-2/LGP85 deficiency causes ureteric pelvic junction obstruction, deafness and peripheral neuropathy in mice. *Hum. Mol. Genet.* **12,** 631–46 (2003).

111. Balreira, A. *et al.* A nonsense mutation in the LIMP-2 gene associated with progressive myoclonic epilepsy and nephrotic syndrome. *Hum. Mol. Genet.* **17,** 2238–2243 (2008).

112. Gaspar, P. *et al.* Action myoclonus-renal failure syndrome: diagnostic applications of activity-based probes and lipid analysis. *J. Lipid Res.* **55,** 138–145 (2014).

113. Ferraz, M. J. *et al.* Lysosomal glycosphingolipid catabolism by acid ceramidase: formation of glycosphingoid bases during deficiency of glycosidases. *FEBS Lett.* **590,** 716–725 (2016).

114. Smid, B. E. *et al.* Biochemical response to substrate reduction therapy versus enzyme replacement therapy in Gaucher disease type 1 patients. *Orphanet J. Rare Dis.* **11,** 28 (2016).

115. Biegstraaten, M., van Schaik, I. N., Aerts, J. M. F. G. & Hollak, C. E. M. 'Non-neuronopathic' Gaucher disease reconsidered. Prevalence of neurological manifestations in a Dutch cohort of type I Gaucher disease patients and a systematic review of the literature. *J. Inherit. Metab. Dis.* **31,** 337–349 (2008).

116. Langeveld, M. *et al.* Type I Gaucher Disease, a Glycosphingolipid Storage Disorder, Is Associated with Insulin Resistance. *J. Clin. Endocrinol. Metab.* **93,** 845–851 (2008).

117. Abrahamov, A. *et al.* Gaucher's disease variant characterised by progressive calcification of heart valves and unique genotype. *Lancet (London, England)* **346,** 1000–3 (1995).

118. Chabás, A. *et al.* Unusual expression of Gaucher's disease: cardiovascular calcifications in three sibs homozygous for the D409H mutation. *J. Med. Genet.* **32,** 740–2 (1995).

119. George, R., McMahon, J., Lytle, B., Clark, B. & Lichtin, A. Severe valvular and aortic arch calcification in a patient with Gaucher's disease homozygous for the D409H mutation. *Clin. Genet.* **59,** 360–3 (2001).

120. Pasmanik-Chor, M. *et al.* The glucocerebrosidase D409H mutation in Gaucher disease. *Biochem. Mol. Med.* **59,** 125–33 (1996).

121. de Fost, M. *et al.* Immunoglobulin and free light chain abnormalities in Gaucher disease type I: data from an adult cohort of 63 patients and review of the literature. *Ann. Hematol.* **87,** 439–49 (2008).

122. Cox, T. M., Rosenbloom, B. E. & Barker, R. A. Gaucher disease and comorbidities: B-cell malignancy and parkinsonism. *Am. J. Hematol.* **90,** S25–S28 (2015).

123. de Fost, M. *et al.* Increased incidence of cancer in adult Gaucher disease in Western Europe. *Blood Cells. Mol. Dis.* **36,** 53–8 (2006).

124. Hrebícek, M. *et al.* A case of type I Gaucher disease with cardiopulmonary amyloidosis and chitotriosidase deficiency. *Virchows Arch.* **429,** 305–9 (1996).

125. van Dussen, L. *et al.* Markers of bone turnover in Gaucher disease: modeling the evolution of bone disease. *J. Clin. Endocrinol. Metab.* **96,** 2194–205 (2011).

126. Mistry, P. K. *et al.* Glucocerebrosidase gene-deficient mouse recapitulates Gaucher disease displaying cellular and molecular dysregulation beyond the macrophage. *Proc. Natl. Acad. Sci.* **107,** 19473–19478 (2010).

127. van Weely, S., Brandsma, M., Strijland, A., Tager, J. M. & Aerts, J. M. Demonstration of

the existence of a second, non-lysosomal glucocerebrosidase that is not deficient in Gaucher disease. *Biochim. Biophys. Acta* **1181,** 55–62 (1993).

128. Yildiz, Y. *et al.* Mutation of β-glucosidase 2 causes glycolipid storage disease and impaired male fertility. *J. Clin. Invest.* **116,** 2985–2994 (2006).
129. Boot, R. G. *et al.* Identification of the non-lysosomal glucosylceramidase as beta-glucosidase 2. *J. Biol. Chem.* **282,** 1305–12 (2007).
130. Mistry, P. K. *et al.* Glucocerebrosidase 2 gene deletion rescues type 1 Gaucher disease. *Proc. Natl. Acad. Sci.* **111,** 4934–4939 (2014).
131. Marques, A. R. A. *et al.* Reducing GBA2 Activity Ameliorates Neuropathology in Niemann-Pick Type C Mice. *PLoS One* **10,** e0135889 (2015).
132. Marques, A. R. A. *et al.* Glucosylated cholesterol in mammalian cells and tissues: formation and degradation by multiple cellular β-glucosidases. *J. Lipid Res.* **57,** 451–463 (2016).
133. Nair, S. *et al.* Clonal Immunoglobulin against Lysolipids in the Origin of Myeloma. *N. Engl. J. Med.* **374,** 555–561 (2016).
134. Pavlova, E. V. *et al.* B cell lymphoma and myeloma in murine Gaucher's disease. *J. Pathol.* **231,** 88–97 (2013).
135. Pavlova, E. V *et al.* Inhibition of UDP-glucosylceramide synthase in mice prevents Gaucher disease-associated B-cell malignancy. *J. Pathol.* **235,** 113–124 (2015).
136. Ferraz, M. J. *et al.* Lyso-glycosphingolipid abnormalities in different murine models of lysosomal storage disorders. *Mol. Genet. Metab.* **117,** 186–193 (2016).
137. Suzuki, K. Twenty five years of the "psychosine hypothesis": a personal perspective of its history and present status. *Neurochem. Res.* **23,** 251–9 (1998).
138. Aerts, J. M. *et al.* Elevated globotriaosylsphingosine is a hallmark of Fabry disease. *Proc. Natl. Acad. Sci.* **105,** 2812–2817 (2008).
139. Formichi, P. *et al.* Psychosine-induced apoptosis and cytokine activation in immune peripheral cells of Krabbe patients. *J. Cell. Physiol.* **212,** 737–43 (2007).
140. Tanaka, K., Nagara, H., Kobayashi, T. & Goto, I. The twitcher mouse: accumulation of galactosylsphingosine and pathology of the sciatic nerve. *Brain Res.* **454,** 340–6 (1988).
141. Choi, L. *et al.* The Fabry disease-associated lipid Lyso-Gb3 enhances voltage-gated calcium currents in sensory neurons and causes pain. *Neurosci. Lett.* **594,** 163–8 (2015).
142. Sanchez-Niño, M. D. *et al.* Lyso-Gb3 activates Notch1 in human podocytes. *Hum. Mol. Genet.* **24,** 5720–5732 (2015).
143. Brady, R. O. Enzyme replacement therapy: conception, chaos and culmination. *Philos. Trans. R. Soc. B Biol. Sci.* **358,** 915–919 (2003).
144. Barton, N. W., Furbish, F. S., Murray, G. J., Garfield, M. & Brady, R. O. Therapeutic response to intravenous infusions of glucocerebrosidase in a patient with Gaucher disease. *Proc. Natl. Acad. Sci. U. S. A.* **87,** 1913–6 (1990).
145. Barton, N. W. *et al.* Replacement therapy for inherited enzyme deficiency--macrophage-targeted glucocerebrosidase for Gaucher's disease. *N. Engl. J. Med.* **324,** 1464–70 (1991).
146. Aerts, J. M., Hollak, C., Boot, R. & Groener, A. in 193–208 (Springer Berlin Heidelberg, 2003). doi:10.1007/978-3-642-55742-2_11
147. Desnick, R. J. & Schuchman, E. H. Enzyme Replacement Therapy for Lysosomal Diseases: Lessons from 20 Years of Experience and Remaining Challenges. *Annu. Rev.*

Genomics Hum. Genet. **13,** 307–335 (2012).

148. Aerts, J. M. F. G., Yasothan, U. & Kirkpatrick, P. Velaglucerase alfa. *Nat. Rev. Drug Discov.* **9,** 837–8 (2010).
149. Zimran, A. *et al.* Pivotal trial with plant cell-expressed recombinant glucocerebrosidase, taliglucerase alfa, a novel enzyme replacement therapy for Gaucher disease. *Blood* **118,** 5767–73 (2011).
150. de Fost, M. *et al.* Superior effects of high-dose enzyme replacement therapy in type 1 Gaucher disease on bone marrow involvement and chitotriosidase levels: a 2-center retrospective analysis. *Blood* **108,** 830–5 (2006).
151. Pastores, G. M. *et al.* Therapeutic goals in the treatment of Gaucher disease. *Semin. Hematol.* **41,** 4–14 (2004).
152. Platt, F. M. *et al.* Inhibition of substrate synthesis as a strategy for glycolipid lysosomal storage disease therapy. *J. Inherit. Metab. Dis.* **24,** 275–90 (2001).
153. Aerts, J. M. F. G., Hollak, C. E. M., Boot, R. G., Groener, J. E. M. & Maas, M. Substrate reduction therapy of glycosphingolipid storage disorders. *J. Inherit. Metab. Dis.* **29,** 449–456 (2006).
154. Cox, T. *et al.* Novel oral treatment of Gaucher's disease with N-butyldeoxynojirimycin (OGT 918) to decrease substrate biosynthesis. *Lancet* **355,** 1481–1485 (2000).
155. Elstein, D. *et al.* Sustained therapeutic effects of oral miglustat (Zavesca, N-butyldeoxynojirimycin, OGT 918) in type I Gaucher disease. *J. Inherit. Metab. Dis.* **27,** 757–766 (2004).
156. Cox, T. M. *et al.* Eliglustat compared with imiglucerase in patients with Gaucher's disease type 1 stabilised on enzyme replacement therapy: a phase 3, randomised, open-label, non-inferiority trial. *Lancet* **385,** 2355–2362 (2015).
157. Mistry, P. K. *et al.* Effect of Oral Eliglustat on Splenomegaly in Patients With Gaucher Disease Type 1. *JAMA* **313,** 695 (2015).
158. Hughes, D. A. & Pastores, G. M. Eliglustat for Gaucher's disease: trippingly on the tongue. *Lancet* **385,** 2328–2330 (2015).
159. Overkleeft, H. S. *et al.* Generation of specific deoxynojirimycin-type inhibitors of the non-lysosomal glucosylceramidase. *J. Biol. Chem.* **273,** 26522–7 (1998).
160. Ghisaidoobe, A. T. *et al.* Identification and Development of Biphenyl Substituted Iminosugars as Improved Dual Glucosylceramide Synthase/Neutral Glucosylceramidase Inhibitors. *J. Med. Chem.* **57,** 9096–9104 (2014).
161. Boyd, R. E. *et al.* Pharmacological Chaperones as Therapeutics for Lysosomal Storage Diseases. *J. Med. Chem.* **56,** 2705–2725 (2013).
162. Fan, J.-Q. A contradictory treatment for lysosomal storage disorders: inhibitors enhance mutant enzyme activity. *Trends Pharmacol. Sci.* **24,** 355–60 (2003).
163. Brooks, D. A. Getting into the fold. *Nat. Chem. Biol.* **3,** 84–5 (2007).
164. Araki, K. & Nagata, K. Protein Folding and Quality Control in the ER. *Cold Spring Harb. Perspect. Biol.* **3,** a007526–a007526 (2011).
165. Benito, J. M., García Fernández, J. M. & Ortiz Mellet, C. Pharmacological chaperone therapy for Gaucher disease: a patent review. *Expert Opin. Ther. Pat.* **21,** 885–903 (2011).
166. Jung, O., Patnaik, S., Marugan, J., Sidransky, E. & Westbroek, W. Progress and potential of non-inhibitory small molecule chaperones for the treatment of Gaucher disease and its implications for Parkinson disease. *Expert Rev. Proteomics* **13,** 471–9 (2016).

167. Zechel, D. L. *et al.* Iminosugar Glycosidase Inhibitors: Structural and Thermodynamic Dissection of the Binding of Isofagomine and 1-Deoxynojirimycin to β-Glucosidases. *J. Am. Chem. Soc.* **125,** 14313–14323 (2003).
168. Chang, H.-H., Asano, N., Ishii, S., Ichikawa, Y. & Fan, J.-Q. Hydrophilic iminosugar active-site-specific chaperones increase residual glucocerebrosidase activity in fibroblasts from Gaucher patients. *FEBS J.* **273,** 4082–92 (2006).
169. Steet, R. A. *et al.* The iminosugar isofagomine increases the activity of N370S mutant acid beta-glucosidase in Gaucher fibroblasts by several mechanisms. *Proc. Natl. Acad. Sci. U. S. A.* **103,** 13813–8 (2006).
170. Yu, Z., Sawkar, A. R., Whalen, L. J., Wong, C.-H. & Kelly, J. W. Isofagomine- and 2,5-anhydro-2,5-imino-D-glucitol-based glucocerebrosidase pharmacological chaperones for Gaucher disease intervention. *J. Med. Chem.* **50,** 94–100 (2007).
171. Steet, R. *et al.* Selective action of the iminosugar isofagomine, a pharmacological chaperone for mutant forms of acid-beta-glucosidase. *Biochem. Pharmacol.* **73,** 1376–83 (2007).
172. Kornhaber, G. J. *et al.* Isofagomine Induced Stabilization of Glucocerebrosidase. *ChemBioChem* **9,** 2643–2649 (2008).
173. Tropak, M. B. *et al.* Identification of Pharmacological Chaperones for Gaucher Disease and Characterization of Their Effects on β-Glucocerebrosidase by Hydrogen/Deuterium Exchange Mass Spectrometry. *ChemBioChem* **9,** 2650–2662 (2008).
174. Lieberman, R. L., D'aquino, J. A., Ringe, D. & Petsko, G. A. Effects of pH and iminosugar pharmacological chaperones on lysosomal glycosidase structure and stability. *Biochemistry* **48,** 4816–27 (2009).
175. Khanna, R. *et al.* The pharmacological chaperone isofagomine increases the activity of the Gaucher disease L444P mutant form of beta-glucosidase. *FEBS J.* **277,** 1618–38 (2010).
176. Sun, Y. *et al.* Ex Vivo and in Vivo Effects of Isofagomine on Acid -Glucosidase Variants and Substrate Levels in Gaucher Disease. *J. Biol. Chem.* **287,** 4275–4287 (2012).
177. Maegawa, G. H. B. *et al.* Identification and Characterization of Ambroxol as an Enzyme Enhancement Agent for Gaucher Disease. *J. Biol. Chem.* **284,** 23502–23516 (2009).
178. Babajani, G., Tropak, M. B., Mahuran, D. J. & Kermode, A. R. Pharmacological chaperones facilitate the post-ER transport of recombinant N370S mutant β-glucocerebrosidase in plant cells: evidence that N370S is a folding mutant. *Mol. Genet. Metab.* **106,** 323–9 (2012).
179. Zimran, A., Altarescu, G. & Elstein, D. Pilot study using ambroxol as a pharmacological chaperone in type 1 Gaucher disease. *Blood Cells, Mol. Dis.* **50,** 134–137 (2013).
180. Bendikov-Bar, I., Maor, G., Filocamo, M. & Horowitz, M. Ambroxol as a pharmacological chaperone for mutant glucocerebrosidase. *Blood Cells. Mol. Dis.* **50,** 141–5 (2013).
181. Petersen, N. H. T. & Kirkegaard, T. HSP70 and lysosomal storage disorders: novel therapeutic opportunities. *Biochem. Soc. Trans.* **38,** 1479–1483 (2010).
182. Kalmar, B., Lu, C.-H. & Greensmith, L. The role of heat shock proteins in Amyotrophic Lateral Sclerosis: The therapeutic potential of Arimoclomol. *Pharmacol. Ther.* **141,** 40–54 (2014).
183. Biffi, A. Gene therapy for lysosomal storage disorders: a good start. *Hum. Mol. Genet.* **25,** R65–R75 (2016).
184. Correll, P. H. & Karlsson, S. Towards therapy of Gaucher's disease by gene transfer into hematopoietic cells. *Eur. J. Haematol.* **53,** 253–64 (1994).
185. Dahl, M. *et al.* Lentiviral gene therapy using cellular promoters cures type 1 Gaucher disease in mice. *Mol. Ther.* **23,** 835–844 (2015).
186. Maeder, M. L. & Gersbach, C. A. Genome-editing Technologies for Gene and Cell Therapy. *Mol. Ther.* **24,** 430–446 (2016).
187. Willemsen, R. *et al.* An immunoelectron microscopic study of glucocerebrosidase in type 1 Gaucher's disease spleen. *Ultrastruct. Pathol.* **12,** 471–8
188. Aerts, J. M. *et al.* Comparative study on glucocerebrosidase in spleens from patients with Gaucher disease. *Biochem. J.* **269,** 93–100 (1990).
189. Aerts, J. M. *et al.* A procedure for the rapid purification in high yield of human glucocerebrosidase using immunoaffinity chromatography with monoclonal antibodies. *Anal. Biochem.* **154,** 655–63 (1986).
190. Herrera Moro Chao, D. *et al.* Visualization of Active Glucocerebrosidase in Rodent Brain with High Spatial Resolution following In Situ Labeling with Fluorescent Activity Based Probes. *PLoS One* **10,** e0138107 (2015).
191. Marques, A. R. A. *et al.* A Specific Activity-Based Probe to Monitor Family GH59 Galactosylceramidase, the Enzyme Deficient in Krabbe Disease. *ChemBioChem* **18,** 402–412 (2017).
192. Willems, L. I. *et al.* Synthesis of α- and β-Galactopyranose-Configured Isomers of Cyclophellitol and Cyclophellitol Aziridine. *European J. Org. Chem.* **2014,** 6044–6056 (2014).
193. Jiang, J. *et al.* Comparing Cyclophellitol N-Alkyl and N-Acyl Cyclophellitol Aziridines as Activity-Based Glycosidase Probes. *Chemistry* **21,** 10861–10869 (2015).
194. Jiang, J. *et al.* In vitro and in vivo comparative and competitive activity-based protein profiling of GH29 α-l -fucosidases. *Chem. Sci.* **6,** 2782–2789 (2015).
195. Jiang, J. *et al.* Detection of Active Mammalian GH31 α-Glucosidases in Health and Disease Using In-Class, Broad-Spectrum Activity-Based Probes. *ACS Cent. Sci.* **2,** 351–358 (2016).
196. Chandrasekar, B. *et al.* Broad-range Glycosidase Activity Profiling. *Mol. Cell. Proteomics* **13,** 2787–2800 (2014).
197. Urano, Y. Novel live imaging techniques of cellular functions and in vivo tumors based on precise design of small molecule-based 'Activatable' fluorescence probes. *Curr. Opin. Chem. Biol.* **16,** 602–608 (2012).
198. Yadav, A. K. *et al.* Fluorescence-quenched substrates for live cell imaging of human glucocerebrosidase activity. *J. Am. Chem. Soc.* **137,** 1181–9 (2015).
199. Wennekes, T. *et al.* Development of adamantan-1-yl-methoxy-functionalized 1-deoxynojirimycin derivatives as selective inhibitors of glucosylceramide metabolism in man. *J. Org. Chem.* **72,** 1088–97 (2007).
200. Gold, H. *et al.* Quantification of Globotriaosylsphingosine in Plasma and Urine of Fabry Patients by Stable Isotope Ultraperformance Liquid Chromatography-Tandem Mass Spectrometry. *Clin. Chem.* **59,** 547–556 (2013).
201. Wisse, P. *et al.* Synthesis of a Panel of Carbon-13-Labelled (Glyco)Sphingolipids. *European J. Org. Chem.* **2015,** 2661–2677 (2015).
202. Haberkant, P. & Holthuis, J. C. M. Fat & fabulous: Bifunctional lipids in the spotlight. *Biochim. Biophys. Acta - Mol. Cell Biol. Lipids* **1841,** 1022–1030 (2014).
203. Haberkant, P. *et al.* Bifunctional Sphingosine for Cell-Based Analysis of Protein-

Sphingolipid Interactions. *ACS Chem. Biol.* **11,** 222–230 (2016).

204. Hehre, E. J. Glycosyl transfer: a history of the concept's development and view of its major contributions to biochemistry. *Carbohydr. Res.* **331,** 347–368 (2001).

205. Aguilera, B. Transglycosidase Activity of Chitotriosidase: IMPROVED ENZYMATIC ASSAY FOR THE HUMAN MACROPHAGE CHITINASE. *J. Biol. Chem.* **278,** 40911–40916 (2003).

206. Vanderjagt, D. J., Fry, D. E. & Glew, R. H. Human glucocerebrosidase catalyses transglucosylation between glucocerebroside and retinol. *Biochem. J.* **300,** 309–15 (1994).

207. Akiyama, H., Kobayashi, S., Hirabayashi, Y. & Murakami-Murofushi, K. Cholesterol glucosylation is catalyzed by transglucosylation reaction of β-glucosidase 1. *Biochem. Biophys. Res. Commun.* **441,** 838–43 (2013).

208. Nair, S. *et al.* Type II NKT-TFH cells against Gaucher lipids regulate B-cell immunity and inflammation. *Blood* **125,** 1256–71 (2015).

209. Salio, M. & Cerundolo, V. NKT-dependent B-cell activation in Gaucher disease. *Blood* **125,** 1200–2 (2015).

210. Liu, J. *et al.* Gaucher disease gene GBA functions in immune regulation. *Proc. Natl. Acad. Sci.* **109,** 10018–10023 (2012).

Thesis Outline

Thesis Outline

This thesis describes biochemical investigations on glucocerebrosidase (GBA), initially conducted at the premises of the Department of Medical Biochemistry at the Academic Medical Centre in Amsterdam and later performed at the Department of Medical Biochemistry at the Leiden Institute of Chemistry of the Leiden University. In parts of the studies use is made of novel chemical biology tools designed and synthesized at the Department of Bio-organic Synthesis at the Leiden Institute of Chemistry.

The central theme of this thesis is formed by biochemical studies on factors influencing the intralysosomal stability and survival of GBA. The steady-state GBA content of lysosomes determines the capacity of cells to degrade glucosylceramide, a reaction deficient in patients suffering from Gaucher disease (GD). The conducted investigations were aimed to increase knowledge about turnover of GBA molecules in lysosomes and to establish the feasibility of pharmacological augmentation of intralysosomal GBA degradative capacity.

Chapter 1 describes an investigation of the role of proteases in lysosomal GBA content. Building on the observation that leupeptin, a broad-specific protease inhibitor, reduces intralysosomal degradation of GBA, the nature of proteases involved in the process was analyzed in more detail. Making use of fluorescent activity-based probes directed against a number of lysosomal cysteine-proteins, the identity of cathepsins involved in proteolytic degradation of GBA was determined. An increase in functional GBA capacity in cultured lymphoblasts of GD patients with N370S enzyme was reached by inhibition of multiple cysteine cathepsins.

Chapter 2 presents an investigation of the effect of occupancy of the active site of GBA with glyco-mimetics. Permanent occupancy of the active site by covalent binding of β-glucoside configured cyclophellitols is shown to markedly stabilize GBA in its conformation and to provide protection against proteolytic degradation in cultured cells and mice.

Chapter 3 reports a new methodology to probe GBA using cyclophellitol-type activity-based probes and photoactivatable diazirine-functionalized clickable glucosylceramide (pacGlcCer). Labeling of GBA by fluorescent pacGlcCer is shown to occur with high affinity and to be prevented by prior labeling of enzyme with fluorescent β-glucopyranosyl-configured cyclophellitol. The GBA specific activity-based probe competes the binding of pacGlcCer to GBA. Cholesterol, a known lipid acceptor in transglucosylation by GBA also inhibits binding of pacGlcCer. The methodology might potentially be employed in screens for interactors with GBA.

Chapter 4 reports on the observed intralysosomal stabilization of GBA by its cellular transporter protein LIMP-2. Transient interactions of GBA with LIMP-2 in lysosomes seem to promote conformational stability of GBA and thus reduce proteolytic turnover of the enzyme. The potential implication for efficacy of high-dose enzyme replacement therapy is discussed.

Moreover, the findings suggest that treatment of AMRF patients with GBA enzyme replacement therapy is not a promising avenue.

Chapter 5 describes an investigation of LIMP-2 deficient mice with respect to abnormalities in lysosome composition, tissue GBA content and glycosphingolipid levels. Except for the absence of LIMP-2 and very marked reduction in GBA, no significant abnormalities in the proteome of isolated lysosomes of hepatocytes were identified. The tissue and cell-type specific differences in deficiency of GBA in LIMP-2 deficient mice are demonstrated, as revealed by measurement of enzymatic activity and detection of active enzyme molecules with activity-based probes. The cause for the exceptionally high residual GBA in LIMP-2 deficient white blood cells is experimentally investigated, rendering indications for re-uptake of faulty secreted GBA. An inventory of lipid abnormalities in the LIMP-2 deficient mice is also presented, revealing the successful prevention of glucosylceramide accumulation in tissues by its conversion to glucosylsphingosine.

Chapter 6 presents a review on biochemical adaptations developing during inherited primary deficiency of a glycosphingolipid-degrading lysosomal glycosidase. The active generation of glycosphingoid bases from accumulating glycosphingolipids by lysosomal acid ceramidase is described and the potential pathophysiological consequences of excessive glycosphingoid bases are discussed. In addition, the increased metabolism of glucosylceramide by the cytosolic β-glucosidase GBA2 during deficiency of lysosomal GBA activity is reviewed and the potential consequences of the related excessive formation of ceramide and glucosylated metabolites in the cytosol are considered.

Chapter 7 deals with the catalytic versatility of GBA. Next to hydrolyzing β-glucosides, the enzyme also cleaves β-xylosides, although with lower affinity. Moreover, GBA is able to act as a xylosyltransferase. Incubation of enzyme with 4-methylumbelliferyl-β-xyloside (4MU-β-Xyl) leads to formation of xyloslated cholesterol (XylChol) and dixylosylated sterol (Xyl$_2$Chol). Incubation of cultured cells with 4MU-β-Xyl also causes formation of XylChol and Xyl$_2$Chol, a reaction promoted by U18666A induced lysosomal cholesterol accumulation and being prevented by inactivation of GBA with conduritol B-epoxide.

The *Addendum* describes the multiplex quantitation of a series of glycosphingoid bases in plasma samples using ^{13}C encoded internal standards. It is further demonstrated that glycosphingolipids in the same sample can be quantified following microwave-assisted de-acylation to the corresponding bases.

The *Discussion* concludes the thesis and concerns the implications of the findings in view of recent literature and insights. Envisioned future directions of research are indicated.

The *Summary* presents an overview of the various studies presented in this thesis.

1

Augmentation of lysosomal glucocerebrosidase by the inhibition of its lysosomal proteolysis

Augmentation of lysosomal glucocerebrosidase by the inhibition of its lysosomal proteolysis

Based on

S.V. Oussoren[1], S. Hoogendoorn[2], M. Verdoes[3], S. Scheij[4], M. Verhoek[1], M. Artola[2], R.G. Boot[1], H.S. Overkleeft[2], J.M.F.G. Aerts[1]

[1]Dept. of Medical Biochemistry, LIC, Leiden University
[2]Dept. of Bio-Organic Synthesis, LIC, Leiden University
[3]Dept. of Tumor Immunology, RIMLS, Nijmegen
[4]Dept. of Medical Biochemistry, AMC, University of Amsterdam

Manuscript in preparation

Abstract

Patients suffering from the lysosomal storage disorder Gaucher disease (GD) have defects in lysosomal glucocerebrosidase (GBA) and consequently an impaired turnover of the glycosphingolipid glucosylceramide (GlcCer). GBA is known to be degraded by lysosomal cysteine cathepsins: the broad-specific inhibitors leupeptin and E64d protect lysosomal GBA in GD patient fibroblasts and lymphoblasts as revealed by labelling of enzyme with activity-based probes and enzymatic activity assays. Inhibition of the proteolytic GBA turnover might in principle offer a novel therapeutic avenue to increase lysosomal GBA levels. Indeed, we observed that the inhibition of multiple cysteine cathepsins with E64d in cultured GD lymphoblasts results in a reduction of glucosylsphingosine, the base formed from accumulating GlcCer. Thus, a functional correction in GBA capacity can be accomplished in this manner. We next studied the contribution of various cysteine proteases in the lysosomal breakdown of GBA using activity-based probes with an E64 scaffold and shRNA or CRISPR-Cas mediated reduction of specific cysteine cathepsins. The candidate proteases predominantly involved in lysosomal GBA breakdown were first narrowed down to cathepsins B, F and L. Deletion of each of these cathepsins was insufficient to significantly reduce the turnover of GBA in cultured cells. We therefore conclude that multiple cysteine cathepsins are able to degrade GBA in lysosomes and would need to be concomitantly inhibited to render the desired increase in lysosomal GBA level. Such approach is unattractive since it would lead to a broad interference in lysosomal turnover of proteins.

Introduction

Patients with Gaucher disease (GD) are deficient in the activity of glucocerebrosidase (GBA), a lysosomal β-glucosidase encoded by the *Gba* gene at locus 1q21[1–3]. Several hundred mutations have been identified in *Gba* of GD patients of which many cause single amino acid substitutions in the enzyme[4]. GBA is a 495-amino acid polypeptide with four N-linked glycans at Asn19, Asn59, Asn146 and Asn270[1]. Inside lysosomes, GBA degrades glucosylceramide (GlcCer), a crucial step in cellular glycosphingolipid turnover[5]. The degradation of GlcCer by GBA is assisted by saposin C, as indicated by the consequences of inherited defects in this activator protein[6]. Recently it has become clear that naturally occurring glucosylated cholesterol is also a physiological substrate for the enzyme[7]. All cells of GD patients have impaired GBA, but macrophages in patient tissues most prominently accumulate GlcCer[8–10]. The lipid-laden macrophages of GD patients (Gaucher cells) produce and secrete specific proteins[10,11]. Moreover, by the action of acid ceramidase GBA-deficient cells generate from accumulating GlcCer through de-acylation the water-soluble base glucosylsphingosine (GlcSph)[11]. Elevated plasma levels of GlcSph and Gaucher cell-derived chitotriosidase, CCL18, gpNMB and sCD136 are employed as biomarkers to monitor disease progression[12–17]. The clinical presentation of GD is remarkably heterogeneous, ranging from fatal symptoms in skin and brain early in life to a virtually asymptomatic course of disease[1]. The most common manifestation of GD among Caucasians does not involve the central nervous system (non-neuronopathic type 1 GD). Marked hepatosplenomegaly, thrombocytopenia and skeletal disease are characteristic symptoms of type 1 GD patients[1]. Hetero- and homo-allelic presence of mutant *Gba* coding for N370S GBA, the prevalent mutation among Caucasian GD patients, is associated with a non-neuronopathic type 1 course of disease[1,18,19].

Otherwise, *Gba* genotype – GD phenotype correlations are relatively poor, explicitly illustrated by the occurrence of phenotypically discordant monozygotic twins[20,21]. N370S GBA is almost normally folded in the endoplasmic reticulum and transported to lysosomes, but the mutant enzyme presents catalytic abnormalities and reduced stability[22,23]. Many of the other mutations in GBA observed in GD patients lead to defective folding and reduced transport to lysosomes[24]. One example in this respect is L444P GBA[25]. Only a small fraction of newly formed L444P enzyme is correctly folded and transported to lysosomes. Most L444P GBA molecules are destined for degradation in proteasomes. Homozygosity for L444P GBA is usually accompanied by a severe neuropathic disease, again with marked individual variability[1]. The 3D structure of the enzyme has been solved by X-ray diffraction crystal analysis, revealing a typical $(\beta/\alpha)_8$ TIM barrel catalytic core domain III, a three-strand antiparallel β-sheet flanked by a loop and a perpendicular strand (domain I) and an Ig-like fold formed by two β-sheets (domain II)[25,26]. *In silico* molecular modeling of the 3D structure does not render a reliable prediction of clinical severity of amino acid substitutions in GBA. Crystallography has confirmed earlier biochemical studies indicating that GBA is a retaining β-glucosidase, employing the double-displacement mechanism for catalysis in which Glu340 acts as nucleophile residue and Glu235 as acid/base residue[27,28]. As reaction intermediate the glucose of the substrate GlcCer becomes covalently linked to E340 and is released by subsequent

attack of a hydroxide. Based on this is the irreversible inhibition of GBA by conduritol B-epoxide and cyclophellitol that form permanent conjugates with Glu340[29]. Cyclophellitol scaffolds have been successfully used to design functionalized activity-based probes allowing in situ visualization of active GBA molecules[30,31].

The life cycle of GBA is fundamentally different from that of most other lysosomal hydrolases[10,19]. In general, lysosomal hydrolases are glycoproteins, acquiring in the Golgi apparatus mannose-6-phosphate recognition signals in their N-glycans, allowing binding to mannose-6-phosphate receptors and subsequent delivery to lysosomes. In sharp contrast to this, the glycans of GBA are predominantly complex-type and lack mannose-6-phosphate groups[32]. Newly formed GBA is transported to lysosomes through binding to the triple helical structure in the apical region of integral membrane protein LIMP-2 (lysosome integral membrane protein 2, encoded by the *Scarb2* gene) with trafficking information in its cytoplasmic tail[33]. The GBA-LIMP-2 complex reaches late endosomes/lysosomes where the enzyme dissociates at the local acid pH[34]. Defects in LIMP-2 cause major reductions in GBA in most cell types except mononuclear phagocytes, likely contributing to the different clinical picture of GD and action myoclonus renal failure syndrome (AMRF), due to LIMP-2 deficiency[35]. Trafficking of newly formed GBA from the ER to lysosomes takes relatively long and the half-life of GBA in lysosomes is only a few days, at least as observed in the cultured cells studied[36,37]. GBA does not undergo proteolytic processing but is subject to modification of its N-glycans by the action of lysosomal glycosidases[38].

Brady and colleagues developed so-called enzyme replacement therapy (ERT), an approach based on two-weekly intravenous administration of macrophage-targeted GBA[39]. ERT has proven to offer a very effective treatment for type 1 GD patients, resulting in impressive corrections in organomegaly and hematological abnormalities accompanied by corrections in biomarkers[40]. Presently several recombinantly produced GBA preparations are registered for ERT of type 1 GD[41,42]. Neurological manifestations in more severely affected GD patients are not prevented by ERT since the enzyme does not pass the blood-brain barrier[43]. More recently, substrate reduction therapy (SRT) has been developed as alternative treatment for type 1 GD[44]. Here, oral administration of an inhibitor of glucosylceramide synthase aims to reduce bodily GlcCer. Two inhibitors are registered for SRT of type 1 GD: *Miglustat* (N-butyldeoxynojirimycin) and lately the more potent *Eligustat* (*N*-[(1*R*,2*R*)-1-(2,3-Dihydro-1,4-benzodioxin-6-yl)-1-hydroxy-3-(1-pyrrolidinyl)-2-propanyl]octanamide). Both drugs have been reported to result in clinical benefit to type 1 GD patients[45,46]. Another approach actively pursued by academic researchers and pharmaceutical industry is based on small compound chaperones, assisting folding of mutant enzyme in the ER[47,48]. Theoretically, some chaperones might also promote structural stability of GBA inside the lysosome and thus reduce sensitivity for proteolytic degradation. Small compound therapies for GD are appealing since they might provide treatment of neuropathology in GD, an unmet clinical need. An impairment of GBA, even at the level of GD carriers, has been found to significantly increase the risk for development of alpha-synucleinopathies[49].
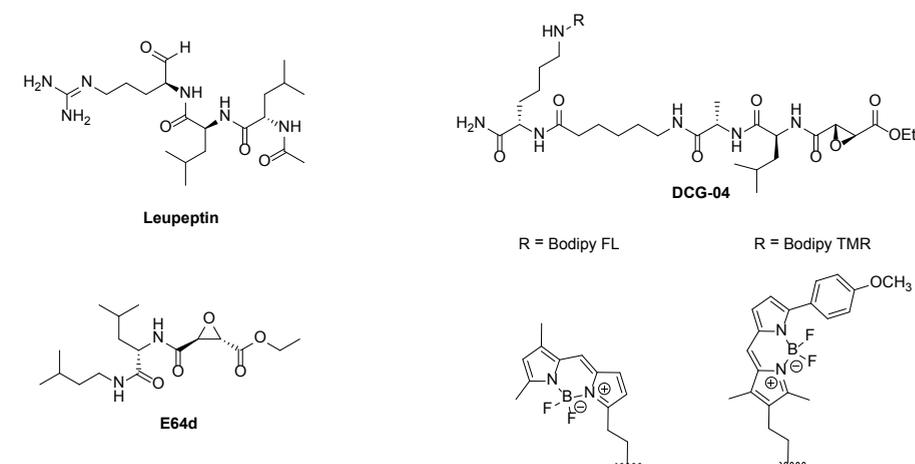
Scheme 1. Overview of the protease inhibitors used in this study. Top left: Leupeptin; reversible inhibitor of serine and cysteine proteases. Middle left: E64d; the cell-penetrable form of E64, irreversible inhibitor of cysteine proteases. Lower left: DCG-04; the activity based probe based on E64. Lower right: Bodipy FL and Bodipy TMR; fluorescent tags (R) of DCG-04. Upper right: reaction mechanism of E64d; cysteine protease alkylation.

GBA is degraded in lysosomes by proteases sensitive to inhibition by leupeptin (*N*-acetyl-L-leucyl-L-leucyl-L-argininal), a naturally occurring protease inhibitor produced by actinomycetes (see Scheme 1)[50]. In the eighties several researchers have reported that incubation of cultured cells with leupeptin results in increased levels of GBA as detected with specific antibodies[36,51]. Augmentation of lysosomal GBA by means of inhibition of lysosomal proteases has not actively been studied as therapeutic approach. Given its potential to increase intralysosomal GBA capacity, we revisited the protection of the enzyme by protease inhibitors. We first demonstrated that also E64d ((2*S*,3*S*)-trans-epoxysuccinyl-L-leucylamido-3-methylbutane ethyl ester; Scheme 1) protects GBA against proteolytic degradation and is able to functionally increase GBA capacity in GD lymphoblasts as reflected by a reduction in glucosylsphingosine. Next, we made use of activity-based probes (ABPs) with E64 as scaffold (DCG-04, Scheme 1)[52,53] to visualize the cysteine proteases potentially involved in GBA breakdown. Based on ABP labeling of cathepsins in fibroblasts and lymphoblasts the most

likely candidates for degrading GBA are cathepsins S, H, B, L and F. *In vitro* degradation of GBA with each of these cathepsins led to breakdown of GBA, although very little with cathepsins S and H. Next, we investigated the role of cathepsins B and F by their knock-out with CRISPR-Cas and that of cathepsin L by knock-down using shRNA. Reduction of neither of these cathepsins was sufficient to increase GBA in cultured cells. Apparently, multiple cathepsins may degrade GBA in lysosomes. The implications of these findings are discussed.

Results

Stabilization of GBA in fibroblasts exposed to leupeptin and E64d.
We first recapitulated the earlier findings by Jonsson et al. that GBA in cultured fibroblasts is protected against degradation by the presence of leupeptin, an inhibitor of serine and cysteine proteases[36]. For this, fibroblasts homozygous for wildtype and N370S GBA were cultured for 5 days in the presence of 20 µM leupeptin. The cell lysates were analyzed on GBA content by western blot, labeling of active GBA with ABP MDW933 (Figure S1) and enzyme activity measurement. All three methods showed stabilization of GBA (Figure 1), confirming earlier results[36].

Next, we investigated the effect of E64d, a more specific cysteine protease inhibitor. The same stabilizing effect on GBA, visualized with MDW933 labeling and western blot, was induced by the presence of E64d in the culture medium of fibroblasts homozygous for wildtype and N370S GBA as observed for leupeptin (see Figure 2A). An increased enzyme activity in cells treated with E64d was also noted (Figure 2B).
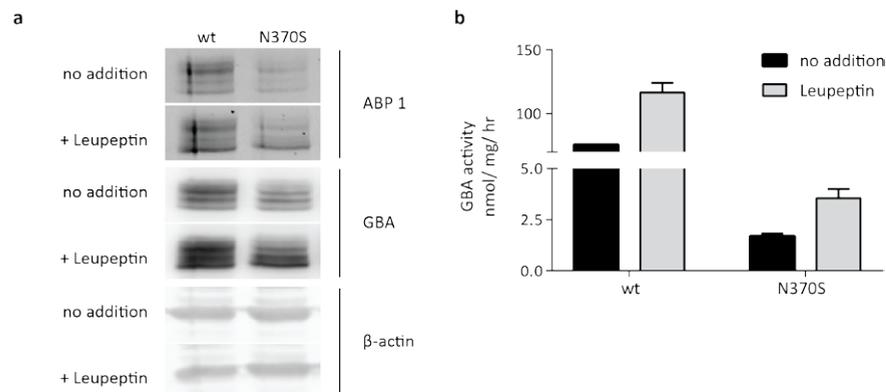

Figure 1. Increased GBA levels in cells cultured with leupeptin. Wildtype and homozygous N370S GBA GD fibroblasts were cultured with or without 20 µM leupeptin for 5 days. Medium supplemented with or without leupeptin was refreshed on a daily basis. **(a)** Fluorescent labeling of cell lysates with ABP 1 and subsequent western blotting with anti-GBA and anti-β-actin as described in Methods. **(b)** GBA activities measured in the same protein lysates with 4MU-β-D-Glc substrate as described in Methods.

The proteases targeted by E64 have earlier been determined by Greenbaum and colleagues. They synthesized the compound DCG-04 based on E64 as scaffold[52]. DCG-04 has a P2 leucine and was shown to target the same broad set of cysteine proteases as E64. The affinity tag of DCG-04 allowed purification of targeted proteases and their subsequent identification by proteomics. Among the identified proteases were the cathepsins C, S, F, H, K, V, B and L[53]. We tested the presence of these cathepsins in lysates of fibroblasts using fluorescent DCG-04 as ABP (see Figure 2). Based on apparent molecular weight, cathepsins B, F, H, L, and S were detectable with BODIPY DCG-04 (Figure 2c and d). Subsequently, BODIPY DCG-04 was administered to intact cells and gave rise to increases in GBA (as detected by enzyme activity) comparable to those observed with E64d (see Figure 2e).
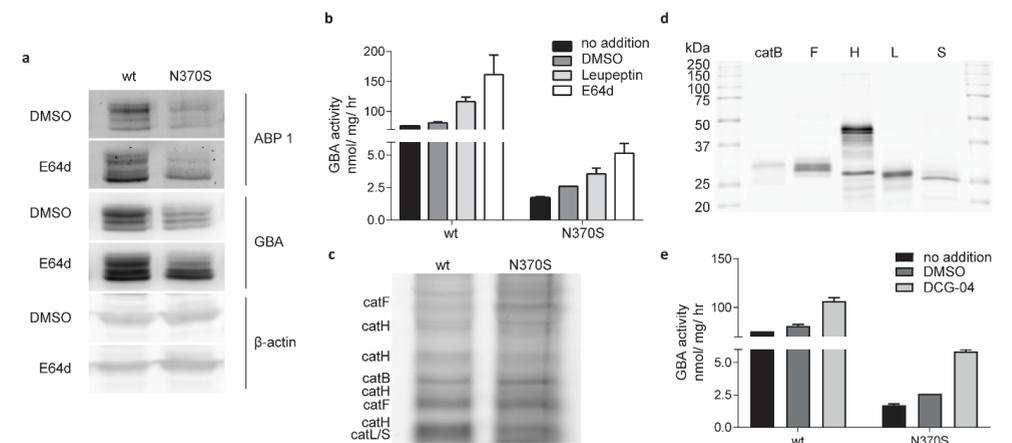

Figure 2. Increased GBA levels in cells cultured with E64d and BODIPY DCG-04. Wildtype and homozygous N370S Gaucher fibroblasts were cultured with or without 20 µM E64d or 10 µM BODIPY DCG-04 for 5 days. Medium supplemented with or without E64d or BODIPY DCG-04 was refreshed daily. **(a)** Fluorescent labeling of cell lysates with ABP 1 and subsequent western blotting with anti-GBA and anti-β-actin as described in Methods. **(b)** GBA activities measured in the same protein lysates with 4MU-β-D-Glc substrate as described in Methods. **(c)** Wildtype and N370S fibroblasts labeled with BODIPY DCG-04; cathepsins are indicated based on apparent molecular weight. **(d)** Fluorescent labeling of recombinant cathepsins with BODIPY DCG-04. **(e)** GBA activities measured with 4MU-β-D-Glc substrate in the same control and DMSO treated protein lysates as shown in **(b)**, now compared to cells treated with BODIPY DCG-04.

We subsequently investigated immortalized lymphoblasts of type 1 GD patients, each with at least one N370S *Gba* allele (N370S/N370S; N370S/R463 IVS10; N370S/X, uncharacterized mutation). The presence of E64d in the culture medium for 12 days led to increased active GBA as visualized with ABP ME569 (Figure 3a, 3b and S1). E64d treatment also resulted in

elevated GBA activity (Figure 3c and d). Finally, we determined glucosylsphingosine (GlcSph) in untreated and treated GD lymphoblasts (Figure 3 e and f). E64d treatment led to a decreased GlcSph content of GD lymphoblasts, demonstrating a functional correction in GBA capacity. The lymphoblasts showing the largest increase in GBA activity also showed the largest reduction in GlcSph.

Next, we investigated whether one specific cathepsin among the candidates B, F, H, L and S plays a major role in intralysosomal stability of GBA. The ability of commercial recombinant cathepsins to degrade GBA was determined (Figure 4). For this purpose, we looked into *in vitro* degradation of recombinant (60 kDa) GBA by equal quantities of commercial recombinant cathepsins at acid pH 5.0, mimicking the lysosomal environment. Cathepsin B, F and L generated GBA fragments when 30 ng cathepsin and 250 ng GBA was used (Figure 4).
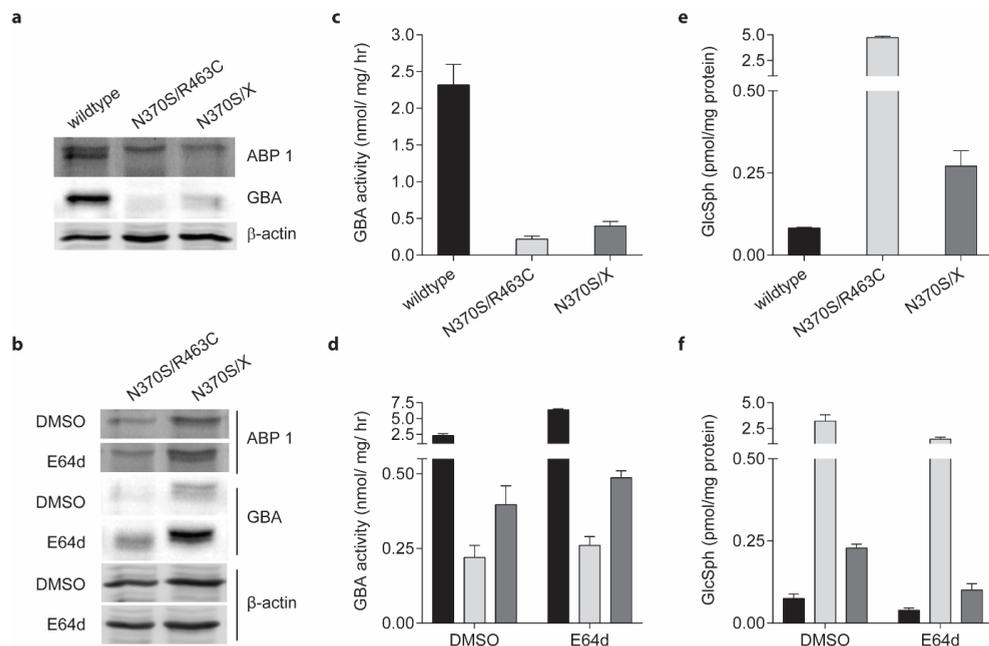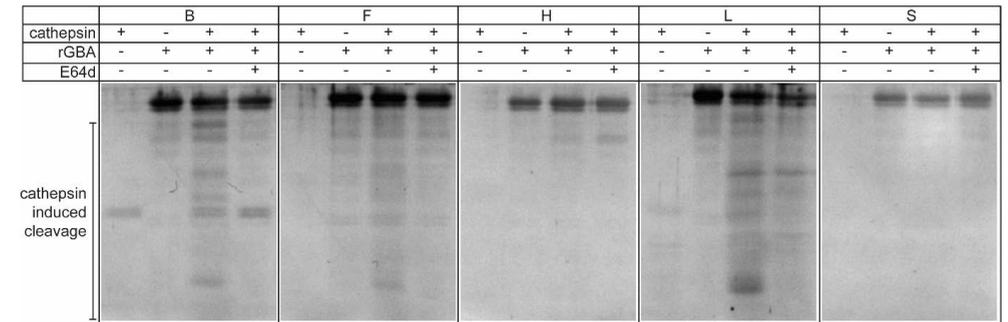

Figure 4. In vitro digestion of pure GBA by recombinant cathepsins. Silver staining of SDS-PAGE gels of recombinant human GBA (250 ng) digested *in vitro* by recombinant cathepsins (30 ng) at pH 5.0 for 1 hour.

Finally, we generated by CRISPR-Cas cells lacking cathepsin B and F. No effect on GBA as detected by ABP labeling or Western blotting was detected in the protease deficient cells (Figure 5a). The generation of cathepsin L-KO cells by CRISPR-Cas was not successful. Therefore, a knockdown in cathepsin L was generated using shRNA (Figure 5b). A major reduction in cathepsin L was obtained, however without effect on cellular GBA level as detected with ABP or Western blotting. Unfortunately, there are no truly specific inhibitors of various cathepsins commercially available to further validate the findings.
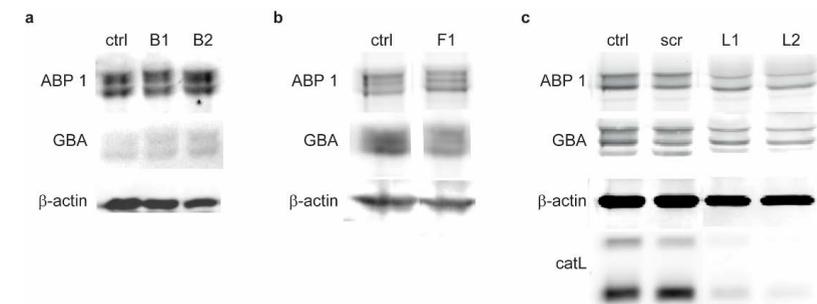
Figure 5. Impact of reduction of cathepsins B, F and L on cellular GBA. (a), (b) A knock-out of cathepsin B and cathepsin F was generated in HEK293T cells by CRISPR-Cas as described in M&M. Cellular GBA was analyzed by ABP labeling and Western blotting with anti-GBA antibody. B1, B2 and F1: CRISPR-Cas clones of cathepsin B and F. **(c)** Knock-downs of cahepsin L were generated in fibroblast cells using a specific shRNA. Reduction of cathepsin L was determined by Western blotting. Cellular GBA was analyzed by ABP labeling and Western blotting with anti-GBA antibody. Ctrl: untransduced cells, scr: cells transduced with unspecific scrambled shRNA, L1 and L2: generated catL knockdowns 1 and 2.

Figure 3. Cathepsin inhibition in lymphoblast cell lines. (a) Active GBA labeling with Cy5 tagged GBA-ABP ME569 in lysates of wildtype and GD lymphoblasts (upper panel), western blotting of GBA (middle panel) and β-actin loading control. **(b)** Idem to (a), except for cells being prior treated with E64d for 12 days. **(c)** GBA activity in wildtype and GD lymphoblasts measured by 4MU assay; **(d)** Idem to (c), except for cells treated with E64d for 12 days. **(e)** Glucosylsphingosine (GlcSph) in GD lymphoblasts. **(f)** GlcSph levels in same GD lymphoblasts treated for 12 days with E64d.

Discussion

There remains a need for alternative treatments of GD for a variety of reasons. Firstly, the existing ERT fails to prevent neurological manifestations due to poor brain penetrance of the therapeutic enzyme and moreover it is extremely costly and therefore not always accessible. Present substrate reduction therapies are neither able to prevent neuropathology in GD patients. Another need for improving GBA capacity stems from the recent realization that carriers of mutant GBA have a 30-fold increased risk for developing Parkinson disease. Thus, the lysosomal GBA capacity appears to be critical for normal functioning of neuronal cells, in particular motor neurons[54]. It is known that the lysosomal breakdown of GBA is mediated by cysteine and/or serine cathepsins inhibited by leupeptin and is abnormally fast in the case of the common mutant N370S GBA. Of note, cathepsins are found to be increased in plasma as well as tissues of GD patients[55,56]. We therefore set out to identify which cathepsins are involved in the turnover of GBA with the aim to assess whether it is feasible to significantly increase the half-life of (mutant) GBA in lysosomes by the specific inhibition of one particular cathepsin (see Scheme 2).

Our investigation first revealed that the protective effect on GBA exerted by leupeptin is also observed with E64d and the structurally related DCG-04, inhibitors of multiple cysteine cathepsins, but not serine proteases. E64d and DCG-04 treatment both lead to the desired functional increase of GBA capacity in cultured GD lymphoblasts as reflected by reduction of glucosylsphingosine, the base formed from accumulating GlcCer in lysosomes. Using fluorescent activity-based DCG-04 probes, we next narrowed down the cysteine cathepsins likely involved in lysosomal GBA turnover to the cathepsin B, F, L, H and S. Based on the observed ability of each of these five proteases to digest *in vitro* GBA, the cathepsins B, F and L were considered as prime candidates to mediate lysosomal turnover of GBA. Knockout of cathepsins B and F did not significantly reduce the turnover of GBA in cultured cells. Neither did knockdown of cathepsin L. We therefore conclude that multiple cysteine cathepsins, most likely combinations of cathepsins B, F and L, are able to degrade GBA in lysosomes.

Analysis	Candidate protease
Protective effect leupeptin	Serine and cysteine proteases
Protective effect E64d and DCG-04	Cathepsins B, C, F, H, K, L and S
Presence in lysosomes of fibroblasts and lymphoblasts	Cathepsins B, F, H, L and S
Knock-out/down of Cathepsin B, F and L	Combination of at least two of cathepsins B, F and L

Scheme 2. Candidate proteases involved in lysosomal GBA turnover.

Our findings suggest that in order to increase the half-life of GBA in lysosomes one would need to concomitantly inhibit multiple cysteine cathepsins. Such approach is unattractive for various reasons. Cathepsin F has been reported to influence LIMP-2, the transporter of newly formed GBA to lysosomes[57]. Moreover, cathepsin F deficiency causes Kufs disease type B, characterized by dementia and motor deficits[58]. Cathepsin L is highly expressed in neurons of the cerebral cortex and in Purkinje cells of the cerebellum. It is considered to exert a protective effect, as for example observed in cathepsin B deficient mice that develop lethal hypotrophy and motility defects in the absence of cathepsin L[59]. In conclusion, our study did not reveal a single cathepsin as target to pharmacologically modulate the half-life of GBA in lysosomes and thus boost GBA activity.

Materials & Methods

Materials.

All chemicals used were research grade and obtained from Sigma-Aldrich if not indicated differently. The GBA ABP, MDW933 (cyclophellitol, BODIPY FL)[30] as well as BODIPY TMR and Cy5 DCG-04, the ABP for cysteine proteases[53,60] were synthesized at the Leiden Institute of Chemistry as described previously. For synthesis of GBA ABP ME569 (cyclophellitol, Cy5) see methods. Recombinant human GBA (Cerezyme[TM]) was a gift from Sanofi-Genzyme (Cambridge, MA, USA). Recombinant cathepsin B and S were purchased at EMD Millipore, cathepsin H was from R&D Systems and cathepsins F and L were from Enzo Life Sciences. The fluorogenic substrate 4-methylumbelliferyl-β-glucose was from Glycosynth (Warrington, UK). A SpeedVac Eppendorf concentrator Plus was used during lipid extractions. The antibody for cathepsin L was purchased at Sigma-Aldrich, antibodies for β-actin and GAPDH were from Cell Signaling.

Methods.

Cell culture.

Skin fibroblasts and lymphoblasts of GD patients and controls were obtained after consent and diagnosis was confirmed by genotyping. Lymphoblasts were generated as follows. Leukocytes from healthy donors and from GD patients were isolated by sedimentation on Ficoll-Hypaque density gradients. Mononuclear cells were resuspended in RPMI 1640 medium containing 10% fetal calf serum and EBV viral supernatants (10^7 mononuclear cells/ml) and incubated for 2 h at 37 °C. Cultures were maintained in 25 cm^2 tissue culture flask for 3 weeks containing 1 μg/mL cyclosporin A. The cells were washed twice with PBS and then cultured in IMDM medium containing 10 % fetal calf serum and 5 % Pen/Strep (Life Technologies). Fibroblasts were cultured in Dulbecco's modified Eagle's medium (DMEM) F12 supplemented with 10 % fetal calf serum, 2 mM L-glutamine and 1 % Pen/Strep (Sigma Aldrich). Fibroblasts were cultured for 5 days and lymphoblasts for 12 days with or without 20 μM leupeptin or

E64d. E64d is the cell permeable variant of E64. Medium and inhibitors were refreshed daily for fibroblasts and every other day for lymphoblasts. DMSO levels were kept constant between different conditions. Cell lysates were made in K_2HPO_4 - KH_2PO_4 buffer pH 6.5 with 0.1 % Triton X-100.

Lentiviral knockdown and CRISPR knockouts.
Wildtype fibroblast cells transduced with scrambled were infected with non-target shRNA TRC 002. Fibroblast knockdowns of cathepsin L (L1 & L2) were obtained by infection with shRNA TRC 677. CRISPR cathepsin B knockouts were obtained by transfection of HEK293T cells with wildtype cas9 and guideRNA tcaacaaacggaataccac**gtgg** (the PAM site indicated in bold). Primers gatcccatagacacctcagctc, tttcaacagtccaggacaatgtt, gacccacataacagagaggtgtc and ccgacatgactcagggtcagg were used for PCR of relevant genomic cathepsin B fragments. CRISPR cathepsin B clone 1 (B1) was found to contain a 10bp deletion and a 113bp deletion. No other mutations were found, but judging by the frequency with which the 10bp deletion was found, it was concluded that two out of three alleles must have this mutation. Cathepsin B clone 2 (B2) was found to have an allele with a 351 bp deletion, another allele with a 107bp insertion and a third allele with the same 10bp deletion as clone 1. A CRISPR cathepsin F knockout (F1) was obtained by transfection of HEK293T cells with wildtype cas9 and guideRNA tgtgcgcggccgcgtccgcc**ggg**. Primers ccattccccatcaccagagatc and acctacttcagagattgctacgc were used for PCR of cathepsin F fragments. The CRISPR clone for cathepsin F contained a 50bp deletion. No other mutations, nor wildtype sequence were found, so it was assumed that all alleles contained this deletion.

GBA activity measurement.
Activity of GBA was measured with 4-methylumbellifryl-β-glucoside as substrate in McIlvaine buffer (pH 5.2) containing 0.1 % (v/v) Triton X-100 and 0.2 % (w/v) taurocholate at 37 °C as described earlier[61]. Briefly, protein lysates were incubated with substrate for 30 minutes at 37 °C, after which the reaction was stopped with NaOH-glycine (pH 10.3), and fluorescence was measured with a fluorimeter LS55 (Perkin-Elmer, Beaconsfield, UK) at λ_{ex} 366 nm and λ_{ex} 445 nm.

Protein determination.
For quantification of protein the Pierce™ BCA Protein Assay Kit (Pierce Biotechnology Inc., No. 23225), was used according to the manufacturer's protocol.

Labeling of cathepsins with fluorescent DCG-04 probe.
Equal amounts of protein in cell lysates were incubated in 50 mM MES buffer (50 mM MES, 50 mM NaCl, 5 mM DTT, 0.0125 % (w/v) digitonin, pH 5.5 with 1 µM BODIPY TMR or Cy5 DCG-04 for 60 minutes at 37 °C. Of recombinant cathepsins 1 µg protein was labeled with 1 µM Cy5 DCG-04 for the same duration at 37 °C.

Labeling of GBA with GBA ABPs
Equal amounts of protein were incubated with 100 nM MDW933 (BODIPY FL) or ME569 (Cy5) for GBA in McIlvaine buffer (pH 5,2) containing 0.1 % triton X-100 as well as 0.2 % taurocholate for 30 minutes at 37 °C.

Gel electrophoresis, fluorescence scanning and Western blotting.
Equal amounts of protein were denatured with 5× Laemmli buffer (50 % (v/v) 1 M Tris-HCl, pH 6.8, 50 % (v/v) 100 % glycerol, 8 % (w/v) DTT, 10 % (w/v) SDS, 0.01 % (w/v) bromophenol blue), boiled for 5 minutes at 100 °C and electrophoresed on a 10 % (w/v) SDS-PAGE gel running at 75 V for 30 minutes and afterwards at 150 V. Wet slab-gels were scanned on fluorescence with a Typhoon Variable Mode Imager (Amersham Biosciences) using λ_{EX} 488 nm and λ_{EM} 520 nm (band pass filter 40 nm) for green fluorescent ABP 1 and λ_{EX} 635 nm and λ_{EM} 670 nM (band pass filter 30 nm) for Cy5 labeled GBA ABP. After fluorescence scanning, semi-dry blotting was performed and antigens on blot were visualized by incubation with antibodies as described earlier[30]. Monoclonal anti-human GBA antibody 8E4 was produced by hybridoma cells as described previously[62]. Scanning of blots was carried out with a Fujifilm LAS-4000 Imager (GE Healthcare Bio-Sciences, Uppsala, Sweden) for ECL and Cy5 fluorescence.

In vitro digestion of recombinant human GBA with recombinant cathepsins.
Recombinant human GBA (Cerezyme™, 250 ng) was incubated with 30 ng recombinant cathepsin B, F, H, L or S in 20 mM MES buffer pH 5.0 containing 150 mM NaCl, 1 mM DTT and 250 mM EDTA. A 40 mM DMSO stock of E64d was diluted into MES buffer to come to a final concentration of 50 µM in the incubation mixture. Cathepsin alone, GBA alone, GBA with cathepsin, or GBA with cathepsin and E64d was incubated at 37 °C for 60 minutes. Subsequently 5x Laemmli buffer was added, samples were boiled and run on a 12.5 % SDS-page gel after which silver staining was performed using the SilverQuest™ Staining Kit from Invitrogen (Carlsbad CA, USA).

Lipid measurements by UPLC-ESI-MS/MS procedures.
GlcSph was determined as described earlier[63,64]. An internal standard mix ($^{13}C_5$-Sph and $^{13}C_5$-GlcSph) was added for quantification of the glycosphingoid bases. Briefly, after protein precipitation with $CHCl_3$:MeOH 1:1 (v:v), lipid extraction was performed at the ratio $CHCl_3$:MeOH:H_2O 1:1:0.9 (v:v:v). GlcSph is recovered in the upper phase. The upper phase was dried under N_2 gas stream and the pellet re-dissolved in solution A (10 mM ammonium formate in MeOH). Lipids were measured by UPLC-ESI-MS/MS with an Acquity TQD (Waters Inc.).

Synthesis of ME569 (cyclophellitol Cy5)
Cyclophellitol Cy5 ME569 was synthesized by copper–catalyzed click chemistry of azidocyclophellitol with Cy5 alkyne.

Cyclophellitol Cy5 ME569: Azidocyclophellitol[65] (24.2 mg, 0.12 mmol) and the desired Cy5-alkyne (84 mg, 0.15 mmol) were dissolved in BuOH/toluene/H_2O (6 mL, 1:1:1, v/v/v). $CuSO_4$ (0.024 mL, 1 M in H_2O) and sodium ascorbate (0.024 mL, 1 M in H_2O) were added and the reaction mixture was heated at 80 ºC for 18 h. Then, the solution was diluted with CH_2Cl_2, washed with H_2O, dried over $MgSO_4$ and concentrated under reduced pressure. The crude was purified by silica gel column chromatography (CH_2Cl_2 to CH_2Cl_2/MeOH 9:1), subsequently purified by semipreparative reversed-phase HPLC (linear gradient: 45 to 48% B in A, 12 min, solutions used A: 50 mM NH_4HCO_3 in H_2O, B: MeCN) and lyophilized to yield cyclophellitol ME569 as a blue powder (33.5 mg, 44 μmol, 37%). ^1H NMR (400 MHz, CD_3OD): δ 8.25 (t, J = 13.1 Hz, 2H), 7.91 (d, J = 3.3 Hz, 1H), 7.49 (d, J = 7.4 Hz, 2H), 7.44 − 7.39 (m, 2H), 7.31 − 7.24 (m, 4H), 6.63 (t, J = 12.4 Hz, 1H), 6.29 (d, J = 13.8 Hz, 2H), 4.81 (dd, J = 13.9, 3.8 Hz, 1H), 4.61 (dd, J = 13.9, 8.6 Hz, 1H), 4.42 (s, 2H), 4.09 (t, J = 7.4 Hz, 2H), 3.63 (s, 3H), 3.60 (d, J = 8.0 Hz, 1H), 3.24 − 3.20 (m, 1H), 3.12 (t, J = 14.9 Hz, 1H), 3.02 − 3.00 (m, 1H), 2.41 − 2.35 (m, 1H), 2.25 (t, J = 7.3 Hz, 2H), 1.91 (s, 6H), 1.85 − 1.78 (m, 2H), 1.72 (s, 12H), 1.50 − 1.43 (m, 2H) ppm; ^{13}C NMR (101 MHz, CD_3OD): δ 175.8, 175.4, 174.6, 155.5, 155.5, 146.2, 144.2, 143.5, 142.6, 142.5, 129.8, 129.7, 126.7, 126.2, 126.2, 125.2, 123.4, 123.3, 112.0, 111.8, 104.5, 104.3, 78.2, 72.5, 68.6, 57.6, 55.5, 50.8, 50.5, 50.5, 44.8, 44.6, 36.5, 35.6, 31.6, 28.1, 28.0, 27.3, 26.4 ppm; HRMS: calcd. for $C_{42}H_{53}N_6O_5$ [M]$^+$ 721,4072, found: 721.4070.

References

1. E. Beutler, G. A. G. in *C.R. Scriver,W.S. Sly, D. Valle (Eds.), The Metabolic and Molecular Bases of Inherited Disease, 8th ed.* 3635–3668 (McGraw-Hill, New York, 2001).
2. Brady, R. O., Kanfer, J. N., Bradley, R. M. & Shapiro, D. Demonstration of a deficiency of glucocerebroside-cleaving enzyme in Gaucher's disease. *J. Clin. Invest.* **45,** 1112–1115 (1966).
3. Patrick, A. A deficiency of glucocerebrosidase in Gaucher's disease. *Biochem J.* **97,** 17C–18C (1965).
4. Hruska, K. S., LaMarca, M. E., Scott, C. R. & Sidransky, E. Gaucher disease: mutation and polymorphism spectrum in the glucocerebrosidase gene (GBA). *Hum. Mutat.* **29,** 567–583 (2008).
5. Kolter, T. & Sandhoff, K. Lysosomal degradation of membrane lipids. *FEBS Lett.* **584,** 1700–1712 (2010).
6. Vaccaro, A. M. *et al.* Saposin C mutations in Gaucher disease patients resulting in lysosomal lipid accumulation, saposin C deficiency, but normal prosaposin processing and sorting. *Hum. Mol. Genet.* **19,** 2987–2997 (2010).
7. Marques, A. R. A. *et al.* Glucosylated cholesterol in mammalian cells and tissues: formation and degradation by multiple cellular β-glucosidases. *J. Lipid Res.* **57,** 451–463 (2016).
8. Bussink, A. P., van Eijk, M., Renkema, G. H., Aerts, J. M. & Boot, R. G. The biology of the Gaucher cell: the cradle of human chitinases. *Int. Rev. Cytol.* **252,** 71–128 (2006).
9. Boven, L. A. *et al.* Gaucher cells demonstrate a distinct macrophage phenotype and resemble alternatively activated macrophages. *Am. J. Clin. Pathol.* **122,** 359–69 (2004).
10. Ferraz, M. J. *et al.* Gaucher disease and Fabry disease: New markers and insights in pathophysiology for two distinct glycosphingolipidoses. *Biochim. Biophys. Acta - Mol. Cell Biol. Lipids* **1841,** 811–825 (2014).
11. Ferraz, M. J. *et al.* Lysosomal glycosphingolipid catabolism by acid ceramidase: formation of glycosphingoid bases during deficiency of glycosidases. *FEBS Lett.* **590,** 716–725 (2016).
12. Dekker, N. *et al.* Elevated plasma glucosylsphingosine in Gaucher disease: relation to phenotype, storage cell markers, and therapeutic response. *Blood* **118,** e118–e127 (2011).
13. Boot, R. G. *et al.* Marked elevation of the chemokine CCL18/PARC in Gaucher disease: a novel surrogate marker for assessing therapeutic intervention. *Blood* **103,** 33–9 (2004).
14. Kramer, G. *et al.* Elevation of glycoprotein nonmetastatic melanoma protein B in type 1 Gaucher disease patients and mouse models. *FEBS Open Bio* **6,** 902–913 (2016).
15. van Dussen, L. *et al.* Value of plasma chitotriosidase to assess non-neuronopathic Gaucher disease severity and progression in the era of enzyme replacement therapy. *J. Inherit. Metab. Dis.* **37,** 991–1001 (2014).
16. Schoonhoven, A. *et al.* Monitoring of Gaucher patients with a novel chitotriosidase assay. *Clin. Chim. Acta.* **381,** 136–9 (2007).
17. Møller, H. J. *et al.* Soluble CD163: a marker molecule for monocyte/macrophage activity in disease. *Scand. J. Clin. Lab. Invest. Suppl.* **237,** 29–33 (2002).
18. Boot, R. G. *et al.* Glucocerebrosidase genotype of Gaucher patients in The Netherlands: limitations in prognostic value. *Hum. Mutat.* **10,** 348–58 (1997).
19. Aerts, J. M., Hollak, C., Boot, R. & Groener, A. Biochemistry of glycosphingolipid storage disorders: implications for therapeutic intervention. *Philos. Trans. R. Soc. Lond. B. Biol. Sci.* **358,** 905–14 (2003).
20. Biegstraaten, M. *et al.* A monozygotic twin pair with highly discordant Gaucher phenotypes. *Blood Cells. Mol. Dis.* **46,** 39–41 (2011).
21. Lachmann, R. H., Grant, I. R., Halsall, D. & Cox, T. M. Twin pairs showing discordance of phenotype in adult Gaucher's disease. *QJM* **97,** 199–204 (2004).
22. Ohashi, T. *et al.* Characterization of human glucocerebrosidase from different mutant alleles. *J. Biol. Chem.* **266,** 3661–7 (1991).
23. van Weely, S. *et al.* Role of pH in determining the cell-type-specific residual activity of glucocerebrosidase in type 1 Gaucher disease. *J. Clin. Invest.* **91,** 1167–75 (1993).
24. Schmitz, M., Alfalah, M., Aerts, J. M. F. G., Naim, H. Y. & Zimmer, K.-P. Impaired trafficking of mutants of lysosomal glucocerebrosidase in Gaucher's disease. *Int. J. Biochem. Cell Biol.* **37,** 2310–20 (2005).
25. Dvir, H. *et al.* X-ray structure of human acid-β-glucosidase, the defective enzyme in Gaucher disease. *EMBO Rep.* **4,** 704–709 (2003).
26. Brumshtein, B. *et al.* Cyclodextrin-mediated crystallization of acid β-glucosidase in complex with amphiphilic bicyclic nojirimycin analogues. *Org. Biomol. Chem.* **9,** 4160 (2011).
27. Rempel, B. P. & Withers, S. G. Covalent inhibitors of glycosidases and their applications in biochemistry and biology. *Glycobiology* **18,** 570–586 (2008).
28. Kallemeijn, W. W. *et al.* A Sensitive Gel-based Method Combining Distinct Cyclophellitol-based Probes for the Identification of Acid/Base Residues in Human Retaining -Glucosidases. *J. Biol. Chem.* **289,** 35351–35362 (2014).

29. Witte, M. D., van der Marel, G. a, Aerts, J. M. F. G. & Overkleeft, H. S. Irreversible inhibitors and activity-based probes as research tools in chemical glycobiology. *Org. Biomol. Chem.* **9,** 5908–5926 (2011).

30. Witte, M. D. *et al.* Ultrasensitive in situ visualization of active glucocerebrosidase molecules. *Nat. Chem. Biol.* **6,** 907–913 (2010).

31. Kallemeijn, W. W. *et al.* Novel activity-based probes for broad-spectrum profiling of retaining β-exoglucosidases in situ and in vivo. *Angew. Chemie - Int. Ed.* **51,** 12529–12533 (2012).

32. Aerts, J. M. *et al.* Glucocerebrosidase, a lysosomal enzyme that does not undergo oligosaccharide phosphorylation. *Biochim. Biophys. Acta* **964,** 303–8 (1988).

33. Reczek, D. *et al.* LIMP-2 Is a Receptor for Lysosomal Mannose-6-Phosphate-Independent Targeting of β-Glucocerebrosidase. *Cell* **131,** 770–783 (2007).

34. Rothaug, M. *et al.* LIMP-2 expression is critical for -glucocerebrosidase activity and -synuclein clearance. *Proc. Natl. Acad. Sci.* **111,** 15573–15578 (2014).

35. Gaspar, P. *et al.* Action myoclonus-renal failure syndrome: diagnostic applications of activity-based probes and lipid analysis. *J. Lipid Res.* **55,** 138–145 (2014).

36. Jonsson, L. M. V *et al.* Biosynthesis and maturation of glucocerebrosidase in Gaucher fibroblasts. *Eur. J. Biochem.* **164,** 171–179 (1987).

37. Aerts, J. M. *et al.* Comparative study on glucocerebrosidase in spleens from patients with Gaucher disease. *Biochem. J.* **269,** 93–100 (1990).

38. Van Weely, S. *et al.* Function of oligosaccharide modification in glucocerebrosidase, a membrane-associated lysosomal hydrolase. *Eur. J. Biochem.* **191,** 669–77 (1990).

39. Barton, N. W. *et al.* Replacement therapy for inherited enzyme deficiency--macrophage-targeted glucocerebrosidase for Gaucher's disease. *N. Engl. J. Med.* **324,** 1464–70 (1991).

40. Smid, B. E. *et al.* Biochemical response to substrate reduction therapy versus enzyme replacement therapy in Gaucher disease type 1 patients. *Orphanet J. Rare Dis.* **11,** 28 (2016).

41. Aerts, J. M. F. G., Yasothan, U. & Kirkpatrick, P. Velaglucerase alfa. *Nat. Rev. Drug Discov.* **9,** 837–8 (2010).

42. Zimran, A. *et al.* Pivotal trial with plant cell-expressed recombinant glucocerebrosidase, taliglucerase alfa, a novel enzyme replacement therapy for Gaucher disease. *Blood* **118,** 5767–73 (2011).

43. Desnick, R. J. & Schuchman, E. H. Enzyme Replacement Therapy for Lysosomal Diseases: Lessons from 20 Years of Experience and Remaining Challenges. *Annu. Rev. Genomics Hum. Genet.* **13,** 307–335 (2012).

44. Platt, F. M. *et al.* Inhibition of substrate synthesis as a strategy for glycolipid lysosomal storage disease therapy. *J. Inherit. Metab. Dis.* **24,** 275–90 (2001).

45. Cox, T. *et al.* Novel oral treatment of Gaucher's disease with N-butyldeoxynojirimycin (OGT 918) to decrease substrate biosynthesis. *Lancet* **355,** 1481–1485 (2000).

46. Cox, T. M. *et al.* Eliglustat compared with imiglucerase in patients with Gaucher's disease type 1 stabilised on enzyme replacement therapy: a phase 3, randomised, open-label, non-inferiority trial. *Lancet* **385,** 2355–2362 (2015).

47. Steet, R. *et al.* Selective action of the iminosugar isofagomine, a pharmacological chaperone for mutant forms of acid-beta-glucosidase. *Biochem. Pharmacol.* **73,** 1376–83 (2007).

48. Benito, J. M., García Fernández, J. M. & Ortiz Mellet, C. Pharmacological chaperone therapy for Gaucher disease: a patent review. *Expert Opin. Ther. Pat.* **21,** 885–903 (2011).

49. Siebert, M., Sidransky, E. & Westbroek, W. Glucocerebrosidase is shaking up the synucleinopathies. *Brain* **137,** 1304–1322 (2014).

50. Hozumi, M., Ogawa, M., Sugimura, T., Takeuchi, T. & Umezawa, H. Inhibition of tumorigenesis in mouse skin by leupeptin, a protease inhibitor from Actinomycetes. *Cancer Res.* **32,** 1725–8 (1972).

51. Sun, Y., Qi, X. & Grabowski, G. A. Saposin C is required for normal resistance of acid beta-glucosidase to proteolytic degradation. *J. Biol. Chem.* **278,** 31918–23 (2003).

52. Greenbaum, D., Medzihradszky, K. F., Burlingame, A. & Bogyo, M. Epoxide electrophiles as activity-dependent cysteine protease profiling and discovery tools. *Chem. Biol.* **7,** 569–581 (2000).

53. Greenbaum, D. *et al.* Chemical approaches for functionally probing the proteome. *Mol. Cell. Proteomics* **1,** 60–8 (2002).

54. Aflaki, E., Westbroek, W. & Sidransky, E. The Complicated Relationship between Gaucher Disease and Parkinsonism: Insights from a Rare Disease. *Neuron* **93,** 737–746 (2017).

55. Moran, M. T. *et al.* Pathologic gene expression in Gaucher disease: up-regulation of cysteine proteinases including osteoclastic cathepsin K. *Blood* **96,** 1969–1978 (2000).

56. Vitner, E. B. *et al.* Altered expression and distribution of cathepsins in neuronopathic forms of Gaucher disease and in other sphingolipidoses. *Hum. Mol. Genet.* **19,** 3583–90 (2010).

57. Zunke, F. *et al.* Characterization of the complex formed by β-glucocerebrosidase and the lysosomal integral membrane protein type-2. *Proc. Natl. Acad. Sci.* **113,** 3791–3796 (2016).

58. Smith, K. R. *et al.* Cathepsin F mutations cause Type B Kufs disease, an adult-onset neuronal ceroid lipofuscinosis. *Hum. Mol. Genet.* **22,** 1417–23 (2013).

59. Sevenich, L., Pennacchio, L. A., Peters, C. & Reinheckel, T. Human cathepsin L rescues the neurodegeneration and lethality in cathepsin B/L double-deficient mice. *Biol. Chem.* **387,** 885–91 (2006).

60. Hillaert, U. *et al.* Receptor-Mediated Targeting of Cathepsins in Professional Antigen Presenting Cells. *Angew. Chemie Int. Ed.* **48,** 1629–1632 (2009).

61. Aerts, J. M. *et al.* The occurrence of two immunologically distinguishable beta-glucocerebrosidases in human spleen. *Eur. J. Biochem.* **150,** 565–74 (1985).

62. Aerts, J. M. *et al.* A procedure for the rapid purification in high yield of human glucocerebrosidase using immunoaffinity chromatography with monoclonal antibodies. *Anal. Biochem.* **154,** 655–63 (1986).

63. Mirzaian, M. *et al.* Mass spectrometric quantification of glucosylsphingosine in plasma and urine of type 1 Gaucher patients using an isotope standard. *Blood Cells, Mol. Dis.* **54,** 307–314 (2015).

64. Mirzaian, M. *et al.* Simultaneous quantitation of sphingoid bases by UPLC-ESI-MS/MS with identical 13C-encoded internal standards. *Clin. Chim. Acta* **466,** 178–184 (2017).

65. Li, K.-Y. *et al.* Synthesis of Cyclophellitol, Cyclophellitol Aziridine, and Their Tagged Derivatives. *European J. Org. Chem.* **2014,** 6030–6043 (2014).

Supplemental Figures

Table S1. Cathepsin gene expression and protein levels in human Gaucher spleens versus control spleens. Gene expression of proteases was determined via qPCR and statistical significance was determined by unpaired t-tests. Protein levels were analyzed via quantification of Western Blots of spleen tissue lysates.

	Gene expression		Protein
	Fold change GD vs Wt	Significance	Fold change GD vs Wt
catA	2.9	0,0091	0.63
catB	2.1	n.s.	4.21
catC	1.2	n.s.	1.27
catD	11.4	0,0035	1.65
catF	3.1	n.s.	0.43
catH	0.8	n.s.	5.90
catK	47.3	0,045	0.77
catL	1.9	n.s.	2.12
catS	8.2	0,0089	0.76
catW	0.2	n.s.	1.19
catZ	3.8	0,004	3.28
LGMN	4.6	0,0081	0.92

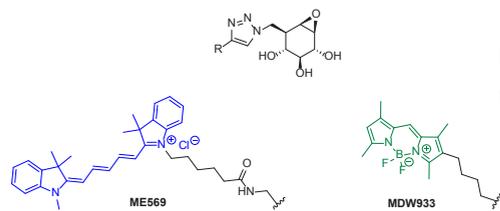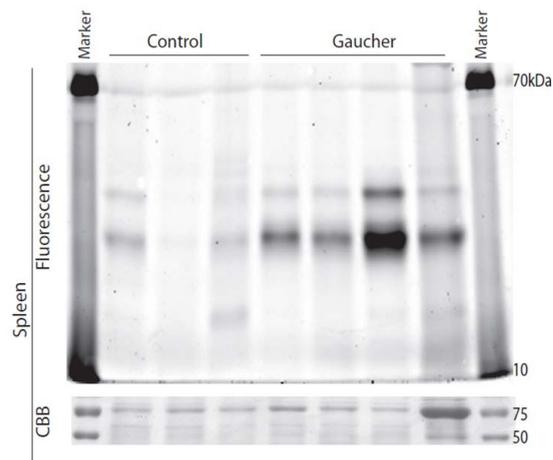Decreased compared to Wt
Increased compared to Wt

Figure S1. Chemical structures of GBA ABPs used in this work.

Figure S2. Labeling of active cysteine cathepsins in spleen homogenates at pH5.5 using BODIPY TMR DCG-04 ABP. CBB: Coomassie Brilliant Blue staining.

2

Stabilization of glucocerebrosidase by active-site occupancy

Stabilization of glucocerebrosidase by active-site occupancy

Fredj Ben Bdira[a]*, Wouter W. Kallemeijn[b]*, Saskia V. Oussoren[b], Saskia Scheij[c], Boris Bleijlevens[c], Bogdan I. Florea[d], Cindy P. A. A. van Roomen[c], Roelof Ottenhoff[c], Marielle J. F. M. van Kooten[a], Marthe T. C. Walvoort[d], Martin D. Witte[d], Rolf G. Boot[b], Marcellus Ubbink[a], Herman S. Overkleeft[d], Johannes M. F. G. Aerts[b,c]

[a]Dept. of Macromolecular Biochemistry, LIC, Leiden University
[b]Dept. of Medical Biochemistry, LIC, Leiden University
[c]Dept. of Medical Biochemistry, AMC, University of Amsterdam
[d]Dept. of Bio-organic Synthesis, LIC, Leiden University

Abstract

Glucocerebrosidase (GBA) is a retaining lysosomal β-glucosidase degrading glucosylceramide. Its deficiency results in Gaucher disease (GD). We examined the effects of active site occupancy of GBA on its structural stability. For this we made use of cyclophellitol-derived activity-based probes (ABPs) binding irreversibly to the catalytic nucleophile E340 and for comparison the potent reversible inhibitor, isofagomine. We demonstrate that cyclophellitol ABPs improve GBA stability in vitro as revealed by thermodynamic measurements (T_m increase by 21 °C) and its extreme resistance to tryptic digestion. The stabilizing effect of cell-permeable cyclophellitol ABPs is also observed in intact cultured cells containing wildtype, N370S GBA (labile in lysosomes) and L444P GBA (impaired ER folding): all showing marked increases in lysosomal forms of GBA molecules upon exposure to ABPs. The same stabilization effect is observed for endogenous GBA in liver of wild-type mice injected with cyclophellitol ABPs. Similar stabilization effects, as for ABPs, were also noted at high concentrations of the reversible inhibitor isofagomine. In conclusion, we provide evidence that the increase in GBA cellular level by ABPs and reversible inhibitors is in part caused by their ability to stabilize GBA folding and hence increased resistance against breakdown by lysosomal proteases. These effects are more pronounced in the case of the amphiphilic ABPs, presumably due to their high lipophilic potential, which may promote further structural compactness of GBA through hydrophobic interactions. Our study provides further rationale for the design of chaperones for GBA to ameliorate Gaucher disease.

Introduction

The lysosomal β-glucosidase glucocerebrosidase (GBA) cleaves glucosylceramide, an essential step in turnover of cellular glycosphingolipids[1,2]. GBA is co-translationally translocated into the ER where it acquires four N-linked glycans[3]. After removal of its signal peptide, the 495 amino acid polypeptide completely folds and subsequently binds to the triple helical structure in the apical region of the integral membrane protein LIMP-2 (lysosome integral membrane protein 2, encoded by the Scarb2 gene), and containing trafficking information in its cytoplasmic tail[4,5]. Complexed to LIMP2, GBA is transported through the Golgi apparatus where its glycans are converted into complex-type structures[6]. The GBA–LIMP2 complex is routed to late endosomes/lysosomes where GBA dissociates as a result of local acid pH[5,7].

GBA belongs to family 30 of glycoside hydrolase clan A (www.cazy.org), hence its structural topology displays a typical $(\alpha/\beta)_8$TIM barrel fold which forms the catalytic domain, a β-sheets domain and an immunoglobulin like domain, which interacts tightly with the catalytic domain, where few loops are located in the proximity of the enzyme active site[8]. These later seem to adopt multiple conformations, indicating their structural flexibility, presumably reflecting their crucial role in the enzyme conformational stability and/or its substrate turnover[9]. The inspection of GBA crystal structure in complex with NN-DNJ (PDB code:2V3E) shows that the binding site of the enzyme is formed by a hydrophilic glycon binding pocket, where the sugar ring of the inhibitor is accommodated forming multiple hydrogen bonds with its surrounding residues. In addition to the presence of an aglycon binding pocket formed by a narrow hydrophobic channel where the aliphatic tail of the inhibitor resides and forms a cluster of hydrophobic interactions with residues Leu241, Phe246, Tyr313, Leu314, and Tyr244[10].

Deficiency of GBA results in Gaucher disease (GD, OMIM #203800)[11]. At present more than 200 mutations in the Gba gene have been linked with GD, and next to truncations and splicing defects, several hundred amino acid substitutions in GBA have been shown to cause GD[12]. Substitutions in the folding domain positioned far away from the catalytic site proved to destabilize GBA structure, hence decreasing its half-life within the cell. For instance, the substitution L444P in GBA causes faulty folding of most enzyme molecules in the ER and subsequent proteasomal degradation[13]. Homozygosity for L444P GBA nearly always leads to a severe neuronopathic course of GD, albeit with great individual variability in onset and progression[11]. Premature degradation may also occur in the case of GBA molecules with mutations in the catalytic domain. In fact, quite many of the documented mutations in GBA lead to defective folding and reduced transport to lysosomes[14]. An exception is the N370S GBA substitution, the prevalent Gba mutation among Caucasians GD patients. The amino acid substitution is in a loop close to the catalytic pocket and found to affect pH optimum and kinetic parameters such as affinity for substrate and inhibitors[15–19]. The intralysosomal stability of N370S GBA is also reduced[15,16,19]. The survival of wildtype GBA in lysosomes is already relatively short ($t_{1/2}$ ~24-36 hours), at least in cultured cells. The intralysosomal proteolytic breakdown of GBA is known to be mediated by cysteine proteases as suggested by its inhibition by leupeptin[20].

The major symptoms of GD are caused predominantly by the abnormal accumulation of glucosylceramide in lysosomes of tissue macrophages[21,22]. Lysosomal accumulation of glucosylceramide induces a multi-system disorder with various symptoms such as hepatosplenomegaly, cytopenia and bone disease[11]. Severely affected GD patients also develop neurological symptoms and GBA abnormalities have been recognized as risk factor for developing α-synucleinopathies[23]. Enzyme replacement therapy (ERT), chronic intravenous administration of macrophage-targeted recombinant human GBA[24], markedly improves visceral symptomatology in GD patients, but the inability of the infused enzyme to pass the blood-brain barrier prohibits prevention and correction of neurological manifestations[25]. An alternative treatment might be offered by so-called pharmacological chaperones that promote folding and stabilize the fold of (mutant) GBA through interacting with its catalytic site[26–29]. These preferably brain-permeable, small compounds should promote folding of (mutant) GBA in the endoplasmic reticulum, resulting in increased transport of GBA to the lysosome[26–29]. Additionally, pharmacological chaperones might also stabilize GBA intra-lysosomally[15]. Whether the latter is clinically beneficial is debated, since pharmacological chaperones that interact with the active site of GBA will intrinsically also inhibit its enzymatic activity. We wanted to address the question whether occupancy of the binding pocket of GBA may promote its protection against proteolytic degradation in lysosomes.
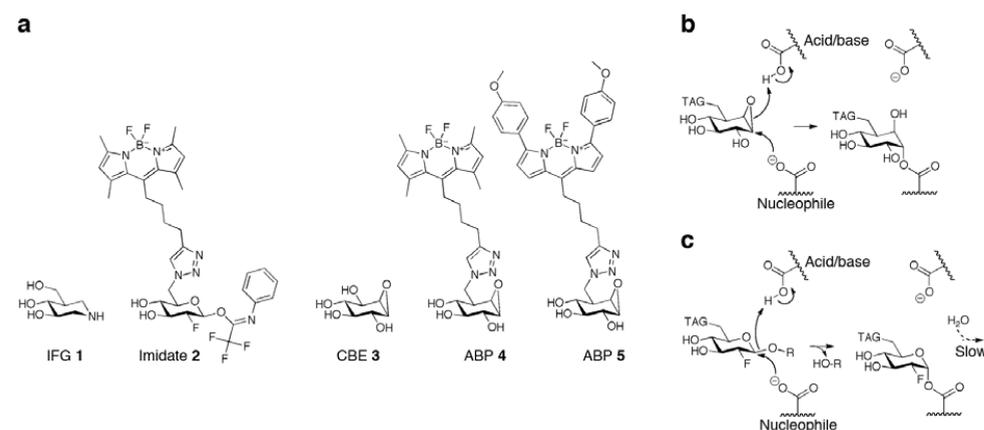

Figure 1. Inhibitors and reaction mechanism. (**a**) Structure formulas of competitive, reversible inhibitor isofagomine (IFG **1**), semi-irreversible inhibitor 2-deoxy-2-fluoro-β-D-glucopyranosyl-2-fluoro-β-d-glucopyranosyl-N-phenyltrifluoroacetimidate[30] (imidate **2**) and irreversible inhibitors conduritol β-epoxide (CBE **3**) and cyclophellitol β-epoxide type ABP **4** (MDW933, green fluorescent) and β-epoxide type ABP **5** (MDW941, red fluorescent)[32]. (**b**) Irreversible binding mechanism of β-epoxide type ABPs to the nucleophile of GBA via its double-displacement mechanism. (**c**) Hydrolysis of imidate **2**, and the temporary trapping of the glycosylated nucleophile adducts of GBA.

In the present study, we first examined pure recombinant glucocerebrosidase regarding stabilizing effects of cyclophellitol-type activity-based probes (ABPs, figure 1a) that permanently bind to the catalytic nucleophile E340 of GBA by utilizing its retaining double-displacement mechanism (figure 1b). These ABPs are β-glucose configured cyclophellitols with attached to the C6 a spacer with hydrophobic green– or red fluorescent BODIPY-moieties (MDW933 **4**, MDW941 **5**, figure 1a)[30,31]. These amphiphilic compounds are supposed to mimic the natural substrate of GBA and bind both its glycon and aglycon binding pockets. We also used CBE **3** as a small hydrophilic covalent inhibitor that is supposed to occupy only the glycon binding pocket of GBA binding site. These mechanism based inhibitors take benefit from the first step of GBA catalysis reaction to trap the enzyme in its intermediate state forming an addict complex, thus providing a valuable tool to dissect the contribution of each compound moiety into the stabilization mechanism by binding site occupancy on GBA.

We also examined the effect of 2-deoxy-2-fluoro-β-d-glucopyranosyl-2-deoxy-2-fluoro-β-d-glucopyranosyl-N-phenyltrifluoroacetimidate (imidate **2**, figure 1a)[32] which forms a transient glycosyl-enzyme intermediate (figure 1c). For comparison, we studied the effect of the potent reversible competitive GBA inhibitor **IFG 1** which has an *in vitro* IC_{50} ~30 nM at pH 5.2 and 5 nM at pH 7.0[27]. All inhibitors, most prominently the amphiphilic ABPs, **4** and **5**, improved stability of GBA and its proteolysis resistance *in vitro* and *in vivo* presumably promoted by their lipophilic tails that occupy the protein aglycon binding pocket, thus "inducing" a more rigid conformation of the protein trough hydrophobic interactions. Similar beneficial action on the stability and proteolysis resistance of GBA wildtype, N370S and L444P in cultured cells were observed. Marked increases in GBA tissue level were also noted for liver of mice infused with cyclophellitol ABPs. The stabilizing effects of the hydrophilic inhibitors IFG **1**, CBE **3** and the semi-reversible fluorosugar imidate **2** were less pronounced, suggesting that permanent occupancy of the glycon and aglycon binding pockets of GBA leads to a superior stabilization effect. The various investigations are here described and the implications are discussed.

Results

Structural stability and flexibility of GBA: impact of pH and glycomimetic ligands
During its life cycle glucocerebrosidase is exposed to a broad range of pH values, from neutral pH in the ER to increasingly acid pH in endosomes and lysosomes (pH 6.5 > pH 4.5–5.0). Therefore, we first investigated the effect of both acid and neutral pH on the structural stability of purified recombinant GBA (rGBA, imiglucerase) by monitoring its thermal unfolding, using circular dichroism. The temperature dependence of rGBA secondary structure at 222 nm was recorded by applying a temperature gradient from 30–80 °C with a heating rate of 1 °C/min (figure 2a). The obtained rGBA melting curve at pH 7.4 shows an apparent T_m value of 57 °C. On the other hand, its melting temperature increased at pH 5.2 with 4 °C to an apparent T_m value of 61 °C. This observed T_m increase at acidic pH is in

agreement with the previously reported measurements by differential scanning calorimetry[15,33,34]. Next, we investigated the effect of isothermal incubation at different pH on the activity of rGBA, and whether this was time-dependent. For this purpose, rGBA was firstly incubated for different lengths of time intervals at 37 °C in 150 mM McIlvaine buffer with a pH of 5.2 or 7.4. Residual activity of rGBA was measured with 4MU-β-D-Glc substrate in 150 mM McIlvaine buffer, pH 5.2 (figure 2b). The obtained data indicate that rGBA preserves its activity under acidic conditions, whereas at pH 7.4 its activity is lost in a time-dependent manner with a half-life of 30 min.

The noted loss of rGBA activity at pH 7.4 could be due to loss of the enzyme's native fold, apparently due to an irreversible process since the remaining activity was measured at pH 5.2. To substantiate this explanation, we performed a trypsin-limited proteolysis reaction to probe the pH effects on rGBA rigidity. For this, rGBA was treated with trypsin in 150 mM McIlvaine buffer at pH 5.2 or 7.4 and the tryptic events were analyzed every 10 min by SDS-PAGE (figure 2c). At pH 5.2, rGBA shows resistance to tryptic digestion over the course of the reaction, while at pH 7.4, rGBA is more sensitive to trypsin digestion, with about 40 % degraded within 60 min. Of note, a tryptic fragment of 34 kDa appears during proteolysis and it persist over the course of the reaction events, which may point to a structured and rigid, nicked domain of rGBA (figure 2c, arrow). Mass spectrometry was used to tentatively identify the trypsin cleavage site in GBA. It suggested that the cleavage site position could be after Lys233 (UniProt:P04062, fasta sequence, see supplemental figure S3) within the polypeptide sequence VNGK_GSL located in a loop close to the active site. This cleavage site seems to be more accessible to trypsin digestion at neutral pH and more protected at acidic pH. Seemingly, due to the different adopted conformation of rGBA under these experimental conditions (figure 2d).
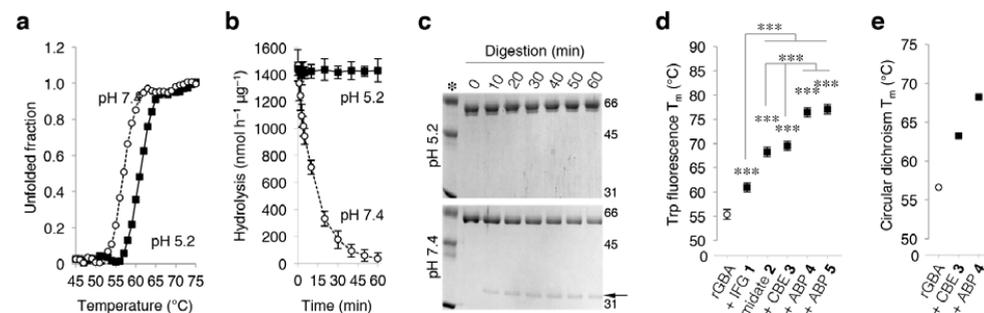

Figure 2. pH affects the rGBA structure. (**a**) rGBA melting curve at pH 5.2 (*closed squares*) and pH 7.4 (*open circles*) as determined by circular dichroism. (**b**) Time-dependent decay of rGBA activity at pH 5.2 (*closed squares*) and pH 7.4 (*open circles*), as determined by hydrolysis of 4MU-β-D-Glc substrate at pH 5.2. Data are average of duplicates ± SD. (**c**) Coomassie brilliant blue (CBB) staining of time-dependent, tryptic digestion of rGBA with a trypsin/rGBA ratio of 1/10 (w/w) at pH 5.2 and 7.4 (*top*, *bottom*, respectively). Arrow highlights the 35 kDa tryptic

fragment. (**d**) Melting temperature (T_m) determined by tryptophan fluorescence of rGBA in absence (control) or presence of saturating inhibitor concentrations of IFG **1**, imidate **2**, CBE **3**, β-epoxide ABPs **4** and **5**. Statistical analysis of $n = 3$ experiments, two-way ANOVA, $p < 0.001^{***}$. (**e**) T_m determined by circular dichroism of rGBA in absence or presence of saturating inhibitor concentrations of **3** and **4**. Statistical analysis of $n = 2$, two-way ANOVA, $p < 0.001^{***}$.

Thermal stability of rGBA: impact of glycomimetic ligands

The effects of the competitive inhibitor isofagomine (IFG **1**), the semi-irreversible inhibitor 2-deoxy-2-fluoro-β-D-glucopyranosyl-trichloroacetimidate (imidate **2**) and the irreversible inhibitors conduritol β-epoxide (CBE **3**) and lipophilic cyclophellitol β-epoxide type ABPs **4/5** on thermal stability of rGBA were investigated at pH 5.2, mimicking lysosomal conditions. For this purpose, rGBA was incubated with saturating concentrations of inhibitors for 1 h at 37 °C and next gradually heated whilst measuring tryptophan fluorescence[35,36], which decays as a result of tertiary structure unfolding. As depicted in figure 3a, IFG **1** increased the T_m of rGBA (55.2 °C) by +5.6 °C, **2** by +12.9 °C, irreversible inhibitor **3** by +14.1 °C and ABPs **4** and **5** by +21.0 and +21.7 °C, respectively. Another analysis of biophysical stability was performed by circular dichroism[37]. rGBA without inhibitors was compared to enzyme saturated by **3** and β-epoxide **4** (figure 3a). The calculated melting temperatures of rGBA preparations follow a similar trend as observed with tryptophan fluorescence decay (figure 3b). Again, β-epoxide **4** is found to exert the most prominent stabilization of rGBA.

Glycomimetic ligands influence the intrinsic fluorescence of GBA.

We next exploited the twelve tryptophan-residues present in GBA to probe the effects of ligand binding on the general folding of GBA. Notably, Trp178 and Trp381 are in close proximity of the substrate binding pocket, and residues Trp348 (loop 2), Trp393 (loop 3) reside on the protein surface, while the other Trp residues are buried into the hydrophobic core of the protein[8]. For this purpose, rGBA emission spectra were acquired by exciting tryptophan residues at 295 nm and recording the emission spectrum by scanning from 300–450 nm, in the presence or absence of various (ir)reversible inhibitors (figure 3c). In its free form, rGBA exhibits a maximum emission of 336.5 nm (similar as previous reported[36]). A slight blue shift of the spectrum by 2 nm was observed upon complex formation with CBE **3** with a maximum emission at 334.5 nm, reflective of a more hydrophobic environment of the Trp residues within the complex state (see figure 2c). rGBA exhibits a slightly larger blue shift when bound to ABPs **4** and **5**, with emission maximums of 333 nm. These data suggest that CBE **3** and ABPs **4/5** cause changes in rGBA folding, with higher effects of the latter ABPs presumably promoted by their lipophilic tails. Serendipitously, the blue shifts induced by ABP **4** and **5** were concomitant with fluorescence quenching. As ABP **4** and **5** contain a BODIPY fluorescence moiety (green and red fluorescent, respectively), we speculate that part of intrinsic GBA tryptophane-emitted fluorescence is transferred to these fluorophores through

an intrinsic FRET (iFRET) mechanism[38]. To test this, the fluorescence spectra of ABP **4**– and ABP **5**-labeled rGBA were acquired by exciting at 295 nm and extending the scanning range to 700 nm. Indeed, two peaks appear at a maximum emission of 515 nm and 610 nm, which represent the maximum emission for both ABP-incorporated BODIPYs (figure 3d). This iFRET mechanism is also supported by the overlaps between rGBA and ABPs emission spectra (Supplemental Figure S1).
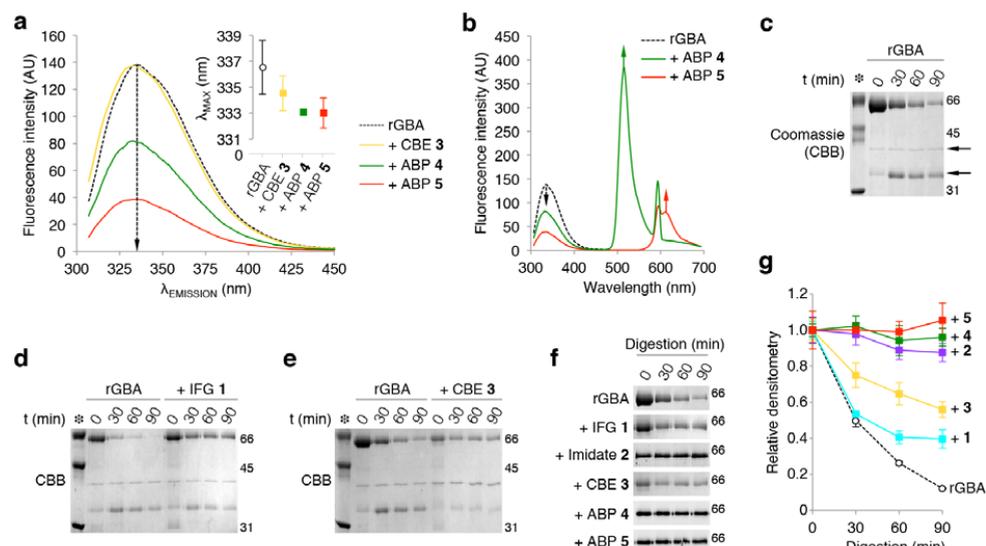

Figure 3. rGBA conformational changes monitored by intrinsic fluorescence. (a) rGBA fluorescence spectra with λ_{EX} 295 nm in the absence of additives (control, blue) with a maximum λ_{EM} 335 nm, in complex with CBE **3** (yellow) with a maximum λ_{EM} 333 nm, with ABP **4** (green) with a maximum λ_{EM} 332 nm and with ABP **5** (red) with a maximum λ_{EM} 331 nm. **(b)** rGBA fluorescence spectra showing the fluorescence quenching by ABP **5** (red) with the appearance of an emission peak at 610 nm and ABP **4** (green) with the emerge of an emission peak at 515 nm. All the measurements were done in 10 mM phosphate buffer, 150 mM NaCl pH 7.4. **(c)** Time course analysis of rGBA trypsin digestion. Arrows highlight the 40 and 35 kDa tryptic fragments. **(d, e)** Time course analysis of rGBA tryptic digestion in complex with IFG **1** and CBE **3**. **(f)** rGBA band intensities over the course of tryptic digestion stained by CBB or detected by ABP-emitted fluorescence. **(g)** Quantification of rGBA band densitometry over the course of tryptic digestion in the absence and in the presence of ABP **4** (green), imidate **2** (magenta), ABP **5** (red), CBE **3** (yellow) and IFG **1** (blue). Duplicate quantification ± SD.

Glycomimetic ligands variably rigidify the GBA structure.

Protein stabilization by ligands is generally paired with protein rigidification, due to new hydrogen-bond formation, or due to the formation of new clusters of hydrophobic interactions[39]. From the data presented above, we speculate that there is a correlation between the induced conformational changes by the ligand and the thermodynamic stabilization of GBA. We next investigated whether interactions with (ir)reversible inhibitors stabilize GBA by rigidification *in vitro*, by analyzing their effect on the ability of trypsin to digest rGBA. As can already be seen in figure 2c, purified rGBA is rapidly digested by trypsin, forming two major fragments (~35 and ~40 kDa), which remain mostly intact over the course of the experiment. After 90 min, ~10 % of intact rGBA remains. Presence of IFG **1** or CBE **3** increased resistance against tryptic digestion, with 50 % of rGBA remaining intact (figure 3 e,f). Imidate **2** and ABPs **4** and **5** exert prominent effects on the sensitivity of rGBA for tryptic digestion (figure 3 e,f), as such that within 90 min no degradation was observed. These ABPs have long hydrophobic tails of 15–18 Å, which give them a high lipophilic potential, suggesting that GBA rigidifies when interacting with these lipophilic ABPs, plausibly also shielding GBA's hydrophobic core and locking flexible loops in the vicinity of the active site through a cluster of hydrophobic interactions. Altogether, these observations match the increases in melting temperature (figure 3a–b). Of note, the amphiphilic inhibitors **4** and **5** show the lowest IC_{50} values regarding inhibition of GBA enzymatic activity, reflecting their highest binding affinity (see figure 1).

Lipophilic ABPs 4 and 5 stabilize GBA in macrophages and living mice.

As ABPs **4** and **5** exerted the strongest effect on rGBA stability *in vitro*, we assessed their influence on the enzyme *in situ*. Hence, human monocyte-derived macrophages were cultured with 100 nM ABP **5**, completely labeling all active GBA molecules (*in situ* IC_{50} ~10 nM). After a continuous pulse for up to 192 h (8 days), *in situ* ABP **5**-labeled GBA was detected by fluorescence scanning (figure 4a). ABP **5** labeled various molecular weight forms of GBA in the range 58–66 kDa, stemming from modifications in the enzyme's *N*-linked glycans[40]. Earlier investigations have revealed that the 58 kDa form of GBA is formed inside lysosomes as the result of trimming of N-linked glycans by local glycosidases[40]. As seen in figure 4a, the mature 58 kDa form of GBA accumulates when the enzyme is labeled with **5**. This finding suggests that ABP-labeling stabilizes GBA against proteolytic degradation in lysosomes, and does not prohibit the *N*-glycan modifications by lysosomal glycosidases.

To further examine the stabilizing effect of ABPs on GBA *in situ*, we analyzed the fate of exogenous, unlabeled rGBA and identical enzyme pre-labeled with ABP **4** following uptake by human monocyte-derived macrophages (figure 4b). The ABP **4**-labeled enzyme was stable after uptake for at least 48 hours, sharply contrasting with the rapid breakdown of unlabeled rGBA (figure 4c).

Next, we infused mice intravenously with 1 nanomole ABP **4** which subsequently labeled endogenous GBA in various tissues[31,32,41]. In the livers of treated animals, sacrificed six weeks post ABP-administration, ABP **4**-labeled GBA could still be detected (figure 4d). The

amount was around ~35 % of that in the livers of animals that were sacrificed 24 hours after infusion of an identical dose of ABP **4**. This suggests again that ABP-labeling markedly stabilizes GBA *in vivo*, since the half-life of unlabeled GBA is reported to be around 32–48 hours[18,20].
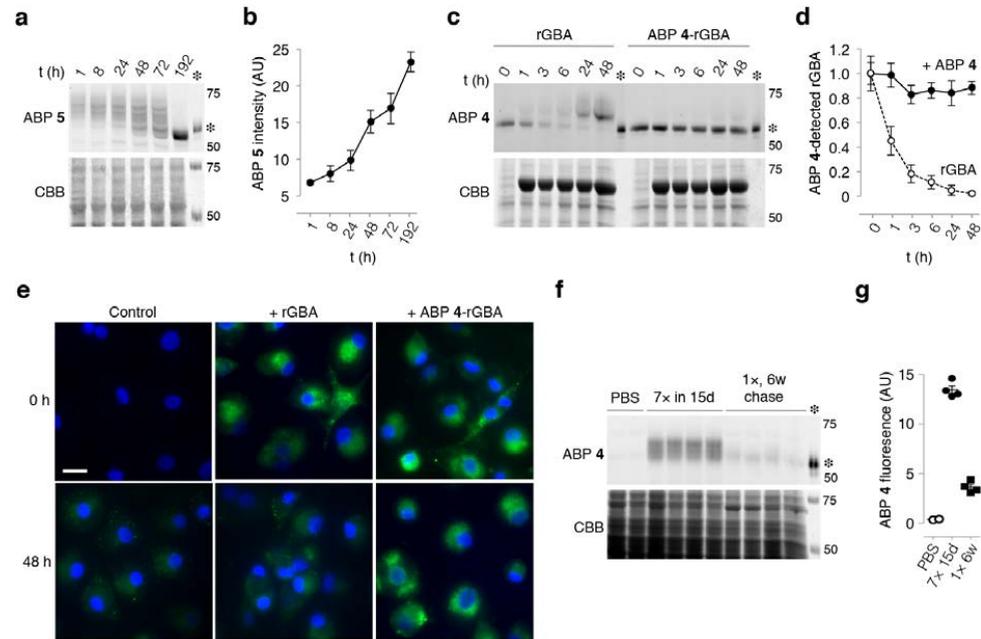

Figure 4. *In situ* **labeling of GBA with ABP 4/5.** (**a**) Continuous labeling of human monocyte-derived macrophage GBA with ABP **5** (*top panel*) and Coomassie staining of protein input (CBB, *bottom*). (**b**) Densitometry of ABP **5**-emitted fluorescence, corrected to CBB (mean of duplicate quantification, ± SD). (**c**) Chase of ABP **4** (pre–) labeled rGBA (imiglucerase) taken up by CBE pre-treated human monocyte-derived macrophages (*top*) and CBB (*bottom*). (**d**) Densitometry of ABP **4**-emitted fluorescence, corrected to CBB, with rGBA (*open circle*) and ABP **4**-labeled rGBA (*closed square*), mean of duplicate quantification ± SD. (**e**) Fluorescence micrographs of chase in (**c**), of control (*left*), and cells treated with unlabeled rGBA (*middle*) and ABP **4**-labeled rGBA, after 0 and 48 h (*top*, *bottom*, respectively). Unlabeled rGBA was labeled 30 min prior to fixation with 10 nM ABP **4**. Scale-bar represents 25 μm. (**f**) Chase of murine hepatic GBA of animals treated either with vehicle or ABP **4** during 15 days (7 injections), or a single dose 6 weeks prior sacrifice (*top panel*) and CBB (*bottom*). (**g**) Densitometry of ABP **4**-emitted fluorescence, corrected to CBB, with untreated (*open circle*), ABP **4** repeatedly (*closed diamond*) and single dose (*closed square*), mean of duplicate quantification ± SEM. All gels contain 50 fmol equimolar ABP **4**– and **5**-labeled ~58 kDa imiglucerase (*asterisk*) as positive control.

Lipophilic ABPs 4 and 5 increase GBA in fibroblasts by protection against lysosomal proteolysis.

To assess whether the accumulation of ABP **4**-labeled 58 kDa GBA stems from a reduced susceptibility towards lysosomal proteases, we treated confluent human control fibroblasts for 3, 5, 7, 9 or 12 days with the cysteine-cathepsin inhibitor leupeptin[20]. After harvesting the cells, GBA present in lysates of control cells and leupeptin-exposed cells was *in vitro* labeled with excess ABP **4**. As shown in figure 5a, the amount of green **4**-labeled GBA in untreated control cells increased slightly with culture time (*top row*). The incubation of cells with leupeptin caused a prominent accumulation of ~58 kDa active GBA over time (*second row*)[20].

Next, we incubated cells with ABP **5**. The inhibitor treatment induced a prominent time-dependent accumulation of ABP-labeled GBA (*third row*, figure 5a). The increase in *in situ* ABP **5**-labeled GBA was slightly further enhanced in cells co-incubated leupeptin (*fourth row*), suggesting **5**-labeled GBA is still prone to some degree of proteolysis within lysosomes (figure 5a). The quantification of GBA levels is shown in figure 5b, indicating that *in situ* stabilization of GBA by leupeptin and ABP **5** is at least partially overlapping.
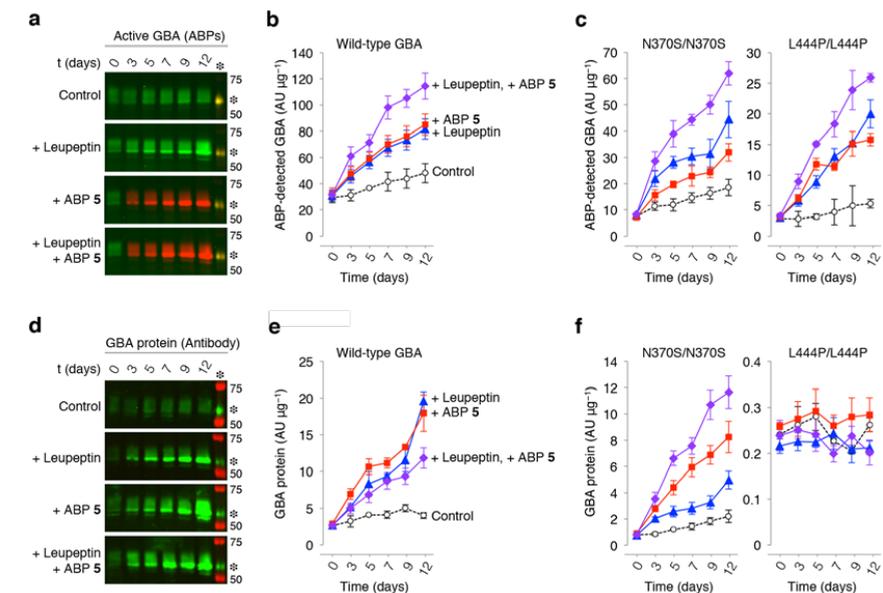
Figure 5. *In situ* **stabilization of GBA by ABP 5 and leupeptin.** Wild-type GBA fibroblasts incubated with leupeptin, ABP **5** (*red*), or both for the indicated length of time. (**a**) GBA levels in untreated fibroblasts (*top row*) and cells incubated with leupeptin (*second row*), visualized *in vitro* with ABP **4** (*green*). Labeling of GBA in cells *in situ* with ABP **5** (*red, third row*) and in combination with leupeptin (*bottom row*). Equal green and red fluorescence yields yellow overlay; fluorescence was calibrated with 50 fmol equimolar green ABP **4**– and red ABP **5**-labeled imiglucerase present on each SDS-PAGE gel (*asterisk*). (**b**) Quantification of ABP-emitted fluorescence from *in vitro* ABP **4**-labeled controls (*open black circles*) and leupeptin

(*blue triangles*), and *in situ* ABP **5**-labeled GBA (*red squares*), and in combination with leupeptin (*purple diamonds*). Data as mean of *n* = 2, ± SD. (**c**) Quantifications of ABP-fluorescence as observed in N370S and L444P Gaucher fibroblasts, *vide supra*. (**d**) Detection of GBA protein (*green*) with Western immunoblotting of gels depicted in **a** (molecular weight ladder in *red*), with quantification in (**c**) and identical analysis of N370S and L444P Gaucher fibroblasts, *vide supra*. All data expressed as average of *n* = 2, ± SD.

Lipophilic ABPs 4 and 5 increase mutant GBA molecules in GD fibroblasts.
In fibroblasts from a homozygous N370S GBA Gaucher patient and a homozygous L444P GBA Gaucher patient, similar stabilizing effects of ABP on enzyme were observed (figure 5c). Both fibroblast cell lines contained less active GBA compared to the control fibroblasts. Incubation of the cells with leupeptin and ABP **5** resulted in stabilization of GBA, more prominent (6– to 8-fold) compared to that seen for GBA in wild-type cells (about 3-fold) (compare figure 5b and 5c). Exposure of both Gaucher fibroblast cell lines to the combination of ABP **5** and leupeptin further increased the stabilizing effect,   again partially overlapping (Figure 5c, see supplemental information for original data). Total GBA protein in cell lysates was also visualized by Western blot using GBA-specific antibody 8E4[42,43] (figure 5d; *corresponding quantification in* figure 5e). Again, prominent stabilization of ~58 kDa GBA was noted with ABP **5** and/or leupeptin in the case of wild-type cells and N370S GBA Gaucher fibroblasts (figure 5f). Comparable analysis of L444P GBA Gaucher fibroblasts was unfortunately not reliable due to the very low quantities of GBA protein. Overall, these findings suggest that the stabilizing effect of ABP **5** is partially caused by protection against breakdown by lysosomal proteases. This effect is specific since the lysosomal glycosidases processing GBA to its 58 kDa form appear to be not inhibited.

The reversible inhibitor IFG and semi-irreversible inhibitor **2** were found to augment GBA to a lesser extent in fibroblasts. Confluent wild-type and homozygous N370S GBA fibroblasts were treated for 12 days with 0–100 µM of **1**. After harvesting, cell lysates were labeled with excess green ABP **4** to visualize residual active GBA molecules (Supplemental information Figure S2)**.** A stabilizing effect of IFG **1** became only evident at concentrations greater than 10 µM, being maximal at 100 µM (*the highest concentration tested*). Western-blot analysis of the same experiment, rendered a similar result (Supplemental information figure S2). The semi-irreversible inhibitor ABP **2** comparably augmented GBA in wild-type and N370S/N370S GD fibroblasts (supplemental information figure S2). The findings made for imidate **2** treatment were confirmed by Western blot analysis (see supplemental information figure S2).

Discussion
In recent years attention has been paid to the design and synthesis of chemical chaperones for GBA. Reviews by Benito *et al.*[28] and Jung *et al.*[44] cover some of the classes of glycomimetics currently under investigation as GBA chaperones. Many of these are reversible competitive, or mixed-type, inhibitors of GBA. The most well studied chemical chaperone so far has been IFG **1**, which was the subject of several pre-clinical studies as well as a clinical study that did not meet the full expectation. Ambroxol[45–48], a weak, mixed-type inhibitor of GBA, has been found to augment the enzyme in cultured GD patient cells and following oral administration to patients. Impressive reductions in spleen and liver volumes, as well as the GD biomarker chitotriosidase, have been documented[47,49]. The beneficial effects of chemical chaperones on GBA in cultured cells are generally attributed to improved chaperone-assisted folding of GBA in the endoplasmic reticulum. Our present investigation suggests an additional beneficial mode of action of inhibitors. i.e. The contribution of hydrophobic interactions of GBA binding pocket occupancy into the enhancement of its structural stability and protection against intralysosomal proteolytic degradation.

The evidence for this notion stems from *in vitro* and *in vivo* experiments testing GBA stabilization by inhibitors. Thermodynamic measurements with pure GBA suggested firstly that, correlating with affinity of inhibition, all inhibitors tested stabilized enzyme. A modest stabilization of GBA was observed for small hydrophilic compounds IFG **1** and conduritol β-epoxide **3**. The lipophilic fluorosugar **2** and β-epoxides **4/5** equipped with hydrophobic fluorophores cause a more dramatic increase of melting temperature up by 21 °C. Next, we analyzed using intrinsic fluorescence the conformational changes of GBA *in vitro* following interaction with inhibitors. Upon complex formation with CBE **3** GBA presents a slight shift toward the blue region of its fluorescence spectra, an indication for a conformation change, possibly resulting from orientation adjustments of indole groups toward a more hydrophobic environment. A higher shift toward the blue region was observed when the protein is in complex with lipophilic ABPs **4** and **5**. Presumably their lipophilic tails provoke further conformational changes in which the indole groups of a tryptophan experience extra hydrophobicity. Of note, equipment of cyclophellitol and cyclophellitol-aziridine with hydrophobic fluorophore tags markedly increases their affinity for GBA[30,31]. Along the same line, Vocadlo and co-workers developed an elegant fluorescence-quenched substrate for GBA for which they exploited the fact that GBA accommodates the hydrophobic ceramide moiety of glucosylceramide and is known to tolerate a hydrophobic modification to the 6-position of glucose[50]. The designed high-affinity fluorescence-quenched substrate harbors a fluorophore attached to the C6-glucose and the hydrophobic quencher to the anomeric site and to a certain extent mimics fluorosugar **2** and ABPs **4** and **5**. This successful substrate design indicates again that the catalytic pocket of GBA in active state accommodates substrate with a hydrophobic modification. At present no crystal structure of GBA has been solved in the presence of the ABPs **2, 4** or **5**. However, the crystal structure of GBA in complex with a lipophilic ligand (*N*-nonyl-DNJ, PDB code 2V3E) suggests that GBA loops 1 and 2 become structured and undergo interactions with the aliphatic tails of *N*-nonyl-DNJ, becoming more

closed and thermostable[34]. Similarly, upon complex formation with the ABPs **2**, **4** and **5**, GBA becomes extremely protected against tryptic digestion, providing strong evidence of its structure rigidification. In the presence of hydrophilic compounds such as IFG **1** or CBE **3**, GBA behaves similarly to its free form, with a moderate enhancement of its tryptic resistance. These observations support the proposition of GBA rigidification by the lipophilic ligands, presumably through a cluster of hydrophobic interactions. Therefore, we presume that the observed differences of the stabilization mechanisms between the tested compounds are mainly due to the difference in their lipophilic potentials.

The predominant trypsin cleavage site in GBA free state is located in a loop (223-241 Uniprot:P04062 fasta sequence) close to the active site. In solution, this loop seems to be accessible for trypsin digestion by adopting a flexible conformation that fits within the protease catalytic site. As it is well known that protease cleavages site for a variety of proteins with solved crystal structure almost never occur in α-helixes, but largely in flexible loops[51]. Interestingly sixteen mutations within this protein region were reported in human to decrease dramatically GBA stability and activity leading to sever symptoms of the disease. For instance, the substitution of L224F decreases GBA normal activity up to 4 % and increases its susceptibility to proteolytic degradation[52]. Another substitution V230E has a dramatic effect on GBA activity and presents in GD patient type 1[53]. Single mutation G232E is present in patients suffering from Parkinson disease and this GBA variant preserve only 7 % of the wildtype normal activity[54]. Moreover, substitution of G234E in GBA sequence has similar effect on Gaucher patients[55]. The position of the latter mutation overlaps with what we found as a major trypsin cleavage site. Based on these findings, it is plausible that this particular region represents a hotspot for maintaining a correct folding of GBA catalytic domain. Upon complex formation with ABPs, this site becomes shielded against proteolytic degradation. Thus it is attractive to hypothesize that complexing the enzyme with ABPs **2**, **4** and **5** prevents GBA to become loose and locally flexible, improving its structural stability and resistance against proteolysis.

We recently noticed a similar stabilization mechanism for another retaining β-glucosidase, endoglycoceramidase II (EGCII) from *Rhodococcus sp*[56]. The stability of EGCII was found to be improved by formation of covalent complexes with cyclophellitols substituted with hydrophobic moieties. The tested compounds seemed to have an induced fit mechanism effect on the protein flexible structure, which makes it adopting a more compact conformation. This was evidenced by the increase of EGCII melting temperature, its resistance against tryptic digestion, the observed changes in its ^{15}N-^{1}H transverse relaxation optimized spectroscopy spectrum, and the decrease of its exposed hydrophobic surface to the solvent as determined by 8-anilino-1-naphthalenesulfonic acid fluorescence. Stabilization of EGCII conformation was correlated with the shape and hydrophobicity of the cyclophellitols substituents. The structural comparison between GBA and EGCII showed a remarkable overlaps of their glycon and aglycon binding pocket[56]. Therefore, it will not be surprising if a similar stabilization mechanism of ABPs takes place in GBA case. Following the observed *in vitro* stabilization of GBA by inhibitors, we extended our study to living cells and mice. We

consistently noted that exposing cells (monocyte-derived macrophages, skin fibroblasts) and mice to cyclophellitol ABPs **4** or **5**, resulted in accumulation of GBA with a molecular weight of approximately 58 kDa, suggestive of a lysosomal localization. Co-incubation of fibroblasts with ABPs and leupeptin, a broad lysosomal cysteine protease inhibitor known to inhibit proteolytic breakdown of GBA, indicated that the stabilizing effect could indeed be partly ascribed to reduced breakdown

Our study reveals that irreversible inhibitors like cyclophellitol ABPs **4** and **5** potently stabilize GBA molecules, but by virtue they are of no use in the treatment of GD patients. Although they provided a valuable tool to dissect the contribution of hydrophobic interactions into GBA stabilization and to selectively label the active form of GBA in cells. Fluoroglucosides, designed by Withers and co-workers[57], in theory may be more attractive as chaperones since they initially covalently bind to the catalytic nucleophile of a retaining glycosidase but are ultimately released again. A true therapeutic application of such compounds in patients will however offer the major challenge to dose the inhibitor adequately to reach concomitant beneficial effects in all tissues: under-dosing in a tissue will be without effect and over-dosing will cause undesired loss of degradative capacity. More relevant is the consideration that the natural substrate glucosylceramide assists in the stabilization of GBA in lysosomes. In such hypothetical scenario, intra-lysosomal GBA levels would be higher during high substrate flux, and *vice versa,* the prolonged absence of substrate would promote degradation of the enzyme. It will be of interest to examine whether reduction of glycosphingolipids in cells by inhibition of glucosylceramide synthase activity is associated with increased lysosomal turnover of GBA.

In conclusion, GBA is significantly stabilized through the dual occupancy of its glycon and aglycon binding pockets by amphiphilic inhibitors (see fig. S4), likely in part by promoting a global structural compactness of the enzyme associated with reduced susceptibility for proteolytic cleavage by lysosomal proteases. On the other hand, the single occupancy of the glycon binding pocket by small hydrophilic compounds seems to induce a local GBA structural rigidification as revealed by its *in vitro* and *in vivo* proteolysis susceptibility. Our findings reveal new insights into a pharmacological chaperone stabilization mechanism that could be further exploited in the design of new compounds to rescue GBA proteostasis in GD patients.

Materials & Methods

General methods.

The ABPs and isofagomine were synthesized as described earlier[31,32,41]. Chemicals were obtained from Sigma-Aldrich if not indicated otherwise. Recombinant GBA (rGBA, imiglucerase) was obtained from Genzyme (Cambridge, MA, USA). Gaucher patients were diagnosed on the basis of reduced GBA activity and demonstration of an abnormal genotype. Fibroblasts were obtained with consent from donors. Cell lines were cultured in HAMF12-DMEM medium (Invitrogen) supplied with 10 % (v/v) FBS. Monoclonal anti-human GBA

antibody 8E4 was produced from hybridoma cells as described earlier[43]. Buffy-coats were purchased at Sanquin Bloodbank (Amsterdam).

Cerezyme purification.
rGBA (imiglucerase) is supplied as a sterile white lyophilized powder in the presence of mannitol and polysorbate 80 NF as stabilizer substances. Thorough purification of rGBA from its additives was conducted by affinity chromatography using a Concanavalin A–Sepharose column, eluting with a 30 min gradient of 0–1 M mannoside in 150 mM McIlvaine buffer (citric acid–Na_2HPO_4, pH 5.2). Next, an additional purification step was performed on pooled fractions using size exclusion chromatography (Superdex 75) and elution occurred either with 150 mM McIlvaine buffer (citric acid–Na_2HPO_4, pH 5.2) or with 20 mM Tris–HCl, pH 7.4, supplemented with 150 mM NaCl. rGBA was concentrated Amicon Ultra-4 centrifugal filter devices (30 kDa cutoff) and kept at 4 °C for further experiments.

Limited proteolysis.
Tryptic digestion of purified rGBA with or without reversible or irreversible inhibitors was performed at 37 °C, either in 150 mM McIlvaine buffer (pH 5.2 or 7.4) or in 20 mM Tris–HCl, pH 7.4, supplemented with 150 mM NaCl, and using a trypsin/rGBA ratio of 1/10 (w/w) as optimum condition for proteolysis. Digestions were stopped with cracking buffer (50 mM Tris–HCl, pH 6.8, supplemented with 1 % (w/v) SDS, 25 % (v/v) glycerol, 1 % (v/v) β-mercaptoethanol and 0.05 % (w/v) bromophenol blue), immediately followed by heating for 10 min at 100 °C. The tryptic digestion products (1.5–5 µg) were separated by SDS-PAGE and analyzed by Coomassie staining, or where stated, by fluorescence scanning (*see below*).

Tryptophan fluorescence.
rGBA (50 µM) was pre-incubated with 1 mM of IFG **1** or imidate **2**, 10 mM conduritol β-epoxide **3**, or 100 µM cyclophellitol ABP **4** or **5** in 150 mM McIlvaine buffer (citric acid–Na_2HPO_4, pH 5.2, supplemented with 0.2 % (w/v) sodium taurocholate and 0.1 % (v/v) Triton X-100 for 3 h at 37 °C. Fluorescence decay curves were obtained by diluting to 1 µM rGBA-inhibitor complex in Nanopure H_2O, followed by determination of tryptophane fluorescence (λ_{EX} 295 nm, slit width 5 nm; λ_{EM} 345 nm, slit width 5 nm) whilst the sample temperature increased 1.5 °C per minute. Sample temperature was controlled *via* a PTP-1 Fluorescence Peltier System (Perkin-Elmer). We defined the inflection point of the temperature-induced decrease in tryptophan fluorescence intensity as the melting temperature (T_m). This value was determined by taking the minimum value of the first-derivative of the slope, at which the negative slope is maximal, using GraphPad Prism 5.1. The tryptophan emission fluorescence spectra was mapped using λ_{EX} 295 nm, slit width 5 nm, and scanning emission at λ_{EM} 300–470, slit width 5 nm (Cary Eclipse Fluorescence Spectrophotometer, Agilent Technologies). Samples comprised of 5 µM of purified rGBA with or without **3**, **4** or **5** in 10 mM potassium phosphate buffer (K_2HPO_4–KH_2PO_4, pH 7.4), supplemented with 150 mM NaCl. Spectral backgrounds were corrected and smoothed using Cary Eclipse Fluorescence Spectrophotometer software. To obtain the different protein-inhibitors complexes, purified rGBA was pre-incubated with inhibitors in excess for 3 hours at 37 °C in 150 mM McIlvaine buffer. After labeling, excess of irreversible inhibitors was removed *via* buffer exchange into 10 mM potassium phosphate buffer using Centriprep filter devices (30 kDa cutoff).

Circular dichroism.
Spectra were recorded on a Chirascan CD spectrometer (Applied Photophysics). Far-UV CD spectra were recorded from 180 to 300 nm in a 1 mm path length quartz cuvette (Hellma) at 20 °C at a concentration of ca. 10 µM. Spectra were collected for 0.5 s per data point at 0.5 nm step size (spectral bandwidth 1 nm) and were corrected for background signals. A Peltier element was used to control the sample temperature and allow ramping at 1 °C per minute. Intensity of the CD signal was monitored at various wavelengths (204, 215 and 235 nm). The unfolding transition point (T_m) of free purified rGBA at different pH (5.2 or 7.4) was measured by following the ellipticity signal decay at 222 nm by applying a heating rate of 1 °C/min, over a temperature gradient from 30–80°C in 10 mM potassium phosphate buffer (K_2HPO_4–KH_2PO_4, pH 5.2 or 7.4), supplemented with 150 mM NaCl. Obtained melting curves were fitted, and the T_ms were calculated using GraphPad Prism 5.1.

Enzyme activity assays.
The residual β-glucosidase activity associated with GBA was assayed at 37 °C by incubating samples with 3.75 mM 4-methylumbelliferyl-β-D-glucopyranoside (4MU-β-D-Glc) as substrate in 150 mM McIlvaine buffer, pH 5.2, supplemented with 0.1 % (w/v) BSA, 0.2 % (w/v) sodium taurocholate, and 0.1 % (v/v) Triton X-100[42]. Time-dependent decay of rGBA activity was assessed by incubating rGBA for 0–60 min at 37 °C, and at various time points, the residual rGBA activity was assessed by adding substrate. Assays were stopped with excess NaOH-glycine (pH 10.3) and fluorescence was measured with a fluorimeter LS30 / LS55 (Perkin Elmer) using λ_{EX} 366 nm and λ_{EM} 445 nm.

Isolation and maturation of macrophages.
Buffy-coats were diluted into PBS supplemented with 0.1 % (w/v) BSA and heparin, subsequently layered on top of Lymphoprep gradient (Stemcell Technologies) and centrifuged at 1,000× *g* for 15 min at RT. After washing the PBMC pellets with PBS supplemented with 0.1 % (w/v) BSA, cells were centrifuged at 750× *g* for 10 min at RT, rinsed and repeated at 500× *g* for 5 min. Hereafter, the pellet was washed with aforementioned PBS, and centrifuged at 250× *g* for 10 min at RT. Then, monocytes were separated on a Percoll gradient. The resulting pellet was resuspended in 2.5 mL 60 % (w/v) SIP, layered with 5 mL 45 % (w/v) SIP and 2.0 mL 34 % (w/v) SIP), and centrifuged at 1750× *g* for 45 min at RT. The upper interface containing monocytes was washed thrice with aforementioned PBS, centrifuged at 500× *g* for 10 min and then twice at 500× *g* for 5 minutes. The cell fraction was then resuspended in RPMI with 1 % (w/v) human serum, the monocytes were counted with

tryphan blue solution and 10^6 monocytes were seeded per well. After 1 h at 37 °C and 5 % (v/v) CO$_2$, non-adhering non-monocyte cells were washed away with aforementioned PBS and the adhering monocytes then were cultured in RPMI with 10 % (v/v) human serum for 7 days prior to experiment initiation.

Continuous β-epoxide ABP 5 pulse in human monocyte-derived macrophages.
Human monocyte-derived macrophages were switched to X-VIVO 15 medium (Lonza) lacking human serum, and continuously pulsed with 100 nM β-epoxide ABP **5**. After 0–192 h (8 d), cells were washed extensively with PBS and lysed by scraping in 25 mM potassium phosphate buffer (pH 6.5, supplemented with 0.1 % (v/v) Triton X-100 and protease inhibitor cocktail (Roche)). Protein concentrations were determined and 10 μg total protein (20 μL) was denatured with 5× Laemmli buffer (50 % (v/v) 1M Tris-HCl, pH 6.8, 50 % (v/v) 100 % glycerol, 10 % (w/v) DTT, 10 % (w/v) SDS, 0.01 % (w/v) bromophenol blue), boiled for 4 min at 100 °C, and separated by electrophoresis on 7.5 % (w/v) SDS-PAGE gel running continuously at 90 V[31,32,41]. Wet slab-gels were scanned on fluorescence using the Typhoon Variable Mode Imager (Amersham Biosciences) using λ$_{EX}$ 488 nm and λ$_{EM}$ 520 nm (band pass filter 40 nm) for green fluorescent imidate ABP **2** and β-epoxide ABP **4** and λ$_{EX}$ 532 nm and λ$_{EM}$ 610 nM (band pass filter 30 nm) for red fluorescent β-epoxide ABP **5**. ABP-emitted fluorescence was quantified using ImageJ software (NIH, Bethesda, USA), and verified in-gel by presence of 50 femtomol equimolar green β-epoxide ABP **4**– and red ABP **5**-labeled imiglucerase. After fluorescence scanning, SDS-PAGE gels were fixed (50/40/10 – MeOH/H$_2$O/HAc) for 1 h, stained for total protein (50/40/10 with 1 % (w/v) CBB-G250) and de-stained (45/45/10). Coomassie brilliant blue-stained gels were scanned on a flatbed scanner.

Determination of *in situ* IC$_{50}$.
Confluent human skin control fibroblasts with wild-type GBA were incubated with 0–100 μM IFG **1**, 0–10 μM imidate ABP **2** or 0–100 nM β-epoxide ABP **4** for 2 h at 37 °C and subsequently GBA-associated β-glucosidase activity was determined by incubation in the presence or absence of 250 μM fluorescein-di-β-D-glucopyranoside (FDG) for 1 h at 37 °C. Next, cells were suspended by trypsinization, fixed in 3 % (w/v) *p*-formaldehyde and analyzed by FACS using FACS Calibur (BD Biosciences), FL1 channel (λ$_{EX}$ 488 nm). In case of reversible inhibitor **1**, all the procedures, including washing with PBS, occurred in the presence of **1** in the corresponding concentration as employed during the *in situ* incubation.

Pulse-chase of exogenous GBA.
rGBA (imiglucerase, 50 μM) was incubated with (out) 100 μM ABP **4** for 1 h in 150 mM McIlvaine buffer, pH 5.2, supplemented with 0.2 % (w/v) sodium taurocholate and 0.1 % (v/v) Triton X-100), and at 37 °C, cleaned three times over a 30 kDa cutoff-filter with PBS. Mature human monocyte-derived macrophages were incubated with 300 μM **3** for 2 h, hereafter cells were washed extensively with PBS, incubated with 100 nM rGBA (control) or **4**–labeled rGBA with for 30 minutes at 37 °C, again washed extensively and medium refreshed. After 0–48 h,

cells were again washed extensively with PBS and lysed by scraping in 25 mM potassium phosphate buffer (pH 6.5, supplemented with 0.1 % (v/v) Triton X-100 and protease inhibitor cocktail (Roche)). Protein concentrations were determined in the lysates and, of the control rGBA-treated cells, 10 μg total protein was labeled *in vitro* with 1 μM β-epoxide ABP **4** in McIlvaine buffer, pH 5.2 and with supplements, for 1 h at 37 °C. Finally, samples were denatured and **4**-labeled proteins visualized by fluorescence scanning of the SDS-PAGE slab-gels. ABP-emitted fluorescence was quantified using ImageJ software (NIH, Bethesda, USA), *vide supra*.

Pulse-chase of GBA in living animals.
The appropriate ethics committee for animal experiments approved all experimental procedures. C57Bl/6J mice were obtained from Charles River (Wilmington, MA, USA) and fed a commercially available lab diet (CRM(E), Special Diet Services, UK). Two male C57BL/6J mice were injected intravenously *via* tail vein with a single dose of 100 μL PBS, four were injected with 100 μL PBS containing 100 picomoles ABP **4** (~2 μg kg⁻¹) six weeks prior sacrifice, and four mice received the same dose every 48 hours for 15 days prior sacrifice. At termination of the experiment, the mice were anesthetized with FFM mix (25/25/50 fentanylcitrate/midazalam/H$_2$O) then perfused *via* the heart into the aortic root with PBS, flowing at 3.0 mL min⁻¹, by using a syringe pump (Harvard apparatus, Holliston, MA, USA). The liver was collected and directly frozen in liquid nitrogen. Homogenates were made in 25 mM potassium phosphate buffer, pH 6.5, supplemented with 0.1 % (v/v) Triton X-100 and ABP **4**-labeled GBA in 10 μg total protein was analyzed *via* SDS-PAGE. After fluorescence scanning, SDS-PAGE gels were fixed and stained with CBB, *vide supra*.

Pulse-chase of normal and Gaucher patient skin fibroblasts.
Confluent human skin fibroblasts homozygous for wild-type, N370S or L444P GBA were cultured with medium supplemented with 100 nM ABP **5**, 100 μM leupeptin or both components. Medium was completely refreshed every fortnight, and after 0–12 days cells were lysed by scraping in 25 mM potassium phosphate buffer (pH 6.5, supplemented with 0.1 % (v/v) Triton X-100 and protease inhibitor cocktail (Roche)). After determination of the protein concentration, 10 μg total protein was incubated with 100 nM ABP **4** (if fibroblasts were not treated by β-epoxide ABP **5** *in situ*), dissolved in 150 mM McIlvaine buffer (pH 5.2, supplemented with 0.2 % (w/v) sodium taurocholate, 0.1 % (v/v) Triton X-100 and protease inhibitor cocktail (Roche)) for 1 h at 37 °C. Finally, samples were analyzed by SDS-PAGE on two gels: one for fluorescence scanning followed by CBB staining, and one for Western blotting; this was accomplished by transfer of the protein for 1 h at 12 V, followed by blocking of the membrane with 2 % (w/v) BSA in TBST buffer (50 mM Tris–HCl, pH 7.4, 150 mM NaCl, 0.1 % (v/v) Tween-20), overnight treatment with 1:1,000 diluted primary mouse α-human GBA mAb (8E4, 2 % (w/v) BSA in TBST), washing with TBST for 20 min (repeated 6 times), followed by 1:10,000 diluted secondary rabbit α-mouse IRD680 (Cell Signaling, 2 % (w/v) BSA in TBST), subsequent washing with TBST for 20 min (repeated 6 times), and read-out on an

Odyssey infrared scanner (Licor). Fluorescence emitted by either ABP-labeled proteins or antibodies was quantified using ImageJ software (NIH, Bethesda, MD, USA), *vide supra*.

In situ treatment with IFG 1 or imidate 2.

Confluent human skin fibroblasts homozygous for wild-type, N370S or L444P GBA were incubated for 12 days with 100 nM ABP **5**, 100 μM leupeptin, both, or with 0.001–100 μM IFG **1** or imidate **2**. Medium was completely refreshed every fortnight, and samples were treated as described earlier, *vide supra*.

Acknowledgments

Conflict of interest

None declared.

References

1. Brady, R. O., Kanfer, J. N., Bradley, R. M. & Shapiro, D. Demonstration of a deficiency of glucocerebroside-cleaving enzyme in Gaucher's disease. *J. Clin. Invest.* **45,** 1112–1115 (1966).
2. Patrick, A. A deficiency of glucocerebrosidase in Gaucher's disease. *Biochem J.* **97,** 17C–18C (1965).
3. Berg-Fussman, A., Grace, M. E., Ioannou, Y. & Grabowski, G. A. Human acid beta-glucosidase. N-glycosylation site occupancy and the effect of glycosylation on enzymatic activity. *J. Biol. Chem.* **268,** 14861–6 (1993).
4. Reczek, D. *et al.* LIMP-2 Is a Receptor for Lysosomal Mannose-6-Phosphate-Independent Targeting of β-Glucocerebrosidase. *Cell* **131,** 770–783 (2007).
5. Zunke, F. *et al.* Characterization of the complex formed by β-glucocerebrosidase and the lysosomal integral membrane protein type-2. *Proc. Natl. Acad. Sci.* **113,** 3791–3796 (2016).
6. Aerts, J. M. *et al.* Glucocerebrosidase, a lysosomal enzyme that does not undergo oligosaccharide phosphorylation. *Biochim. Biophys. Acta* **964,** 303–8 (1988).
7. Saftig, P. & Klumperman, J. Lysosome biogenesis and lysosomal membrane proteins: trafficking meets function. *Nat. Rev. Mol. Cell Biol.* **10,** 623–635 (2009).
8. Dvir, H. *et al.* X-ray structure of human acid-β-glucosidase, the defective enzyme in Gaucher disease. *EMBO Rep.* **4,** 704–709 (2003).
9. Lieberman, R. L. A Guided Tour of the Structural Biology of Gaucher Disease: Acid-β-Glucosidase and Saposin C. *Enzyme Res.* **2011,** 973231 (2011).
10. Brumshtein, B. *et al.* Crystal structures of complexes of N-butyl- and N-nonyl-deoxynojirimycin bound to acid beta-glucosidase: insights into the mechanism of chemical chaperone action in Gaucher disease. *J. Biol. Chem.* **282,** 29052–8 (2007).
11. E. Beutler, G. A. G. in *C.R. Scriver,W.S. Sly, D. Valle (Eds.), The Metabolic and Molecular Bases of Inherited Disease, 8th ed.* 3635–3668 (McGraw-Hill, New York, 2001).
12. Hruska, K. S., LaMarca, M. E., Scott, C. R. & Sidransky, E. Gaucher disease: mutation and polymorphism spectrum in the glucocerebrosidase gene (GBA). *Hum. Mutat.* **29,** 567–583 (2008).
13. Tan, Y. L. *et al.* ERdj3 is an endoplasmic reticulum degradation factor for mutant glucocerebrosidase variants linked to Gaucher's disease. *Chem. Biol.* **21,** 967–76 (2014).
14. Schmitz, M., Alfalah, M., Aerts, J. M. F. G., Naim, H. Y. & Zimmer, K.-P. Impaired trafficking of mutants of lysosomal glucocerebrosidase in Gaucher's disease. *Int. J. Biochem. Cell Biol.* **37,** 2310–20 (2005).
15. Wei, R. R. *et al.* X-ray and Biochemical Analysis of N370S Mutant Human Acid -Glucosidase. *J. Biol. Chem.* **286,** 299–308 (2011).
16. van Weely, S. *et al.* Role of pH in determining the cell-type-specific residual activity of glucocerebrosidase in type 1 Gaucher disease. *J. Clin. Invest.* **91,** 1167–75 (1993).
17. Sawkar, A. R. *et al.* Chemical chaperones increase the cellular activity of N370S beta -glucosidase: a therapeutic strategy for Gaucher disease. *Proc. Natl. Acad. Sci. U. S. A.* **99,** 15428–33 (2002).
18. Grace, M. E., Graves, P. N., Smith, F. I. & Grabowski, G. A. Analyses of catalytic activity and inhibitor binding of human acid beta-glucosidase by site-directed mutagenesis. Identification of residues critical to catalysis and evidence for causality of two Ashkenazi Jewish Gaucher disease type 1 mutations. *J. Biol. Chem.* **265,** 6827–35 (1990).
19. Ohashi, T. *et al.* Characterization of human glucocerebrosidase from different mutant alleles. *J. Biol. Chem.* **266,** 3661–7 (1991).
20. Jonsson, L. M. V *et al.* Biosynthesis and maturation of glucocerebrosidase in Gaucher fibroblasts. *Eur. J. Biochem.* **164,** 171–179 (1987).
21. Ferraz, M. J. *et al.* Gaucher disease and Fabry disease: New markers and insights in pathophysiology for two distinct glycosphingolipidoses. *Biochim. Biophys. Acta - Mol. Cell Biol. Lipids* **1841,** 811–825 (2014).
22. Dekker, N. *et al.* Elevated plasma glucosylsphingosine in Gaucher disease: relation to phenotype, storage cell markers, and therapeutic response. *Blood* **118,** e118–e127 (2011).
23. Siebert, M., Sidransky, E. & Westbroek, W. Glucocerebrosidase is shaking up the synucleinopathies. *Brain* **137,** 1304–1322 (2014).
24. Barton, N. W. *et al.* Replacement therapy for inherited enzyme deficiency--macrophage-targeted glucocerebrosidase for Gaucher's disease. *N. Engl. J. Med.* **324,** 1464–70 (1991).
25. Desnick, R. J. & Schuchman, E. H. Enzyme Replacement Therapy for Lysosomal Diseases: Lessons from 20 Years of Experience and Remaining Challenges. *Annu. Rev. Genomics Hum. Genet.* **13,** 307–335 (2012).
26. Zechel, D. L. *et al.* Iminosugar Glycosidase Inhibitors: Structural and Thermodynamic Dissection of the Binding of Isofagomine and 1-Deoxynojirimycin to β-Glucosidases. *J. Am. Chem. Soc.* **125,** 14313–14323 (2003).
27. Steet, R. A. *et al.* The iminosugar isofagomine increases the activity of N370S mutant

acid beta-glucosidase in Gaucher fibroblasts by several mechanisms. *Proc. Natl. Acad. Sci. U. S. A.* **103,** 13813–8 (2006).

28. Benito, J. M., García Fernández, J. M. & Ortiz Mellet, C. Pharmacological chaperone therapy for Gaucher disease: a patent review. *Expert Opin. Ther. Pat.* **21,** 885–903 (2011).

29. Jung, O., Patnaik, S., Marugan, J., Sidransky, E. & Westbroek, W. Progress and potential of non-inhibitory small molecule chaperones for the treatment of Gaucher disease and its implications for Parkinson disease. *Expert Rev. Proteomics* **13,** 471–9 (2016).

30. Walvoort, M. T. C. *et al.* Tuning the leaving group in 2-deoxy-2-fluoroglucoside results in improved activity-based retaining β-glucosidase probes. *Chem. Commun.* **48,** 10386–10388 (2012).

31. Li, K.-Y. *et al.* Synthesis of Cyclophellitol, Cyclophellitol Aziridine, and Their Tagged Derivatives. *European J. Org. Chem.* **2014,** 6030–6043 (2014).

32. Kallemeijn, W. W. *et al.* Novel activity-based probes for broad-spectrum profiling of retaining β-exoglucosidases in situ and in vivo. *Angew. Chemie - Int. Ed.* **51,** 12529–12533 (2012).

33. Abian, O. *et al.* Therapeutic strategies for Gaucher disease: miglustat (NB-DNJ) as a pharmacological chaperone for glucocerebrosidase and the different thermostability of velaglucerase alfa and imiglucerase. *Mol. Pharm.* **8,** 2390–7 (2011).

34. Lieberman, R. L., D'aquino, J. A., Ringe, D. & Petsko, G. A. Effects of pH and iminosugar pharmacological chaperones on lysosomal glycosidase structure and stability. *Biochemistry* **48,** 4816–27 (2009).

35. LASCH, J., BESSMERTNAYA, L., KOZLOV, L. V. & ANTONOV, V. K. Thermal Stability of Immobilized Enzymes Circular Dichroism, Fluorescence and Kinetic Measurements of alpha-Chymotrypsin Attached to Soluble Carriers. *Eur. J. Biochem.* **63,** 591–598 (1976).

36. Qi, X. & Grabowski, G. A. Acid β-Glucosidase: Intrinsic Fluorescence and Conformational Changes Induced by Phospholipids and Saposin C[†]. *Biochemistry* **37,** 11544–11554 (1998).

37. MITCHELL, S. A Photo-electric Method for Measuring Circular Dichroism. *Nature* **166,** 434–435 (1950).

38. Kim, J. H., Sumranjit, J., Kang, H. J. & Chung, S. J. Discovery of coumarin derivatives as fluorescence acceptors for intrinsic fluorescence resonance energy transfer of proteins. *Mol. BioSyst.* **10,** 30–33 (2014).

39. Celej, M. S., Montich, G. G. & Fidelio, G. D. Protein stability induced by ligand binding correlates with changes in protein flexibility. *Protein Sci.* **12,** 1496–1506 (2003).

40. Van Weely, S. *et al.* Function of oligosaccharide modification in glucocerebrosidase, a membrane-associated lysosomal hydrolase. *Eur. J. Biochem.* **191,** 669–77 (1990).

41. Witte, M. D. *et al.* Ultrasensitive in situ visualization of active glucocerebrosidase molecules. *Nat. Chem. Biol.* **6,** 907–913 (2010).

42. Aerts, J. M. *et al.* The occurrence of two immunologically distinguishable beta-glucocerebrosidases in human spleen. *Eur. J. Biochem.* **150,** 565–74 (1985).

43. Aerts, J. M. *et al.* A procedure for the rapid purification in high yield of human glucocerebrosidase using immunoaffinity chromatography with monoclonal antibodies. *Anal. Biochem.* **154,** 655–63 (1986).

44. Jung, O., Patnaik, S., Marugan, J., Sidransky, E. & Westbroek, W. Progress and potential of non-inhibitory small molecule chaperones for the treatment of Gaucher disease and its implications for Parkinson disease. *Expert Rev. Proteomics* **13,** 471–479 (2016).

45. Maegawa, G. H. B. *et al.* Identification and Characterization of Ambroxol as an Enzyme Enhancement Agent for Gaucher Disease. *J. Biol. Chem.* **284,** 23502–23516 (2009).

46. Babajani, G., Tropak, M. B., Mahuran, D. J. & Kermode, A. R. Pharmacological chaperones facilitate the post-ER transport of recombinant N370S mutant β-glucocerebrosidase in plant cells: evidence that N370S is a folding mutant. *Mol. Genet. Metab.* **106,** 323–9 (2012).

47. Zimran, A., Altarescu, G. & Elstein, D. Pilot study using ambroxol as a pharmacological chaperone in type 1 Gaucher disease. *Blood Cells, Mol. Dis.* **50,** 134–137 (2013).

48. Bendikov-Bar, I., Maor, G., Filocamo, M. & Horowitz, M. Ambroxol as a pharmacological chaperone for mutant glucocerebrosidase. *Blood Cells. Mol. Dis.* **50,** 141–5 (2013).

49. Narita, A. *et al.* Ambroxol chaperone therapy for neuronopathic Gaucher disease: A pilot study. *Ann. Clin. Transl. Neurol.* **3,** 200–215 (2016).

50. Yadav, A. K. *et al.* Fluorescence-quenched substrates for live cell imaging of human glucocerebrosidase activity. *J. Am. Chem. Soc.* **137,** 1181–9 (2015).

51. Fontana, A. *et al.* Probing protein structure by limited proteolysis. *Acta Biochim. Pol.* **51,** 299–321 (2004).

52. Liou, B. *et al.* Analyses of variant acid beta-glucosidases: effects of Gaucher disease mutations. *J. Biol. Chem.* **281,** 4242–53 (2006).

53. Miocić, S. *et al.* Identification and functional characterization of five novel mutant alleles in 58 Italian patients with Gaucher disease type 1. *Hum. Mutat.* **25,** 100 (2005).

54. Neumann, J. *et al.* Glucocerebrosidase mutations in clinical and pathologically proven Parkinson's disease. *Brain* **132,** 1783–94 (2009).

55. Grace, M. E., Desnick, R. J. & Pastores, G. M. Identification and expression of acid beta-glucosidase mutations causing severe type 1 and neurologic type 2 Gaucher disease in non-Jewish patients. *J. Clin. Invest.* **99,** 2530–7 (1997).

56. Ben Bdira, F. *et al.* Hydrophobic Interactions Contribute to Conformational Stabilization of Endoglycoceramidase II by Mechanism-Based Probes. *Biochemistry* **55,** 4823–35 (2016).

57. Rempel, B. P., Tropak, M. B., Mahuran, D. J. & Withers, S. G. Tailoring the specificity and reactivity of a mechanism-based inactivator of glucocerebrosidase for potential therapeutic applications. *Angew. Chem. Int. Ed. Engl.* **50,** 10381–3 (2011).
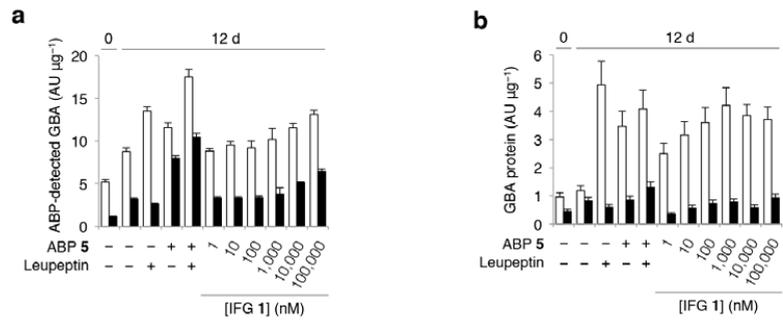
Supplemental data

Figure S1. *In situ* GBA stabilization by IFG. Wild-type GBA (*open columns*) and N370S GBA (*closed columns*) fibroblasts were grown for 12 days in the absence or presence of incubated with leupeptin, ABP **5**, both, or 0.001–100 μM IFG **1**. (**a**) Quantification of ABP-emitted fluorescence from *in vitro* ABP **4**-labeled controls, leupeptin– and IFG **1**-treated cells, compared to fluorescence of *in situ* ABP **5**-labeled GBA. (**b**) Quantification of GBA peptide after treatment. All data expressed as average of *n* = 2, ± SD.
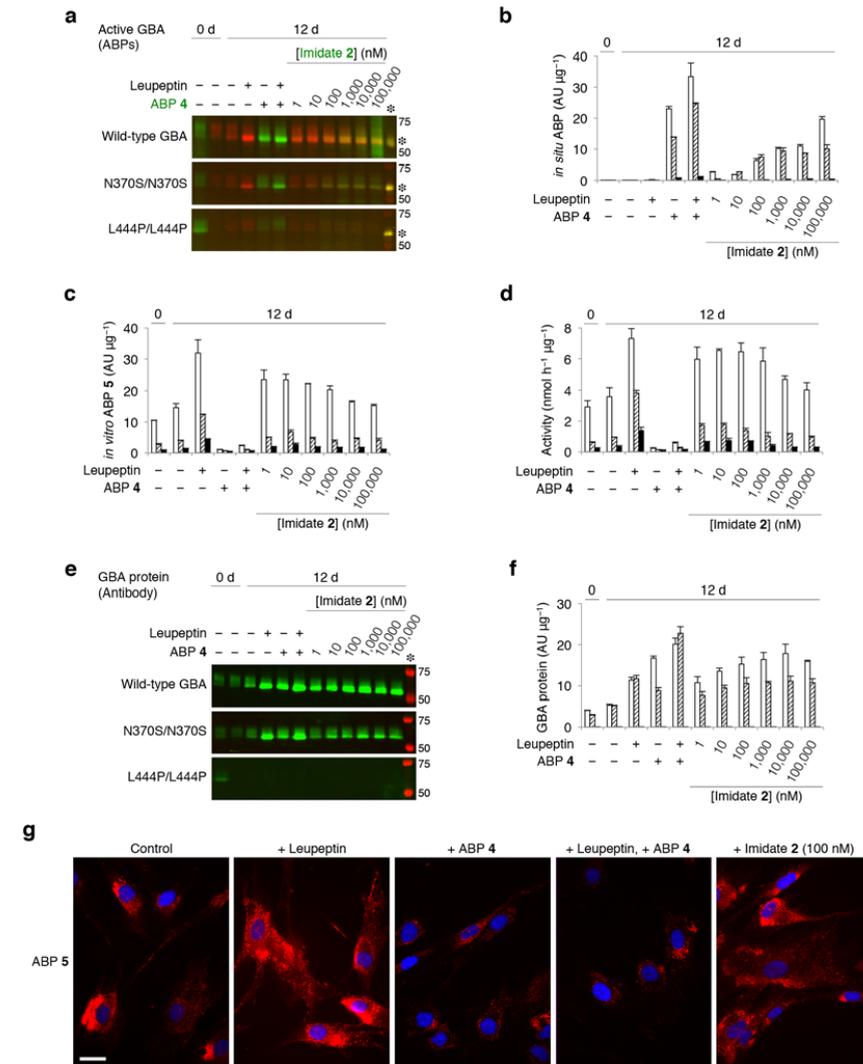

Figure S2. *In situ* stabilization of GBA by imidate 2. (**a**) Wild-type (*top*), N370S (*middle*) and L444P GBA (*bottom row*) Gaucher patient fibroblasts were grown for 12 days in the absence or presence of leupeptin, green β-epoxide **4**, both, or 0.001–100 μM green imidate **2**. Gel depicts *in situ* labeling of active GBA by imidate **2** or β-epoxide **4** followed by *in vitro* labeling of residual active GBA molecules with excess red ABP **5**. Equal green– and red fluorescence yields yellow overlay; fluorescence calibrated with 50 fmol equimolar ABP **4**– and **5**-labeled imiglucerase present on each SDS-PAGE gel (*asterisk*). (**b**) Quantification of *in situ* GBA labeling by imidate **2** or ABP **4**, with wild-type (*white columns*), N370S (*dashed columns*) and L444P (*black*) fibroblasts. (**c**) Quantification of *in vitro* labeling of residual active GBA molecules with excess ABP **5**. (**d**) Residual GBA-associated β-glucosidase activity. (**e**) Detection of GBA protein (*green*) by Western immunoblotting of gels depicted in **a** (molecular weight ladder in *red*) of fibroblasts with wild-type (*top*), N370S (*middle*) and L444P GBA (*bottom row*),

after aforementioned treatments, *vide supra*. (**f**) Quantification of GBA protein levels. Data expressed as mean of duplicate quantifications ± SD. (**g**) Fluorescence micrographs depicting red-fluorescent ABP **5**-labeling of residual active N370S GBA molecules in GD patient fibroblasts. From *left* to *right*: cells grown for 12 days in absence of additives, with leupeptin, with 100 nM green fluorescent ABP **4**, both, or with 100 nM imidate **2**. GBA was post-labeled for 2 h with 10 nM ABP **5**. Scale-bar represents 25 μm. All data expressed as average of *n* = 2, ± SD.
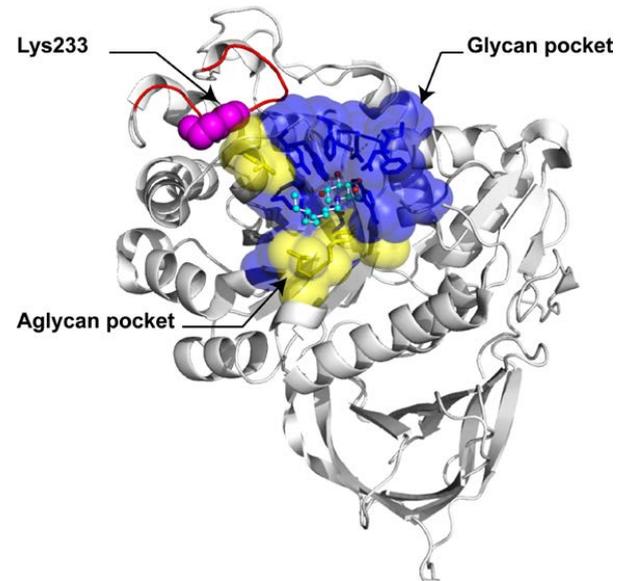

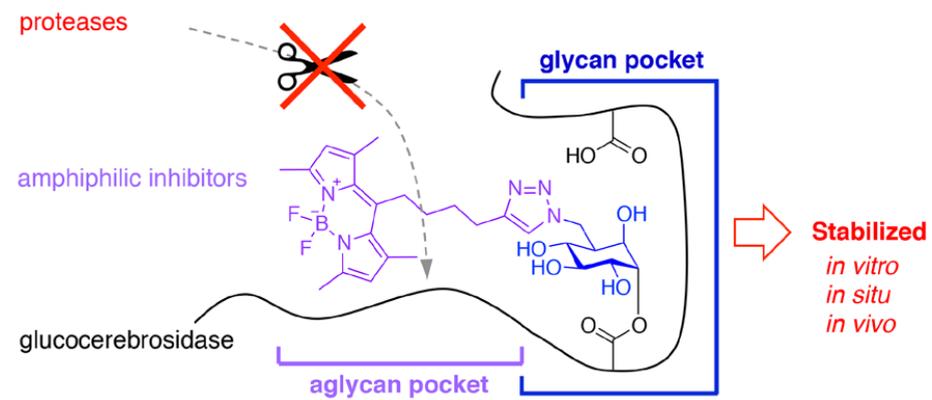**Figure S3. GBA structure and the trypsin cutting site.**

Figure S4. Proposed graphical abstract.

3

Chemical probing of the catalytic pocket of glucocerebrosidase with photoactivatable glucosylceramide and activity-based probes

Chemical probing of the catalytic pocket of glucocerebrosidase with photoactivatable glucosylceramide and activity-based probes

Based on

Saskia Oussoren[1], Jasper Wermink[1], Jianbing Jang[2], Herman S. Overkleeft[2],
Johannes M. Aerts[1], Per Haberkant[1]

[1]Dept. of Medical Biochemistry, LIC, Leiden University
[2]Dept. of Bio-Organic Synthesis, LIC, Leiden University

Manuscript in preparation

Abstract

Glucocerebrosidase (GBA) is the lysosomal retaining β-glucosidase degrading glucosylceramide (GlcCer) and glucosylated cholesterol (GlcChol). Deficiency of GBA causes Gaucher disease. Carriers of this disorder are at increased risk for alpha-synucleinopathies. Information on structure-function relationships in GBA stems from conventional enzymology and crystallography. To extend insight, we investigated human GBA with two new classes of chemical biology tools: pacGlcCer and fluorescent β-glucose configured cyclophellitols binding to the catalytic nucleophile residue E340 in mechanism-based manner (ABP). We here demonstrate that pacGlcCer binds to the catalytic pocket of GBA. Binding requires correctly folded, active enzyme and follows the pH optimum of enzymatic activity. We show that two different kinds of ABP, the irreversible inhibitors cyclophellitol and conduritol B-epoxide and the reversible inhibitor AMP-DNM compete the binding of pacGlcCer. Likewise, pacGlcCer is competed by the substrates glucosylsphingosine, GlcChol and 4-methylumbelliferyl-β-glucose. Known lipid acceptors in the transglucosylation reaction of GBA (cholesterol, retinol and sphingosine) also inhibit binding of pacGlcCer but not that of ABP. In conclusion, newly available probes offer novel possibilities to investigate the catalytic pocket of GBA.

Introduction

Glucocerebrosidase (GBA) is a retaining β-glucosidase encoded by the *Gba* gene at locus q21 of chromosome 1[1,2]. It is synthesized as 497 amino acid polypeptide acquiring 4 N-linked glycans[3–5]. Binding of GBA to LIMP-2 (lysosomes integral membrane protein 2) governs transport to lysosomes independent of the mannose-6-phosphate receptor system[6–10]. In the acid lysosome, GBA cleaves the glycosphingolipid β-D-glucosyl-ceramide (GlcCer) to ceramide (Cer), an essential step in glycosphingolipid turnover[11]. Mutations in the *Gba* gene cause Gaucher disease (GD)[12]. GBA has a catalytic and presumed folding domain[13,14]. Mutations in the latter domain, such as L444P, may impair folding and result in subsequent proteasome-mediated degradation[15,16]. In contrast, the common N370S substitution in GBA is close to the catalytic pocket and reported to affect kinetic parameters, pH optimum and lysosomal stability[14,17–19]. GBA is activated by saposin C and inherited deficiency of this activator protein also leads to lysosomal GlcCer accumulation as well as GD-like disease manifestations[20–22]. Defects in LIMP-2 cause secondary deficiency of GBA, but patients with the associated disease (action myoclonus renal failure syndrome; AMRF) show no GD-like symptoms[23]. The clinical presentation of GD is heterogeneous, ranging from skin defects incompatible with terrestrial life to an almost asymptomatic course of disease[12]. The correlation between *Gba* genotype and phenotypic manifestations of GD patients is limited. Discordant monozygotic GD twins illustrate most prominently the existence of elusive disease modifiers[24,25]. Carriers of mutant *Gba* alleles do not develop GD but show a significantly increased risk for Parkinsonism and Lewy-body dementia[26]. Prominent in symptomatic GD patients are GlcCer-laden macrophages (Gaucher cells)[27,28]. These alternatively activated lipid-laden macrophages are thought to underlie symptoms like splenomegaly and hepatomegaly[12]. As recently recognized, the catalytic functions of GBA may be broader as hitherto assumed. Tissues contain β-D-glucosyl-cholesterol (GlcChol) which is a substrate for GBA[29]. At normal conditions GBA degrades GlcChol, but during excessive accumulation of cholesterol in lysosomes, as in Niemann Pick type C, GBA can generate GlcChol via transglucosylation[29]. An effective treatment for non-neuronopathic (type 1) GD is enzyme replacement therapy (ERT), based on two-weekly intravenous administration of modified human recombinant GBA to supplement macrophages with enzyme[30]. ERT results in reversal of organomegaly and hematological complications as well as stabilization of skeletal disease[31,32]. An alternative registered treatment is substrate reduction therapy (SRT), based on oral administration of an inhibitor of glycosphingolipid biosynthesis; two drugs (*Miglustat, Eliglustat*) have been registered for SRT[33–36].

The clinical interest in GBA has stimulated fundamental investigations on the enzyme, including its catalytic pocket. For catalysis, GBA employs the double-displacement mechanism with E340 as nucleophile E235 and acid/base[37]. As reaction intermediate glucose becomes covalently linked to E340, to be released by attack of a hydroxide. Cyclophellitol irreversibly inhibits GBA by forming a permanent conjugate with E340[38]. Cyclophellitol scaffolds are used in functionalized activity-based probes, allowing *in situ* visualization of GBA and probing of the enzyme's catalytic pocket[39,40]. One class of such ABPs, cyclophellitol-epoxides, requires correctly folded, active enzyme molecules for labeling[40].

Crystallography has been used to study the catalytic pocket of GBA[13,14]. Although this increased knowledge on structural determinants relevant for the interaction of enzyme and sugar-moiety of substrate, it did not shed light on the aglycon interaction. Only indirect information on this has been acquired by studies on inhibitory effects of lipids[19]. More recently developed photoactivatable lipid analogs can be activated by UV light to form a covalent

linkage to their protein-binding partners[41]. Lipids with small photoactivatable groups, limiting interference with the physicochemical properties of the native molecule, such as diazirine-functionalized and clickable fatty acid (pacFA), sphingosine (pacSph) and GlcCer (pacGlcCer) are available[42,43]. Following UV light-mediated binding to the protein, a fluorescent detection group can be installed by click chemistry[41].

In theory, pacGlcCer may be very suitable to study features of the catalytic pocket of GBA, including the aglycon binding site. Here we report the probing of human GBA with pacGlcCer. We demonstrate that specific binding of pacGlcCer to GBA occurs via the catalytic pocket. The interaction depends on correctly folded, active enzyme and follows the pH optimum of enzymatic activity. It is competed by the reversible inhibitor AMP-DNM and the irreversible inhibitors conduritol β-epoxide and cyclophellitol[44]. Prior binding of ABPs to GBA also prohibits pacGlcCer labeling. Known acceptors in transglucosylation like sphingosine and retinol but in particular cholesterol[29,45], also reduce the binding of pacGlcCer to GBA. Thus, the catalytic pocket of GBA can be probed with sugar analogues (ABPs) and with the lipid analogue pacGlcCer, for example to monitor the stabilizing effects of the chaperones N-butyldeoxynojirimycin and Ambroxol.

Results

Labeling of GBA with pacGlcCer.
We first examined the feasibility of labeling GBA with pacGlcCer. Pure recombinant enzyme was incubated with pacGlcCer, photo-crosslinked, ligated with fluorophore by click chemistry and subjected to gel electrophoresis and fluorescence scanning (see scheme 1). Increasing the concentration of pacGlcCer led to increased labeling, the maximum reached at 250 pmol per incubation (16,7 µM) (figure 1a). Denaturation of GBA prohibited labeling by pacGlcCer (fig 1a). Variation of pH of the incubation revealed optimal labeling at pH 5.2, coinciding with the pH optimum of enzymatic activity of GBA towards 4-methylumbelliferyl-β-D-glucose (4MU-β-D-Glc)[39] (fig 1b). Next, we examined competition of labeling by substrates of GBA: 4MU-β-D-Glc and glucosylsphingosine (GlcSph) (fig 1c). Partial competition of labeling was observed at high substrate concentrations, most prominently with GlcSph. The competitive inhibitor N-adamantanemethyloxypentyl-1-deoxynojirimycin (AMP-DNM, IC$_{50}$ 200 nM) led at 500 µM to 73 % reduction of pacGlcCer labeling of GBA. Next, we studied whether pacGlcCer serves as substrate for GBA. For this, the lipid was incubated with enzyme and formation of pacCer was detected after click chemistry (fig 1d). We finally compared the labeling of GBA by pacGlcCer, pacCer and pacSpho (fig 1e). The most efficient labeling by far was observed with pacGlcCer.

Competition of labeling by sugar analogue inhibitors.
Competition of pacGlcCer labeling of GBA by the irreversible inhibitors cyclophellitol and conditurol β-epoxide (CBE) was prominent following 30 minutes pre-incubation of enzyme with inhibitors (fig 2 a, b). This finding suggests that occupancy of E340 by the relatively small

inhibitors interferes markedly with the interaction of pacGlcCer and GBA. To further substantiate this, we pre-incubated GBA with increasing concentrations of the ABP **1** and ABP **2**. After incubation, click chemistry and gel electrophoresis, fluorescence scanning was performed at respective wavelengths following detection of bound ABP as well as bound pacGlcCer (fig 2c, d).

Efficiency of covalent labeling of GBA with pacGlcCer and ABP.
To assess the percentage of GBA molecules to which pacGlcCer was covalently bound we determined residual enzyme activity following labeling at optimal conditions as described in Methods. A very high residual enzyme activity was noted at saturating pacGlcCer concentrations (fig 3), suggesting that the efficiency of photo-cross linking of diazirine to protein is not very high. In sharp contrast, the cross-linking of ABP to the catalytic nucleophile E340 of GBA is very efficient and leads to complete loss of enzyme activity at low concentrations (fig 3)[39].

Reaction mechanism pacGlcCer
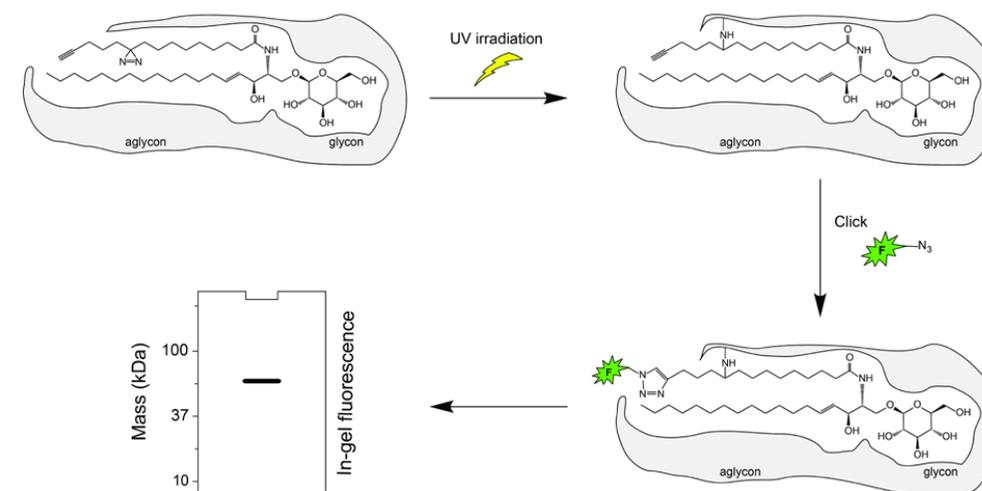
Scheme 1. Hypothetical pacGlcCer binding to GBA. Bifunctional GlcCer is covalently linked to GBA by UV-induced crosslinking. Subsequently, click chemistry is applied to label the alkyne group of the cross-linked GlcCer with azide-conjugated Cy5 (F-N3). PacGlcCer-modified GBA protein is detected by in-gel fluorescence.
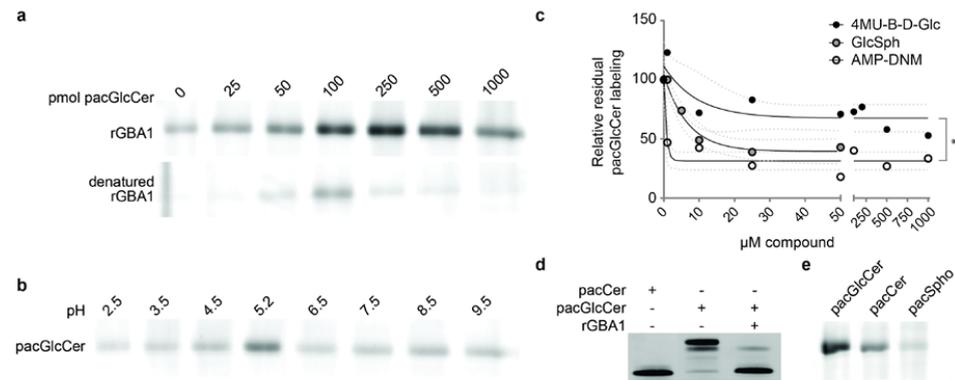
Figure 1. Binding of pacGlcCer to GBA. (a) Titration of pacGlcCer. 0.5 µg GBA was incubated with 0-1000 pmol pacGlcCer for 15 minutes on ice after which samples were UV irradiated. Lower panel: impact of prior denaturation of GBA on pacGlcCer labeling; **(b)** pH dependence of pacGlcCer labeling of GBA. For incubations McIlvaine buffer with taurocholate and Triton X-100 was used at indicated pH values. GBA was incubated with 250 pmol pacGlcCer; **(c)** Competition of pacGlcCer labeling by 4MU-β- D-Glc, GlcSph and AMP-DNM. GBA was incubated on ice simultaneously with pacGlcCer and compound. Data, indicated as one phase exponential decay with 90% confidence interval, were analyzed by the Kruskal-Wallis test and subsequent Dunn's multiple comparison test (p = 0.0130 for 4MU-β-D-Glc vs. AMP-DNM) and are representative for multiple experiments; **(d)** GBA degradation of pacGlcCer to pacCer as visualized by HPTLC; **(e)** Comparative labeling of GBA by pacGlcCer, pacCer and pacSpho.
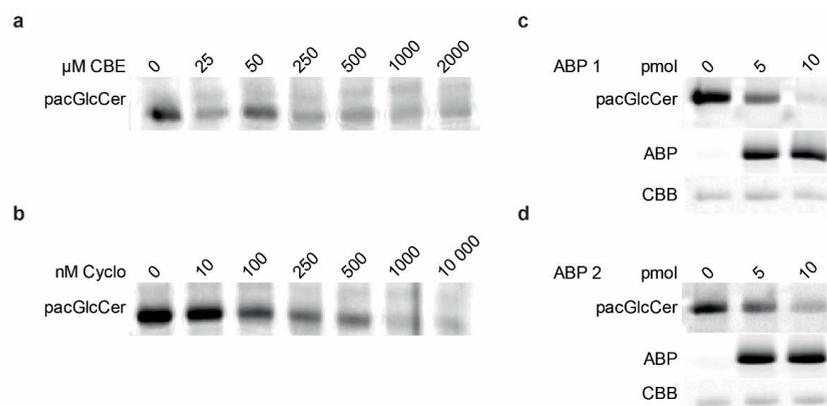

Figure 2. Prevention of pacGlcCer binding to GBA by irreversible inhibitors. Inhibition of pacGlcCer labeling by prior labeling with **(a)** CBE; **(b)** cyclophellitol (cyclo); **(c)** ABP **1** (epoxide); **(d)** ABP **2** (aziridine). Samples were incubated with CBE or cyclophellitol for 30 minutes at 37 °C before incubation on ice for 15 minutes with pacGlcCer. Incubation with ABP was

performed for 15 minutes on ice simultaneously with pacGlcCer. ABP and pacGlcCer fluorescence were visualized separately. CBB: Coomassie Brilliant Blue protein stain.
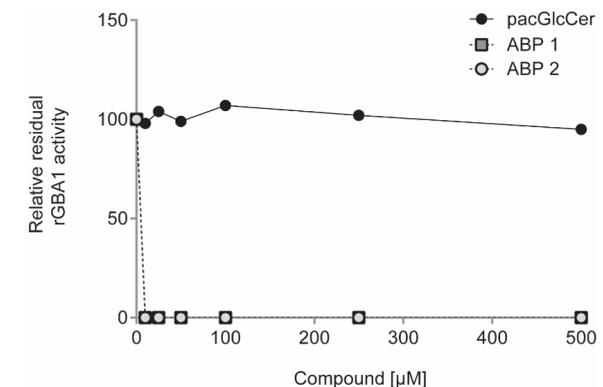

Figure 3. Inhibition of GBA activity by pacGlcCer, ABP 1 and ABP 2. GBA was incubated on ice for 15 minutes with pacGlcCer, ABP **1** or **2**. Next, all samples were UV irradiated for 10 minutes and incubated with 4MU-β-D-Glc for 30 minutes at 37 °C after which the reaction was stopped and released 4MU was measured. Data are indicated as residual GBA activity relative to incubation without added compound.

Competition of pacGlcCer interaction with GBA by lipid acceptors in transglucosylation.

Since GBA uses acceptors in transglucosylation, we compared the effects of such compounds (cholesterol, retinol and sphingosine) on enzyme labeling with pacGlcCer and ABP **1**. For this, enzyme was first shortly exposed to these lipids after which pacGlcCer was added, the mixture incubated and labeled GBA detected (fig 4). Competition of pacGlcCer labeling of GBA was exerted by all lipids tested, being most prominent for cholesterol (fig 4a, b). Of note, as shown in figure 4c, ABP **1** labeling was not competed by the lipid acceptors retinol, sphingosine or cholesterol (fig 4c, d).

Discussion

We studied the potential value of a photoactivatable GlcCer analogue, pacGlcCer, as additional tool to probe the catalytic pocket of GBA. Our investigation revealed that the catalytic pocket of GBA is labeled with high affinity by pacGlcCer. Maximal labeling by pacGlcCer was already reached at 250 pmol/15 µl (16,7 µM). At the same concentration the labeling of enzyme by pacCer and pacSpho was far from maximal. GBA is labeled by pacGlcCer in specific manner via its catalytic pocket as indicated by the following observations. Labeling is most efficient at the pH optimum of activity (pH 5.2) and denaturation of GBA prohibits labeling. GBA substrates glucosylsphingosine and 4-methylumbelliferyl-β-D-glucose compete labeling. The hydrophobic iminosugar AMP-DNM, a competitive inhibitor, also competes the

cross-linking of pacGlcCer to GBA. Importantly, prior incubation of GBA with two small irreversible inhibitors, conduritol β-epoxide and cyclophellitol, as well as two cyclophellitol-type activity based probes with tagged fluorophores almost completely prevents labeling of enzyme with pacGlcCer. This indicates that occupancy of the catalytic nucleophile E340 and adjacent glycon binding site negatively impacts on the interaction of pacGlcCer with the enzyme. Thus, pacGlcCer seems to preferentially interact with GBA via the catalytic pocket. Indeed, pacGlcCer is found to be an excellent substrate for GBA.
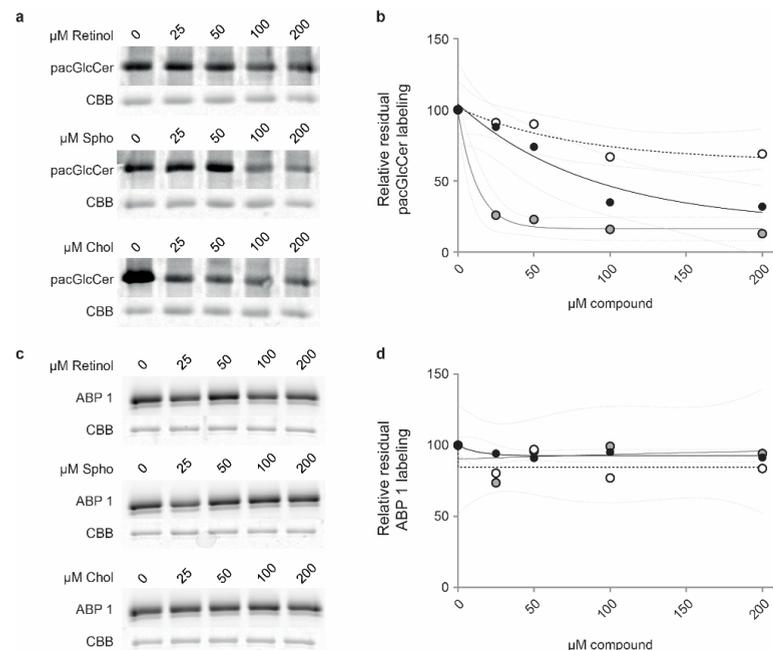

Figure 4. Competition of pacGlcCer labeling by lipid acceptors in transglucosylation. Competition of pacGlcCer labeling by retinol (open symbol), sphingosine (Spho) (closed symbol) and cholesterol (Chol) (grey symbol): **(a)** Gel – fluorescence scan and subsequent CBB staining; **(b)** Quantification (Cy5 fluorescence without added lipid is set at 100 %). Shown result is representative for multiple independent experiments and is indicated as one phase exponential decay with 90 % confidence interval. Kruskal-Wallis test and subsequent Dunn's multiple comparison test did not reveal significant difference between the three competitors; Spho vs. Chol p = 0.4674 and Retinol vs. Chol p = 0.1408, Spho vs. Retinol p > 0.99. **(c)** Competition of ABP **1** labeling by retinol, sphingosine and cholesterol. **(d)** Quantification of c.

We comparatively studied the labeling of GBA by fluorescent ABPs[37,39]. An enormous advantage of ABPs to pacGlcCer is found in the efficiency of labeling. All active GBA molecules are labeled by ABPs at very low concentrations whereas the efficiency of cross-linking

pacGlcCer to GBA is low at saturating lipid concentration. Following incubation with excessive amounts of pacGlcCer less than 5 % of enzyme activity was lost. The intensity of protein-bound fluorescence per mg GBA was consistently far less with pacGlcCer (Cy5 tagged) than ABP labeling with BODIPY-FL. The low efficiency of UV-mediated cross-linking of diazirine to protein has indeed been reported earlier[46]. In practice, the poor efficiency of cross-linking pacGlcCer to GBA is a major drawback because of significantly less sensitive detection which is far surpassed by ABP labeling.

Of recent interest are the hydrophobic acceptors in the newly recognized transglucosylation reactions catalyzed by GBA. Labeling of GBA with ABP is not influenced by the presence of known acceptors such as cholesterol, sphingosine or retinol, likely due to fact that bound ABP inhibitor does not overlap with the binding sites of the acceptors. In contrast to this, labeling of GBA by pacGlcCer is competed by lipid acceptors, most prominently by cholesterol and least striking retinol, coinciding with different rates of their respective transglucosylation. Thus, pacGlcCer offers a tool to identify potential acceptors in transglucosylation and could contribute to future identification of yet unknown glucosylated metabolites. Several academic researchers and pharmaceutical companies pursue the development of chemical chaperones, small glycomimetics, which would promote/stabilize folding of GBA through their transient binding within the catalytic pocket[47–49]. Another application for pacGlcCer labeling of GBA might be found in the probing of stabilization of GBA conformation by potential small compound chaperones as for example N-butyldeoxynojirimycin (NB-DNJ) and Ambroxol[50–56]. In conclusion, our investigation provides evidence that β-glucose-configured cyclophellitol-type ABPs and pacGlcCer offer novel possibilities to investigate the catalytic pocket of GBA.

Materials and Methods.

Materials.
Recombinant human GBA (Cerezyme[TM]) was a gift from Sanofi-Genzyme (Cambridge, MA, USA). Chemicals were purchased from Sigma-Aldrich if not indicated otherwise. Conduritol β-epoxide (CBE) was from Enzo Life Sciences, ABP MDW933 (epoxide) (**1**) and ABP JJB70 (aziridine) (**2**) (scheme 2)[39,40], AMP-DNM[57], N-butyldeoxynojirimycin (NB-DNJ), cyclophellitol and GlcChol were synthesized at the Leiden Institute of Chemistry[29,39]. Retinol and cholesterol were from Sigma-Aldrich. The fluorogenic substrate 4-methylumbelliferyl-β-glucose was from Glycosynth (Warrington, UK). Glucosylsphingosine (D-glucosyl-β1-1'-D-erythrosphingosine), sphingosine, pacChol and pacGlcCer were purchased from Avanti Polar lipids (Alabaster, USA). PacCer and pacSpho were synthesized earlier[42,43]. A SpeedVac Eppendorf concentrator Plus was used to dry lipid compounds in order to dissolve them into reaction buffer. For UV irradiation (350 nm) a Caprotec Caprobox (Berlin, Germany) was used.

Methods.

GBA activity measurements.

Enzymatic activity of GBA was measured with 4-methylumbelliferyl-β-D-glucose (4MU-β-D-Glc) as described previously[58]. Briefly, enzyme was incubated for 30 minutes at 37 °C with 3.7 mM 4MU-β-D-Glc in 150 mM McIlvaine buffer (pH 5.2) with 0.1 % (v/v) Triton X-100 and 0.2 % (w/v) taurocholate. The reaction was stopped with NaOH-glycine (pH 10.3), and fluorescence was measured with a fluorimeter LS55 (Perkin-Elmer, Beaconsfield, UK) at λ_{ex} 366 nm and λ_{ex} 445 nm.

PacGlcCer labeling experiments.

Binding assays with recombinant GBA were performed at optimal conditions for enzymatic activity: 150 mM McIlvaine buffer (pH 5.2) with 0.1 % (v/v) Triton X-100 and 0.2 % (w/v) taurocholate was used as reaction buffer. For pacGlcCer binding, in a total volume of 15 μL reaction buffer, 0.5 μg GBA was incubated on ice for 15 minutes with 0-1000 pmol pacGlcCer, after which samples were UV irradiated for 10 minutes at 4 °C. Subsequently "click-mix" was added as described previously and samples were incubated in the dark at room temperature for 40 minutes[42]. If not indicated differently, 0.5 μg GBA labeling was performed with 250 pmol pac GlcCer.

To denature GBA, enzyme was boiled for 5 minutes at 100 °C. For ABP binding, 0.5 μg GBA was incubated on ice with probe (**1** or **2**). For competition experiments, 0.5 μg GBA was pre-incubated at 37 °C for 30 minutes with CBE or cyclophellitol, or without pre-incubation with ABP **1** or ABP **2**, followed by 15 minute incubation on ice with 250 pmol pac lipid.

For competition with non-covalent inhibitors, substrate and other lipids, 0.5 μg GBA was incubated for 15 minutes on ice with 250 pmol pac lipid and 4MU-β-D-Glc, AMP-DNM, GlcSph, GlcChol, retinol, sphingosine, or cholesterol in reaction buffer.

Labeling with other pac-sphingolipids and pac-cholesterol

Labeling of GBA with other pac-sphingolipids and pac-cholesterol (each 250 pmol) was performed similar to that with pacGlcCer as described above.

ABP labeling experiments

To label GBA, 0.5 μg enzyme was incubated with 10 pmol ABP for 30 minutes at 37 °C. Labeled GBA was visualized after gel electrophoresis as described below.

Gel electrophoresis and fluorescence scanning.

Samples were denatured with 5× Laemmli buffer (50 % (v/v) 1 M Tris-HCl, pH 6.8, 50 % (v/v) 100 % glycerol, 8 % (w/v) DTT, 10 % (w/v) SDS, 0.01 % (w/v) bromophenol blue), boiled for 5 minutes at 100 °C and separated by electrophoresis on 10 % (w/v) SDS-PAGE gel running at 75 V for 30 minutes and subsequently at 200 V. Wet slab-gels were scanned on fluorescence using the Typhoon Variable Mode Imager (Amersham Biosciences) using λEX 488 nm and λEM 520 nm (band pass filter 40 nm) for green fluorescent ABP **1** and **2** and λEX 635nm and λEM 670nM (band pass filter 30 nm) for Cy5 labeled pac lipids. After fluorescence scanning, SDS-PAGE gels were stained for total protein for 1 hour using Coomassie brilliant blue (CBB)-R250 and de-stained with 10 % ethanol (96%) in MilliQ water. CBB-stained gels were scanned on a BioRad Universal Hood III.
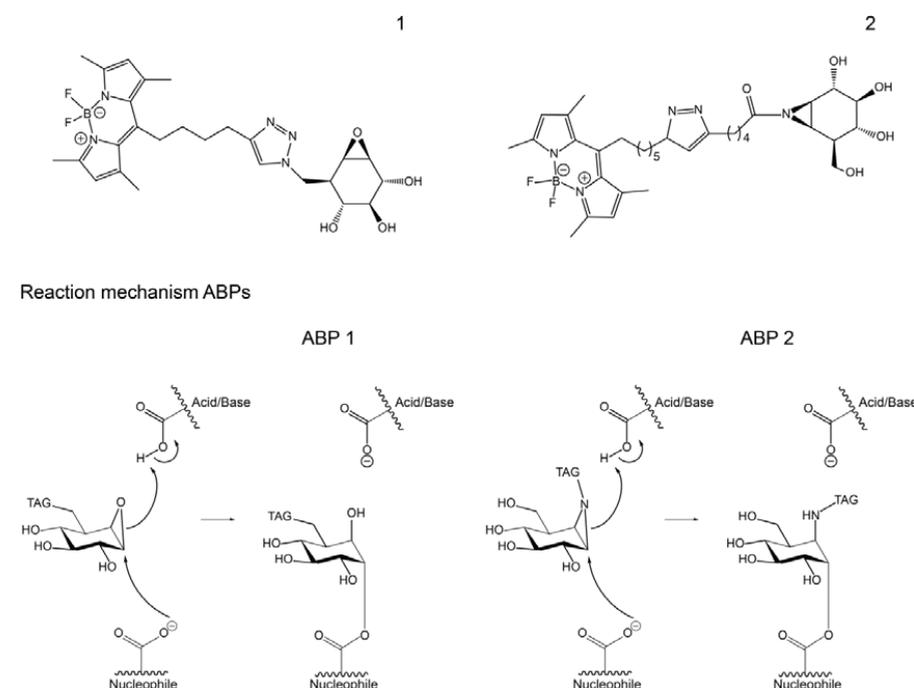
Scheme 2. Labeling of GBA with fluorophore tagged β-glucose-configured cyclophellitol-epoxide ABP 1 and cyclophellitol-aziridine ABP 2.

Scheme 2. Labeling of GBA with fluorophore tagged β-glucose-configured cyclophellitol-epoxide ABP 1 and cyclophellitol-aziridine ABP 2. Reaction mechanism involves covalent conjugation of cyclophellitol to nucleophile E340[37]. ABP-labeled protein can be quantitatively detected by in-gel fluorescence.

Degradation of pacGlcCer by GBA.

PacGlcCer was incubated for 30 minutes at 37 °C with GBA in 150 mM McIlvaine buffer (pH 5.2) with 0.1% (v/v) Triton X-100 and 0.2 % (w/v) taurocholate. Lipids were extracted, the fluorescent tag was installed by click chemistry, and subjected to HPTLC as described earlier[59]. Fluorescent pacGlcCer and the degradation product pacCer were visualized by fluorescence scanning.

Data processing and representation.

In-gel fluorescence intensities were quantified using ImageJ software (NIH, Bethesda, USA), acquired data were processed in Microsoft Excel and finally Graphpad Prism 7 (Graph Pad

Software, Inc., San Diego, USA) was used to present quantification data of Cy5 labeled pac lipids and activity measurements. ChemDraw Professional 15.0.0.106 (PerkinElmer Informatics) was used to make the chemical structures presented in scheme 1 and 2.

Statistical Analysis.
Data were analyzed by nonparametric Kruskal-Wallis test succeeded by a Dunn's multiple comparison test (fig 1c). *P* values < 0.05 were considered significant; * *P* < 0.05. Statistics were carried out using GraphPad Prism.

References

1. Kallemeijn, W. W., Witte, M. D., Wennekes, T. & Aerts, J. M. F. G. Mechanism-based inhibitors of glycosidases: design and applications. *Adv. Carbohydr. Chem. Biochem.* **71,** 297–338 (2014).
2. Horowitz, M. *et al.* The human glucocerebrosidase gene and pseudogene: structure and evolution. *Genomics* **4,** 87–96 (1989).
3. Erickson, A. H., Ginns, E. I. & Barranger, J. A. Biosynthesis of the lysosomal enzyme glucocerebrosidase. *J. Biol. Chem.* **260,** 14319–24 (1985).
4. Takasaki, S. *et al.* Structure of the N-asparagine-linked oligosaccharide units of human placental beta-glucocerebrosidase. *J. Biol. Chem.* **259,** 10112–7 (1984).
5. Berg-Fussman, A., Grace, M. E., Ioannou, Y. & Grabowski, G. A. Human acid beta-glucosidase. N-glycosylation site occupancy and the effect of glycosylation on enzymatic activity. *J. Biol. Chem.* **268,** 14861–6 (1993).
6. Reczek, D. *et al.* LIMP-2 Is a Receptor for Lysosomal Mannose-6-Phosphate-Independent Targeting of β-Glucocerebrosidase. *Cell* **131,** 770–783 (2007).
7. Zunke, F. *et al.* Characterization of the complex formed by β-glucocerebrosidase and the lysosomal integral membrane protein type-2. *Proc. Natl. Acad. Sci.* **113,** 3791–3796 (2016).
8. Aerts, J. M., Hollak, C., Boot, R. & Groener, A. Biochemistry of glycosphingolipid storage disorders: implications for therapeutic intervention. *Philos. Trans. R. Soc. Lond. B. Biol. Sci.* **358,** 905–14 (2003).
9. Jonsson, L. M. V *et al.* Biosynthesis and maturation of glucocerebrosidase in Gaucher fibroblasts. *Eur. J. Biochem.* **164,** 171–179 (1987).
10. Aerts, J. M. *et al.* Glucocerebrosidase, a lysosomal enzyme that does not undergo oligosaccharide phosphorylation. *Biochim. Biophys. Acta* **964,** 303–8 (1988).
11. Schulze, H. & Sandhoff, K. Sphingolipids and lysosomal pathologies. *Biochim. Biophys. Acta* **1841,** 799–810 (2014).
12. E. Beutler, G. A. G. in *C.R. Scriver,W.S. Sly, D. Valle (Eds.), The Metabolic and Molecular Bases of Inherited Disease, 8th ed.* 3635–3668 (McGraw-Hill, New York, 2001).
13. Dvir, H. *et al.* X-ray structure of human acid-β-glucosidase, the defective enzyme in Gaucher disease. *EMBO Rep.* **4,** 704–709 (2003).
14. Wei, R. R. *et al.* X-ray and Biochemical Analysis of N370S Mutant Human Acid -Glucosidase. *J. Biol. Chem.* **286,** 299–308 (2011).
15. Ohashi, T. *et al.* Characterization of human glucocerebrosidase from different mutant alleles. *J. Biol. Chem.* **266,** 3661–7 (1991).
16. Zimmer, K. P. *et al.* Intracellular transport of acid beta-glucosidase and lysosome-associated membrane proteins is affected in Gaucher's disease (G202R mutation). *J Pathol* **188,** 407–414 (1999).
17. Gatt, S., Dinur, T., Osiecki, K., Desnick, R. J. & Grabowski, G. A. Use of activators and inhibitors to define the properties of the active site of normal and Gaucher disease lysosomal beta-glucosidase. *Enzyme* **33,** 109–19 (1985).
18. van Weely, S. *et al.* Role of pH in determining the cell-type-specific residual activity of glucocerebrosidase in type 1 Gaucher disease. *J. Clin. Invest.* **91,** 1167–75 (1993).
19. Grace, M. E., Newman, K. M., Scheinker, V., Berg-Fussman, A. & Grabowski, G. A. Analysis of human acid beta-glucosidase by site-directed mutagenesis and heterologous expression. *J. Biol. Chem.* **269,** 2283–91 (1994).
20. Morimoto, S. *et al.* Interaction of saposins, acidic lipids, and glucosylceramidase. *J. Biol. Chem.* **265,** 1933–7 (1990).
21. Kolter, T. & Sandhoff, K. Lysosomal degradation of membrane lipids. *FEBS Lett.* **584,** 1700–1712 (2010).
22. Tylki-Szymańska, A. *et al.* Gaucher disease due to saposin C deficiency, previously described as non-neuronopathic form — No positive effects after 2-years of miglustat therapy. *Mol. Genet. Metab.* **104,** 627–630 (2011).
23. Gaspar, P. *et al.* Action myoclonus-renal failure syndrome: diagnostic applications of activity-based probes and lipid analysis. *J. Lipid Res.* **55,** 138–145 (2014).
24. Lachmann, R. H., Grant, I. R., Halsall, D. & Cox, T. M. Twin pairs showing discordance of phenotype in adult Gaucher's disease. *QJM* **97,** 199–204 (2004).
25. Biegstraaten, M. *et al.* A monozygotic twin pair with highly discordant Gaucher phenotypes. *Blood Cells. Mol. Dis.* **46,** 39–41 (2011).
26. Siebert, M., Sidransky, E. & Westbroek, W. Glucocerebrosidase is shaking up the synucleinopathies. *Brain* **137,** 1304–1322 (2014).
27. Bussink, A. P., van Eijk, M., Renkema, G. H., Aerts, J. M. & Boot, R. G. The biology of the Gaucher cell: the cradle of human chitinases. *Int. Rev. Cytol.* **252,** 71–128 (2006).
28. Boven, L. A. *et al.* Gaucher cells demonstrate a distinct macrophage phenotype and resemble alternatively activated macrophages. *Am. J. Clin. Pathol.* **122,** 359–69 (2004).
29. Marques, A. R. A. *et al.* Glucosylated cholesterol in mammalian cells and tissues: formation and degradation by multiple cellular β-glucosidases. *J. Lipid Res.* **57,** 451–463 (2016).
30. Barton, N. W. *et al.* Replacement Therapy for Inherited Enzyme Deficiency — Macrophage-Targeted Glucocerebrosidase for Gaucher's Disease. *N. Engl. J. Med.* **324,** 1464–1470 (1991).
31. Aerts, J. M. F. G., Yasothan, U. & Kirkpatrick, P. Velaglucerase alfa. *Nat. Rev. Drug Discov.* **9,** 837–8 (2010).
32. Zimran, A. *et al.* Pivotal trial with plant cell-expressed recombinant glucocerebrosidase, taliglucerase alfa, a novel enzyme replacement therapy for Gaucher disease. *Blood* **118,** 5767–73 (2011).
33. Cox, T. *et al.* Novel oral treatment of Gaucher's disease with N-butyldeoxynojirimycin (OGT 918) to decrease substrate biosynthesis. *Lancet* **355,** 1481–1485 (2000).
34. Platt, F. M. *et al.* Inhibition of substrate synthesis as a strategy for glycolipid lysosomal storage disease therapy. *J. Inherit. Metab. Dis.* **24,** 275–90 (2001).
35. McEachern, K. A. *et al.* A specific and potent inhibitor of glucosylceramide synthase for substrate inhibition therapy of Gaucher disease. *Mol. Genet. Metab.* **91,** 259–267 (2007).

36. Cox, T. M. *et al.* Eliglustat compared with imiglucerase in patients with Gaucher's disease type 1 stabilised on enzyme replacement therapy: a phase 3, randomised, open-label, non-inferiority trial. *Lancet* **385,** 2355–2362 (2015).

37. Kallemeijn, W. W. *et al.* A Sensitive Gel-based Method Combining Distinct Cyclophellitol-based Probes for the Identification of Acid/Base Residues in Human Retaining -Glucosidases. *J. Biol. Chem.* **289,** 35351–35362 (2014).

38. Willems, L. I. *et al.* From Covalent Glycosidase Inhibitors to Activity-Based Glycosidase Probes. *Chem. - A Eur. J.* **20,** 10864–10872 (2014).

39. Witte, M. D. *et al.* Ultrasensitive in situ visualization of active glucocerebrosidase molecules. *Nat. Chem. Biol.* **6,** 907–913 (2010).

40. Kallemeijn, W. W. *et al.* Novel activity-based probes for broad-spectrum profiling of retaining β-exoglucosidases in situ and in vivo. *Angew. Chemie - Int. Ed.* **51,** 12529–12533 (2012).

41. Haberkant, P. & Holthuis, J. C. M. Fat & fabulous: Bifunctional lipids in the spotlight. *Biochim. Biophys. Acta - Mol. Cell Biol. Lipids* **1841,** 1022–1030 (2014).

42. Haberkant, P. *et al.* In vivo profiling and visualization of cellular protein-lipid interactions using bifunctional fatty acids. *Angew. Chemie - Int. Ed.* **52,** 4033–4038 (2013).

43. Haberkant, P. *et al.* Bifunctional Sphingosine for Cell-Based Analysis of Protein-Sphingolipid Interactions. *ACS Chem. Biol.* **11,** 222–230 (2016).

44. Ferraz, M. J. *et al.* Gaucher disease and Fabry disease: New markers and insights in pathophysiology for two distinct glycosphingolipidoses. *Biochim. Biophys. Acta - Mol. Cell Biol. Lipids* **1841,** 811–825 (2014).

45. Vanderjagt, D. J., Fry, D. E. & Glew, R. H. Human glucocerebrosidase catalyses transglucosylation between glucocerebroside and retinol. *Biochem. J.* 309–15 (1994).

46. Sakurai, K., Ozawa, S., Yamada, R., Yasui, T. & Mizuno, S. Comparison of the reactivity of carbohydrate photoaffinity probes with different photoreactive groups. *Chembiochem* **15,** 1399–403 (2014).

47. Sawkar, A. R. *et al.* Chemical chaperones increase the cellular activity of N370S beta - glucosidase: a therapeutic strategy for Gaucher disease. *Proc. Natl. Acad. Sci. U. S. A.* **99,** 15428–33 (2002).

48. Steet, R. *et al.* Selective action of the iminosugar isofagomine, a pharmacological chaperone for mutant forms of acid-beta-glucosidase. *Biochem. Pharmacol.* **73,** 1376–83 (2007).

49. Benito, J. M., García Fernández, J. M. & Ortiz Mellet, C. Pharmacological chaperone therapy for Gaucher disease: a patent review. *Expert Opin. Ther. Pat.* **21,** 885–903 (2011).

50. Abian, O. *et al.* Therapeutic Strategies for Gaucher Disease: Miglustat (NB-DNJ) as a Pharmacological Chaperone for Glucocerebrosidase and the Different Thermostability of Velaglucerase Alfa and Imiglucerase. *Mol. Pharm.* **8,** 2390–2397 (2011).

51. Sánchez-Ollé, G. *et al.* Promising results of the chaperone effect caused by imino sugars and aminocyclitol derivatives on mutant glucocerebrosidases causing Gaucher disease. *Blood Cells. Mol. Dis.* **42,** 159–66 (2009).

52. Alfonso, P. *et al.* Miglustat (NB-DNJ) works as a chaperone for mutated acid beta-glucosidase in cells transfected with several Gaucher disease mutations. *Blood Cells. Mol. Dis.* **35,** 268–76 (2005).

53. Parenti, G., Andria, G. & Valenzano, K. J. Pharmacological Chaperone Therapy: Preclinical Development, Clinical Translation, and Prospects for the Treatment of Lysosomal Storage Disorders. *Mol. Ther.* **23,** 1138–48 (2015).

54. Maegawa, G. H. B. *et al.* Identification and Characterization of Ambroxol as an Enzyme Enhancement Agent for Gaucher Disease. *J. Biol. Chem.* **284,** 23502–23516 (2009).

55. Zimran, A., Altarescu, G. & Elstein, D. Pilot study using ambroxol as a pharmacological chaperone in type 1 Gaucher disease. *Blood Cells, Mol. Dis.* **50,** 134–137 (2013).

56. Narita, A. *et al.* Ambroxol chaperone therapy for neuronopathic Gaucher disease: A pilot study. *Ann. Clin. Transl. Neurol.* **3,** 200–215 (2016).

57. Overkleeft, H. S. *et al.* Generation of specific deoxynojirimycin-type inhibitors of the non-lysosomal glucosylceramidase. *J. Biol. Chem.* **273,** 26522–7 (1998).

58. Aerts, J. M. *et al.* The occurrence of two immunologically distinguishable beta-glucocerebrosidases in human spleen. *Eur. J. Biochem.* **150,** 565–74 (1985).

59. Thiele, C. *et al.* Tracing fatty acid metabolism by click chemistry. *ACS Chem. Biol.* **7,** 2004–11 (2012).

4

Intralysosomal stabilization of glucocerebrosidase by LIMP-2: potential implications for efficacy of ERT

Intralysosomal stabilization of glucocerebrosidase by LIMP-2: potential implications for efficacy of ERT

Based on

Paulo Gaspar[1], Saskia Oussoren[2], Saskia Scheij[1], Marri Verhoek[2], Rolf Boot[2], Hermen S. Overkleeft[3], Jan Aten[4], Johannes M. Aerts[2]

[1]Dept. Med. Biochem, AMC, Amsterdam
[2]Dept. Med.Biochem., Leiden University
[3]Dept. Bio.Synthesis, Leiden University
[4]Dept. Patholopgy, AMC, Amsterdam

Manuscript in preparation

Abstract

Deficiency of the lysosomal enzyme glucocerebrosidase (GBA) occurs in patients with Gaucher disease (GD) as well as individuals with Action Myoclonus Renal Failure (AMRF). GD is caused by mutations in the *Gba* gene encoding GBA, whilst AMRF is due to mutations in the *SCARB2* gene encoding the lysosomal membrane protein LIMP-2 that governs transport of newly formed GBA to lysosomes. AMRF manifests primarily as a neurological disorder without major visceral complications except for late onset renal disease. In contrast, the common non-neuronopathic (type 1) manifestation of GD is caused by visceral complications due to accumulation of macrophages laden with glucosylceramide, the major GBA substrate. For type 1 GD macrophage-targeted enzyme replacement therapy (ERT) is a registered treatment. For AMRF no treatment is presently available. Since deficiency of GBA is the prominent biochemical abnormality in AMRF patients, we studied the feasibility to supplement LIMP-2 deficient cells with recombinant enzyme. Studies were conducted with normal and AMRF fibroblasts as well as normal and LIMP-2 deficient HEK293 cells transduced with mannose receptor to promote uptake of mannose-terminated recombinant GBA. In LIMP-2 deficient cells, the endocytosed enzyme is abnormally fast proteolytically degraded in lysosomes. The half-life of the GBA in LIMP-2 deficient lysosomes is much shorter than in corresponding normal organelles. This suggests that inside the lysosome transient interactions of GBA with LIMP-2 stabilize the conformation of the enzyme and thus slow down proteolytic breakdown. Such mechanism implies that the efficacy with which lysosomes can be supplemented with GBA is intrinsically capped by LIMP-2 presence. In conclusion, the membrane protein LIMP-2 seems to fulfil a dual purpose in the life cycle of GBA, as transporter and as intralysosomal chaperone.

Introduction

GD is an autosomal recessive disorder caused by impaired glucosylceramide (GlcCer) catabolism as the result of GBA deficiency. The defect leads to prominent storage of GlcCer in lysosomes of macrophages that transform to "Gaucher cells" (lipid-laden macrophages), the hallmark of the disease[1]. GBA is encoded by the *GBA* gene and more than 200 different mutations have been described in GD patients[2,3]. The symptomatology of GD is remarkably heterogeneous, ranging from severe neonatal forms to an almost asymptomatic course. Based on the occurrence and age of onset of the neurological involvement, GD has been classified into acute and juvenile neuropathic forms (types 2 and 3) and the non-neuronopathic forms (type 1)[1,4,5]. Although there are no strict genotype-phenotype correlations, some mutations are associated with type 1 GD, like the homo- or heteroallelic presence of *GBA* with the N370S mutation. On the other hand, homozygosity for the *GBA* allele with the L444P mutation is associated with a neuropathic form of the disease[1,6]. Characteristic visceral symptoms of all types of GD are cytopenia, hepatosplenomegaly and skeletal abnormalities[7,8].

It was unknown for a long time how GBA reaches the lysosome. In contrast to other lysosomal enzymes, GBA does not acquire phosphomannosyl moieties in its 4 N-linked glycans[9]. The enzyme is targeted to lysosomes by a mechanism independent of the mannose-6-phosphate receptor[10,11]. Only in 2007, lysosomal integral membrane protein, type 2 (LIMP-2) was identified as the protein responsible for the intracellular sorting of GBA: its absence causes GBA deficiency in almost all organs[12]. Mutations in the *SCARB2* gene, encoding the LIMP-2 protein, are the cause of a disorder called Action Myoclonus Renal Failure (AMRF). This disease is characterized by reduced levels of GBA in the majority of cells. Patients develop heterogeneous symptoms such as glomerulosclerosis, progressive myoclonus epilepsy, and ataxia[13–16]. In addition, accumulation of undefined storage material in the brain has been reported[17]. Although LIMP-2 deficient individuals share a GBA deficiency with GD patients, AMRF presents markedly different from GD. Most striking is the absence of "Gaucher cells" in AMRF patients and the corresponding lack of elevated plasma chitotriosidase and CCL18[18]. Additionally, AMRF patients do not show visceromegaly[16].

Mutations in the *GBA* gene have recently also been linked to Parkinson disease (PD) and Lewy-Body dementia[19–21]. Such increased risk has also been reported for mutations in the *SCARB2* gene[22–24]. In mice treated with the GBA inhibitor conduritol β-epoxide (CBE), the reduction in GBA activity induces the storage of α-synuclein[25,26]. Consistently, adenoviral overexpression of GBA in the brain decreases α-synuclein in transgenic mouse models of GD and PD[27]. Recently, α-synuclein storage was also described in *LIMP-2 KO* mice[28].

Already in 1991 enzyme replacement therapy (ERT) for type 1 GD was applied using alglucerase (Ceredase®) isolated from human placenta[29]. This was replaced in 1994 by imiglucerase (Cerezyme®) (hr*GBA*), a recombinant enzyme produced in Chinese hamster ovary cells[30]. Alternative recombinant enzyme preparations became subsequently available: velaglucerase alfa (VPRIV®) produced in a human fibroblast cell line[31] and Taliglucerase alfa (Elelyso®), produced in carrots[32,33]. All therapeutic GBAs expose terminal mannose residues in order to be efficiently captured by the mannose receptor expressed by macrophages, the

most prominently affected cells in type 1 GD patients[29]. All ERT treatments are effective for the majority of type 1 GD patients, but the inability of the therapeutic enzymes to cross the blood-brain-barrier prohibits correction or prevention of neuropathology in type 2 and type 3 GD patients. An entirely different approach to treat GD is substrate reduction therapy (SRT). This aims to reduce the levels of GlcCer by inhibiting the biosynthetic enzyme GlcCer synthase (GCS)[34–38]. Another approach for treating GD is the use of pharmacological chaperones. These compounds are able to promote folding of mutant GBA, promoting its delivery to lysosomes. Inside the lysosome, the chaperone and GBA ideally dissociate and thus the enzyme becomes available to degrade the substrate[39,40]. Presently, there is no therapy available for AMRF. Although GD and AMRF differ in phenotype, they both share the deficiency in GBA activity. It is therefore of interest to investigate the potential beneficial impact of treating AMRF with approaches similar to the ones successfully employed for GD. Here, we report the outcome of supplementing AMRF cell lines with Cerezyme® (hrGBA). Our investigation has revealed a stabilizing role for GBA of LIMP-2 inside lysosomes. The potential consequences of this interaction are discussed.

Results

LIMP-2 and lysosomal proteolysis of GBA.

To evaluate lysosomal proteolytic degradation, fibroblasts (wild type and AMRF (W178X/W178X SCARB2)) were treated during 4 days with leupeptin, a cysteine and serine protease inhibitor, known to inhibit intralysosomal turnover of GBA[41] (fig. 1). As expected, the presence of leupeptin resulted in increased cellular GBA activity, as detected by enzymatic assay (fig. 1, left panel) and by ABP labelling of active GBA molecules (fig. 1, right panel), both in wild type and AMRF fibroblasts.

The same fibroblast cell lines were supplemented with recombinant GBA (hrGBA) in the medium for 4 days, in the presence or absence of leupeptin (fig. 2). Addition of hrGBA to the medium led to an increase in cellular GBA in the case of control fibroblasts. In contrast, in AMRF fibroblasts almost no increase was observed. The same experiment was conducted in the presence of leupeptin. In all cell lines GBA increased more prominently as measured by enzymatic activity and ABP labeling (fig. 2, left and right panel). Of note, the positive effect of leupeptin was more striking in the case of the AMRF fibroblasts, suggesting that endocytosed GBA is particularly sensitive to lysosomal degradation in these cells.
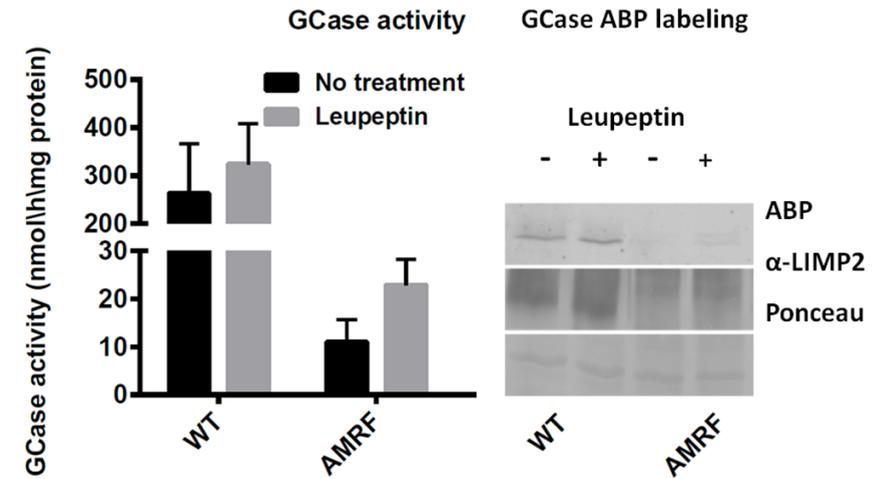
Figure 1. Effect of leupeptin on cellular GBA. Left panel: enzymatic activity of GBA was determined with 4MU-β-Glc; Right panel: ABP labelling followed by SDS-PAGE and fluorescence scanning and detection of LIMP-2 by Western blot. Symbols: − = no treatment; + = Leupeptin 20 µM; WT= wild type; AMRF = LIMP-2 deficient cell line; GD = Gaucher cell line; ABP = activity based probe; GCase = GBA.

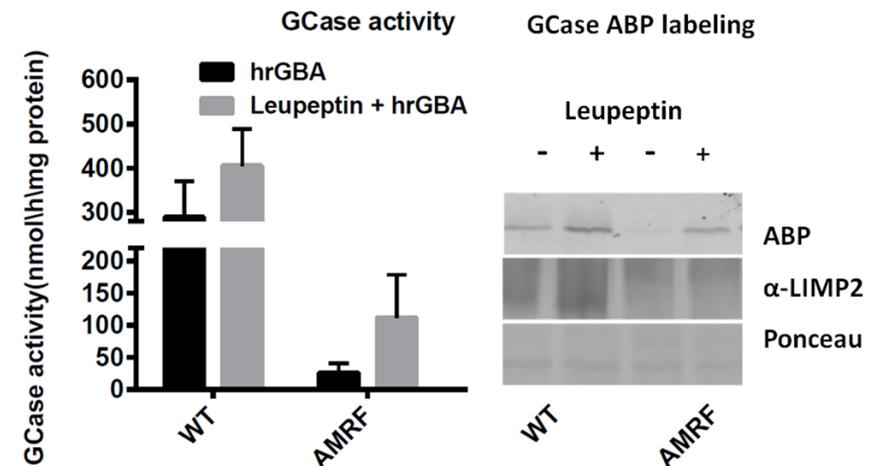**Figure 2. Supplementation of fibroblasts with hrGBA, cultured with or without leupeptin.** Left panel: enzymatic activity of GBA was measured with 4MU-β-Glc substrate; Right panel: ABP labelling followed by SDS-PAGE and fluorescence scanning. Detection of LIMP-2 by Western blot. Symbols: − = hr*GBA*; + = 20 µM Leupeptin plus hrGBA; WT = wild type; AMRF = LIMP-2 deficient cell line; ABP = activity based probe for GBA; GCase = GBA.

Cellular localization of endocytosed hrGBA.

To assess whether hrGBA indeed reaches the lysosome in the case of LIMP-2 deficiency, immunofluorescence experiments were carried out with wild type and AMRF fibroblasts. For this purpose, we combined detection of GBA by ABP labelling with immunohistochemical detection of lysosome using as markers LAMP-2 and LIMP-2 (fig. 3).

Wild type fibroblasts were pre-treated or not with leupeptin and cultured in the presence or absence of hr*GBA*. In all conditions tested, GBA co-localized with the lysosome marker (LAMP-2) and the amount of active GBA was increased (fig. 3, left panel). In untreated AMRF fibroblasts GBA was barely detectable. In the case of cells treated with leupeptin, some lysosomal GBA in lysosomes became apparent. The amount of GBA was clearly higher in cells that had been exposed to hrGBA (fig. 3, right panel). However, when hrGBA was added to cells in the absence of leupeptin, almost no increase of lysosomal GBA was observed (fig. 3, right panel). These findings suggest that GBA, either endogenous or exogenously added, is particularly sensitive to lysosomal degradation in AMRF fibroblasts.

Role of LIMP-2 in stability of hrGBA as assessed in modified HEK293 cells.

Given the observed marked instability of GBA in lysosomes of AMRF fibroblasts, we attempted to reproduce this finding in cells with an introduced LIMP-2 deficiency. For this, we constructed HEK293 cells deficient in LIMP-2 by knock-out of the *SCARB2* gene using CRISPR technology. In addition, HEK293 cells were stably transfected with cDNA encoding the mannose receptor (MR). MR-positive cells can more efficiently internalize hrGBA with terminal mannose residues in its N-linked glycans. With the different HEK293 cell lines (+/- LIMP2; +/- MR), the same experiments were conducted as with fibroblasts (fig. 4). Wild type HEK293 cells (expressing MR or not) showed a modest increase in cellular GBA in the presence of leupeptin. LIMP-2 deficient HEK293 cells showed a more evidently increased GBA activity in the presence of leupeptin (fig. 4, left panel). Thus, the findings with fibroblasts were recapitulated with the modified HEK293 cells.

The presence of hrGBA in the culture medium led to marked increase in cellular GBA in wild type HEK293 cells, particularly those transfected with MR. Cellular GBA activity was only slightly further increased by leupeptin (fig. 4, right panel). In contrast, in LIMP-2 deficient HEK293 cells the exposure to hrGBA hardly increased GBA activity, even in those cells expressing MR (fig 4, right panel). However, concomitant presence of leupeptin resulted in a very prominent increase of cellular GBA activity. Levels of cellular GBA in the LIMP-2 deficient HEK293 cells were almost identical to those in corresponding wild type cells (fig 4, right panel). Thus, endogenous as well as exogenous GBA in lysosomes of LIMP-2 deficient cells appears to be more susceptible to leupeptin-sensitive proteolytic degradation.
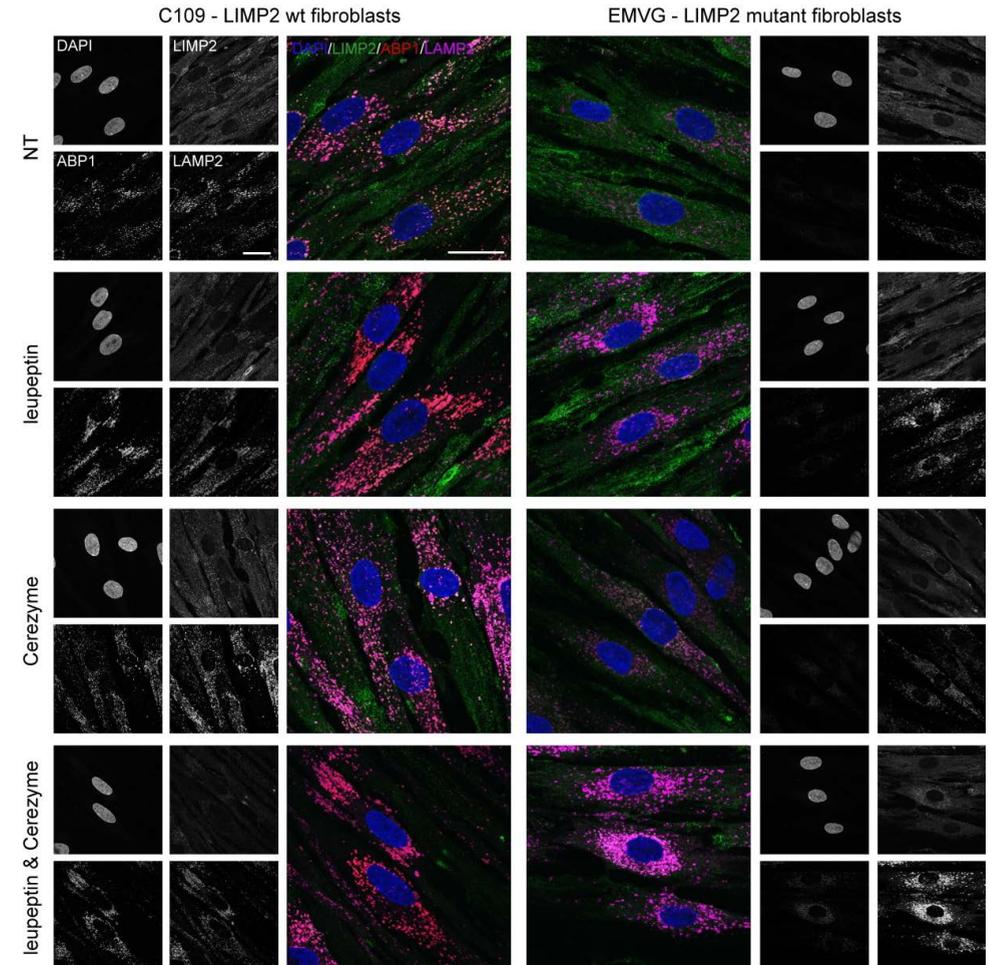

Figure 3. Detection of GBA in wild type and AMRF fibroblasts. Cells were treated with or without leupeptin and with hrGBA. Left panel: wild type fibroblasts; Right panel; AMRF fibroblasts. ABP1 = Activity based probe for GBA; DAPI = Nucleus staining.
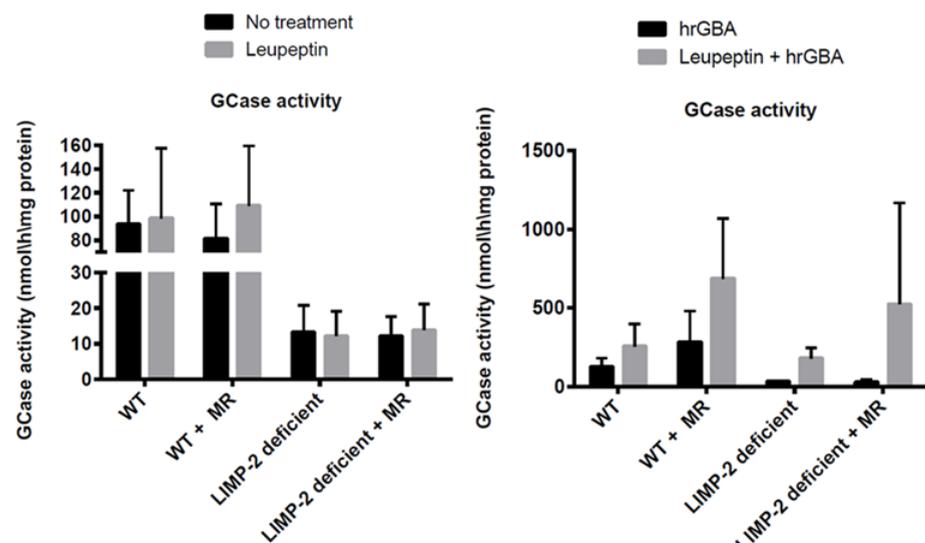
Figure 4. GBA activities in WT and LIMP-2 deficient HEK293 cells with or without MR: effect of LIMP-2 on supplementation by exogenous GBA (hrGBA). Cellular GBA was measured with 4MU-β-Glc substrate. Left panel: Cells not exposed to exogenous hr*GBA*; Right panel: Cells exposed to exogenous hr*GBA*. MR = mannose receptor; GCase = GBA.

Comparable uptake of hrGBA by wild type and LIMP-2 deficient HEK293 cells.

To evaluate whether the uptake of hrGBA is normal in LIMP-2 deficient cells, excess hrGBA was added to the various HEK293 cells with or without MR at 10 ˚C to saturate surface receptors. Next, cells were chased at 37 ˚C for 15 min in the presence of enzyme, washed and chased further without enzyme for different time periods. Cells were harvested at different time points (triplicate wells) and analyzed on GBA. Leupeptin was present during the entire experiment.

Uptake of hrGBA was very similar in wild type and LIMP-2 deficient HEK293 cells without MR for the first 15 min (Table 1). Uptake was equally higher in wild type and LIMP-2 deficient HEK293 cells expressing MR (Table 1).

Lack of overt change in lysosomal proteases in LIMP-2 deficient cells.

We determined the proteome of isolated lysosomes from hepatocytes of wild type and LIMP-2 KO mice. Careful inspection of soluble lysosomal proteases showed no significant differences, see Table 2.

The intralysosomal breakdown of GBA is prevented by the lysosomal cysteine cathepsin inhibitors E64 and the structurally related activity-based probe DCG-04[42–44]. Fluorescently (BODIPY) tagged DCG-04 allows visualization of its target cathepsins. Figure 5 shows no differences in labeled cathepsins in wild type and LIMP-2 deficient HEK239 cells. Thus, GBA

itself seems more prone for degradation in LIMP-2 deficient lysosomes compared to normal organelles.

Table 1. **Uptake of hrGBA in HEK293 cells.** HEK293 cells (+/- LIMP-2; +/- MR) were pre-loaded 10 ˚C with saturating hrGBA, chased for 15 minutes at 37 ˚C, washed and chased firther until 1 h without enzyme. Cells were harvested at indicated time points. Cellular GBA was measured with the fluorescent substrate 4MU-β-Glc. The cellular GBA present prior to uptake was subtracted: shown is the increment in cellular GBA activity.

TIME (MIN)	Increment in cellular GBA in HEK293 cells exposed to hrGBA and leupeptin (nmol hydrolysis/ h/ mg protein)			
	WT	LIMP2 DEF	WT + MR	LIMP2 DEF +MR
0	18 ± 5	17 ± 6	58 ± 11	54 ± 13
5	22 ± 6	19 ± 7	60 ± 10	55 ± 10
7.5	36 ± 6	34 ± 5	93 ± 9	88 ± 11
10	51 ± 9	48 ± 8	133 ± 22	116 ± 15
12.5	64 ± 18	61 ± 10	150 ± 23	147 ± 18
15	70 ± 12	71 + 49	180 ± 11	157 ± 12
20	83 ± 19	80 ± 15	232 ± 32	193 ± 13
25	90 ± 13	84 ± 16	259 ± 22	245 ± 19
30	93 ± 24	82 ± 10	230 ± 18	251 ± 11
40	98 ± 15	83 ± 9	240 ± 10	220 ± 9
60	99 ± 13	76 ± 20	262 ± 15	218 ± 20

Stability of hrGBA in wild type and LIMP-2 deficient lysosomes.

Next, fibroblasts from a control subject and AMRF patient (W178X/W178X *SCARB2*) were incubated with hrGBA for 4 days and then chased for different time points (fig. 6). The reduction in cellular GBA activity during the chase was very prominent in AMRF fibroblasts when compared to wild type and GD cells (fig 6a). The half-life of GBA in the AMRF fibroblasts was only about 6-8 h vs >48 h in the corresponding wild type cells (fig. 6b).

To assess whether the lifetime of hrGBA differs in wild type and LIMP-2 deficient lysosomes, a 9 h chase of endocytosed hrGBA was performed in wild type and AMRF fibroblasts in the presence of leupeptin (fig. 7). In the presence of the protease inhibitor the stability of GBA following uptake was very similar in various fibroblasts as determined by enzymatic assay and ABP labeling. This observation, combined with the findings in the absence of leupeptin (fig. 6), indicates that leupeptin-sensitive proteolytic turnover of exogenous hrGBA occurs faster in AMRF lysosomes than in wild type lysosomes.

4

Table 2. Lysosomal matrix proteases in tritosomes obtained from wild type and LIMP-2 deficient mouse livers.

| PROTEIN NAME	ACCES Nº	DESCRIPTION	RATIO
CATH_MOUSE	P49935	Pro cathepsin H OS Mus musculus GN Ctsh PE 2 SV 2	1.22
CATL1_MOUSE	P06797	Cathepsin L1 OS Mus musculus GN Ctsl1 PE 1 SV 2	0.98
CATZ_MOUSE	Q9WUU7	Cathepsin Z OS Mus musculus GN Ctsz PE 2 SV 1	1.12
DPP2_MOUSE	Q9ET22	Dipeptidyl peptidase 2 OS Mus musculus GN Dpp7 PE 2 SV 2	0.87
LGMN_MOUSE	O89017	Legumain OS Mus musculus GN Lgmn PE 1 SV 1	0.96
RISC_MOUSE	Q920A5	Retinoid inducible serine carboxypeptidase OS Mus musculus GN Scpep1 PE 2 SV 2	1.12
PCP_MOUSE	Q7TMR0	Lysosomal Pro X carboxypeptidase OS Mus musculus GN Prcp PE 2 SV 2	0.64
CATF_MOUSE	Q9R013	Cathepsin F OS Mus musculus GN Ctsf PE 2 SV 1	0.62
CATS_MOUSE	O70370	Cathepsin S OS Mus musculus GN Ctss PE 2 SV 2	0.78
NICA_MOUSE	P57716	Nicastrin OS Mus musculus GN Ncstn PE 1 SV 3	1.15
CATB_MOUSE	P10605	Cathepsin B OS Mus musculus GN Ctsb PE 1 SV 2	0.98
TPP1_MOUSE	O89023	Tripeptidyl peptidase 1 OS Mus musculus GN Tpp1 PE 1 SV 2	1.22
PPGB_MOUSE	P16675	Lysosomal protective protein OS Mus musculus GN Ctsa PE 1 SV 1	1.40
CATD_MOUSE	P18242	Cathepsin D OS Mus musculus GN Ctsd PE 1 SV 1	n.d.
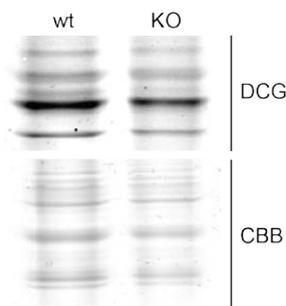
Figure 5. Labeling of cathepsins in wild type and LIMP-2 deficient HEK293 cells with BODIPY DCG-04. HEK293 cells were incubated for 60 minutes with BODIPY DCG-04 and labeled cathepsins were visualized by fluorescence scanning after SDS-PAGE (upper panel); Total cellular protein as visualized by staining with CBB (lower panel).
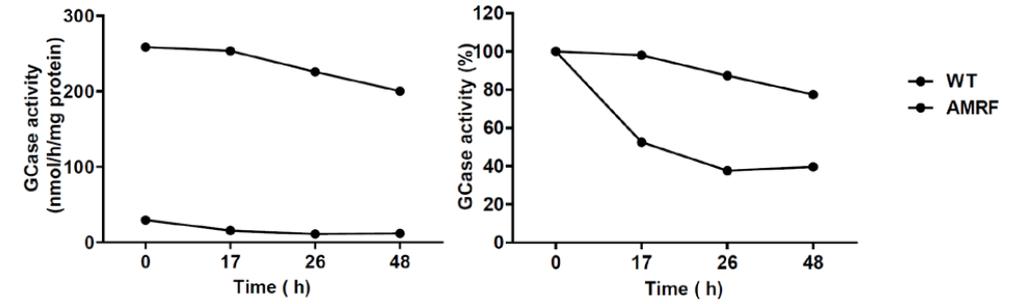
Figure 6. Chase of endocytosed hrGBA in different fibroblast cell lines. Fibroblasts were incubated with hrGBA for 4 days. Cells were harvested and GBA activities were measured with the fluorescent substrate 4MU-β-Glc. Left panel: absolute GBA activity; Right panel: Half-life of GBA. Upper lines: WT fibroblasts; Lower lines: AMRF fibroblasts; GCase = GBA.
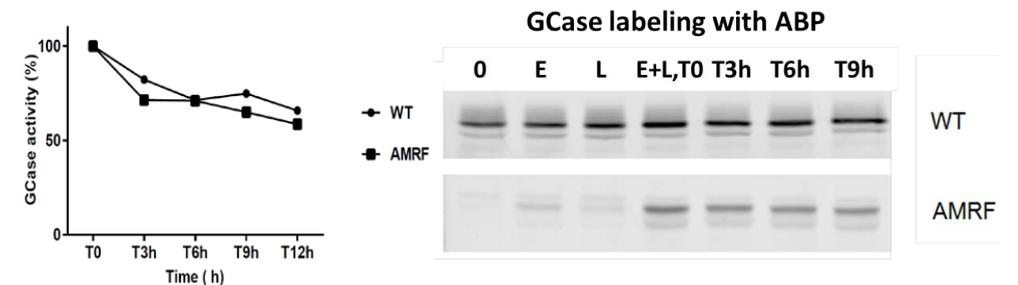
Figure 7. Half-life of hr*GBA* in the presence (+) of leupeptin. Fibroblasts were incubated with hrGBA **(E)** in the absence and presence of leupeptin **(L)**, and chased for 9 hours. Cells were harvested and GBA activity was determined in lysates using 4MU-β-Glc substrate. Left panel: activity at T0 is expressed as 100 % for each cell line. Active GBA (GCase = GBA) was visualized by ABP labeling (right panel).

Lastly, the half-life of exogenous GBA was determined in HEK293 cells expressing MR in the absence of protease inhibitor. Cells were cultured for 3 days with hrGBA, extensively washed and chased in the same medium for different time points. Every two days the medium was refreshed. The cellular GBA content at the start of the chase was lower in LIMP-2 deficient cells (Table 3). It also declined much faster in LIMP-2 deficient HEK cells than the wild type counter parts. The estimated half-life of GBA was 28.3 h in wild type HEK293 cells and only 6.2 h in LIMP-2 deficient cells.

Table 3. Chase of hrGBA in HEK293 cells with MR, following uptake of enzyme for 3 days, in the absence of protease inhibitor: estimated half-life.

	WT +MR	LIMP2 DEF + MR
Cellular GBA After 3 D Pulse With hrGBA (nmol/H/ mg prot)	520 ± 120	36 ± 9
Half-Life GBA During Chase (H)	28.3 ± 3.2	6.2± 1.4

Discussion

The key role of LIMP-2 in sorting GBA from the ER to lysosomes has been unequivocally demonstrated. Binding of newly formed GBA to a specific domain in LIMP-2 governs its routing[12,45,46]. It has been proposed that at low pH the complex LIMP-2/GBA dissociates and enzyme is released[47]. However, binding of GBA to LIMP-2 is not completely abolished at pH values below 6.0. It is therefore conceivable that even inside lysosomes GBA and LIMP-2 may transiently bind, with beneficial effects on the conformation of GBA and subsequent increased resistance of the enzyme against proteolytic breakdown. To study this possibility we exposed wild type and LIMP-2 deficient HEK293 cells to leupeptin, an inhibitor of the lysosomal serine and cysteine proteases. Leupeptin is well known from metabolic labeling experiments using 35C-methionine incorporation to effectively reduce intralysosomal degradation of GBA[41]. Indeed we noted an increase in cellular GBA of wild type fibroblasts with enzyme assay and ABP-labeling alike in the presence of leupeptin. In the case of AMRF fibroblasts however, leupeptin lead to a much more pronounced increase in cellular GBA. This suggests that the small amount of GBA that manages to reach lysosomes during LIMP-2 deficiency has to be far more prone to intralysosomal leupeptin-inhibitable proteolytic degradation. This difference between wild type and LIMP-2 fibroblasts became even more apparent when cells were incubated with recombinant GBA (hrGBA). Again, in AMRF cells, the endocytosed hrGBA appeared far more sensitive to proteolytic, leupeptin-inhibitable, degradation as compared to the situation in wild type fibroblasts. The average half-life of endocytosed hrGBA in AMRF fibroblasts in the absence of leupeptin was surprisingly short, being only about 6 - 8 h.

To exclude that the observed differences between wild type and AMRF fibroblasts were due to other genetic differences beyond the *SCARB2* gene, we generated LIMP-2 deficient HEK293 cells by CRISPR technology. Comparison of wild type and LIMP-2 deficient HEK293 cells, equipped or not with mannose receptor, again revealed that exogenous GBA in LIMP-2 deficient lysosomes is far more vulnerable to leupeptin-inhibitable proteolytic breakdown.

We investigated with the same HEK293 cells whether LIMP-2 may be involved in uptake of GBA, a possible mechanism since low amounts of LIMP-2 are supposedly transiently present at the cell surface. However, no evidence for this was obtained in experiments with wild type and LIMP-2 deficient HEK293 cells, equipped with mannose receptor or not. In these experiments we pre-loaded receptors at the cell surface with hrGBA at 10 °C and chased cells for different time periods at 37 °C. During the first hour of chase, leupeptin-inhibitable degradation of GBA was still very small and a good impression could be obtained about uptake rate. Of note, Malini *et al.* recently also reported that hrGBA cellular uptake is independent of LIMP-2[46].

Longer chase periods allowed us to determine the half–life of endocytosed exogenous GBA, particularly in HEK293 cells expressing mannose-receptor that endocytosed large amounts of enzyme. In wild type HEK293 cells the half-life was 28.3 h, following saturating pre-loading with hrGBA. In comparable LIMP-2 deficient cells expressing mannose receptor it was just 6.2 h. The presence of leupeptin abolished the difference in stability of GBA in wild type and LIMP-2 deficient cells, extending it far over 48 h. Since there are no experimental indications for a different make-up of acid cysteine and serine proteases in LIMP-2 deficient lysosomes, it is attractive to speculate that transient interactions between LIMP-2 and GBA in lysosomes render protection against proteolytic break down of the enzyme. Indeed, Zunke et al. recently described that a LIMP-2 helix 5-derived peptide interacts with GBA in lysosomes in intact cells and activates the enzyme in the process[48].

Our findings may have important implications. It can be envisioned that the amount of LIMP-2 in lysosomes installs an intrinsic limit for the efficacy of ERT. LIMP-2 might become rate-limiting regarding stabilization of exogenous GBA. When too much enzyme is taken up, lack of interaction with the limited amount of LIMP-2 will promote more rapid proteolytic breakdown. Consistent with this is our observation that increase in cellular GBA in mannose receptor expressing HEK293 cells does not seem limited by binding capacity of surface expressed receptor, but rather by intralysosomal stability of endocytosed GBA which relatively decreases with higher dose. A simplified scheme is shown in figure 8, depicting the hypothesis formulated here.

Thus, effectiveness of GBA-ERT may be maximized by the finite presence of LIMP-2 in lysosomes. ERT at very high doses of hrGBA would theoretically result in far excess of exogenous GBA over endogenous LIMP-2 in lysosomes, and the intralysosomal stability of administered enzyme could consequently be poor. Theoretically, administration of very large amounts of hrGBA to cells may even reduce the stability of endogenous GBA due to competition for LIMP-2 stabilization inside lysosomes. It should be considered that the stabilizing effect of LIMP-2 on intralysosomal GBA is more critical in GD patients who concomitantly are carriers for LIMP-2 deficiency. Indeed, it has been reported that carriership for LIMP-2 deficiency acts as modifier and worsens the clinical course of GD[49].
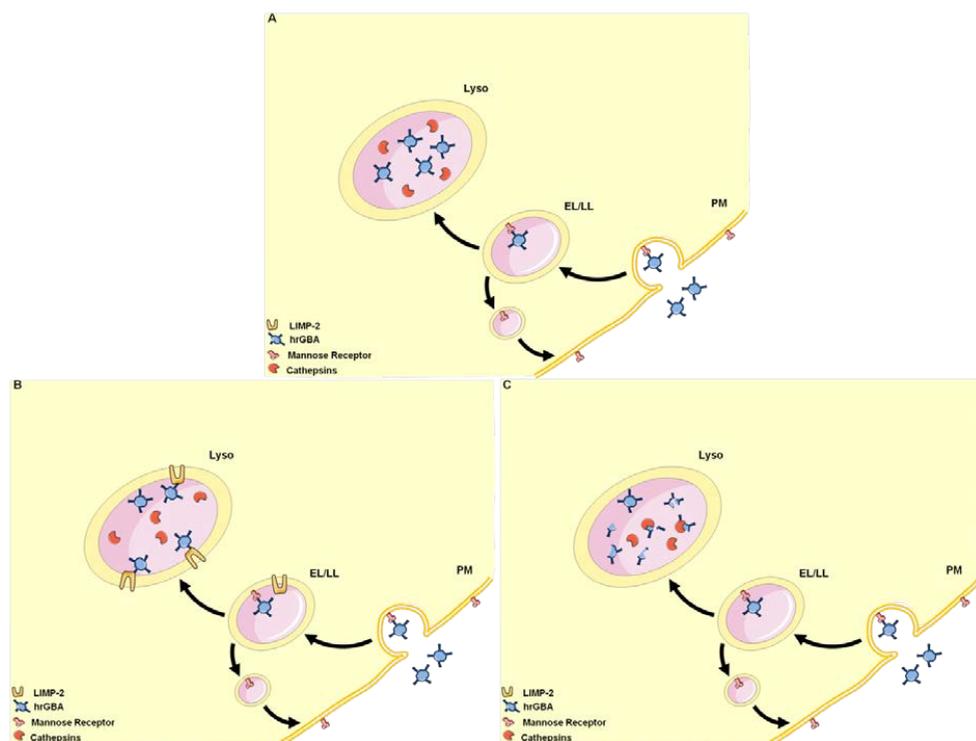
Figure 8. Stability of exogenous hrGBA in wild type and LIMP-2 deficient cells. A. Presently broadly accepted view, ERT for Gaucher Disease; **B.** Proposed model for LIMP-2 as a (lysosomal) chaperone in WT cells; **C.** Proposed model for the detrimental effect of LIMP-2 deficiency in cells, the chaperone lacking in AMRF.

Based on our present concept, ERT of AMRF with recombinant GBA seems not a wise approach. The presently used therapeutic GBAs in ERT of type 1 GD are neither attractive as drug for neurologically affected AMRF patients since these enzymes seem not to pass well the BBB. Other therapeutic approaches such as gene therapy or pharmacological manipulation of the glycosphingolipid metabolism seem to be more attractive to ameliorate abnormalities in AMRF patients. Future studies with LIMP-2 KO mice will be useful to determine which approach is the most appealing to treat AMRF, a disorder with still unmet clinical need.

In conclusion, LIMP-2 seems to influence GBA at various stages of its life cycle. Firstly, LIMP-2 transports newly formed GBA to lysosomes. Secondly, LIMP-2 likely stabilizes GBA also in the lysosome and consequently protects it against proteolytic breakdown. Thus, LIMP-2 seems to have a dual action as transporter and as lysosomal chaperone of GBA.

Materials & Methods

Materials
MDW941 (Inhibody Red) was synthesized at the Leiden Institute of Chemistry as described earlier [50,51]. The rabbit polyclonal anti-LIMP-2 antibody was acquired from Novus Biologicals, Littleton, USA (NB400-129). Human recombinant glucocerebrosidase (hrGBA: Cerezyme™) was a gift from Genzyme, Boston, USA. All other chemicals were obtained from Sigma.

Methods

SCARB2 gene knock-out
In human embryonic kidney 293 (HEK293) cells (ATCC CRL 1573) a *SCARB2* gene knock-out was generated using the CRISPR/Cas9 system. Guide RNA sequences were selected using the optimized CRISPR design tool (http://crispr.mit.edu) using the individual *SCARB2* exon sequences as template. For the selected guides two complementary oligo´s containing the *SCARB2* guide sequences and BbsI ligation adapters were annealed and ligated into pX335 (pX335-U6-Chimeric_BB-CBh-hSpCas9n (D10A, Nickase, Addgene plasmid #42335) and digested with BbsI according to the described protocol[52]. Primers used for *SCARB2* exon 1 are: guide 1 5'- CACCGGACGTTGTCCCTGCTCCTGC-3 and 5'- AAACGCAGGAGCAGGGACAACGTCC-3'. *SCARB2* exon 1 guide 2 5'- CACCGCCGCCGTGTAGAAGCAGCAT-3' and 5'-AAACATGCTGCTTCTACACGGCGGC-3'. For targeting the *SCARB2* exon 7 primers are: guide 1 5'-CACCGTATACCTGAGGGAAACTGCC-3' and 5'-AAACGGCAGTTTCCCTCAGGTATAC-3'. *SCARB2* exon 7 guide 2 5'- CACCGGCCGGCATTGTCTGACGTAT-3' and 5'-AAACATACGTCAGACAATGCCGGCC-3'. HEK293T cells were transfected with a 1:1 ratio of pX335 guide 1 and pX335 guide 2 for either exon 1 or exon 7 of the *SCARB2* gene using FuGene6 (Roche) with a FuGene: DNA ratio of 3:1. Two days after transfection single cell clones were isolated by seeding at 0.5 cell per well in 96 well plates. Clones were checked by PCR and sequencing for the presence of indels. One clone (N1F8) with sequence confirmed indels was shown to secrete GBA. Western blot analysis (data not shown) displayed that clone N1F8 lacks any LIMP-2 protein. HEK293T cells were cultured in DMEM with high glucose, supplemented with 10 % FBS and 100 units/ml Pen/Strep.

Transfection of HEK293 cells with macrophage mannose receptors
HEK293T cells were cultured in DMEM with high glucose (Gibco) supplemented with 10 % FBS (Bodinco) and 100 units/ml Pen/Strep (Gibco). One day before transfection 4×10^5 cells/well were seeded in a 6 well plate. HEK293T cells and HEK293T *SCARB2* knock-out cells (clone N1F8) were infected with a human Mannose Receptor (CD206) pLenti6.3/TO/V5-DEST construct, generated via PCR and the Gateway cloning system (Invitrogen) using primers 5'-GGGGACAAGTTTGTACAAAAAAGCAGGCTTCGGTACCACCATGAGGCTACCCCTGC-3' and 5'-GGGGACCACTTTGTACAAGAAAGCTGGGTCGATGACCGAGTGTTCATTCTG-3',

and pDONR221 as cloning intermediate. All constructs was verified by sequencing. To produce lentiviral particles, HEK293T cells were transfected with pLenti6.3-CD206 in combination with the envelope and packaging plasmids pMD2G, pRRE and pRSV. Subsequently, culture supernatant containing viral particles was collected and used for infection of HEK293 cells and HEK293 *SCARB2* knockout cells (clone N1F8). Infected cells were selected using blasticidin (Sigma) 2.5 µg/ml.

Cell culture and experiments

Fibroblasts were cultured in DMEM medium supplemented with 10 % fetal bovine serum and 1 % Pen/Strep. HEK293 cells were seeded one day before the experiment at 1×10^6 cells/well in a 6 well plate. The cells were subjected to the following 4 conditions during 4 days: no treatment; 20 µM of leupeptin (a broad spectrum protease inhibitor); 32 ng/µl of human recombinant GBA (hrGBA); and 32 ng/µl of hrGBA for one hour after 20 µM of leupeptin. At the fourth day of exposure, the cells were harvested. To evaluate the effect of leupeptin on hrGBA, cells were exposed to either leupeptin and hrGBA or hrGBA only. At the fourth day, cells were washed with cold PBS, and the cells subsequently cultured with or without leupeptin, as aforementioned.

Uptake of hrGBA

HEK293 cells were seeded one day prior to the experiment at 1×10^6 cells/well in a 6 well plate. The cells were subjected to 32 ng/µl of hrGBA one hour after addition of 20 µM of leupeptin. The following time points were collected: 0, 10, 20, 30 min.

Preparation of cell homogenates

Isolated fibroblasts and HEK293 cells were homogenized by sonication on ice and cellular protein was measured according to the manufacturer's protocol with Pierce™ BCA Protein Assay Kit (Pierce Biotechnology Inc., No. 23225). When necessary lysates were diluted with MilliQ water.

In vitro activity-based probe labeling of GBA, gel electrophoresis and fluorescence scanning

Homogenate (50 µg total protein) was incubated with 100 nM cyclophellitol-epoxide type activity based probe MDW941[50] in 150 mM McIlvaine buffer (150 mM citrate-Na$_2$HPO$_4$, pH 5.2. with 0.2 % (w/v) sodium taurocholate. 0.1 % Triton X-100) and protease inhibitor cocktail (Roche) for 45 min at 37 °C. Next, protein was denatured in 5x Laemmli buffer (50 % (v/v) 1 M Tris-HCl, pH 6.8, 50 % (v/v) glycerol, 10 % (w/v) DTT, 10 % (w/v) SDS, 0.01 % (w/v) bromophenol blue) by boiling for 10 min at 100 °C. Proteins were separated by electrophoresis on 10 % (w/v) acrylamide SDS-PAGE gels[51]. Wet slab gels were scanned for red fluorescence with a Typhoon variable mode imager (Amersham Bioscience) using λ_{ex} 532 nm and λ_{em} 610 nm (band pass filter 30nm). Fluorescence was quantified using ImageJ software (NiH). Gels were transferred onto a nitrocellulose membrane (Schleicher & Schuell) and protein was visualized with Ponceau S staining[51].

Western blotting

SDS–PAGE gels were electroblotted onto a nitrocellulose membrane (Schleicher&Schuell). Membranes were blocked with 5 % skimmed milk and 0.05 % Tween-20 in Tris-buffered saline (TBS) for 1 h at room temperature and incubated overnight with the primary antibody at 4 °C. Membranes were then washed three times with 0.01 % Tween-20 in TBS and incubated with the appropriate IRDye conjugated secondary antibody for 1 h at room temperature. After washing, detection was performed using the Odyssey® Clx, Infrared Imaging System (LI-COR).

Immunofluorescence analysis

Fibroblasts were cultured on glass slides. The cells were subjected to the following 4 conditions during 4 days: no treatment; 20 µM of leupeptin; 32 ng/µl of hr*GBA*; 32 ng/µl of hr*GBA* one hour after of 20 µM of leupeptin. Cells were incubated overnight with 1 nM MDW941 in HAM/DMEM with 10 % FCS. Next, cells were washed, fixed with 3 % (v/v) paraformaldehyde in PBS for 60 min, washed with PBS and incubated with 0.1 % saponin in PBS. They were washed again with PBS, incubated with 0.1 mM NH$_4$Cl in PBS for 10 min and then with normal antibody diluent (BD09-999; Immunologic, Duiven, The Netherlands) for 2 h. Nuclei were stained with DAPI, LIMP-2 protein with rabbit IgG anti-LIMP-2 antibody (NB400-129, Novus Biologicals, Abingdon, UK) and LAMP-2 protein with mouse IgG1 anti-LAMP-2 antibody (clone H4B4; 9840-01, Southern Biotechnology Associates, Birmingham, AL). Second step antibodies were Alexa Fluor 488-conjugated goat IgG anti-rabbit IgG (A11034; Life Technologies, Bleiswijk, The Netherlands) and ATTO647N-conjugated goat IgG anti-mouse IgG (610-156-121; Rockland, Limerick, PA). Slides were mounted with ProLong Gold (Life Technologies). Imaging was performed by means of confocal laser scanning microscopy using a TCS SP8 X mounted on a DMI 6000 microscope with a Plan APO 63x/1.40 Oil CS2 objective. For excitation were applied a 405 nm UV diode for DAPI, and a 470-670 nm WLL Pulsed laser, sequentially set at 488 nm, 592 nm and 647 nm for the respective fluorochromes. PMT and HyD detection was applied. Recorded images were analyzed and overlayed using LAS X software (Leica Microsystems, Son, The Netherlands).

GBA activity assay

Activity assays were performed as described earlier[53]. Briefly, GBA activity was measured with 3.73 mM 4-methylumbelliferyl-β-D-glucopyranoside (4MU-β-Glc), dissolved in 150 mM McIlvaine buffer (pH 5.2 supplemented with 0.2 % (w/v) sodium taurocholate, 0.1 % (v/v) Triton X-100) and 0.1 % BSA. After stopping the reaction with NaOH-glycine (pH 10.3), fluorescence was measured with a fluorimeter LS55 (Perkin-Elmer, Beaconsfield, UK) at λ_{ex} 366 nm and λ_{ex} 445 nm.

References

1. E. Beutler, G. A. G. in *C.R. Scriver,W.S. Sly, D. Valle (Eds.), The Metabolic and Molecular Bases of Inherited Disease, 8th ed.* 3635–3668 (McGraw-Hill, New York, 2001).
2. Lee, J.-Y. *et al.* Clinical and genetic characteristics of Gaucher disease according to phenotypic subgroups. *Korean J. Pediatr.* **55,** 48–53 (2012).
3. Hruska, K. S., LaMarca, M. E., Scott, C. R. & Sidransky, E. Gaucher disease: mutation and polymorphism spectrum in the glucocerebrosidase gene (GBA). *Hum. Mutat.* **29,** 567–83 (2008).
4. Baris, H. N., Cohen, I. J. & Mistry, P. K. Gaucher disease: the metabolic defect, pathophysiology, phenotypes and natural history. *Pediatr. Endocrinol. Rev.* **12 Suppl 1,** 72–81 (2014).
5. Mehta, A. Epidemiology and natural history of Gaucher's disease. *Eur. J. Intern. Med.* **17 Suppl,** S2-5 (2006).
6. Ohashi, T. *et al.* Characterization of human glucocerebrosidase from different mutant alleles. *J. Biol. Chem.* **266,** 3661–7 (1991).
7. Boven, L. A. *et al.* Gaucher cells demonstrate a distinct macrophage phenotype and resemble alternatively activated macrophages. *Am. J. Clin. Pathol.* **122,** 359–69 (2004).
8. Bussink, A. P., van Eijk, M., Renkema, G. H., Aerts, J. M. & Boot, R. G. The biology of the Gaucher cell: the cradle of human chitinases. *Int. Rev. Cytol.* **252,** 71–128 (2006).
9. Aerts, J. M. *et al.* Glucocerebrosidase, a lysosomal enzyme that does not undergo oligosaccharide phosphorylation. *Biochim. Biophys. Acta* **964,** 303–8 (1988).
10. Rijnboutt, S., Aerts, H. M., Geuze, H. J., Tager, J. M. & Strous, G. J. Mannose 6-phosphate-independent membrane association of cathepsin D, glucocerebrosidase, and sphingolipid-activating protein in HepG2 cells. *J. Biol. Chem.* **266,** 4862–8 (1991).
11. Rijnboutt, S., Kal, A. J., Geuze, H. J., Aerts, H. & Strous, G. J. Mannose 6-phosphate-independent targeting of cathepsin D to lysosomes in HepG2 cells. *J. Biol. Chem.* **266,** 23586–92 (1991).
12. Reczek, D. *et al.* LIMP-2 Is a Receptor for Lysosomal Mannose-6-Phosphate-Independent Targeting of β-Glucocerebrosidase. *Cell* **131,** 770–783 (2007).
13. Berkovic, S. F. *et al.* Array-Based Gene Discovery with Three Unrelated Subjects Shows SCARB2/LIMP-2 Deficiency Causes Myoclonus Epilepsy and Glomerulosclerosis. *Am. J. Hum. Genet.* **82,** 673–684 (2008).
14. Badhwar, A. *et al.* Action myoclonus-renal failure syndrome: characterization of a unique cerebro-renal disorder. *Brain* **127,** 2173–2182 (2004).
15. Balreira, A. *et al.* A nonsense mutation in the LIMP-2 gene associated with progressive myoclonic epilepsy and nephrotic syndrome. *Hum. Mol. Genet.* **17,** 2238–2243 (2008).
16. Chaves, J. *et al.* Progressive myoclonus epilepsy with nephropathy C1q due to SCARB2/LIMP-2 deficiency: clinical report of two siblings. *Seizure* **20,** 738–40 (2011).
17. Fu, Y.-J. *et al.* Progressive myoclonus epilepsy: extraneuronal brown pigment deposition and system neurodegeneration in the brains of Japanese patients with novel SCARB2 mutations. *Neuropathol. Appl. Neurobiol.* **40,** 551–63 (2014).
18. Gaspar, P. *et al.* Action myoclonus-renal failure syndrome: diagnostic applications of activity-based probes and lipid analysis. *J. Lipid Res.* **55,** 138–145 (2014).
19. Schapira, A. H. V. Glucocerebrosidase and Parkinson disease: Recent advances. *Mol. Cell. Neurosci.* **66,** 37–42 (2015).
20. Siebert, M., Sidransky, E. & Westbroek, W. Glucocerebrosidase is shaking up the synucleinopathies. *Brain* **137,** 1304–1322 (2014).
21. Sidransky, E. *et al.* Multicenter analysis of glucocerebrosidase mutations in Parkinson's disease. *N. Engl. J. Med.* **361,** 1651–61 (2009).
22. Michelakakis, H. *et al.* Evidence of an association between the scavenger receptor class B member 2 gene and Parkinson's disease. *Mov. Disord.* **27,** 400–5 (2012).
23. Hopfner, F. *et al.* The role of SCARB2 as susceptibility factor in Parkinson's disease. *Mov. Disord.* **28,** 538–40 (2013).
24. Maniwang, E., Tayebi, N. & Sidransky, E. Is Parkinson disease associated with lysosomal integral membrane protein type-2?: challenges in interpreting association data. *Mol. Genet. Metab.* **108,** 269–71 (2013).
25. Sardi, S. P., Cheng, S. H. & Shihabuddin, L. S. Gaucher-related synucleinopathies: The examination of sporadic neurodegeneration from a rare (disease) angle. *Prog. Neurobiol.* **125,** 47–62 (2015).
26. Sardi, S. P., Singh, P., Cheng, S. H., Shihabuddin, L. S. & Schlossmacher, M. G. Mutant GBA1 expression and synucleinopathy risk: first insights from cellular and mouse models. *Neurodegener. Dis.* **10,** 195–202 (2012).
27. Sardi, S. P. *et al.* Augmenting CNS glucocerebrosidase activity as a therapeutic strategy for parkinsonism and other Gaucher-related synucleinopathies. *Proc. Natl. Acad. Sci. U. S. A.* **110,** 3537–42 (2013).
28. Rothaug, M. *et al.* LIMP-2 expression is critical for -glucocerebrosidase activity and -synuclein clearance. *Proc. Natl. Acad. Sci.* **111,** 15573–15578 (2014).
29. Barton, N. W. *et al.* Replacement therapy for inherited enzyme deficiency--macrophage-targeted glucocerebrosidase for Gaucher's disease. *N. Engl. J. Med.* **324,** 1464–70 (1991).
30. Grabowski, G. A. *et al.* Enzyme therapy in type 1 Gaucher disease: comparative efficacy of mannose-terminated glucocerebrosidase from natural and recombinant sources. *Ann. Intern. Med.* **122,** 33–9 (1995).
31. Zimran, A. & Elstein, D. Management of Gaucher disease: enzyme replacement therapy. *Pediatr. Endocrinol. Rev.* **12 Suppl 1,** 82–7 (2014).
32. Grabowski, G. A., Golembo, M. & Shaaltiel, Y. Taliglucerase alfa: An enzyme replacement therapy using plant cell expression technology. *Mol. Genet. Metab.* **112,** 1–8 (2014).
33. Zimran, A. *et al.* Pivotal trial with plant cell-expressed recombinant glucocerebrosidase, taliglucerase alfa, a novel enzyme replacement therapy for Gaucher disease. *Blood* **118,** 5767–73 (2011).
34. Aerts, J. M. F. G., Hollak, C. E. M., Boot, R. G., Groener, J. E. M. & Maas, M. Substrate reduction therapy of glycosphingolipid storage disorders. *J. Inherit. Metab. Dis.* **29,** 449–456 (2006).
35. Cox, T. *et al.* Novel oral treatment of Gaucher's disease with N-butyldeoxynojirimycin (OGT 918) to decrease substrate biosynthesis. *Lancet* **355,** 1481–1485 (2000).
36. Hughes, D. A. & Pastores, G. M. Eliglustat for Gaucher's disease: trippingly on the tongue. *Lancet* **385,** 2328–2330 (2015).
37. Cox, T. M. *et al.* Eliglustat compared with imiglucerase in patients with Gaucher's disease type 1 stabilised on enzyme replacement therapy: a phase 3, randomised, open-label, non-inferiority trial. *Lancet* **385,** 2355–2362 (2015).
38. Mistry, P. K. *et al.* Effect of Oral Eliglustat on Splenomegaly in Patients With Gaucher Disease Type 1. *JAMA* **313,** 695 (2015).

39. Benito, J. M., García Fernández, J. M. & Ortiz Mellet, C. Pharmacological chaperone therapy for Gaucher disease: a patent review. *Expert Opin. Ther. Pat.* **21,** 885–903 (2011).

40. Boyd, R. E. *et al.* Pharmacological chaperones as therapeutics for lysosomal storage diseases. *J. Med. Chem.* **56,** 2705–25 (2013).

41. Jonsson, L. M. V *et al.* Biosynthesis and maturation of glucocerebrosidase in Gaucher fibroblasts. *Eur. J. Biochem.* **164,** 171–179 (1987).

42. Greenbaum, D., Medzihradszky, K. F., Burlingame, A. & Bogyo, M. Epoxide electrophiles as activity-dependent cysteine protease profiling and discovery tools. *Chem. Biol.* **7,** 569–581 (2000).

43. Greenbaum, D. *et al.* Chemical approaches for functionally probing the proteome. *Mol. Cell. Proteomics* **1,** 60–8 (2002).

44. Hillaert, U. *et al.* Receptor-Mediated Targeting of Cathepsins in Professional Antigen Presenting Cells. *Angew. Chemie Int. Ed.* **48,** 1629–1632 (2009).

45. Blanz, J. *et al.* Disease-causing mutations within the lysosomal integral membrane protein type 2 (LIMP-2) reveal the nature of binding to its ligand -glucocerebrosidase. *Hum. Mol. Genet.* **19,** 563–572 (2010).

46. Malini, E. *et al.* Role of LIMP-2 in the intracellular trafficking of β-glucosidase in different human cellular models. *FASEB J.* **29,** 3839–52 (2015).

47. Zachos, C., Blanz, J., Saftig, P. & Schwake, M. A Critical Histidine Residue Within LIMP-2 Mediates pH Sensitive Binding to Its Ligand β-Glucocerebrosidase. *Traffic* **13,** 1113–1123 (2012).

48. Zunke, F. *et al.* Characterization of the complex formed by β-glucocerebrosidase and the lysosomal integral membrane protein type-2. *Proc. Natl. Acad. Sci.* **113,** 3791–3796 (2016).

49. Velayati, A. *et al.* A mutation in SCARB2 is a modifier in Gaucher disease. *Hum. Mutat.* **32,** 1232–8 (2011).

50. Witte, M. D. *et al.* Ultrasensitive in situ visualization of active glucocerebrosidase molecules. *Nat. Chem. Biol.* **6,** 907–913 (2010).

51. Kallemeijn, W. W. *et al.* Novel activity-based probes for broad-spectrum profiling of retaining β-exoglucosidases in situ and in vivo. *Angew. Chemie - Int. Ed.* **51,** 12529–12533 (2012).

52. Ran, F. A. *et al.* Genome engineering using the CRISPR-Cas9 system. *Nat. Protoc.* **8,** 2281–308 (2013).

53. Aerts, J. M. *et al.* The occurrence of two immunologically distinguishable beta-glucocerebrosidases in human spleen. *Eur. J. Biochem.* **150,** 565–74 (1985).

4

5

Lipid abnormalities in
LIMP-2 deficient mice

Lipid abnormalities in LIMP-2 deficient mice

Based on

Paulo Gaspar[1, 2, 3], Maria J. Ferraz[1,4], Markus Damme[5], André R. A. Marques[1], Saskia V. Oussoren[4], GertJan Kramer[1], Mina Mirzaian[4], Marion Gijbels[1], Roelof Ottenhoff[1], Cindy van Roomen[1], Wilma E. Donker-Koopman [1], Michael Schwake[5], Saskia Heybrock[5], Kondababu Kurakula[1], Maria Carmo Macário[6], Clara Sá Miranda[2], Paul Saftig[5], Johannes M. Aerts[1,4]

[1]Dept. of Med Biochem, AMC, Amsterdam
[2]Organelle Biogenesis & Function Group, I3S, IBMC, Porto, Portugal
[3]ICBAS, Universidade do Porto, Porto, Portugal
[4]Dept. of Med Biochem, LIC, Leiden University
[5]Dept. of Biochem, Christian-Albrechts-University of Kiel, Germany
[6]Neurology Dept., Coimbra Hospital and University Centre, Portugal

Abstract

Mutations in *Gba* encoding glucocerebrosidase (GBA) cause Gaucher disease (GD). The lysosomal integral membrane protein type 2 (LIMP-2) transports GBA to lysosomes. LIMP-2 deficiency leads to reduced cellular GBA levels and causes Action Myoclonic Renal Failure Syndrome (AMRF). We investigated the cause for the different clinical manifestation of GD and AMRF. No abnormalities in lysosomal matrix proteins, except GBA, were observed with lysosomes isolated from liver of LIMP-2-deficient mice. Measurement of enzymatic activity of GBA as well as detection of active enzyme molecules with an activity-based probe revealed a variable deficiency along LIMP-2-deficient tissues. GBA is relatively high in leukocytes of LIMP-2 deficient mice. Endocytotic re-uptake of GBA by white blood cells may underlie this and explain the absence of macrophage-related symptoms in AMRF patients. GBA degrades glucosylceramide (GlcCer). GlcCer levels do not correlate with reductions in GBA in LIMP-2 deficient tissues. However, increased glucosylsphingosine and glucosylated cholesterol do correlate with enzyme levels. Glucosylsphingosine and glucosylated cholesterol are also increased in isolated lysosomes of LIMP2-deficient liver. In conclusion, our findings point to an important impact of LIMP-2 deficiency in the regulation of glycosphingolipid metabolism.

Introduction

Gaucher disease (GD) is due to defects in glucocerebrosidase (GBA), a lysosomal β-glucosidase degrading glucosylceramide (GlcCer)[1]. In its most common type 1 variant, GD presents as macrophage disorder[1].The lysosomal integral membrane protein, type 2 (LIMP-2), encoded by the *SCARB2* gene*,* mediates the transport newly formed GBA to lysosomes[2–4]. Mutations in the *SCARB2* gene cause Action Myoclonic Renal Failure Syndrome (AMRF), a progressive myoclonic epilepsy (PME)[3–13]. AMRF patients may develop proteinuria, kidney failure with glomerular sclerosis and neurological symptoms including epilepsy and ataxia[2,9,14]. Most AMRF patients show severe renal disease, but in some the disease is restricted to the CNS[5,6,10,11,15]. LIMP-2, a member of the CD36 superfamily, is a lysosomal membrane protein that transverses the membrane twice with a large luminal domain and a 20 amino acid C-terminal cytoplasmic tail[16,17]. A leucine-isoleucine motif in the cytoplasmic tail governs its transport to lysosomes[18–20]. The luminal domain of LIMP-2 shows a cavity that might be involved in lipid transport as observed for other members of the same protein family, CD36 and SRB-I[21]. LIMP-2 binds via its triple helical structure (aa 152-167) correctly folded GBA in the endoplasmic reticulum[22,23]. Next, the complex is transported to acidic (pre)lysosomal compartments where dissociation occurs[24]. The small fraction of GBA that manages to exit the endoplasmic reticulum in the absence of LIMP-2 is largely secreted[25]. Unlike the situation in GD patients, macrophages of AMRF patients develop no prominent GlcCer storage[3,9]. Chitotriosidase and CCL18, biomarkers of lipid-laden phagocytes of GD patients[26–28], are in the normal range in plasma of AMRF patients[3,9].

The scarcity of AMRF patients has limited investigations regarding the consequences of GBA deficiency, for example at lipid level. A mouse model for AMRF phenotypically resembles human AMRF[29]. Symptoms of *Limp2-/-* mice include neuropathology and sclerosis of glomeruli, as is observed in AMRF patients[14]. We therefore investigated GBA and its lipid metabolites in *Limp2-/-* mice. We analyzed GBA by measurement of its activity as well as through labeling with a fluorescent activity-based probe[30,31]. We also determined GlcCer, the lipid substrate of GBA, as well as glucosylsphingosine (GlcSph), the deacylated GlcCer that is several hundred fold increased in tissues and plasma of GD patients[32–34]. In addition, we measured glucosylated cholesterol (GlcChol), a recently discovered metabolite linked to GlcCer[35]. Our investigation revealed prominent cell-type and tissue specific differences in functional reductions of GBA in LIMP-2 deficient mice. In particular, LIMP-2 deficient white blood show high residual GBA which offers an explanation for the lack of macrophage pathology in AMRF patients.

Results

Impact of LIMP-2 deficiency on the protein composition of lysosomes.

To determine whether LIMP-2 deficiency influences other lysosomal matrix proteins besides GBA, we determined the proteome of isolated lysosomes (tritosomes) from liver of *wt* and *Limp2-/-* mice using LC-MS/MS. Comparing the protein composition of *wt* and *Limp2-/-* tritosomes, no significant differences in any of the lysosomal proteins other than GBA were observed (Table S1, supplemental data). Close to 70 lysosomal matrix proteins could be quantified (Table 1). Lysosomal acid lipase, sphingomyelin phosphodiesterase, cathepsin C

and β-galactosidase 1 were about two fold reduced in tritosomes of *Limp2-/-* mice. Cathepsin H and N-acetylglucosamine 6 sulfatase were about two-fold increased. GBA and LIMP-2 protein were both found to be absent in *Limp2-/-* tritosomes. Thus, absence of LIMP-2 results in a very specific deficiency in GBA and not of other lysosomal matrix proteins, at least in the studied hepatocytes.

Pathology

Limp2-/- mice develop relatively benign disease. Despite the marked absence of lysosomal GBA in hepatocytes, no abnormalities in the liver are observed (fig. S1). An experienced pathologist observed no gross abnormalities in any organ of mice of 6 and 12 months old, with the exception of signs of hidrosis nephro without clear abnormalities in the glomerulus. An additional abnormality is the marked thickness of sciatic nerve (fig. S2).

Table 1. Examples of differential proteins in tritosomes isolated from *Limp2-/-* and *wt* mice.

Protein Name	Accession No.	Description	Limp2-/- vs wt
LICH	Q9Z0M5	Lysosomal acid lipase	0.44
ASM	Q04519	Sphingomyelin phosphodiesterase	0.59
E9Q2Q0	E9Q2Q0	Cathepsin C	0.59
F7AF87	F7AF87	Acid beta-galactosidase1	0.60
D3Z437	D3Z437	Cathepsin H	2.14
GALNS	Q571E4	N acetylgalactosamine 6 sulfatase	2.16

Levels of active GBA in tissues by enzymatic activity measurement

In homogenates of tissues collected from *Limp2-/-* and *wt* mice of 4 months of age, GBA activity was determined using the fluorogenic substrate 4-methylumbelliferyl-β-D-glucopyranoside (4MU-β-Glc) (Table 2). Activity was clearly reduced in most analyzed tissues (eye, pancreas, heart, spleen, liver and lungs). As an exception to this, the intestine (divided in duodenum, ileum and jejunum) showed similar enzymatic activity among the genotypes. This is likely caused by bacterial glycosidases stemming from the microbiome. Moreover, endogenous lactase-phloridzin hydrolase (LPH) in the duodenum also hydrolyzes the artificial substrate[31]. A significant but less prominent reduction of GBA activity than in other organs was found in the sciatic nerve, leukocytes (peripheral blood mononuclear cells; PBMC), brain, and skin of *Limp2-/-* mice (Table 2). Of further note, whereas plasma from *wt* animals shows virtually no GBA activity, the activity is demonstrable in plasma of *Limp2-/-* mice. This is likely due to faulty secretion of mistargeted enzyme during LIMP-2 deficiency.

Table 2. GBA activity in several tissues obtained from *Limp2-/-* mice and matched *wt* animals at 4 months of age. Expressed as nmol/h/g wet weight; for plasma in nmol/h/mL; for leukocytes nmol/h/mg protein.

Abbreviations used from now on: IF (Inguinal fat), AF (Abdominal fat), OF (Omental fat), EF (Epidydimal fat), BM (Bone marrow), BAT (Brown adipose tissue), SG (Salivary gland), AG (Adrenal gland), LN (Lymph node), TE (Testis) and SN (Sciatic nerve).

Tissue	GBA activity	
	wt	*Limp2-/-*
Duodenum	728.58 ± 262.33	463.51 ± 54.80
Jejunum	660.35 ± 167.74	812.48 ± 23.79
Liver	142.05 ± 31.02	22.65 ± 11.43
Ileum	114.95 ± 20.20	78.20 ± 51.22
Testis (TE)	103.23 ± 10.02	39.85 ± 3.32
Thymus	98.06 ± 35.16	27.23 ± 9.45
Abdominal fat (AF)	96.79 ± 33.68	16.44 ± 3.79
Bone Marrow (BM)	96.34 ± 7.65	21.09 ± 1.06
Pancreas	94.77 ± 20.09	9.81 ± 2.20
Omental fat (OF)	93.13 ± 22.63	16.16 ± 2.47
Epidydimal fat (EF)	90.02 ± 35.69	16.96 ± 3.96
Epididymis (EP)	88.01 ± 26.59	45.33 ± 32.51
Inguinal fat (IF)	79.57 ± 24.69	10.81 ± 6.32
Lymph node (LN)	62.88 ± 2.21	20.59 ± 1.93
Spleen	60.30 ± 13.20	10.79 ± 2.52
Adrenal gland (AG)	58.00 ± 3.82	18.64 ± 0.35
Lungs	57.36 ± 12.87	9.59 ± 0.83
Salivary gland (SG)	55.97 ± 10.60	16.27 ± 1.52
Brain	54.20 ± 0.69	32.14 ± 2.74
Brown adipose tissue (BAT)	48.92 ± 1.35	11.41 ± 4.02
Leukocytes (PBMC)	46.78 ± 2.98	31.73 ± 1.47
Kidney	34.94 ± 4.11	9.76 ± 0.51
Skin	33.39 ± 4.24	18.75 ± 2.03
Heart	29.32 ± 6.03	3.95 ± 1.29
Sciatic nerve (SN)	23.97 ± 0.46	22.36 ± 12.78
Eye	4.65 ± 2.05	0.85 ± 0.28
Plasma	0.78 ± 0.10	8.48 ± 1.59

5

5

Detection of active GBA molecules in tissues by ABP labeling.

Active GBA in tissue homogenates was visualized with ABP MDW941 (fig. 1). The tissues of *Limp2*^{-/-} mice generally showed an absence or a strongly reduced amount of enzyme.
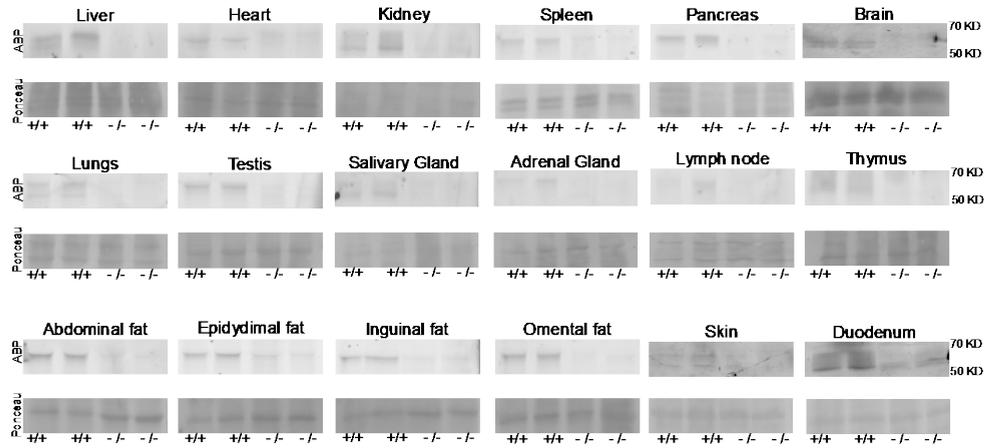

Figure 1. Visualization of GBA with fluorescent ABP MDW941. Upper panels: Detection of active GBA in tissues and organs. Homogenates (50 µg) labelled with ABP followed by SDS-PAGE and visualization by fluorescence imaging. (+/+) = *wt*; (-/-) = *Limp2*^{-/-} mice. Lower panels: Ponceau total protein staining.

We ranked tissues of *Limp2*^{-/-} mice based on residual enzyme activity in homogenates (fig 2A). Fig 2B presents a comparison of residual GBA determined by enzymatic assay and ABP labeling, revealing a strong correlation of the results with both methods. The marked tissue dependence of the reduction in GBA during LIMP-2 deficiency is illustrated in fig. 2. Of interest, considerable residual GBA, although significantly reduced, was detected for brain, leukocytes and SN.

Detection of lipid metabolite abnormalities in *Limp2*^{-/-} mice.

To demonstrate functional deficiency of GBA, we determined lipid metabolites in tissues of *Limp2*^{-/-} and *wt* mice. We first determined the concentration of GlcCer, the primary storage lipid during GBA deficiency. Table 3 shows that GlcCer concentrations differ among tissues and are most prominently increased in leukocytes, OF, AF and LN of *Limp2*^{-/-} mice. The presented values for GlyCer in brain and SN are the sum of galactosylceramide and GlcCer, indistinguishable with the used procedure.

Next, we measured GlcSph in tissues. Clear abnormalities were detected: GlcSph being increased in almost every tissue and most prominently in the pancreas, heart and OF (Table

3). GlcSph accumulation and residual GBA activity in tissues show a trend. The OF, kidney, SG, LN and the different parts of the intestine are exceptions in this regard.

To study whether other catabolic pathways are also affected by LIMP-2 deficiency, the globoside Gb3 and its deacylated form lysoGb3 were analyzed. No significant increase in these lipids in relation to LIMP-2 status was detected (Table S2, supplemental data). Interestingly, Gb3 and lysoGb3 in spleen, thymus and testis of the *Limp2*^{-/-} were about half of that in corresponding *wt* tissues (Table S2). We also determined GlcChol in tissues of *Limp2*^{-/-} and *wt* mice (Table S3, supplemental data). In most tissues, GlcChol was 1.5 fold elevated, with particularly adipose tissues showing an increase.
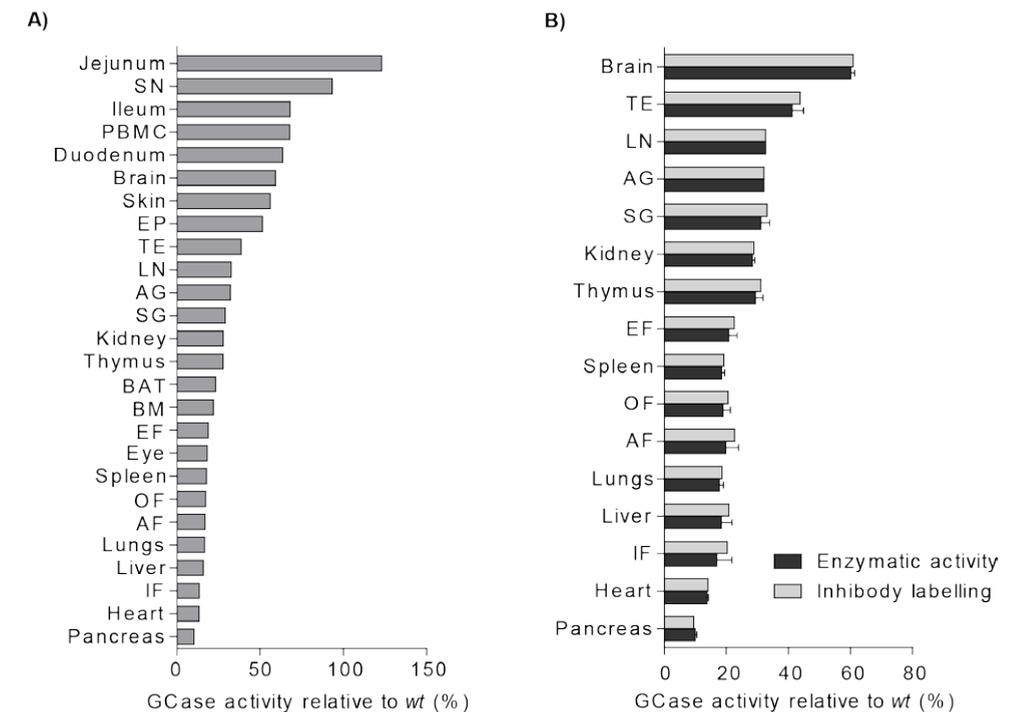
Figure 2. Residual GBA activity in tissue of *Limp2*^{-/-} mice. A) Ranking of the homogenates according to the residual enzymatic activity. **B)** Comparison of residual GBA activity by enzymatic assay and ABP labeling.

Lipid content of tritosomes.

The lipid composition of tritosomes isolated from liver of wt and *Limp2*^{-/-} mice was subsequently determined. None of the neutral glycosphingolipids (Cer, GlcCer, LacCer, and Gb3), or sphingosine and lysoGb3 showed a significant difference. Only a prominent increase

in GlcSph (3.1 vs 30.1 pmol/mg protein) and GlcChol (17.5 vs 66.0 pmol/ mg protein) was detected.

Table 3. Glucosylceramide and glucosylsphingosine levels in tissues of *Limp2-/-* and *wt* mice. Tissue levels are expressed in nmol/g wet weight tissue; Leukocytes in nmol/mg protein; plasma, bile and urine in nmol/mL. * Glycosylceramide= galactosylceramide + glucosylceramide.

Tissue/ Organ	GlcCer			GlcSph		
Genotype	wt	Limp2-/-	Limp2-/-: wt	wt	Limp2-/-	Limp2-/-: wt
Pancreas	9.6 ± 4.3	15.4 ± 1.9	1.61	2.3 ± 0.7	178.4 ± 24.1	76.55
Heart	4.2 ± 2.6	3.0 ± 0.4	0.72	3.3 ± 1.0	86.7 ± 20.5	26.04
Inguinal fat	8.2 ± 6.3	27.5 ± 11.9	3.37	3.0 ± 0.9	31.9 ± 17.5	10.64
Liver	22.2 ± 13.3	23.4 ± 13.0	1.06	32.1 ± 2.6	214.9 ± 157.9	6.70
Lungs	30.5 ± 9.5	42.5 ± 14.8	1.39	34.9 ± 8.0	738.4 ± 285.0	21.18
Abdominal fat	8.8 ± 5.1	57.7 ± 29.3	6.59	1.9 ± 0.7	40.5 ± 35.7	20.88
Omental fat	3.3 ± 1.5	14.7 ± 4.4	4.35	1.0 ± 0.7	128.4 ± 41.0	132.41
Spleen	75.0 ± 8.0	73.8 ± 6.6	0.98	20.6 ± 2.3	400.0 ± 143.7	19.37
Eye	571.8 ± 179.1	171.0 ±107.2	0.30	62.9 ± 5.7	892.6 ± 189.7	14.19
Epididimal fat	3.5 ± 2.0	3.9 ± 0.4	1.13	4.2 ± 1.9	11.0 ± 0.2	2.61
Bone Marrow (BM)	0.5 ± 0.3	0.7 ± 0.4	1.49	0.2 ± 0.1	2.0 ± 0.8	10.05
Brown adipose tissue	32.6 ± 15.2	41.2 ± 10.2	1.26	4.1 ± 1.7	49.7 ± 38.8	12.20
Thymus	70.54±13.6	70.9 ± 15.4	1.01	13.4 ± 2.4	85.6 ± 23.1	6.37
Kidney	17.8 ± 4.5	7.8 ± 10.2	0.44	25.8 ± 0.7	557.5 ± 115.4	21.59
Salivary gland	22.6 ± 8.6	41.4 ± 9.6	1.83	5.0 ± 1.6	95.2 ± 37.4	19.15
Adrenal gland	33.2 ± 12.4	53.4 ± 26.2	1.61	7.0 ± 5.1	75.7 ± 65.1	10.75
Lymph node	40.0 ± 20.2	97.5 ± 28.5	2.44	5.0 ± 4.3	95.6 ± 69.0	19.23
Testis	13.4 ± 2.5	13.3 ± 6.0	0.99	5.2 ± 1.8	24.7 ± 7.0	4.77
Epidydimal	13.3 ± 6.7	14.0 ± 5.9	1.05	29.4 ± 4.3	233.2 ± 112.1	7.93
Skin	23.3 ± 5.1	23.7 ± 14.2	1.02	9.3 ± 4.9	29.6 ± 13.6	3.20
Brain*	3067± 837	3 249 ± 474	1.06	112.8 ± 5.8	230.5 ± 14.5	2.04
Duodenum	64.3 ± 7.1	68.4 ± 9.0	1.06	8.8 ± 3.8	139.0 ± 26.5	15.81
PBMCs	0.1 ± 0.1	0.7 ± 0.8	7.30	0.3 ± 0.3	1.7 ± 0.3	5.57
Ileum	25.1± 3.8	28.1 ± 5.5	1.12	9.3 ± 1.3	180.5 ±22.9	19.39
Sciatic nerve*	10 493 ± 1 020	4 898 ± 1 016	0.47	1 112 ± 652	860.9 ± 543.6	0.77
Jejunum	41.4 ± 9.2	47.9 ± 11.2	1.16	8.2 ± 1.6	140.7 ± 15.3	17.24
Plasma	3.2 ± 0.9	1.8 ± 1.1	0.57	1.1 ± 1.3	3.6 ± 1.7	3.13
Bile	4.8 ± 5.7	2.1 ± 0.8	0.43	1.4 ± 0.5	6.3 ± 2.2	4.54
Urine	0.3 ± 0.1	0.2 ± 0.1	0.73	0.6 ± 1.2	0.4 ± 0.2	0.55

Biochemical course of disease

We then investigated how lipid abnormalities develop with age in several tissues of *Limp2-/-* mice. At various ages, the changes in GlcCer were very small in all the examined tissues from *Limp2-/-* mice (fig. 3). Only kidney and SG showed a very slight increase at older age. In sharp

contrast, already in 2 months old animals, GlcSph was clearly elevated. The sphingoid base did not increase further with age in most tissues of *Limp2-/-* mice, except for the thymus (fig. 4). GlcChol was also already increased in tissues at the youngest age examined (2 months) and no accumulation with increasing age was detected (fig. 5). The concentrations of globosides Gb3 and lysoGb3 showed no differences from *wt* animals at various ages, except for increasingly reduced levels in spleen (fig. S3 and S4).
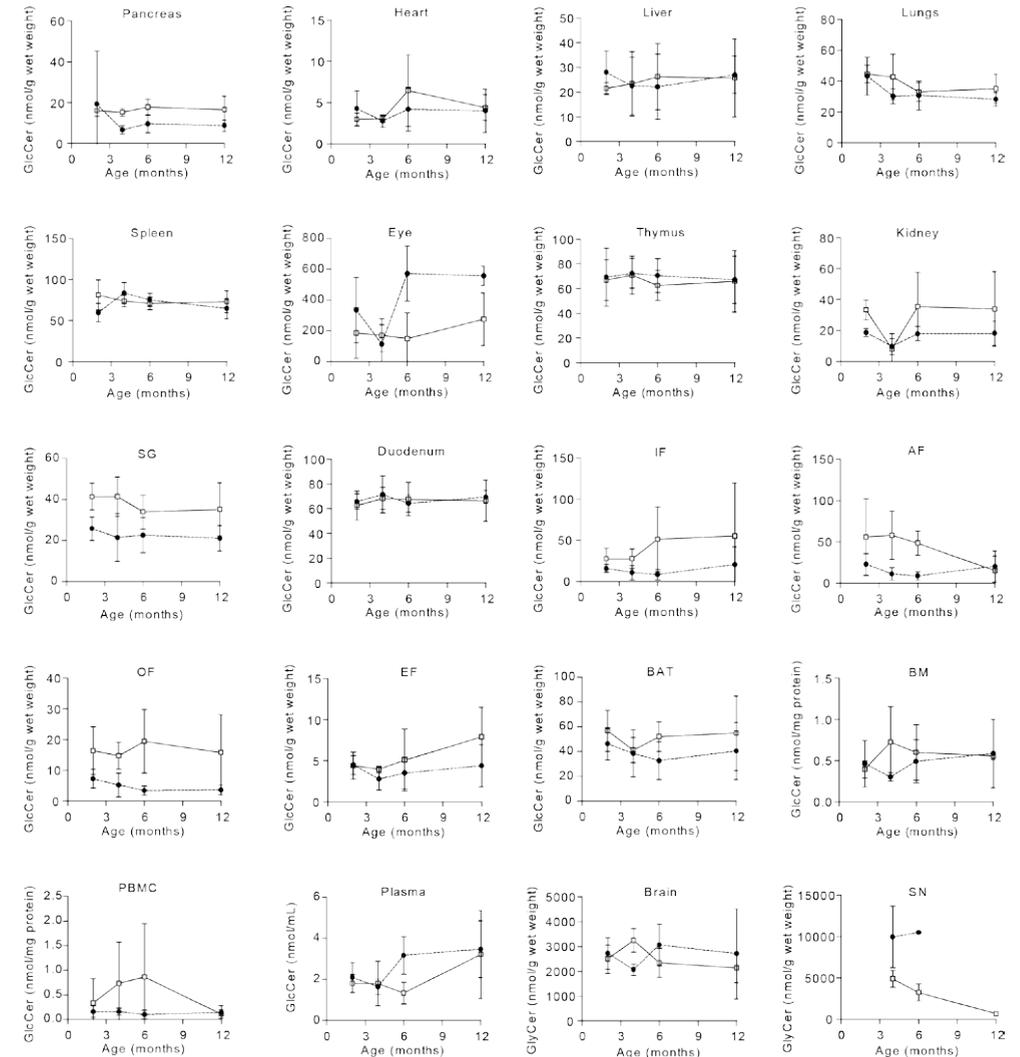
Figure 3. Glucosylceramide levels in *wt* and *Limp2-/-* mice at different ages. Black circle = *wt*; Open square= *Limp2-/-* mice.
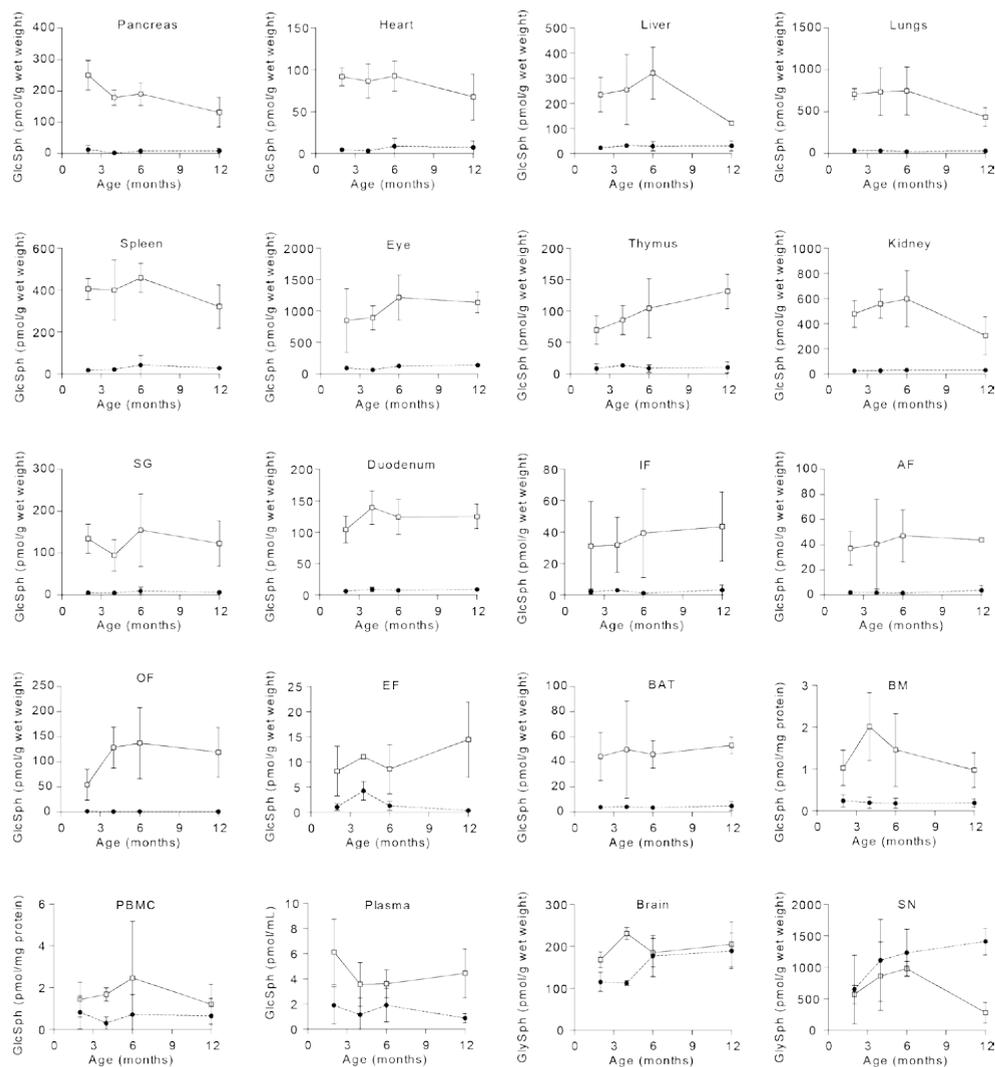
Figure 4. Glucosylsphingosine levels in *wt* and *Limp2*^{-/-} mice at different ages.
Black circle= *wt*; Open square= *Limp2*^{-/-} mice.
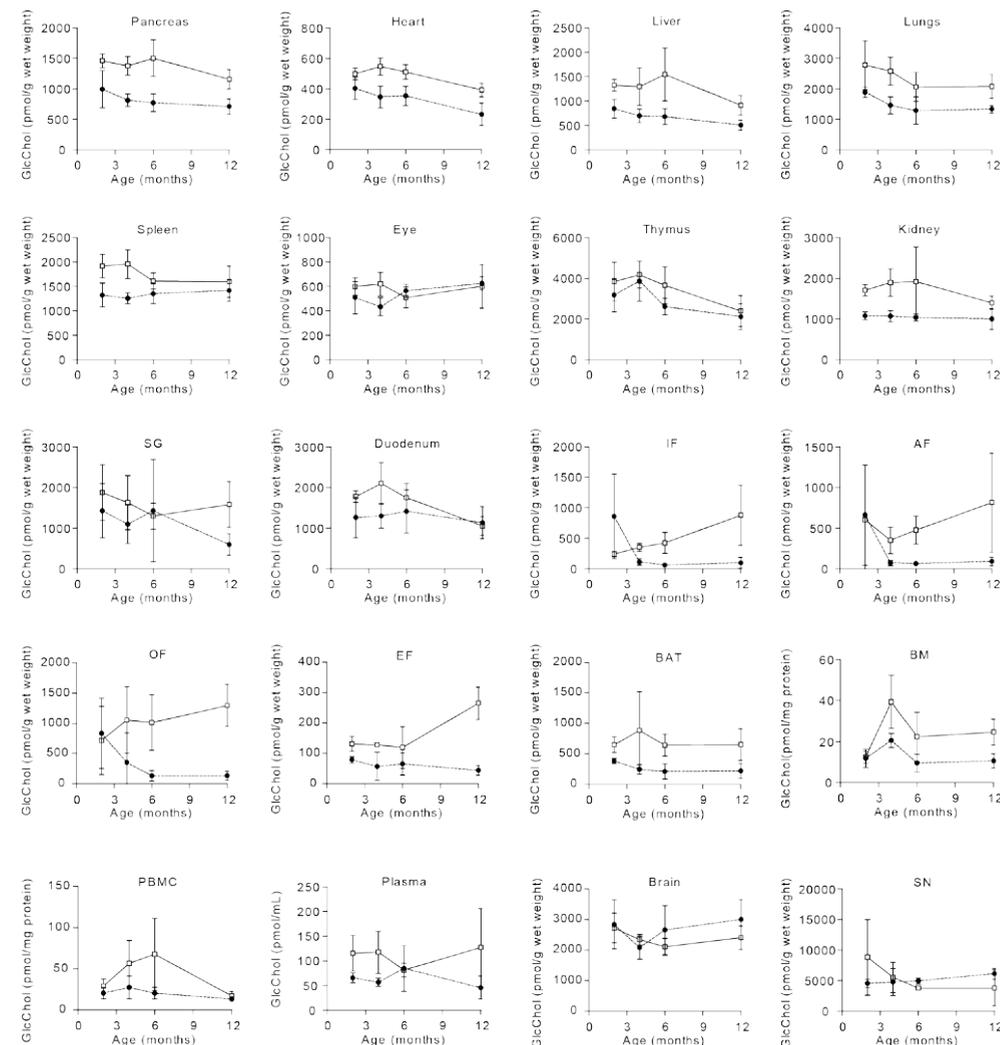
Figure 5. Glucosyl-cholesterol levels in *wt* and *Limp2*^{-/-} mice at different ages.
Black circle= *wt*; Open square= *Limp2*^{-/-} mice.

Lipids in brain and SN

In most tissues GlcCer concentrations exceed those of galactosylceramide, but not in brain and nerves. This also holds for the de-acylated glycosphingosine bases. The used HPLC procedure does not fully separate glucosyl-and galactosyl-lipid and therefore only allows determination of the two lipids together, (gly)ceramide and (gly)sphingosine. We observed no differences in the levels of (gly)ceramide and (gly)sphingosine in brain of Limp2^{-/-} mice (see Fig. 3 and 4, respectively). In the case of the SN, (gly)ceramide was significantly lower and to a lesser extent also (gly)sphingosine. No clear differences in the total (gly)ceramide in brain of

wt and *Limp2*^{-/-} mice were observed at any age analyzed (fig. 3). Digestion of brain and SN homogenates with recombinant GBA allows a discrimination between glucosyl- and galactosylceramide. With this method the GlcCer content of brain from *Limp2*^{-/-} mice was found to be normal (fig. 6). Only a small decrease in galactosylceramide was detected. In the SN of *Limp2*^{-/-} mice, (gly)ceramide was clearly reduced: a prominent reduction in galactosylceramide developing with increasing age. In the SN, ceramide is increased, maximally at 4 months of age.

Figure 6. Glycosphingolipids and ceramide levels in brain and sciatic nerve. Lipids were determined as described in M&M. To distinguish GlcCer and GalCer, digestion with GBA was performed. GalCer is no substrate for the enzyme. Black circle= *wt*; Open square= *Limp2*^{-/-} mice
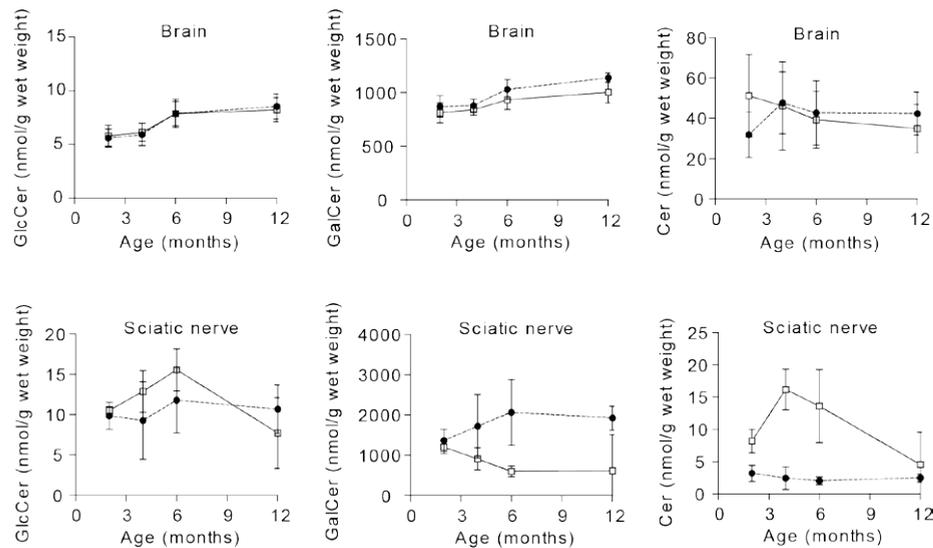
Secretion and re-capture of GBA

Leukocytes of AMRF patients and *Limp2*^{-/-} mice show a relative high (~65 %) residual GBA activity. To create AMRF-like leukocytes, LIMP-2 was reduced in THP-1 cells using lentiviral *SCARB2* siRNA. Reduced expression of *SCARB2* was verified by qPCR and Western Blot (fig. S5). Accompanying reduction of GBA was determined via activity measurement (fig. S5). Cultured immortalized AMRF lymphocytes, fibroblasts, AMRF-like THP-1 cells and the corresponding control cells were incubated with a potent inhibitor of dynamin (Dynasore) inhibiting endocytosis[36]. The presence of Dynasore caused a 50 % reduction of cellular GBA in the immortalized AMRF lymphocytes and AMRF-like THP-1 cells. No alterations were observed in AMRF fibroblasts (fig. 7). This finding suggests that re-uptake of secreted GBA occurs in blood cells but not fibroblasts.
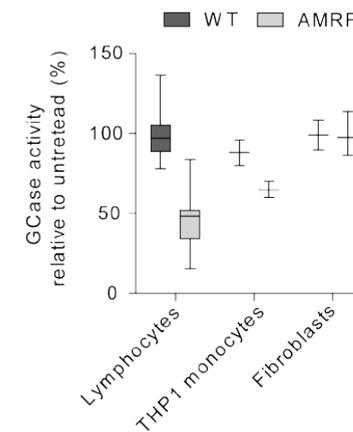

Figure 7. Effect of an endocytosis inhibitor on cellular GBA. Relative amount (%) of GBA activity in different cell lines after treatment with Dynasore, when compared to not treated.

Discussion

GBA is uniformly deficient in all cells and tissues of GD patients[37]. Lysosomal storage of GlcCer is particularly prominent in macrophages of GD patients[1]. These so-called Gaucher cells accumulate in spleen, liver and bone marrow. Intriguingly, the secondary GBA deficiency in AMRF patients does not result in a true phenocopy of GD with characteristic Gaucher cells. The available *Limp2*^{-/-} mice allowed us to study the impact of LIMP-2 on GBA and find an explanation for the different clinical manifestation of GD and AMRF.

We first studied the impact of the absence of LIMP-2 on other lysosomal proteins. Purified lysosomes from hepatocytes of *Limp2*^{-/-} and *wt* mice showed no differences in their proteome, except for the absence of LIMP-2 and GBA. Noteworthy, absence of GBA in lysosomes does not seem to dramatically affect hepatocytes macroscopically or in their function.

We next examined GBA in various tissues of *Limp2*^{-/-} mice. A deficiency in GBA was observed in most tissues, this however showed considerable variation among tissues as revealed by enzymatic activity measurements and labeling of active GBA molecules with a fluorescent activity-based probe. Many tissues of *Limp2*^{-/-} mice like pancreas, heart and liver show little GBA, whereas leukocytes have relatively high residual enzyme levels. The functional consequences of reduced GBA were studied by lipid analysis. GlcCer, the primary substrate of GBA, is only slightly increased in tissues of *Limp2*^{-/-} mice. In contrast, GlcSph, formed by lysosomal deacylation of GlcCer[34], is strongly elevated in LIMP-2 deficient tissues. Likewise, GlcSph, but not GlcCer, was found to be increased in purified lysosomes of liver of *Limp2*^{-/-} mice. Apparently, accumulating GlcCer is efficiently converted to GlcSph during LIMP-2 deficiency. GlcSph is highest in tissues of *Limp2*^{-/-} mice with the lowest GBA. The maximal increase in tissue GlcSph and GlcCer already occurs at 2 month of age. The apparent

5

5

stabilization of lipid accumulation in *Limp2⁻/⁻* mice might be accomplished by the ongoing removal of GlcSph by its secretion from the body via liver and bile[34].

In this connection, *Limp2⁻/⁻* leukocytes are of interest. They accumulate almost no GlcCer and show relatively little GlcSph. The mutant leukocytes seem to produce less GlcSph compared to other cell types. The leukocytes of *Limp2⁻/⁻* mice have a high residual GBA, reaching about 65 % of normal values, and consequently active conversion of GlcCer to GlcSph may be small in these cells.

Our findings with *Limp2⁻/⁻* mice differ from observations of mice with inducible GBA deficiency in cells of the white blood cell lineage that accumulate GlcCer-laden macrophages in tissues[38,39]. Macrophages in these animals do not manage to sufficiently convert GlcCer to GlcSph to avoid Gaucher cell formation. The high residual GBA capacity of *Limp2⁻/⁻* leukocytes prevents formation of GlcCer-laden macrophages in AMRF patients and *Limp2⁻/⁻* mice. We examined the cause for this. Inhibition of endocytosis prohibited high cellular GBA in cultured AMRF lymphoblasts and LIMP-2 deficient THP-1 cells. Apparently, re-uptake of extracellular GBA through (dynamin-dependent) endocytosis provides GBA to THP-1 cells and lymphoblasts with reduced LIMP-2. Such corrective uptake is not observed with LIMP-2 deficient fibroblasts. Based on these findings, it seems likely that leukocytes and macrophages of AMRF patients, with significant GBA in plasma[25], are sufficiently corrected by uptake of faulty secreted GBA to prevent formation of Gaucher cells.

Comparing the various tissues of *Limp2⁻/⁻* mice, the correlation of occurrence of pathology with residual GBA, as well as noted lipid abnormalities, is not evident. For example, *Limp2⁻/⁻* mice, as some AMRF patients, develop tubular proteinuria[4,14,29]. *Limp2⁻/⁻* kidney shows similar residual GBA levels and comparable anomalies in lipids to other tissues. Spleen and liver show no hypertrophy, despite a low GBA and lipid abnormalities similar to kidney. Brain of *Limp2⁻/⁻* mice has a slightly higher residual GBA compared to viscera, but no remarkable difference in lipid abnormalities. Possibly, we missed in our brain lipid analyses specific anomalies in neuronal cells, associated with epileptic attacks occurring in AMRF patients. Peripheral demyelinating neuropathy is a hallmark of AMRF[29]. Strikingly swollen sciatic nerves (SN) in *Limp2⁻/⁻* mice were observed by us already at young age. The residual GBA is relatively high in the SN and GlcCer and GlySph levels are close to normal. The elevated ceramide might be more relevant for the observed pathology of the SN. The decrease in galactosylceramide of *Limp2⁻/⁻* SN likely stems from ongoing peripheral demyelination reflected by the tremors observed in the mice.

Abnormal glucosylceramide metabolism is associated with neuropathology. Severe cases of GD develop neuropathology and type I GD patients as well as GD carriers have an increased risk for Parkinson disease[40]. Michelakakis and colleagues firstly reported on a similar increased risk imposed by heterozygosity for *SCARB2* mutations, a finding confirmed by others[41,42]. *Limp2⁻/⁻* mice develop α-synuclein deposits and associated pathology of dopaminergic neurons[43]. This has prompted the hypothesis that the modulation of LIMP-2 to increase GBA might offer a therapy for α-synucleinopathies[43]. Indeed, very recently it has been demonstrated that a peptide derived from helix 5 of LIMP-2 interacts with GBA, increases

enzymatic activity and reduces α-synuclein levels[23]. Of note, a specific microRNA, miR-127-5p, has been found to reduce GBA by down-regulation of LIMP-2[44]. In view of the above, the physiological relevance of this type of regulation merits further research.

LIMP-2 belongs to the CD36 superfamily of scavenger receptor proteins that also includes SR-BI which is involved in cholesterol transport and CD36, a fatty-acid transporter and receptor of modified lipoproteins. The crystal structure of LIMP-2 reveals a cavity over the entire length of the protein[45]. Mutagenesis experiments have shown that the same cavity in the homologous SR-BI mediates transport of cholesterol(esters) to the membrane. In this regard, the recent observation of a direct link between GBA and cholesterol metabolism is intriguing[34,35]. Glucosylated cholesterol (GlcChol) was shown to be a substrate for GBA. Moreover, GlcChol is formed by GBA via transglucosylation using glucosylceramide as glucose donor and cholesterol as acceptor[34,45]. The apparent interaction between GBA and sterol furthermore warrants investigations on possible impact of LIMP-2 on lysosomal cholesterol homeostasis. In view of the above, our finding of significant increases in GlcChol in purified *Limp2⁻/⁻* lysosomes as well as tissues of *Limp2⁻/⁻* mice is of great interest.

In conclusion, our study sheds new light on the consequences of systemic LIMP-2 deficiency regarding tissue specific GBA reduction and associated compensatory deacylation of GlcCer to GlcSph. While most *Limp2⁻/⁻* tissues manifest a marked deficiency in GBA, *Limp2⁻/⁻* leukocytes appear relatively protected by re-uptake of secreted enzyme. This correction offers a plausible explanation for the different symptomatology of AMRF and GD.

Materials & Methods

Animal studies

All animal protocols were approved by the Institutional Animal Welfare Committee of the Academic Medical Centre Amsterdam in the Netherlands (DBC3021, DBC101698, DBC102873, DBC100757-125 and DBC17AC). *Limp-2⁻/⁻* mice were generated was described earlier[29]. Homozygous wild type (*wt*) animals (*Limp-2⁺/⁺*) and homozygous affected animals (*Limp2⁻/⁻*) were obtained by crossing heterozygous (*Limp2⁺/⁻*) mice. Genotype was determined by PCR using genomic DNA from a small piece of the ear. The mice were housed at the Institute Animal Core Facility in a temperature- and humidity-controlled room with a 12-h light/dark cycle and given free access to food and water *ad libitum*. A total of 45 animals were used, equally distributed by genotype (*wt*; *Limp2⁻/⁻*), gender (male, female) and by age (2, 4, 6 and 12 months).

Tissue collection

Animals were anesthetized with a dose of Hypnorm (0.315 mg/mL phenyl citrate and 10 mg/ml fluanisone) and Dormicum (5 mg/mL midazolam) according to their weight. The given dose was 80 µL/10 g body weight. The animals were sacrificed by cervical dislocation. Blood was collected via heart puncture into EDTA tubes and used for lipid measurements. Tissues

and organs were collected by surgery and rinsed with PBS. Each one was sliced in half: one half was directly snap-frozen in liquid nitrogen and stored at -80 °C and the other half was conserved in 10 % (v/v) formaldehyde for later pathology analysis. Bile was collected for 15 min via cannulation of the gall bladder. Urine was collected through aspiration of the bladder. Bone marrow was extracted from the hind legs. The skin and flesh were removed, in order to expose the tibia and femur. Both ends of the collected femur were excised and bone marrow was removed by rinsing with ice cold PBS and the fluid was collected in a 50 mL tube. The cells in the aspirate were centrifuged for 10 min at 2500 rpm (4 °C). The supernatant was discarded and the pellet was washed again. The pellet was taken up into 1 mL ice cold PBS, transferred to a 1.5 mL Eppendorf tube and centrifuged for 5 min at 13 200 rpm (4 °C). The supernatant was discarded and the pellet stored at -80 °C.

Plasma and leukocytes

Blood in EDTA tubes was centrifuged for 10 min at 4 000 rpm and the collected plasma was stored at -80 °C. The collected leukocyte layer was transferred to a 50 mL tube with 45 mL of erythrocyte lysis buffer (NH_4Cl/EDTA buffer, pH 7.4). After 20 min shaking at 4 °C on a roller mixer, the tube was centrifuged at 2500 rpm for 10 min (4 °C). The supernatant was discarded and 45 mL of lysis buffer was added. This procedure was repeated to get rid of all erythrocytes. The pellet was then resuspended in 1 mL ice cold PBS and transferred to a 1.5 mL Eppendorf tube and centrifuged for 5 minutes at 13 200 rpm (4 °C). The supernatant was discarded and the leukocyte pellet was stored at -80 °C.

Tissue homogenization

Homogenization was performed with RNAse-free glass beads in 2 mL screwcap Eppendorf tubes. 25 mM potassium phosphate buffer (pH 6.5), containing 0.1 % (v/v) Triton X-100 and protease inhibitor cocktail (Roche) was added to tissues in a 1:5 ratio. For homogenization, a Tissue Lyzer FastPrep (R)-24 (M. P. Biomedicals, Irvine, CA, USA) set 6 ms^{-1} for 30 s. Homogenates were cooled for 1 min on ice in between runs. Smaller tissues (eye, salivary gland, sciatic nerve, lymph node, epididymis and adrenal gland) were homogenized by sonication (40 % power. 40 % amplitude for 6 s) using the sonicator Vibra Cell$^{(TM)}$ Model no. CV18 (Sonics, Danburry, CT, USA). In the case of leukocyte and bone marrow preparations, 100 µl of the same extraction buffer was added to the pellets and these were homogenized by sonication as described above. All homogenates were stored at -80 °C.

Protein measurement with the Bicinchoninic acid (BCA^{TM}) assay

For protein quantification the the Pierce™ BCA Protein Assay Kit (Pierce Biotechnology Inc., No. 23225) was used according to the manufacturer's protocol.

Isolation of lysosomes

Lysosomes were purified as follows. Briefly, mice were treated by a single injection of 0.75 mg of tyloxapol (Triton WR1339 Sigma) per g of body weight, 4 days before liver collection. This treatment causes accumulation of non-digestible tylopaxol in lysosomes of hepatocytes. Four days after the tyloxapol administration, animals were sacrificed and the livers collected. Cells were gently disrupted, leaving lysosomes intact. The density of tyloxapol-laden lysosomes (Tritosomes) is below 1 g/mL, enabling their separation from other cell organelles. The isolation of tritosomes from tyloxapol-treated mice included differential centrifugation and isopycnic centrifugation and resulted in a lysosome-enriched fraction as described earlier[46].

LC-MS/MS proteomics

Tritosomes for LC-MS/MS were prepared using Rapigest detergent (Waters Corporation) and tryptic fragments were analyzed by label-free data-independent LC-MS/MS as described before[47].

Activity-based probe (ABP) labeling of GBA

Tissue homogenates (50 µg total protein) were incubated with 100 nM of red BODIPY-MDW941[30] in 150 mM McIlvaine buffer (150 mM citrate-Na_2HPO_4, pH 5.2. with 0.2 % (w/v) sodium taurocholate, 0.1 % Triton X-100) and protease inhibitor cocktail (Roche) for 45 min at 37 °C. In the case of THP-1 cell homogenates, 20 µg total protein was used for ABP labeling.Afterwards protein was denatured in 5x Laemmli buffer (50 % (v/v) 1 M Tris-HCl, pH 6.8, 50 % (v/v) glycerol, 10 % (w/v) DTT, 10 % (w/v) SDS, 0.01 % (w/v) bromophenol blue) by boiling for 10 min at 100 °C and separated by electrophoresis on 10 % (w/v) acrylamide SDS-PAGE gels running at 90 V. Wet slab gels were scanned for fluorescence with a Typhoon variable mode imager (Amersham Bioscience) using λ_{ex} 532 nm and λ_{em} 610 nm (band pass filter 30nm). Fluorescence was quantified with ImageJ software (NIH, USA). Gels were electroblotted onto a nitrocellulose membrane (Schleicher&Schuell) and the protein bands detected with Ponceau S staining.

Enzymatic assays

Activity measurements were performed for GBA as described[48]. Activity was measured with 3.73 mM 4-methylumbelliferyl-β-D-glucopyranoside (4MU-β-Glc), dissolved in 150 mM McIlvaine buffer (pH 5.2 supplemented with 0.2 % (w/v) sodium taurocholate, 0.1 % (v/v) Triton X-100) and 0.1 % BSA. The reaction was stopped with NaOH-glycine (pH 10.3), and fluorescence was measured with a fluorimeter LS55 (Perkin-Elmer, Beaconsfield, UK) at λ_{ex} 366 nm and λ_{ex} 445 nm.

HPLC and MS/MS lipid measurements

Neutral glycosphingolipids, LysoGb3, GlcSph and GlcChol were determined in the homogenates as described earlier[35,49–51]. An internal standard mix ($^{13}C_5$-Lyso-Gb3, $^{13}C_5$-GlcSph and $^{13}C_6$-GlcChol) was added to the samples for calculation. After protein precipitation with $CHCl_3$:MeOH 1:1 (v:v), one step of extraction and two washing steps were carried out, always with the ratio $CHCl_3$:MeOH;H_2O 1:1:0.9 (v:v:v). With this procedure, LysoGb3 and GlcSph are in the hydrophilic phase (upper phase), and GlcChol and neutral lipids will be in the

hydrophobic phase (lower phase). The upper phase was dried under N_2 gas stream and the pellet redissolved in MeOH (LysoGb3 and GlcSph). One-half of the lower phase, for GlcChol measurement, was dried under a N_2 gas stream and the pellet redissolved in solution A (10 mM ammonium formate in MeOH). Lipids were measured using an Acquity TQD (Waters Inc.). For determination of neutral glycosphingolipids, a known amount of internal standard (C_{17}-Sphinganine) was added to the sample after the extraction and then deacylated with 0.1 M NaOH in MeOH in a microwave for 1h. Neutral lipids were next analyzed using a Dionex HPLC system with a C18 reversed-phase chromatography and automated derivatization with fluorescent o-phthaldialdehyde (OPA). The fluorescent derivatized structures derived from glycosphingolipids were quantitatively detected by fluorescence measurement at λ_{ex} 340 nm and λ_{ex} 435 nm. Quantification of GlcCer in brain and sciatic nerves required an optimized protocol, given the abundant presence of interfering galactosylceramide in these materials. After total lipid extraction by adapted Folch extraction[52], glycosphingolipids were separated from neutral lipids (ceramides and phospholipids) by solid phase extraction (SPE) using a silica gel (SiOH) SPE column. After deacylation with sphingolipid ceramide N-deacylase (SCDase, Takara Bio Inc., Japan), GlcCer was digested with recombinant GBA (Imiglucerase, Genzyme). The subsequent increase in ceramide levels after digestion, measured as described above, was assumed to be derived from GlcCer degradation[53].

Lymphocyte immortalization

Materials from donors and patients were obtained after informed consent. B95–8 culture supernatants containing the transforming strain of Epstein-Barr virus (EBV) were used to establish lymphoblastoid cell lines *in vitro*. In short, leukocytes from healthy donors and from two LIMP-2 deficient patients homozygous for the *SCARB2* mutation W178X[3] were isolated by sedimentation on Ficoll-Hypaque density gradients. Mononuclear cells were resuspended in RPMI 1640 medium containing 10 % fetal calf serum and viral supernatants (10^7 mononuclear cells/ml) and incubated for 2 h at 37 °C. Cultures were maintained in 25 cm^2 tissue culture flask for 3 weeks containing 1 µg/mL cyclosporin A. The cells were washed twice with PBS and then cultured in RPMI 1640 medium containing 10 % fetal calf serum and 5 % Pen/Strep (Life Technologies).

Generation of lentivirus particles and infection

Recombinant lentivirus particles encoding shRNAs targeting *SCARB2* were produced, concentrated and titrated as described previously[54]. Cultured THP-1 were infected with recombinant lentivirus particles for 24 h in 400 mL of RPMI 1640 medium containing 10 % fetal calf serum and 5 % Pen/Strep. The next day, 400 mL RPMI 1640 medium containing 10 % fetal calf serum and 5 % Pen/Strep were added. After 48 h, the cells were carefully washed and cultured for another 48 h before harvesting. Transduction efficiency was determined by western-blot and RT-PCR.

RNA Extraction and quantitative RT-PCR

Total RNA was harvested from cells using the Total RNA mini kit (Bio-Rad) or Trizol reagent (Invitrogen) according to the manufacturer's instructions. cDNA was made using the iScript cDNA synthesis kit (Bio-Rad). Real-time reverse transcription PCR was performed using the MyIQ system (Bio-Rad) with the primer LIMP-2 forward (*5'*-TTGGCCCTCTGGACATTATC-*3')* and the LIMP-2 reverse (*5'*-AGAACCGCATGAAGTGAACC-*3')*. Acidic ribosomal phosphoprotein P0 was determined as an internal control for cDNA content of the samples, with the primer P0 forward (*5'*-TCGACAATGGCAGCATCTAC-*3')* and P0 reverse (*5'*-ATCCGTCTCCACAGACAAGG-*3')*

SDS-PAGE Western Blotting

Homogenates containing 20 µg of total protein were denatured in 5x Laemmli buffer (50 % (v/v) 1 M Tris-HCl, pH 6.8, 50 % (v/v) glycerol, 10 % (w/v) DTT, 10 % (w/v) SDS, 0.01 % (w/v) bromophenol blue) by boiling for 10 min at 100 °C, and separated by electrophoresis on 10 % acrylamide (w/v) SDS-PAGE gels running at 90 V. SDS–PAGE gels were electroblotted onto a nitrocellulose membrane (Schleicher & Schuell). Membranes were blocked with 5 % skimmed milk and 0.05 % Tween-20 in Tris-buffered saline (TBS) for 1 h at room temperature and incubated overnight with the rabbit polyclonal anti-LIMP-2 antibody (NB400-129, Novus Biologicals) at 4 °C. Membranes were then washed three times with 0.01 % Tween-20 in TBS and incubated with the appropriate IRDye conjugated secondary antibody for 1 h at room temperature. After washing, detection was performed using the Odyssey® Clx. Infrared Imaging System (LI-COR).

Inhibition of endocytosis by cultured cells

Immortalized lymphocytes and THP-1 cells were seeded at $1x10^6$ cells/well in 6-well plates containing 1 mL of medium RPMI 1640 with 5 % Pen/Strep. Fibroblasts were obtained from skin biopsies of control subjects and AMRF patients after informed consent. The patient's cells were homozygous for the *SCARB2* mutation W178X[3]. Fibroblasts were cultured in Dulbecco's modified Eagle's medium (DMEM) supplemented with 10 % fetal bovine serum, 2 mM L-glutamine, 1 % Pen/Strep. 100 mg/mL kanamycin sulfate and 2.5 mg/mL fungizone (Gibco, Invitrogen). Fibroblasts were cultured almost to confluency in 6-well plates. Next, the medium was changed to 1 mL of DMEM supplemented with 1 % Pen/Strep (Gibco, Invitrogen). A pre-dilution of Dynasore to 160 µM was made in RPMI 1640 or DMEM containing 5 % Pen/Strep. One mL of this solution was added to cells to achieve a final concentration of 80 µM. After 8 h of incubation, the cells were washed with PBS and collected. Treatment of cells with mannan at a concentration of 1 mg/mL was performed overnight. Cells were disrupted by sonication (40 % power, 40 % amplitude for 6 s) in the sonicator Vibra Cell (TM) Model no. CV18. (Sonics, Danburry, CT, USA). Dynasore, a dynamin inhibitor impairing endocytosis, was obtained from Sigma-Aldrich.

References

1. Beutler, E. & Grabowski, G. A. *Glucosylceramide lipidosis-Gaucher disease. In: CR Scriver, Al Beaudet, WS Sly, D Valle (Eds) The metabolic and molecular bases of inherited diseases*. (McGraw-Hill, New York, 2001).
2. Reczek, D. *et al.* LIMP-2 is a receptor for lysosomal mannose-6-phosphate-independent targeting of beta-glucocerebrosidase. *Cell* **131,** 770–83 (2007).
3. Balreira, A. *et al.* A nonsense mutation in the LIMP-2 gene associated with progressive myoclonic epilepsy and nephrotic syndrome. *Hum. Mol. Genet.* **17,** 2238–2243 (2008).
4. Berkovic, S. F. *et al.* Array-Based Gene Discovery with Three Unrelated Subjects Shows SCARB2/LIMP-2 Deficiency Causes Myoclonus Epilepsy and Glomerulosclerosis. *Am. J. Hum. Genet.* **82,** 673–684 (2008).
5. Fu, Y.-J. *et al.* Progressive myoclonus epilepsy: extraneuronal brown pigment deposition and system neurodegeneration in the brains of Japanese patients with novel SCARB2 mutations. *Neuropathol. Appl. Neurobiol.* **40,** 551–63 (2014).
6. Dibbens, L. M. *et al.* SCARB2 mutations in progressive myoclonus epilepsy (PME) without renal failure. *Ann. Neurol.* **66,** 532–6 (2009).
7. Hopfner, F. *et al.* Novel SCARB2 mutation in action myoclonus-renal failure syndrome and evaluation of SCARB2 mutations in isolated AMRF features. *BMC Neurol.* **11,** 134 (2011).
8. Zeigler, M. *et al.* A novel SCARB2 mutation in progressive myoclonus epilepsy indicated by reduced β-glucocerebrosidase activity. *J. Neurol. Sci.* **339,** 210–3 (2014).
9. Chaves, J. *et al.* Progressive myoclonus epilepsy with nephropathy C1q due to SCARB2/LIMP-2 deficiency: clinical report of two siblings. *Seizure* **20,** 738–40 (2011).
10. Perandones, C., Pellene, L. A. & Micheli, F. A new SCARB2 mutation in a patient with progressive myoclonus ataxia without renal failure. *Mov. Disord.* **29,** 158–9 (2014).
11. Guerrero-López, R. *et al.* A new SCARB2 mutation in a patient with progressive myoclonus ataxia without renal failure. *Mov. Disord.* **27,** 1826–7 (2012).
12. Higashiyama, Y. *et al.* A novel SCARB2 mutation causing late-onset progressive myoclonus epilepsy. *Mov. Disord.* **28,** 552–3 (2013).
13. Perandones, C. *et al.* A case of severe hearing loss in action myoclonus renal failure syndrome resulting from mutation in SCARB2. *Mov. Disord.* **27,** 1200–1 (2012).
14. Desmond, M. J. *et al.* Tubular proteinuria in mice and humans lacking the intrinsic lysosomal protein SCARB2/Limp-2. *Am. J. Physiol. Renal Physiol.* **300,** F1437-47 (2011).
15. Rubboli, G. *et al.* Clinical and neurophysiologic features of progressive myoclonus epilepsy without renal failure caused by SCARB2 mutations. *Epilepsia* **52,** 2356–63 (2011).
16. Saftig, P. & Klumperman, J. Lysosome biogenesis and lysosomal membrane proteins: trafficking meets function. *Nat. Rev. Mol. Cell Biol.* **10,** 623–35 (2009).
17. Calvo, D., Dopazo, J. & Vega, M. A. The CD36, CLA-1 (CD36L1), and LIMPII (CD36L2) gene family: cellular distribution, chromosomal location, and genetic evolution. *Genomics* **25,** 100–106 (1995).
18. Ogata, S. & Fukuda, M. Lysosomal targeting of Limp II membrane glycoprotein requires a novel Leu-Ile motif at a particular position in its cytoplasmic tail. *J. Biol. Chem.* **269,** 5210–7 (1994).
19. Sandoval, I. V *et al.* The residues Leu(Ile)475-Ile(Leu, Val, Ala)476, contained in the extended carboxyl cytoplasmic tail, are critical for targeting of the resident lysosomal membrane protein LIMP II to lysosomes. *J. Biol. Chem.* **269,** 6622–31 (1994).
20. Vega, M. A. *et al.* Targeting of lysosomal integral membrane protein LIMP II. The tyrosine-lacking carboxyl cytoplasmic tail of LIMP II is sufficient for direct targeting to lysosomes. *J. Biol. Chem.* **266,** 16269–72 (1991).
21. Gaspar, P. *et al.* Action myoclonus-renal failure syndrome: diagnostic applications of activity-based probes and lipid analysis. *J. Lipid Res.* **55,** 138–145 (2014).
22. Blanz, J. *et al.* Disease-causing mutations within the lysosomal integral membrane protein type 2 (LIMP-2) reveal the nature of binding to its ligand -glucocerebrosidase. *Hum. Mol. Genet.* **19,** 563–572 (2010).
23. Zunke, F. *et al.* Characterization of the complex formed by β-glucocerebrosidase and the lysosomal integral membrane protein type-2. *Proc. Natl. Acad. Sci.* **113,** 3791–3796 (2016).
24. Zachos, C., Blanz, J., Saftig, P. & Schwake, M. A Critical Histidine Residue Within LIMP-2 Mediates pH Sensitive Binding to Its Ligand β-Glucocerebrosidase. *Traffic* **13,** 1113–1123 (2012).
25. Gaspar, P. *et al.* Action myoclonus-renal failure syndrome: diagnostic applications of activity-based probes and lipid analysis. *J. Lipid Res.* **55,** 138–145 (2014).
26. Ferraz, M. J. *et al.* Gaucher disease and Fabry disease: New markers and insights in pathophysiology for two distinct glycosphingolipidoses. *Biochim. Biophys. Acta - Mol. Cell Biol. Lipids* **1841,** 811–825 (2014).
27. Boot, R. G. *et al.* Marked elevation of the chemokine CCL18/PARC in Gaucher disease: a novel surrogate marker for assessing therapeutic intervention. *Blood* **103,** 33–9 (2004).
28. Hollak, C. E., van Weely, S., van Oers, M. H. & Aerts, J. M. Marked elevation of plasma chitotriosidase activity. A novel hallmark of Gaucher disease. *J. Clin. Invest.* **93,** 1288–1292 (1994).
29. Gamp, A.-C. *et al.* LIMP-2/LGP85 deficiency causes ureteric pelvic junction obstruction, deafness and peripheral neuropathy in mice. *Hum. Mol. Genet.* **12,** 631–46 (2003).
30. Witte, M. D. *et al.* Ultrasensitive in situ visualization of active glucocerebrosidase molecules. *Nat. Chem. Biol.* **6,** 907–913 (2010).
31. Kallemeijn, W. W. *et al.* A Sensitive Gel-based Method Combining Distinct Cyclophellitol-based Probes for the Identification of Acid/Base Residues in Human Retaining -Glucosidases. *J. Biol. Chem.* **289,** 35351–35362 (2014).
32. Dekker, N. *et al.* Elevated plasma glucosylsphingosine in Gaucher disease: relation to phenotype, storage cell markers, and therapeutic response. *Blood* **118,** e118-27 (2011).
33. Rolfs, A. *et al.* Glucosylsphingosine Is a Highly Sensitive and Specific Biomarker for Primary Diagnostic and Follow-Up Monitoring in Gaucher Disease in a Non-Jewish, Caucasian Cohort of Gaucher Disease Patients. *PLoS One* **8,** e79732 (2013).
34. Ferraz, M. J. *et al.* Lysosomal glycosphingolipid catabolism by acid ceramidase: formation of glycosphingoid bases during deficiency of glycosidases. *FEBS Lett.* **590,** 716–25 (2016).
35. Marques, A. R. A. *et al.* Glucosylated cholesterol in mammalian cells and tissues: formation and degradation by multiple cellular β-glucosidases. *J. Lipid Res.* **57,** 451–463 (2016).
36. Kirchhausen, T., Macia, E. & Pelish, H. E. Use of dynasore, the small molecule inhibitor

of dynamin, in the regulation of endocytosis. *Methods Enzymol.* **438,** 77–93 (2008).

37. Beutler, E. & Grabowski, G. A. in *The Metabolic and Molecular Bases of Inherited Disease. 7th ed. New York, NY: McGraw-Hill;* (ed. McGraw-Hill) 2641–2670 (1995).

38. Dahl, M. *et al.* Lentiviral gene therapy using cellular promoters cures type 1 Gaucher disease in mice. *Mol. Ther.* **23,** 835–844 (2015).

39. Mistry, P. K. *et al.* Glucocerebrosidase gene-deficient mouse recapitulates Gaucher disease displaying cellular and molecular dysregulation beyond the macrophage. *Proc. Natl. Acad. Sci.* **107,** 19473–19478 (2010).

40. Siebert, M., Sidransky, E. & Westbroek, W. Glucocerebrosidase is shaking up the synucleinopathies. *Brain* **137,** 1304–1322 (2014).

41. Michelakakis, H. *et al.* Evidence of an association between the scavenger receptor class B member 2 gene and Parkinson's disease. *Mov. Disord.* **27,** 400–5 (2012).

42. Maniwang, E., Tayebi, N. & Sidransky, E. Is Parkinson disease associated with lysosomal integral membrane protein type-2?: challenges in interpreting association data. *Mol. Genet. Metab.* **108,** 269–71 (2013).

43. Rothaug, M. *et al.* LIMP-2 expression is critical for β-glucocerebrosidase activity and α-synuclein clearance. *Proc. Natl. Acad. Sci. U. S. A.* **111,** 15573–8 (2014).

44. Siebert, M. *et al.* Identification of miRNAs that modulate glucocerebrosidase activity in Gaucher disease cells. *RNA Biol.* 1–14 (2015). doi:10.1080/15476286.2014.996085

45. Akiyama, H., Kobayashi, S., Hirabayashi, Y. & Murakami-Murofushi, K. Cholesterol glucosylation is catalyzed by transglucosylation reaction of β-glucosidase 1. *Biochem. Biophys. Res. Commun.* **441,** 838–43 (2013).

46. Damme, M. *et al.* Impaired lysosomal trimming of N-linked oligosaccharides leads to hyperglycosylation of native lysosomal proteins in mice with alpha-mannosidosis. *Mol. Cell. Biol.* **30,** 273–83 (2010).

47. Vissers, J. P. C., Langridge, J. I. & Aerts, J. M. F. G. Analysis and quantification of diagnostic serum markers and protein signatures for Gaucher disease. *Mol. Cell. Proteomics* **6,** 755–66 (2007).

48. Aerts, J. M. *et al.* The occurrence of two immunologically distinguishable beta-glucocerebrosidases in human spleen. *Eur. J. Biochem.* **150,** 565–74 (1985).

49. Groener, J. E. M. *et al.* HPLC for simultaneous quantification of total ceramide, glucosylceramide, and ceramide trihexoside concentrations in plasma. *Clin. Chem.* **53,** 742–7 (2007).

50. Mirzaian, M. *et al.* Mass spectrometric quantification of glucosylsphingosine in plasma and urine of type 1 Gaucher patients using an isotope standard. *Blood Cells, Mol. Dis.* **54,** 307–314 (2015).

51. Aerts, J. M. *et al.* Elevated globotriaosylsphingosine is a hallmark of Fabry disease. *Proc. Natl. Acad. Sci. U. S. A.* **105,** 2812–7 (2008).

52. Folch, J., Lees, M. & SLoane Stanley, G. H. A simple method for the isolation and purification of total lipides from animal tissues. *J. Biol. Chem.* **226,** 497–509 (1957).

53. Marques, A. R. A. *et al.* Reducing GBA2 Activity Ameliorates Neuropathology in Niemann-Pick Type C Mice. *PLoS One* **10,** e0135889 (2015).

54. Bonta, P. I. *et al.* Nuclear receptors Nur77, Nurr1, and NOR-1 expressed in atherosclerotic lesion macrophages reduce lipid loading and inflammatory responses. *Arterioscler. Thromb. Vasc. Biol.* **26,** 2288–94 (2006).

Supplemental data

Table S1. Lysosomal matrix proteins identified in tritosomes. Ratio: amount in *Limp2-/-* versus *wt* tritosomes; n.m.: not measurable; n.d.: below detection limit; n.m.: not measurable due to lack of detection in part of the measurements.

Nº	Protein Name	Acces Nº	Description	Count inj	Limp2-/-: wt
1	A2BFA6	A2BFA6	Alpha N acetylglucosaminidase Sanfilippo disease IIIB OS Mus musculus GN Naglu PE 4 SV 1	9	1.06
2	ARL8B	Q9CQW2	ADP ribosylation factor like protein 8B OS Mus musculus GN Arl8b PE 2 SV 1	9	1.10
3	CATH	P49935	Pro cathepsin H OS Mus musculus GN Ctsh PE 2 SV 2	9	1.22
4	CATL1	P06797	Cathepsin L1 OS Mus musculus GN Ctsl1 PE 1 SV 2	9	0.98
5	CATZ	Q9WUU7	Cathepsin Z OS Mus musculus GN Ctsz PE 2 SV 1	9	1.12
6	CREG1	O88668	Protein CREG1 OS Mus musculus GN Creg1 PE 2 SV 1	9	1.45
7	DPP2	Q9ET22	Dipeptidyl peptidase 2 OS Mus musculus GN Dpp7 PE 2 SV 2	9	0.87
8	GNS	Q8BFR4	N acetylglucosamine 6 sulfatase OS Mus musculus GN Gns PE 2 SV 1	9	0.92
9	LAMP1	P11438	Lysosome associated membrane glycoprotein 1 OS Mus musculus GN Lamp1 PE 1 SV 2	9	1.12
10	LAMP2	P17047	Lysosome associated membrane glycoprotein 2 OS Mus musculus GN Lamp2 PE 2 SV 2	9	1.06
11	LGMN	O89017	Legumain OS Mus musculus GN Lgmn PE 1 SV 1	9	0.96
12	LYAG	P70699	Lysosomal alpha glucosidase OS Mus musculus GN Gaa PE 1 SV 2	9	1.07
13	MA2B1	O09159	Lysosomal alpha mannosidase OS Mus musculus GN Man2b1 PE 2 SV 4	9	0.84
14	MANBA	Q8K2I4	Beta mannosidase OS Mus musculus GN Manba PE 2 SV 1	9	0.76
15	NAGAB	Q9QWR8	Alpha N acetylgalactosaminidase OS Mus musculus GN Naga PE 2 SV 2	9	0.91
16	NPC2	Q9Z0J0	Epididymal secretory protein E1 OS Mus musculus GN Npc2 PE 2 SV 1	9	1.08
17	PLBL2	Q3TCN2	Putative phospholipase B like 2 OS Mus musculus GN Plbd2 PE 1 SV 2	9	0.93
18	PPA5	Q05117	Tartrate resistant acid phosphatase type 5 OS Mus musculus GN Acp5 PE 2 SV 2	9	0.72
19	PPT2	O35448	Lysosomal thioesterase PPT2 OS Mus musculus GN Ppt2 PE 2 SV 1	9	1.12
20	RISC	Q920A5	Retinoid inducible serine carboxypeptidase OS Mus musculus GN Scpep1 PE 2 SV 2	9	1.12
21	RNT2	Q9CQ01	Ribonuclease T2 OS Mus musculus GN Rnaset2 PE 2 SV 1	9	0.82
22	NCUG1	Q9JHJ3	Lysosomal protein NCU G1 OS Mus musculus PE 1 SV 1	8	1.72

|					
23	PCP	Q7TMR0	Lysosomal Pro X carboxypeptidase OS Mus musculus GN Prcp PE 2 SV 2	8	0.64
24	CATF	Q9R013	Cathepsin F OS Mus musculus GN Ctsf PE 2 SV 1	7	0.62
25	CATS	O70370	Cathepsin S OS Mus musculus GN Ctss PE 2 SV 2	7	0.78
26	HEXB	P20060	Beta hexosaminidase subunit beta OS Mus musculus GN Hexb PE 2 SV 2	7	1.37
27	CATC	P97821	Dipeptidyl peptidase 1 OS Mus musculus GN Ctsc PE 2 SV 1	6	n.m.
28	E9PVY4	E9PVY4	Uncharacterized protein OS Mus musculus GN Ppt1 PE 4 SV 1	6	0.96
29	GLCM	P17439	Glucosylceramidase OS Mus musculus GN *GBA* PE 1 SV 1	6	n.d.
30	LICH	Q9Z0M5	Lysosomal acid lipase cholesteryl ester hydrolase OS Mus musculus GN Lipa PE 2 SV 2	6	0.44
31	ARSB	P50429	Arylsulfatase B OS Mus musculus GN Arsb PE 2 SV 3	5	0.92
32	ASM	Q04519	Sphingomyelin phosphodiesterase OS Mus musculus GN Smpd1 PE 2 SV 2	5	0.59
33	GALNS	Q571E4	N acetylgalactosamine 6 sulfatase OS Mus musculus GN Galns PE 2 SV 2	5	2.16
34	NICA	P57716	Nicastrin OS Mus musculus GN Ncstn PE 1 SV 3	5	1.15
35	SCRB2	O35114	Lysosome membrane protein 2 OS Mus musculus GN *SCARB2* PE 1 SV 3	5	n.d.
36	ASAH1	Q9WV54	Acid ceramidase OS Mus musculus GN Asah1 PE 1 SV 1	4	n.m.
37	E9PW67	E9PW67	Uncharacterized protein OS Mus musculus GN Hexa PE 4 SV 1	4	0.97
38	NPC1	O35604	Niemann Pick C1 protein OS Mus musculus GN Npc1 PE 1 SV 1	4	n.m.
39	PPT1	O88531	Palmitoyl protein thioesterase 1 OS Mus musculus GN Ppt1 PE 2 SV 2	4	0.69
40	SIAE	P70665	Sialate O acetylesterase OS Mus musculus GN Siae PE 2 SV 3	4	n.m.
41	ARL8A	Q8VEH3	ADP ribosylation factor like protein 8A OS Mus musculus GN Arl8a PE 2 SV 1	3	n.m.
42	E9Q9I3	E9Q9I3	Uncharacterized protein OS Mus musculus GN Acp2 PE 4 SV 1	3	n.m.
43	RAB7A	P51150	Ras related protein Rab 7a OS Mus musculus GN Rab7a PE 1 SV 2	3	n.m.
44	AGAL	P51569	Alpha galactosidase A OS Mus musculus GN Gla PE 1 SV 1	2	n.m.
45	CD1D1	P11609	Antigen presenting glycoprotein CD1d1 OS Mus musculus GN Cd1d1 PE 1 SV 3	2	n.m.
46	DIAC	Q8R242	Di N acetylchitobiase OS Mus musculus GN Ctbs PE 2 SV 2	2	n.m.
47	E9Q515	E9Q515	Uncharacterized protein OS Mus musculus GN 4930471M23Rik PE 4 SV 1	2	n.m.
48	HEXA	P29416	Beta hexosaminidase subunit alpha OS Mus musculus GN Hexa PE 2 SV 2	2	n.m.
49	HGNAT	Q3UDW8	Heparan alpha glucosaminide N acetyltransferase OS Mus musculus GN Hgsnat PE 1 SV 2	2	n.m.
50	Q3U2B2	Q3U2B2	Uncharacterized protein OS Mus musculus GN Npc1 PE 2 SV 1	2	n.m.
51	CATB	P10605	Cathepsin B OS Mus musculus GN Ctsb PE 1 SV 2	9	0.98
52	Q8C243	Q8C243	Uncharacterized protein OS Mus musculus GN Ctsd PE 2 SV 1	9	0.94
53	SAP	Q61207	Sulfated glycoprotein 1 OS Mus musculus GN Psap PE 1 SV 2	9	0.81
54	SAP3	Q60648	Ganglioside GM2 activator OS Mus musculus GN Gm2a PE 1 SV 2	9	0.68
55	TPP1	O89023	Tripeptidyl peptidase 1 OS Mus musculus GN Tpp1 PE 1 SV 2	9	1.22
56	PPGB	P16675	Lysosomal protective protein OS Mus musculus GN Ctsa PE 1 SV 1	8	1.40
57	F6Y6L6	F6Y6L6	Uncharacterized protein Fragment OS Mus musculus GN Ctsd PE 3 SV 1	7	0.95
58	PAG15	Q8VEB4	Group XV phospholipase A2 OS Mus musculus GN Pla2g15 PE 1 SV 1	4	n.m.
59	CATD	P18242	Cathepsin D OS Mus musculus GN Ctsd PE 1 SV 1	3	n.m.
60	VA0D1	P51863	V type proton ATPase subunit d 1 OS Mus musculus GN Atp6v0d1 PE 1 SV 2	9	1.07
61	D3Z437	D3Z437	Uncharacterized protein OS Mus musculus GN Ctsh PE 4 SV 1	6	2.14
62	E9Q5W3	E9Q5W3	Uncharacterized protein OS Mus musculus GN Ctsz PE 3 SV 1	4	n.m.
63	F6QKK2	F6QKK2	Uncharacterized protein Fragment OS Mus musculus GN Arl8a PE 3 SV 1	4	n.m.
64	VATB2	P62814	V type proton ATPase subunit B brain isoform OS Mus musculus GN Atp6v1b2 PE 1 SV 1	4	n.m.
65	E9Q2Q0	E9Q2Q0	Uncharacterized protein OS Mus musculus GN Ctsc PE 3 SV 1	3	0.59
66	F7AF87	F7AF87	Uncharacterized protein Fragment OS Mus musculus GN Glb1 PE 4 SV 1	3	0.60
67	CD68	P31996-2	Isoform Short of Macrosialin OS Mus musculus GN Cd68	2	n.m.
68	HGNAT	Q3UDW8-2	Isoform 2 of Heparan alpha glucosaminide N acetyltransferase OS Mus musculus GN Hgsnat	2	n.m.
69	LTOR3	O88653	Ragulator complex protein LAMTOR3 OS Mus musculus GN Lamtor3 PE 1 SV 1	2	n.m.
70	STOM	P54116	Erythrocyte band 7 integral membrane protein OS Mus musculus GN Stom PE 1 SV 3	2	n.m.

wt — Limp2 -/-
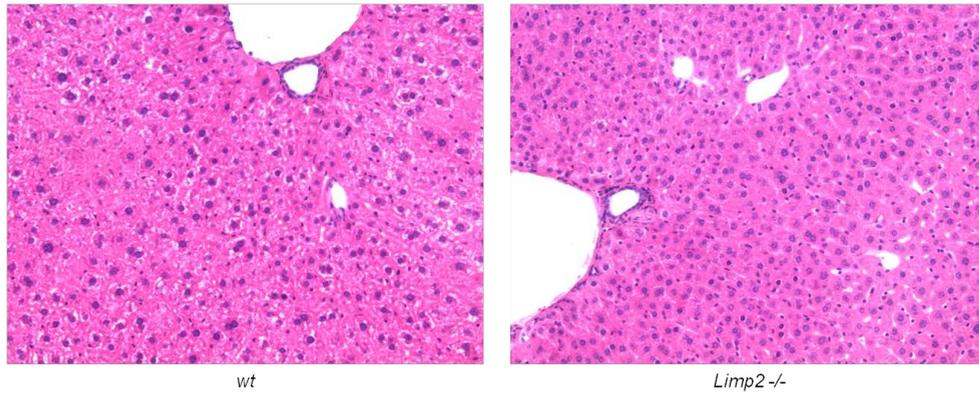
Figure S1. Section of livers of *wt* and *Limp2⁻ᐟ⁻* mice of 6 months of age

Figure S2. Sciatic nerves of *wt* (left) and *Limp2⁻ᐟ⁻* mouse (right).

Table S2. Globotriaosylceramide (Gb3) and LysoGb3 levels in tissues of *Limp2-/-* compared to *wt* mice. Results are presented as ratios.

Tissue/ Organ	Limp2$^{-/-}$: wt	
	Gb3	LysoGb3
Pancreas	1,10	1,37
Heart	1,02	0,96
IF	1,97	1,01
Liver	0,65	0,41
Lungs	1,10	0,61
AF	1,96	1,20
OF	1,70	5,92
Spleen	0,49	0,54
Eye	2,34	0,78
EF	1,62	0,36
BM	1,75	0,68
BAT	1,16	2,12
Thymus	0,33	0,96
Kidney	0,95	0,57
SG	1,53	0,64
AG	1,73	0,46
LN	1,14	0,34
TE	0,48	0,32
EP	0,73	2,18
Skin	1,30	1,26
Brain*	1,77	0,77
Duodenum	0,99	0,61
PBMC	2,51	1,71
Ileum	1,00	0,68
SN*	2,38	0,34
Jejunum	0,96	0,64
Plasma	0,37	0,46
Bile	0,35	0,41
Urine	0,79	0,09

Table S3. Glycosyl-cholesterol levels in tissues of *Limp2⁻/⁻* and *wt* mice. Tissue levels in nmol/g wet weight tissue; leukocytes in nmol/mg protein; plasma, bile and urine in nmol/mL. Limp2⁻/⁻: wt = ratio of GlcChol.

| Tissue	GlcChol levels		
Genotype	*Wt*	*Limp2⁻/⁻*	*Limp2⁻/⁻ : wt*
Pancreas	811,27±102,11	1376,76±153,35	1,74
Heart	345,81±71,91	545,20±57,41	1,53
IF	109,85±54,44	353,53±67,57	3,55
Liver	698,43±143,17	1296,74±387,57	1,95
Lungs	1457,64±275,82	2574,40±455,34	1,70
AF	70,04±34,73	348,71±161,58	5,81
OF	354,12±492,03	1058,44±550,83	2,62
Spleen	1257,83±111,84	1957,10±292,90	1,53
Eye	433,39±73,12	619,27±96,68	1,37
EF	56,74±46,44	128,06±7,10	2,25
BM	20,61±3,45	39,34±12,94	1,90
BAT	245,97±79,47	884,84±633,08	3,73
Thymus	3860,94±975,90	4183,37±660,07	1,16
Kidney	1067,67±136,93	1894,23±339,59	1,79
SG	1095,61±471,00	1624,70±664,56	1,41
AG	971,95±347,59	1433,54±462,36	1,71
LN	1311,46±539,59	2194,95±404,80	1,67
TE	449,02±42,71	438,83±	0,97
EP	169,50±1,07	211,96±	1,25
Skin	585,28±524,36	973,49±654,93	1,47
Brain*	2076,92±374,80	2335,98±176,57	1,15
Duodenum	1299,28±301,07	2099,68±513,31	1,71
PBMC	27,36±13,71	56,68±27,54	2,07
Ileum	1271,41±435,69	2202,11±1360,32	1,69
SN*	4782,98±2217,85	5530,42±2515,20	1,11
Jejunum	1757,52±196,12	3847,03±977,64	2,19
Plasma	56,56±8,15	117,51±42,85	2,03
Bile	29,35±4,76	42,14±12,33	1,44
Urine	n.d.	n.d.	n.d.
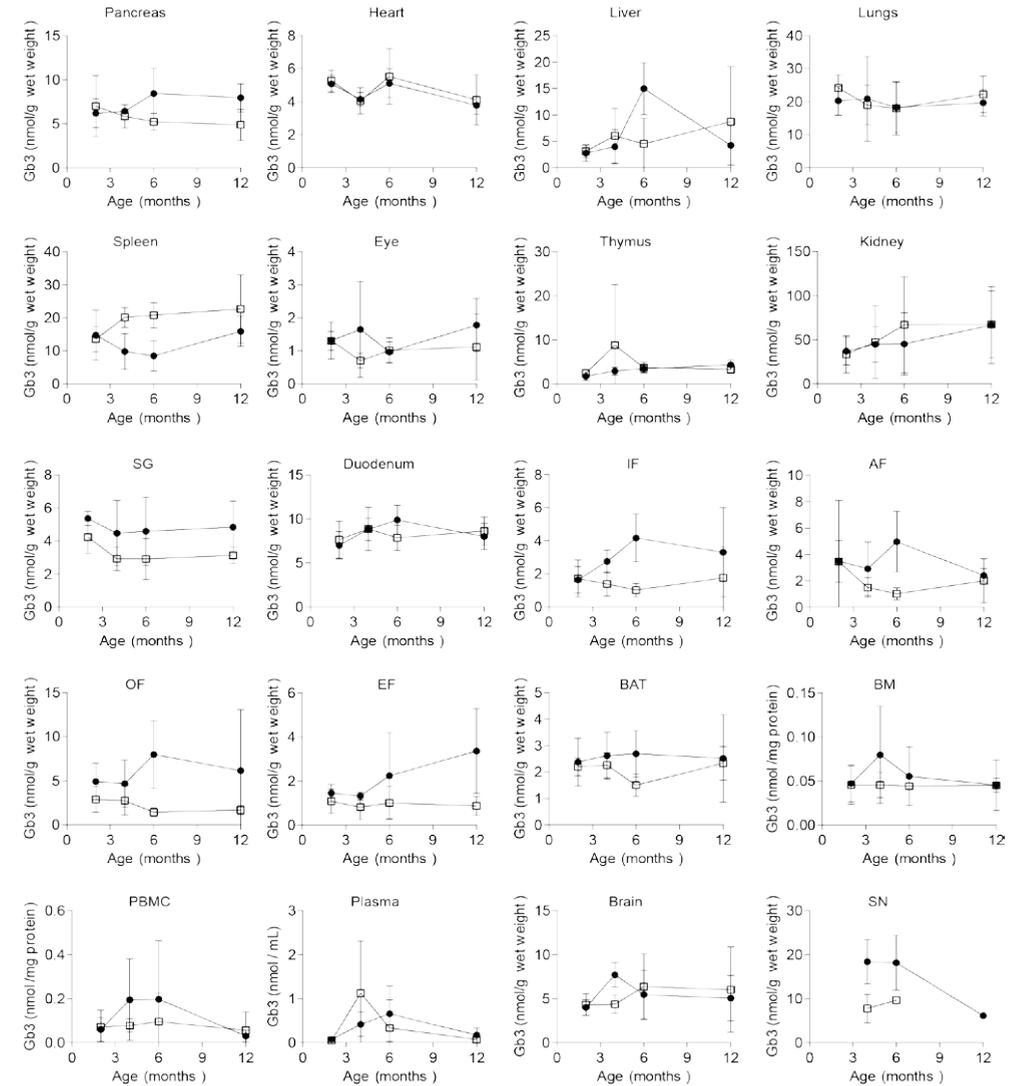
Figure S3. Gb3 levels in wt and *Limp2⁻/⁻* mice with age.
Black circle= *wt*; Open square= *Limp2⁻/⁻* mice.
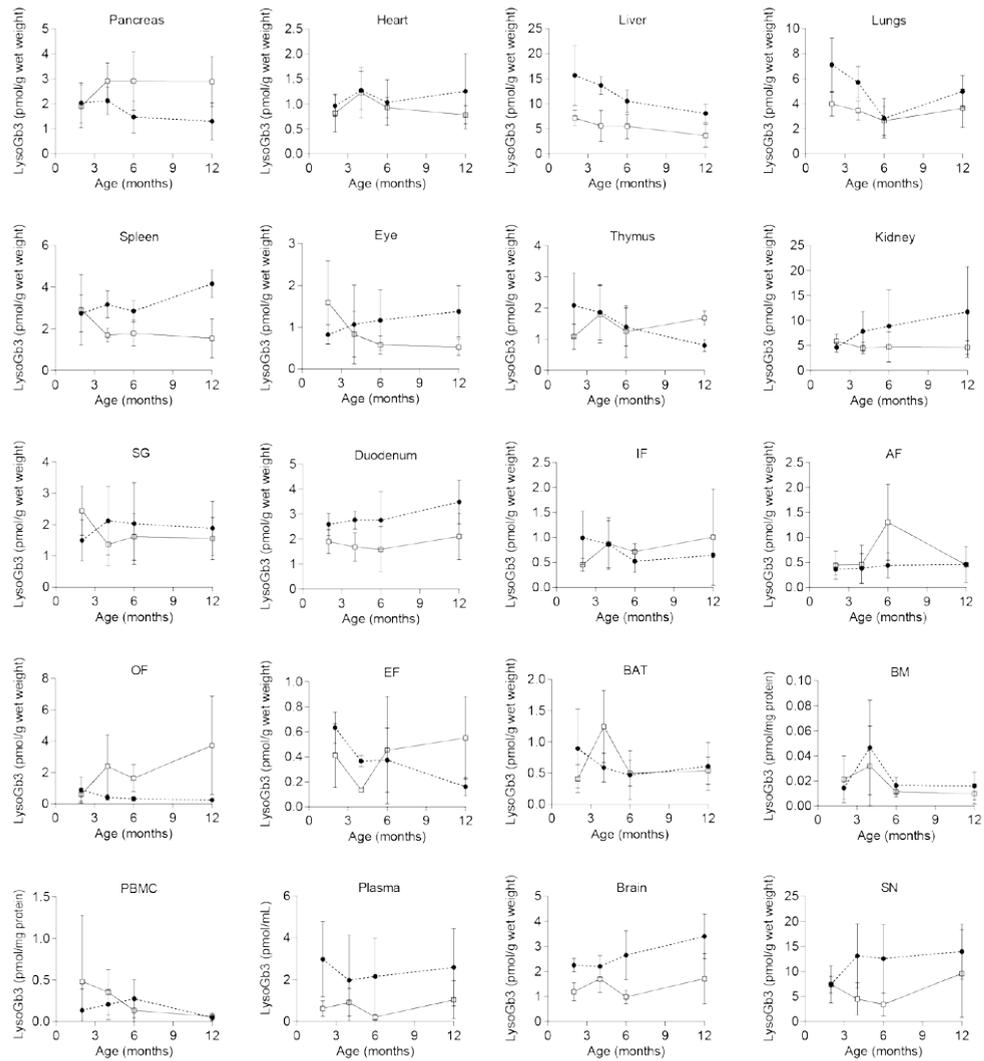
Figure S4. LysoGb3 levels in wt and *Limp2*^{-/-} mice with age.

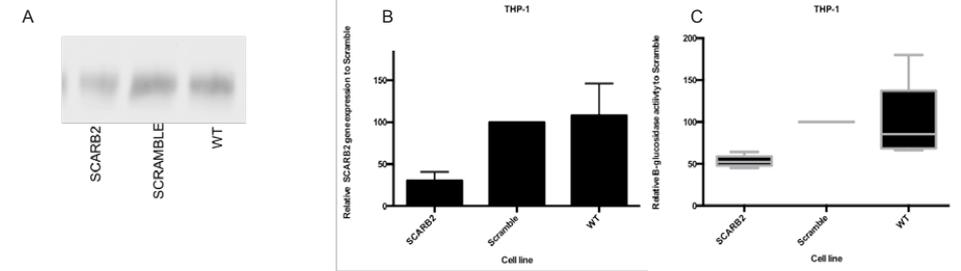Black circle= *wt*; Open square= *Limp2*^{-/-} mice.

Figure S5. Characterization THP-1 cell line with lentiviral *SCARB2* partial knockdown. A. Western blot of LIMP-2 protein in THP-1 treated with *SCARB2* siRNA and scrambled siRNA; **B.** *SCARB2* gene expression (qPCR); **C.** GBA activity measured with 4MU-Glc.

6

Metabolic adaptations to defective lysosomal glycosphingolipid degradation

Metabolic adaptations to defective lysosomal glycosphingolipid degradation

Based on

Johannes M. Aerts[1,2,*], Maria J. Ferraz[2], Mina Mirzaian[1], Saskia V. Oussoren[1], Kassiani Kytidou[1], Ethan Kuo[1], Lindsey Lelieveld[1], Marc Hazeu[2], Daphne Boer[2], Paulo Gaspar[2], Daniela Herrera Moro[2], Tanit L. Gabriel[2], Wouter W. Kallemeijn[1], Patrick Wisse[3], Herman S. Overkleeft[3], Marco van Eijk[1], Rolf G. Boot[1], André R. A. Marques[2]

[1]Dept of Medical Biochemistry, LIC, Leiden University
[2]Dept of Medical Biochemistry, AMC, University of Amsterdam
[3]Dept of Bio-organic Synthesis, LIC, Leiden University

Manuscript submitted

Abstract

The cellular recycling of glycosphingolipids (GSLs) to their building blocks is completed in lysosomes and involves the local hydrolytic action of specific glycosidases. Severe reduction of capacity in one of the down-stream steps in degradation of GSLs in lysosomes should result in progressive and prominent accumulation of the corresponding substrate since turnover of endogenous and endocytosed exogenous GSLs is chronic and considerable. The most common inherited deficiencies in lysosomal GSL catabolism are Gaucher disease (GD) and Fabry disease (FD) caused by defects in lysosomal glucocerebrosidase (GBA) and alpha-galactosidase A (GLA), respectively. The accumulation in cells and tissues of glucosylceramide (GlcCer) in GD and that of globotriaosylceramide (Gb3) in FD tends to level with age, suggesting the existence of biochemical adaptations to the primary defects. These poorly appreciated metabolic adaptations, in and beyond lysosomes, are reviewed here. One important adaptation is the de-acylation of accumulating GSLs in lysosomes by the action of the enzyme acid ceramidase. Thus, the lysosomal storage of GlcCer in GD and that of Gb3 in FD is limited through formation of glucosylsphingosine (GlcSph) and globotriaosylsphingosine (lysoGb3), respectively. In the case of GD, another adaptation in metabolism takes place beyond the lysosome, involving the enzyme GBA2 located in the cytoplasmic leaflet of membranes of the endoplasmic reticulum and Golgi apparatus. GBA2 allows extra-lysosomal degradation of GlcCer and concomitantly generates glucosylated cholesterol. The benefit and harm of these metabolic adaptations in GD and FD are discussed.

The life cycle of glycosphingolipids through various subcellular compartments.

The outer leaflet of the plasma membrane is rich in glycosphingolipids (GSLs) with a hydrophobic ceramide (Cer; N-acylated sphingosine) embedded in the lipid layer. Attached to the C1-hydroxyl of Cer are sugars[1,2]. The glycan starts with glucose or galactose and can be further extended by combinations of monosaccharides[1,2]. GSLs interact with cholesterol molecules by van der Waals forces and thus form transient semi-ordered membrane domains, so-called 'lipid rafts'. In these domains specific proteins are preferentially located and related signaling events occur[3–5]. GSLs undergo several chemical modifications during their life in various subcellular compartments (Figure 1). They are de novo synthesized starting with the formation of 3-ketosphinganine by the enzyme serine palmitoyltransferase (SPT). At the endoplasmic reticulum it catalyzes the condensation of serine and fatty acyl-CoA with preference for palmitoyl-CoA resulting in 18 carbon sphingoid bases[6]. Next, a specific reductase forms sphinganine that is subsequently metabolized by ceramide synthases (CERS) to dihydroceramides. The enzyme dihydroceramide desaturase (DES) converts these to ceramides[6,7]. The newly formed Cer may be next metabolized in the ER to galactosylceramide (GalCer). Alternatively, Cer is transported by the protein CERT to the cytosolic leaflet of membranes of the cis-Golgi apparatus where it is converted to glucosylceramide (GlcCer) by the enzyme glucosylceramide synthase (GCS)[8,9]. Subsequently, translocation of GlcCer to the luminal leaflet of the Golgi membrane may occur via an unknown mechanism whereupon the lipid can be stepwise extended with further sugars by sequential action of glycosyltransferases to complex GSLs like gangliosides and globosides[10,11]. In addition, specific GSLs can be sulfated by sulfotransferases[6]. This metabolism of GSLs and the resulting structural heterogeneity of GSLs is the topic of excellent reviews[1,6,11,12]. From the Golgi apparatus, GSLs move to the outer leaflet of the plasma membrane. GSLs may be exported from the surface of cells through transfer to nascent HDL particles, but most are ultimately internalized. Through endocytosis, GSLs finally end up in multi-vesicular bodies of late endosomes and are subsequently degraded in lysosomes. The degradation of complex GSLs implies sequential removal of terminal sugars by specialized lysosomal glycosidases, often facilitated by specific accessory proteins (GM2 activator protein and saposins A-D)[13]. A common product of GSL fragmentation is Cer, being generated from GlcCer by glucocerebrosidase (GBA) and from GalCer by galactocerebrosidase (GALC). Cer is cleaved in lysosomes by acid ceramidase (AC) to fatty acid and sphingosine ((2S,3R,4E)-2-aminooctadec-4-ene-1,3-diol). The degradation product sphingosine is exported to the cytosol where it may be re-generated to Cer. This salvage pathway is mediated by the CERS enzymes[14]. Alternatively, sphingosine kinases (SK1 and SK2) may convert sphingosine to sphingosine-1-phosphate (S1P) that can be degraded by S1P lysase (SPL) to phosphatidylethanolamine and 2-trans-hexadecenal[15,16].
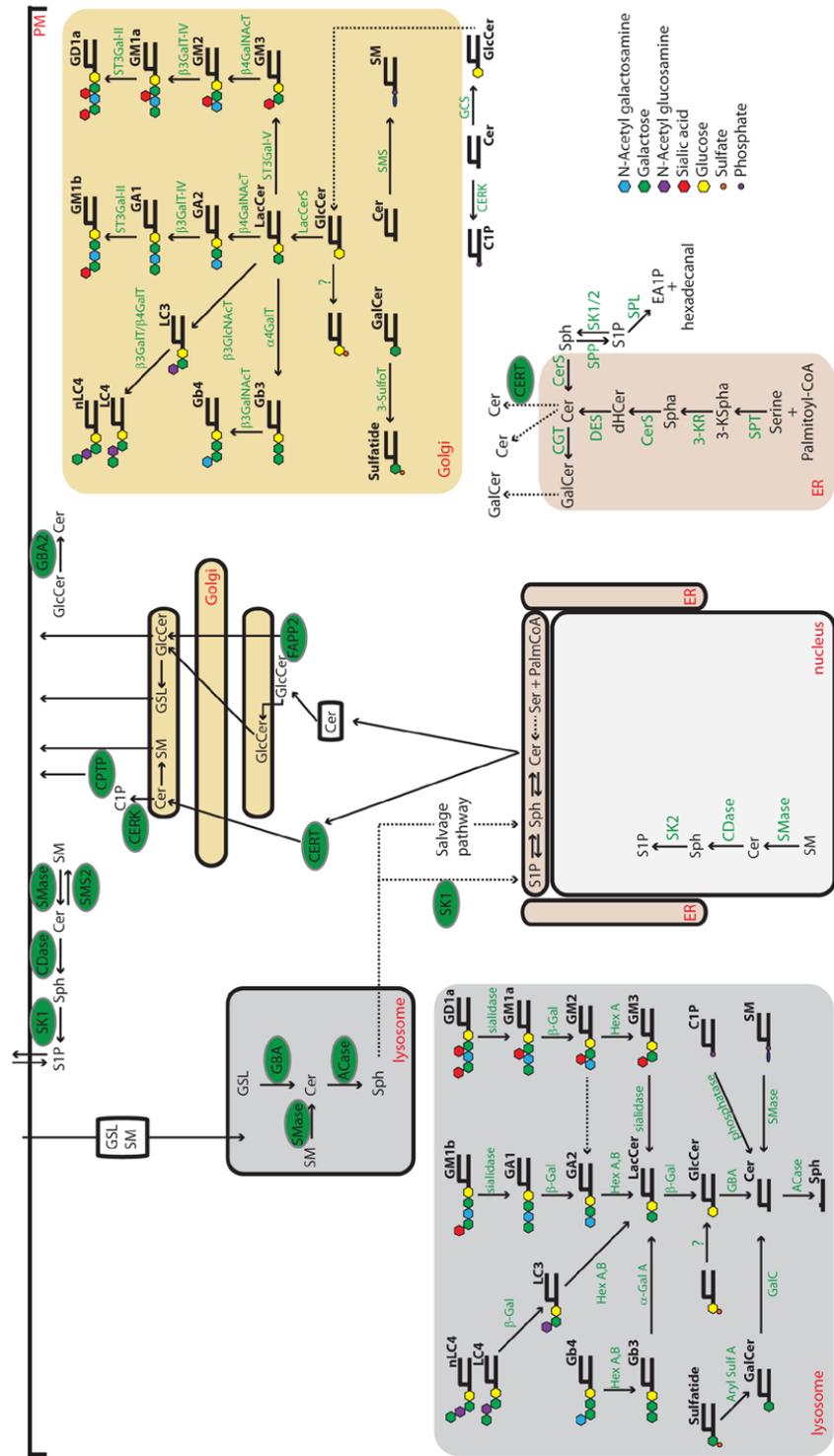
Figure 1. GSL life cycle in the cell. GSLs (black font) are synthesized in the ER (red) and Golgi (yellow) compartments starting with the condensation of serine and palmitoyl-CoA building blocks. Catabolism of GSLs occurs in lysosomes (grey) through the sequential action of various hydrolases (green font).

Impaired lysosomal degradation of GSLs as cause for disease.

A number of inherited deficiencies in lysosomal GSL degradation exist, the so-called glycosphingolipidoses. An inherited disease in man is known for each step in the lysosomal catabolism of the more common glycosphingolipids, except for that of lactosylceramide, (for reviews see references[17–20]). Examples of these disorders are Fabry disease (FD, globotriaosylceramidosis), Gaucher disease (GD, glucosylceramidosis), Krabbe disease (KD, galactosylceramidosis), GM1 gangliosidosis and GM2 gangliosidosis, due to defects in α-galactosidase A, glucocerebrosidase (acid β-glucosidase), galactocerebrosidase, β-galactosidase and β-hexosaminidase, respectively (Table 1). The therapeutic success of supplementing GD patients with lacking enzyme through chronic intravenous infusions (enzyme replacement therapy, ERT) has stimulated similar approaches for other glycosphingolipidoses. This development promoted the screening for individuals with lysosomal glycosidase abnormalities in targeted risk groups as well as newborns[21,22]. The prevalence of the combined glycosphingolipidoses, earlier estimated to be about 1 in 20 000 live births, seems relatively high given the increasingly recognized late onset and atypical variants, particularly for X-linked FD[21].

Table 1. Inherited (glyco)sphingolipidoses.

Disease	Gene	Protein	Main storage material
GM1 gangliosidosis	GLB1	Acid β-galactosidase	GM1 ganglioside
GM2 gangliosidosis (Tay-Sachs)	HEXA	β-hexosaminidase α subunit	GM2 ganglioside
GM2 gangliosidosis (Sandhoff)	HEXB	β-hexosaminidase β subunit	GM2 ganglioside
Fabry	GLA	α-galactosidase A	Globotriaosylceramide (Gb3)
Gaucher	GBA	Glucocerebrosidase	Glucosylceramide (GlcCer)
Metachromatic leukodystrophy	ARSA	Arylsulfatase A	Sulfatide
Krabbe	GALC	Galactosylceramidase	Galactosylceramide (GalCer)
Niemann-Pick type A and B	SMPD1	Acid sphingomyelinase	Sphingomyelin
Niemann-Pick type C	NPC1/NPC2	NPC1/NPC2	Cholesterol, GSLs & sphingomyelin
Farber	ASAH1	Acid ceramidase	Ceramide

The *de novo* synthesis and turnover of GSLs is impressive in most cell types with estimated half-lives in the order of hours[6,11]. Cells may furthermore endocytose significant amounts of

GSL-rich lipoproteins. A (near) complete block in lysosomal catabolism should lead to a rapid, and ongoing, accumulation of a GSL in cells, according to the "critical threshold" hypothesis of Conzelmann and Sandhoff that furthermore predicts a linear increase in storage accumulation[23]. Indeed, in glycosidase-deficient cells lysosomal GSL storage generally develops quickly. It already occurs *in utero* with some glycosidase knockout mouse models[24]. However, patients and mice with a glycosphingolipidosis not always show the predicted ongoing GSL buildup: after fast initial accumulation, the subsequent lipid storage increases only marginally. Equally puzzling is the observation that overt disease manifests relatively late in man and mice with complete absence of a GSL-degrading glycosidase, as for example GBA. The degradative flux through GBA is considerable since its substrate GlcCer is generated in lysosomes from all glycosphingolipids (gangliosides, globosides and lactosylceramide). Despite the considerable *in utero* turnover of GlcCer, mice and humans without GBA develop more or less normally as fetus[24,25]. Only at birth the impairment of skin barrier function becomes fatal in the GBA-deficient collodion baby variant of GD. This skin defect is not attributed to lysosomal lipid storage, but rather an incorrect ratio of Cer and GlcCer in the extruded lamellar bodies forming the stratum corneum[26]. Upon autopsy marked GlcCer deposition is detected in several organs of the collodion baby, but organ function and development do not seem overtly impaired, at least until birth[27,28]. Another example in the same line are males with classic FD lacking any residual GLA protein. This 49 kDa lysosomal enzyme degrades the globoside Gb3 that is abundant in endothelial cells, blood cells, cardiomyocytes and podocytes[25]. Classic FD males with complete deficiency of GLA express only at juvenile age overt symptoms in skin, nociceptive neurons and eye[29]. Deposits of Gb3 in so-called zebra-bodies are already detected in fetal endothelial cells, but pathology of heart, kidney and brain only manifests in adult life[29]. Male FD mice lacking GLA show already in the first months of life prominent Gb3 storage in tissues, but this does not progress further[30,31]. Similar leveling of storage lipid deposition with age occurs in LIMP-2 deficient mice (Gaspar *et al.*, to be published; chapter 5 of this thesis). LIMP-2 essentially mediates the transport of newly synthesized GBA to lysosomes[32]. In the endoplasmic reticulum LIMP-2 binds GBA and the complex is sorted to late endosomes/lysosomes where the acid pH causes dissociation[32,33]. Although most cell types and tissues of LIMP-2 deficient mice are severely deficient in GBA, this is accompanied by marginally increased GlcCer. Moreover, the storage of GlcCer in LIMP-2 mice does not increase with age (Gaspar *et al.,* to be published; chapter 5 of this thesis). The non-linear increase in GSL storage with age in GLA- and LIMP-2 deficient mice is puzzling since it cannot be explained by a simple feedback regulation. No prominent reduction of GSL biosynthesis in response to defective lysosomal degradation is reported. This contrasts sharply to the tight regulation of cellular cholesterol by sensing of sterol concentrations in membranes and the transcriptional and post-translational regulation of biosynthetic and other modifying enzymes[34]. The sensing of lysosomal dysfunction and subsequent responses have been elucidated by Ballabio and colleagues. It has become clear that lysosomal stress by indigestible macromolecules leads to translocation of the transcription factor TFEB to the nucleus. There, it increases transcription of genes encoding protein constituents of lysosomes and

autophagosomes[35]. Although increased *de novo* synthesis of entire lysosomes may contribute to reducing lysosomal lipid storage at short term, the amelioration is ultimately limited by the total cellular volume that can be occupied by lysosomes.

Thus, the paradox presented by the glycosphingolipidoses is the initial rapid accumulation of GSL followed by a far less progressive phase. An explanation for this riddle would be induction of cellular adaptations in metabolism of GSLs in response to increasing storage in lysosomes (figure 2). Such adaptive responses would fit with the observed leveling of GSL storage with age. At present, the nature of the postulated adaptations is largely unknown.
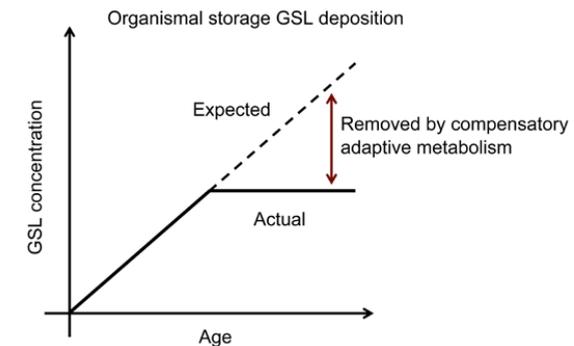

Figure 2. The paradox of glycosphingolipidoses. Theoretical argument for existence of adaptive metabolism for GSL clearance.

Adaptive rescue by lysosomal conversion of glycosphingolipids to glycosphingoid bases.
Glycosphingoid bases corresponding to the primary accumulating GSLs in cells and tissues are markedly increased in plasma of patients suffering from glycosphingolipidoses, (figure 3A). Examples are the 300-fold elevated GlcSph in plasma of GD patients. More modestly, GlcSph is also increased in plasma of GBA-deficient patients suffering from Action Myoclonus Renal failure Syndrome (AMRF) resulting from mutations in the *SCARB2* gene encoding LIMP-2[36–38]. Likewise, lysoGb3 is 200-fold increased in plasma of classic FD patients[39,40]. Furthermore, galactosylsphingosine is increased in Krabbe disease (KD) patients deficient in galactocerebrosidase degrading GalCer[41,42]. Examination of glycosphingoid bases in mouse models with deficiencies in glucocerebrosidase, α-galactosidase A and galactocerebrosidase recapitulated these findings. In plasma and tissues of all mice, the storage of the primary GSL substrate is accompanied by marked increases in corresponding glycosphingoid bases[43].

The question to be addressed next is "how do the excessive amounts of glycosphingoid bases arise?". A first clue was offered by the work of Yamaguchi *et al*. demonstrating that pharmacological inhibition of GBA in fibroblasts results in formation of GlcSph, but not in cells lacking the lysosomal enzyme AC[44]. The putative role of lysosomal AC in formation of glycosphingoid bases was further investigated[45]. The prominent generation of GlcSph upon

inhibition of lysosomal GBA was found to be abolished by genetic loss of AC as well as its pharmacological inhibition[45]. Feeding of cells with $^{13}C_5$-isotope encoded GlcCer (containing the isotope label in the sphingosine moiety) led to prominent formation of $^{13}C_5$- GlcSph when GBA was inhibited in cells. The same observation was made for classic FD fibroblasts: inhibition of AC also abolished the generation of lysoGb3 by these cells[45]. Thus, AC is able to convert accumulating GlcCer and Gb3 in lysosomes to the corresponding glycosphingoid bases GlcSph and lysoGb3. The amphiphilic nature of these glycosphingoid bases allows export from lysosomes and even cells[45]. GlcSph and lysoGb3 are water soluble contrary to their corresponding GSLs. The glycosphingoid bases are not associated with plasma lipoproteins like GlcCer and Gb3 are. In urine, GlcSph and lysoGb3 are not in the proximal tube cell sediment, but recovered in the cell-free supernatant. The concentrations of glycosphingoid bases in plasma and urine correlate with each other, both in FD and GD patients. Most of the urinary GlcSph in GD patients and lysoGb3 in FD patients is more hydroxylated and possibly methylated in their C18-sphingoid base as compared to the major species in plasma[37,46] (figure 3B). These modifications in the bases seem to be directly introduced in the kidney since they are lacking for urinary GlcCer and Gb3. Possibly, local monooxygenase activity of CYPs contributes to the modifications. Another structural heterogeneity observed for plasma as well as urinary GlcCer, GlcSph, Gb3 and lysoGb3 is the presence of an additional double bond in the sphingosine moiety. These 4E,14Z-dienes usually constitute around 10 % of the total glycosphingolipids and glycosphingoid bases.

Formation of glycosphingoid bases, a blessing or a curse?

The conversion of accumulating GSLs into corresponding glycosphingoid bases during deficiency of GBA or GLA explains, at least in part, the non-linear increase of GSL in time in GD and FD (figure 2). The lysosomal de-acylation by AC provides the organism a way to eliminate indigestible GSL as water-soluble glycosphingoid bases from cells and even the body by excretion via bile and urine (figure 3A). This solution mimics the body's handling of excessive non-digestible cholesterol, being secreted as such in bile or as water-soluble metabolite like bile acid. LIMP2-deficient mice illustrate how de-acylation of non-digestible GlcCer allows to efficiently prevent lysosomal storage in most cells. This is exemplified by the liver of LIMP2-deficient mice with near complete absence of GBA. Microscopic examination shows no storage deposits and biochemical analysis reveals only a very modest increase in GlcCer. Concomitantly, hepatic GlcSph is 6.7-fold increased and biliary GlcSph is 4.5-fold elevated (Gaspar *et al.,* unpublished; chapter 5). The normal liver function of LIMP2-deficient mice is likely achieved by the ability to avoid formation of lipid-laden lysosomes in hepatocytes.
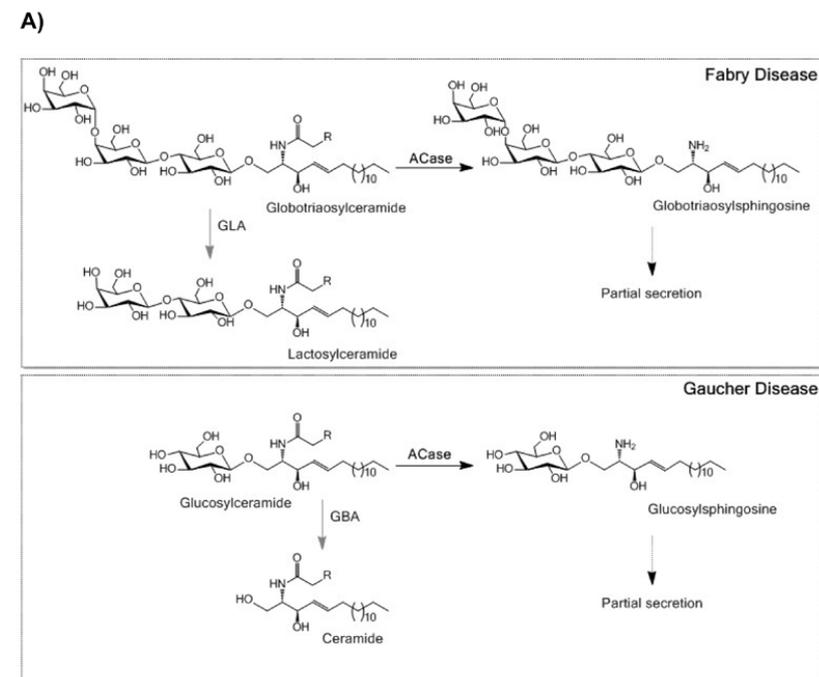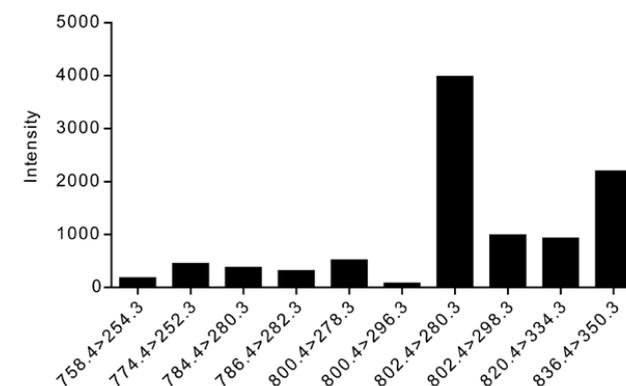
Figure 3. AC-mediated deacylation of GlcCer and Gb3. A) Deacylation by AC of GlcCer and Gb3 to GlcSph and lysoGb3, respectively. **B)** Isoforms of lysoGb3 found in the urine of 2 classical Fabry patients.

There is a prize to pay for the adaptive de-acylation of non-digestible GSL in lysosomes: it exposes the body to chronic high levels of glycosphingoid bases (figure 4). This does not seem to be without long term health risk. Glycosphingoid bases are biologically active and may exert negative effects (for detailed reviews see references[25,47–50]). Briefly, the production of galactosylsphingosine in brain of KD patients contributes to the devastating neuropathology[50].

GlcSph, chronically elevated in GD patients and to lesser extent AMRF patients, is found to be toxic at high concentrations. For example, GlcSph experimentally promotes lysis of red blood cells, impairs cell fission during cytokinesis, damages specific neurons, hampers growth, impairs bone formation by osteoblasts, and promotes chronic inflammation via activation of phospholipase A2[47,48]. It is appealing to speculate that GlcSph contributes to the occurrence of hemolysis, multinucleated macrophages, neuropathology, growth retardation, bone deterioration and chronic low grade inflammation in GD patients. Gammopathies are common in GD patients[51]. Studies by Cox and co-workers firstly demonstrated a correlation between lymphoma and plasma GlcSph levels in mice with inducible GBA knock-down in the white blood cell lineage[52,53]. Recently, Nair and colleagues reported that excessive GlcSph in GD patients may act as auto-antigen driving B-cell proliferation. Thus, GlcSph would directly promote development of multiple myeloma, a blood cell cancer occurring with increased incidence in GD patients[54]. LysoGb3, excessively generated in classic FD patients, is also considered to be toxic[55,56]. It has recently been proposed that lysoGb3 through sensitization of nociceptive neurons plays a direct role in the intense pain experienced by FD patients[57]. Indeed, plasma lysoGb3 in FD patients has been earlier found to correlate with pain[56]. LysoGb3 is also considered as culprit in renal disease in FD patients by causing podocyte damage and fibrosis in the kidney[58]. A correlation of plasma (or urinary) lysoGb3 with renal complications has however not yet been documented. Finally, there is experimental evidence that lysoGb3 promotes proliferation of smooth muscle cells *in vitro* which might explain the characteristic increase in intima media thickness in vasculature of FD patients[39,55]. In theory, GlcSph and lysoGb3 might also be harmful as structural mimic of sphingosine-1-phosphate (S1P), interfering with processes governed by this sphingoid base and its receptors[59]. Minor abnormalities in S1P have been reported for FD patients[60,61]. Of note, the putative toxic effects of GlcSph in GD1 and lysoGb3 in classic FD occur relatively late in patients' lives, implying that associated pathologies require prolonged exposure to high concentrations of glycosphingoid bases. In conclusion, the potential toxicity of glycosphingoid bases urgently warrants further examination.
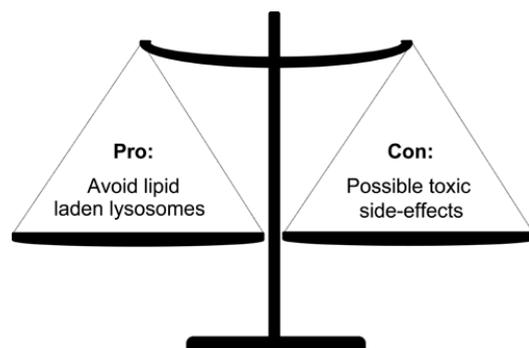

Figure 4. Pro and con of GSL base formation. Pro: avoidance cellular dysfunction by accumulation of dysfunctional lipid laden lysosomes; con: possible toxic side effects.

Employing glycosphingoid base abnormalities for diagnostic purposes and disease monitoring.

The abnormal high concentrations of glycosphingoid bases in blood and urine of patients with a glycosphingolipidosis can be used to biochemically confirm diagnosis and to demonstrate onset of pathological GSL accumulation[25,36,39–41,62,63] (addendum of this thesis). The recent development of very sensitive methods for the quantification of glycosphingoid bases in complex biological samples has been a major step forward[40] (addendum of this thesis). Glycosphingoid bases like GlcSph and lysoGb3 can be in parallel accurately quantified by LC-MS/MS with use of $^{13}C_5$ isotope-encoded natural sphingoid bases as internal standards (figure 5)[37,40,64,65]. With these advanced LC-MS/MS methods, average 300-fold increases in plasma GlcSph in symptomatic GD patients and 200-fold increased lysoGb3 in plasma of males with classic FD were detected (figure 5D)[37,64]. Nowadays, GD and FD patients are identified in screening programs based on detection of gene abnormalities or reduced enzyme activity in dried blood spots. Diagnosis based on these tests is sometimes ambiguous, for example in the case of mutations with unknown consequence or marked residual enzymatic activity. Demonstration of elevated GlcSph allows sensitive and reliable confirmation of diagnosis for GD[37]. Likewise, markedly elevated plasma lysoGb3 confirms diagnosis of FD in males[64]. Glycosphingoid base abnormalities already occur in GD patients and male Fabry patients at very young age, prior to overt symptomatology. Marginal increases in plasma glycosphingoid bases should however be treated with caution since these might not be related to the presumed primary defect. For example, we noted that plasma samples of GD patients show besides more than 100 times increased GlcSph also a modest elevation in lysoGb3 level[45,66]. This is highly relevant since in recent years individuals with abnormalities of unknown significance in the *GLA* gene are increasingly regarded to be at risk for an atypical manifestation of FD[66,67]. Contrary to classic FD patients, atypical patients express no characteristic acroparesthesias and corneal clouding early in life, but only develop one of the isolated late onset symptoms such as unexplained stroke, cardiomyopathy or renal disease. The relative high frequency of such symptoms in the general population makes it conceivable that simply by mere chance an individual with a *GLA* polymorphism develops such a common symptom. It should be avoided that in these cases a faulty diagnosis of FD is made. An incorrect FD diagnosis in a male has serious consequences since all daughters are labelled as obligate carriers that potentially develop disease and require preventive, extremely costly, therapeutic intervention by enzyme replacement therapy. To avoid faulty diagnoses a threshold value of 1.3 pmol/mL plasma lysoGb3 was earlier proposed to distinguish true atypical FD patients from individuals with alpha-galactosidase A abnormalities without significance[68]. This threshold was based on data from 10 non-matched controls. Plasma specimens from individuals with unexplained stroke, cardiomyopathy or renal disease in the presence of normal GLA were not analysed. The strict use of the proposed threshold 1.3 pmol/mL cannot be recommended since plasma lysoGb3 levels in nearly every GD patient examined exceeds this. It is conceivable that diverse causes for lysosomal stress, including

6

chronic exposure to lysomotropic drugs, may cause non-specific modest elevations of glycosphingoid bases in plasma (up to a few pmol/mL).
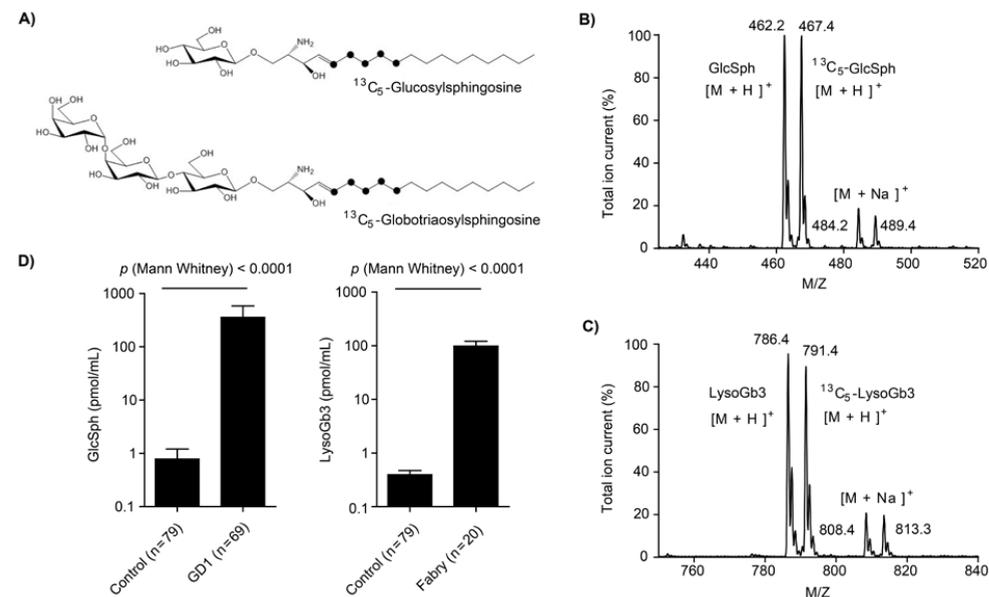

Figure 5. LC-MS/MS quantification of glycosphingoid bases. A) $^{13}C_5$-encoded isotope standards of GlcSph and lysoGb3. **B)** M/z ratio for analyte and internal standard for GlcSph. **C)** M/z ratio for analyte and internal standard for lysoGb3. **D)** GlcSph levels in GD1 patients (n=69) and lysoGb3 in classical FD patients (n=20).

Another application of measurement of glycosphingoid bases is found in monitoring disease manifestation and progression in GD1 patients and classic FD patients[36,69–73]. The origin of circulating glycosphingoid bases is by virtue unknown. Consequently, plasma glycosphingoid bases do not reflect a particular symptom. Regular measurements of plasma glycosphingoid bases in GD and FD patients receiving costly enzyme replacement therapy should nevertheless be advocated since this renders objective information on general efficacy of the intervention. A lack of response in plasma GlcSph of GD patients, or plasma lysoGb3 of FD patients, receiving therapy strongly suggests that the treatment is ineffective. Striking is the noted fast relapse in plasma GlcSph in GD patients following ERT interruption or major dose reductions as well as relapses in plasma lysoGb3 in classic FD males following the formation of neutralizing antibodies against the therapeutic enzyme[69,72]. The measurement of glycosphingoid bases is also of great value to examine the efficacy of experimental therapeutic intervention in animal models. An illustration for this forms the work of Dahl and colleagues on gene therapy in mice with an inducible loss GBA activity in white blood cells[74]. These mice, and similar animals generated by Mistry and colleagues[75] provide valuable

information on the relationship of plasma GlcSph and GlcCer-laden macrophages (Gaucher cells). The induction of Gaucher cells in both mouse models was found to be associated with a marked increase of plasma GlcSph, indicating that these cells are a major source of the circulating glycosphingoid base. Another strong indication for this are the earlier noted proportional changes in plasma GlcSph and chitotriosidase, a validated biomarker for Gaucher cells in most GD patients receiving ERT[36].

Out of the lysosome box: metabolism of GlcCer by the cytosol-faced enzyme GBA2.
The present paradigm on GSL degradation includes its restriction to lysosomes. An exception to this forms GlcCer, the only GSL synthesized and present in the cytosolic leaflet of membranes. Two decades ago the existence of a non-lysosomal glucosylceramidase, presently named GBA2, was discovered[76]. The enzyme differs from GBA in sensitivity for inhibitors and ability to degrade artificial β-xyloside substrates[76]. The strong membrane association of GBA2, and its intrinsic lability upon dissociation from membranes with detergents, hampered purification. Cloning of GBA2 cDNA, independently reported by Yildiz *et al.* and colleagues and Boot *et al.*[77,78], shed the first light on the protein's structural features. GBA2 proves to be a non-glycosylated 927-amino acid protein (figure 6A) that is synthesized in the cytosol and subsequently strongly binds to membranes[78]. Literature reports on its subcellular localization are conflicting, ranging from endosomes to the endoplasmic reticulum[78,79]. GBA2 lacks a true transmembrane domain and most likely the catalytic pocket is inserted in the cytosolic leaflet of membranes, consistent with the early observation that the enzyme preferentially uses substrate while embedded in the membrane[76]. At present, no 3D-structure of GBA2 is available. Very recently a crystal structure was published for the slightly homologous TxGH116 β-glucosidase from Thermoanaerobacterium xylanolyticum, revealing a N-terminal domain, primarily formed by a two-sheet β-sandwich and a C-terminal (α/α)6 solenoid domain[80]. The C-terminal domain contains the residues that were proposed as catalytic nucleophile and general acid/base in the archaeal β-glucosidase from Sulfolobus solfataricus and human GBA2[81]. The residues binding the glucose in the −1 subsite are highly conserved between TxGH116 β-glucosidase and human GBA2[80]. The enzyme is a retaining β-glucosidase using double displacement in catalysis with glutamate 527 as nucleophile and aspartate 677 as acid/base[81]. Hydrophobic iminosugars like AMP-deoxynojirimycin (AMP-DNM, IC_{50} of 1 nM) ((figure 6B) and N-butyl-deoxynojirimycin (Zavesca; IC_{50} of 250 nM)) are potent inhibitors of GBA2[82,83]. A survey of genomes shows that GBA2 is an ancient and evolutionarily conserved protein[84]. GD patients treated for more than a decade with *Zavesca* at concentrations that inhibit GBA2 activity generally tolerate the drug well. On the other hand, there are several reports of patients with defects in the GBA2 gene developing spastic paraplegia and cerebellar ataxia[85–90]. Their disease has an early onset and involves muscle weakness and spasticity in upper and lower limbs, cognitive impairment ataxia, axonal neuropathy and cerebellar and cerebral atrophy. Likewise, knock-down of GBA2 with antisense morpholino oligonucleotides in zebrafish led to abnormal motor behavior and axonal shortening/branching of motor

neurons[91]. However, GBA2 knock-down in mice does not cause any neuropathology[77] (figure 6C). GBA2-deficiency in male mice reduces spermatocyte fertility due to a defect in acrosome formation in early post-meiotic germ cells and causes malformation of the sperm head[92]. These defects are attributed to disorganization of cytoskeletal structures[93]. GBA2 mice also show impaired liver regeneration associated with cytokine- and growth factor-mediated signaling pathways[94].
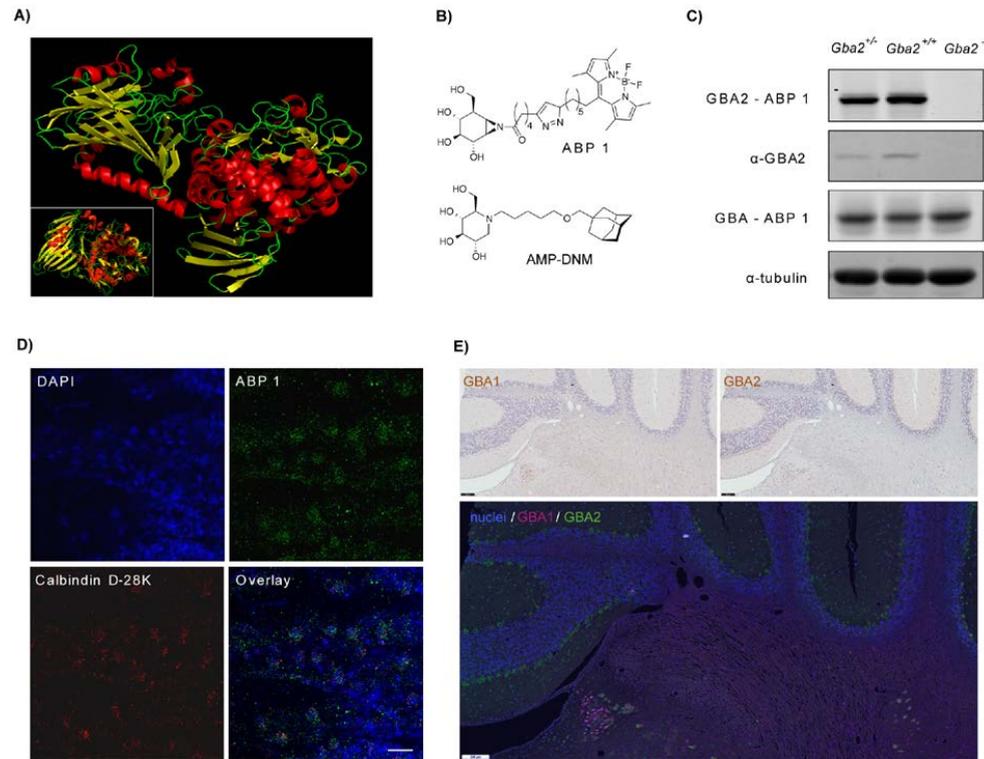
Figure 6. GBA2 *in silico*, *in vitro* and *in vivo*. A) Homology model of GBA2 secondary structure. **B)** Chemical structure of nanomolar GBA2 inhibitor AMP-DNM and activity-based probe (ABP 1) targeted against GBA and GBA2. **C)** Labeling of GBA2 and GBA by ABP 1 and immunoblotting of GBA2 and tubulin in brain homogenates of mice heterozygous, wt and knock-out for *Gba2*. Scale bar = 20 μm. **D)** *In situ* visualization of GBA2 labeled *in vivo* following i.c.v. injection of ABP 1. **E)** Immunostaining of GBA and GBA2 in the cerebellum of wt mouse. Scale bar = 100 μm.

The discovery of GBA2 in the nineties soon led to the speculation that this enzyme might be over-active in GD and that excessive degradation of GlcCer by GBA2 may exert toxic effects contributing to GD symptomatology[95]. Mistry and colleagues tested this hypothesis many years later by crossing in GBA2 deficiency in mice with inducible GBA deficiency. Indeed, the

absence of GBA2 significantly rescued the clinical phenotype of the GD mice[96]. Cells from GD patients have been reported to show higher levels of GBA2 protein as well as increased *in vitro* enzymatic activity when compared to corresponding control cells[97,98]. Recently, an opposite down-regulation of GBA2 activity in GD was reported and ascribed to its inhibition by sphingosine[99]. No explanation is at present available for the conflicting findings. In Niemann-Pick type C, the levels of GBA are significantly reduced in cells and tissues and GlcCer is elevated[100–102]. To test the hypothesis that GBA2 activity during GBA deficiency is harmful, the effect of genetic loss of *Gba2* in *Npc1*[nih] mice developing major motor neuron loss was examined. NPC mice with concomitant GBA2 deficiency lived longer and developed loss of motor coordination at later age (figure 7C)[98]. The survival of Purkinje cells, motor neurons with a relatively high GBA2 content, is prolonged in GBA2-deficient NPC mice (figure 6D-E)[98]. The beneficial effect of reducing GBA2 in NPC mice was recapitulated by daily administration of 1 mg AMP-DNM per kilo to each animal, a dose sufficient to inhibit GBA2 in the brain of mice (figure 7B). This investigation and that by Mistry and colleagues[96], provide evidence that GBA2 activity during GBA deficiency has harmful effects. The molecular mechanism for this remains currently elusive. Excessive generation of Cer from GlcCer by GBA2 in the cytosolic membrane leaflet might be detrimental (figure 7A) in view of the presumed pro-apoptotic role of cytosolic Cer and its stimulation of inflammation through activation of PLA2 resulting in increased prostaglandin E2[95].
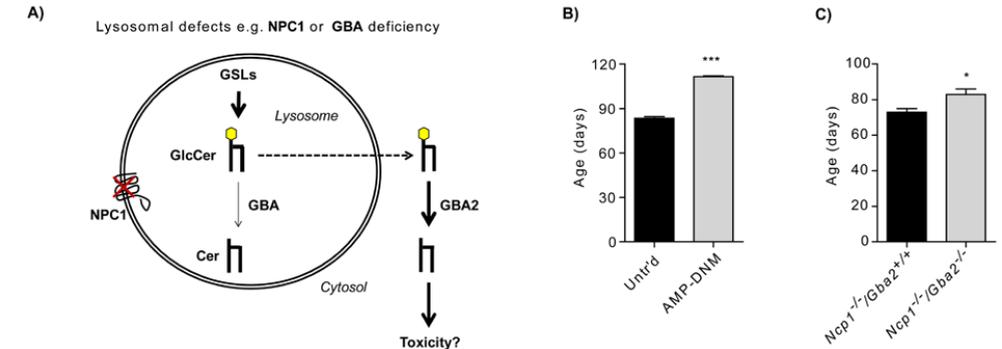
Figure 7. Detrimental role of excessive GBA2 activity during GBA deficiency. A) Scheme of postulated excessive compensatory activity of GBA2 during GBA deficiency. **B)** Mean survival of *Npc1*[nih] mice treated with one mg per kilogram per day of AMP-DNM in the diet and untreated control. **C)** Mean survival of *Npc1*-deficient mice wt or knock-out for *Gba2*.

GBA2, a β-glucosidase generating GlcChol by transglucosylation.
The catalytic mechanism of the retaining β-glucosidases GBA and GBA2[103], coined 'double-displacement' by its discoverer Koshland Jr., deserves closer inspection (figure 8A). The catalytic pocket of these enzymes employs two adjacent carboxylic acid residues, spaced ~5.5 Å apart, with one acting as catalytic nucleophile and the other as acid/base residue. The

deprotonated carboxylate of the nucleophile attacks the substrate's anomeric C1 carbon, while the carboxylic acid side-chain of the acid/base donates a proton to the inter-glycosidic oxygen. The aglycone is next expelled while concurrently a glycosyl-enzyme intermediate is formed, with an inversed configuration at the anomeric center. To deglycosylate the enzyme, the now deprotonated side-chain of the acid/base abstracts a proton from an incoming water molecule, forming a nucleophilic hydroxyl that attacks the anomeric center (C1) of the glycosyl-enzyme adduct and causes release of the sugar with overall retention of configuration (figure 8A). Of interest, several retaining glycosidases can also transglycosylate, i.e. transfer the sugar from substrate to an acceptor other than a free hydroxyl. A thorough historical account of transglycosylation by glycosidases is provided by the review of Hehre[104]. For example, acceptors in the transglycosylation by chitinases are sugars[105]. Glew and co-workers showed that GBA can catalyze the transfer of the glucose from 4-methylumbelliferyl-β-glucoside to retinol and other alcohols[106]. Akiyama and colleagues demonstrated that *in vitro* GBA generates 25-NBD-cholesterol-glucoside from GlcCer and artificial 25-NBD-cholesterol[107]. Marques and colleagues recapitulated their finding with natural cholesterol as acceptor[102]. Artificial β-glucosides like 4-methylumbelliferyl-β-glucoside as well as natural GlcCer were suitable sugar donors to generate glucosyl-β-D-cholesterol or 1-O-cholesteryl-β-D-glucopyranoside (GlcChol) (figure 8B). It was next discovered that also the enzyme GBA2 can generate GlcChol *in vitro* through transglucosylation, again using GlcCer as donor. Expectedly, GlcChol also proved to be an excellent substrate for *in vitro* hydrolysis by GBA and GBA2.
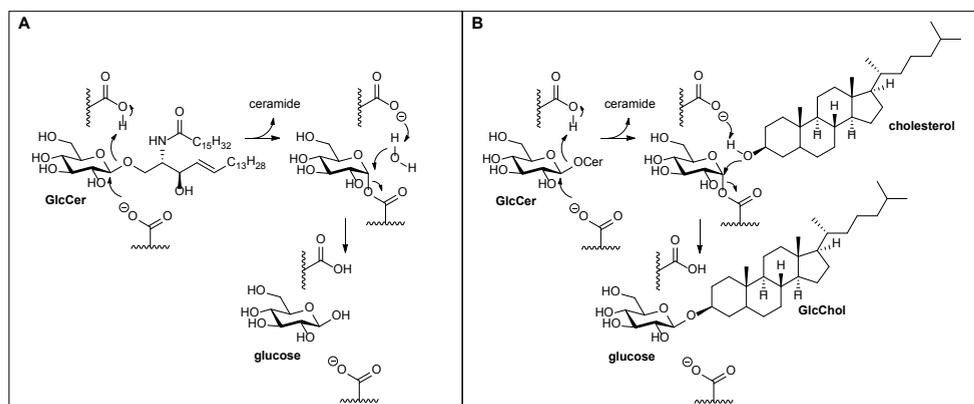

Figure 8. Transglucosylation. A) Hydrolysis of GlcCer by a β-glucosidase yielding free glucose and ceramide. **B)** Transglycosylation of cholesterol catalyzed by a β-glucosidase using GlcCer as donor of the glucose moiety and leading to the formation of GlcChol. Shown in both schemes are the catalytic residues of the β-glucosidase: acid-base (top) and nucleophile (bottom). See also ref[102].

The existence of sterol-glucosides in plant and fungal species is well documented[108], but not for mammals. Murofushi and co-workers proposed the presence of GlcChol in cultured human fibroblasts and gastric mucosa, but solid analytical proof for this was not provided[109,110]. To establish physiological relevance of GlcChol, its natural occurrence in mammalian cells and tissues was investigated. For this, a sensitive quantitative detection of GlcChol by LC-MS/MS using $^{13}C_5$-isotope labeled GlcChol as internal standard was developed. GlcChol was subsequently detected in human plasma and cultured cells. GlcChol was found to be present in all examined tissues of mice[102]. The highest concentration was observed for sciatic nerve[102]. The relative high amounts of GlcChol in the thymus, several nanomoles per gram of wet weight, are of interest in view of noted abnormalities in NKT and B-cells in GBA-deficient GD patients[111–113]. It has been proposed by Mistry and colleagues that elevated GlcCer or GlcSph via binding to CD1 may be causing this[111], but a role for GlcChol should not be excluded in this respect.

The biosynthesis and degradation of GlcChol in cells have been elucidated[102,114]. The enzyme GCS (EC2.4.1.80) forms GlcCer by transfer of glucose from UDP-glucose to Cer[115]. However, GCS does not synthesize GlcChol as firstly demonstrated by Akiyama and colleagues[114]. Next, Marques and co-workers studied GD mice, GBA-deficient LIMP-2 KO mice and GBA2-deficient mice to determine whether GBA or GBA2 is responsible for formation of GlcChol through transglucosylation[102]. Mice deficient in GBA showed modestly elevated GlcChol in several tissues. GBA2-deficient animals presented a very marked reduction in GlcChol in tissues, suggesting that *in vivo* GBA2 largely forms GlcChol and GBA degrades it. Consistent with this interpretation is the observed increase in plasma GlcChol in symptomatic GD patients.

Intrinsically, the local concentrations of donors (GlcCer and GlcChol) and acceptors (ceramide and cholesterol) determine the transglucosylation equilibrium of a retaining β-glucosidase. This is nicely illustrated by the finding that high lysosomal cholesterol concentrations drive GBA to generate GlcChol instead of degrading it[102]. The induction of lysosomal cholesterol accumulation in cells with U18666A causes a rapid increase in GlcChol, which is abolished by selective inactivation of GBA[102]. Consistently, in liver of NPC mice GlcChol is 25-fold elevated[102]. Pharmacological inhibition of GCS leads to reduction of GlcChol in cultured cells and plasma of mice and GD patients[102]. Apparently, availability of GlcCer is essential for formation of GlcChol through transglucosylation. GBA2 is well positioned in the cytosolic membrane leaflet containing GlcCer and cholesterol to generate GlcChol.

The physiological function of GlcChol is at present unclear. GlcChol is far more water soluble than cholesterol and intrinsically more suited for non-vesicular transport between compartments. Tentatively, water soluble GlcChol formed by transglucosylation at one cellular site could be transported to another site. A reverse reaction at the destination site could reconverted back cholesterol without any need for ATP. During pathological conditions such as GD, secondary abnormalities in GlcChol likely occur due to the imbalance in GBA and GBA2 activities. Future research will need to address whether such abnormalities in GlcChol, or in other glucosylated metabolites, contribute to particular GD symptoms.

Conclusion and Outlook

As reviewed, there is compelling evidence for the occurrence of adaptive metabolism in glycosphingolipidoses like GD and FD. Firstly, there is solid proof for formation of glycosphingoid bases in response to intralysosomal accumulation of GSLs. Secondly, there is strong evidence pointing to cytosolic metabolism of GlcCer by GBA2 that may generate GlcChol as side product and this pathway seems increased during GBA deficiency. Other metabolic adaptations in these diseases might still have to be discovered. A potential alternative compensatory reaction comes to mind, i.e. direct enzymatic removal of the entire glycan of GSLs. Such enzymes actually do exist in nature and are named endoglycoceramidases (EGC)[116,117]. At present several EGCs, with little mutual sequence homology, have been identified in mollusk, leech, earthworm and several pathogenic cestode parasites[118]. A search for the existence of such enzymes in mammals seems warranted, particularly since a comparable enzymatic activity has been reported by Basu *et al.* for rats and specific tumor cell lines[119–122]. The recent availability of activity-based probes recognizing various retaining β-glucosidases might assist the discovery of an elusive EGC in mammals. Briefly, cyclophellitol-epoxides and cyclophellitol-aziridines with a particular sugar configuration react with high specificity with corresponding retaining glycosidases through irreversible linkage to the catalytic nucleophilic residue. Cyclophellitol-epoxides tagged at C6 with a fluorophore react specifically with GBA, while cyclophellitol-aziridines tagged at C1 with a fluorophore react with several β-glucosidases[123,124]. Bacterial EGCase has already been found to react well with a β-glucopyranosyl-configured cyclophellitol-aziridine tagged with either a fluorophore or biotin[125]. The biotin-tagged ABP might be employed in a search for the elusive mammalian endoglycoceramidase and facilitate its purification and subsequent identification by proteomics.

The recent recognition of toxic effects of excessive lysoGb3 in FD and excessive GlcSph in GD deserves attention and warrants further research. Could novel drugs be envisioned to ameliorate these pathological effects by specifically reducing the glycosphingoid bases? Unfortunately, inhibition of AC, the enzyme responsible for generation of glycosphingoid bases, seems wise not since this will cause impaired lysosomal degradation of ceramide mimicking Farber disease, a severe neurological disorder[126]. The realization that excessive GBA2 during GBA deficiency is detrimental for motor neurons should be pursued regarding therapy. Further investigations on the therapeutic value of available brain-permeable combined inhibitors of GBA2 and GCS[127] are appealing for the juvenile neuronopathic variant of GD (type 3), in particular given the positive effect of the well tolerated inhibitor AMP-DNM in NPC mice[98,126] and similar positive findings made earlier by other investigators with Sandhoff mice[128], another glycosphingolipidosis.

References

1. Thudichum, J. *A treatise on the chemical constitution of the brain*. (Bailliere Tindall and Cox, 1884).
2. Wennekes, T. *et al.* Glycosphingolipids-Nature, Function, and Pharmacological Modulation. *Angew. Chemie Int. Ed.* **48,** 8848–8869 (2009).
3. Hancock, J. F. Lipid rafts: contentious only from simplistic standpoints. *Nat. Rev. Mol. Cell Biol.* **7,** 456–462 (2006).
4. Sonnino, S. & Prinetti, A. Membrane domains and the 'lipid raft' concept. *Curr. Med. Chem.* (2012).
5. Lingwood, D. & Simons, K. Lipid rafts as a membrane-organizing principle. *Science (80-.).* **327,** 46–50 (2010).
6. Merrill, A. H. Sphingolipid and Glycosphingolipid Metabolic Pathways in the Era of Sphingolipidomics. *Chem. Rev.* **111,** 6387–6422 (2011).
7. Schulze, H. & Sandhoff, K. Sphingolipids and lysosomal pathologies. *Biochim. Biophys. Acta* **1841,** 799–810 (2014).
8. Hanada, K. *et al.* Molecular machinery for non-vesicular trafficking of ceramide. *Nature* **426,** 803–9 (2003).
9. Ichikawa, S., Sakiyama, H., Suzuki, G., Hidari, K. I. & Hirabayashi, Y. Expression cloning of a cDNA for human ceramide glucosyltransferase that catalyzes the first glycosylation step of glycosphingolipid synthesis. *Proc. Natl. Acad. Sci. U. S. A.* **93,** 12654 (1996).
10. D'Angelo, G., Capasso, S., Sticco, L. & Russo, D. Glycosphingolipids: synthesis and functions. *FEBS J.* **280,** 6338–53 (2013).
11. Merrill, A. H., Wang, M. D., Park, M. & Sullards, M. C. (Glyco)sphingolipidology: an amazing challenge and opportunity for systems biology. *Trends Biochem. Sci.* **32,** 457–468 (2007).
12. Yu, R. K., Yanagisawa, M. & Ariga, T. *Comprehensive Glycoscience*. *Comprehensive Glycoscience* (Elsevier, 2007). doi:10.1016/B978-044451967-2/00003-9
13. Kolter, T. & Sandhoff, K. Lysosomal degradation of membrane lipids. *FEBS Lett.* **584,** 1700–1712 (2010).
14. Trinchera, M., Ghidoni, R., Sonnino, S. & Tettamanti, G. Recycling of glucosylceramide and sphingosine for the biosynthesis of gangliosides and sphingomyelin in rat liver. *Biochem. J.* **270,** 815–20 (1990).
15. Pyne, S., Adams, D. R. & Pyne, N. J. Sphingosine 1-phosphate and sphingosine kinases in health and disease: Recent advances. *Prog. Lipid Res.* **62,** 93–106 (2016).
16. Serra, M. & Saba, J. D. Sphingosine 1-phosphate lyase, a key regulator of sphingosine 1-phosphate signaling and function. *Adv. Enzyme Regul.* **50,** 349–62 (2010).
17. Platt, F. M. Sphingolipid lysosomal storage disorders. *Nature* **510,** 68–75 (2014).
18. Schulze, H. & Sandhoff, K. Lysosomal lipid storage diseases. *Cold Spring Harb. Perspect. Biol.* **3,** (2011).
19. Xu, Y.-H., Barnes, S., Sun, Y. & Grabowski, G. A. Multi-system disorders of glycosphingolipid and ganglioside metabolism. *J. Lipid Res.* **51,** 1643–1675 (2010).
20. Futerman, A. H. & van Meer, G. The cell biology of lysosomal storage disorders. *Nat. Rev. Mol. Cell Biol.* **5,** 554–565 (2004).
21. Wang, R. Y., Bodamer, O. A., Watson, M. S. & Wilcox, W. R. Lysosomal storage

diseases: diagnostic confirmation and management of presymptomatic individuals. *Genet. Med.* **13,** 457–484 (2011).

22. Matern, D., Oglesbee, D. & Tortorelli, S. Newborn screening for lysosomal storage disorders and other neuronopathic conditions. *Dev. Disabil. Res. Rev.* **17,** 247–253 (2013).

23. Conzelmann, E. & Sandhoff, K. Partial enzyme deficiencies: residual activities and the development of neurological disorders. *Dev. Neurosci.* **6,** 58–71

24. Farfel-Becker, T., Vitner, E. B. & Futerman, A. H. Animal models for Gaucher disease research. *Dis. Model. Mech.* **4,** 746–752 (2011).

25. Ferraz, M. J. *et al.* Gaucher disease and Fabry disease: New markers and insights in pathophysiology for two distinct glycosphingolipidoses. *Biochim. Biophys. Acta - Mol. Cell Biol. Lipids* **1841,** 811–825 (2014).

26. Holleran, W. M., Takagi, Y. & Uchida, Y. Epidermal sphingolipids: Metabolism, function, and roles in skin disorders. *FEBS Lett.* **580,** 5456–5466 (2006).

27. Staretz-Chacham, O., Lang, T. C., LaMarca, M. E., Krasnewich, D. & Sidransky, E. Lysosomal storage disorders in the newborn. *Pediatrics* **123,** 1191–207 (2009).

28. Sidransky, E., Sherer, D. M. & Ginns, E. I. Gaucher disease in the neonate: a distinct Gaucher phenotype is analogous to a mouse model created by targeted disruption of the glucocerebrosidase gene. *Pediatr. Res.* **32,** 494–8 (1992).

29. Germain, D. P. Fabry disease. *Orphanet J. Rare Dis.* **5,** 30 (2010).

30. Durant, B. *et al.* Sex differences of urinary and kidney globotriaosylceramide and lyso-globotriaosylceramide in Fabry mice. *J. Lipid Res.* **52,** 1742–1746 (2011).

31. Taguchi, A. *et al.* A symptomatic Fabry disease mouse model generated by inducing globotriaosylceramide synthesis. *Biochem. J.* **456,** 373–383 (2013).

32. Reczek, D. *et al.* LIMP-2 is a receptor for lysosomal mannose-6-phosphate-independent targeting of beta-glucocerebrosidase. *Cell* **131,** 770–83 (2007).

33. Blanz, J. *et al.* Disease-causing mutations within the lysosomal integral membrane protein type 2 (LIMP-2) reveal the nature of binding to its ligand -glucocerebrosidase. *Hum. Mol. Genet.* **19,** 563–572 (2010).

34. Goldstein, J. L., DeBose-Boyd, R. A. & Brown, M. S. Protein sensors for membrane sterols. *Cell* **124,** 35–46 (2006).

35. Settembre, C., Fraldi, A., Medina, D. L. & Ballabio, A. Signals from the lysosome: a control centre for cellular clearance and energy metabolism. *Nat. Rev. Mol. Cell Biol.* **14,** 283–96 (2013).

36. Dekker, N. *et al.* Elevated plasma glucosylsphingosine in Gaucher disease: relation to phenotype, storage cell markers, and therapeutic response. *Blood* **118,** e118–e127 (2011).

37. Mirzaian, M. *et al.* Mass spectrometric quantification of glucosylsphingosine in plasma and urine of type 1 Gaucher patients using an isotope standard. *Blood Cells, Mol. Dis.* **54,** 307–314 (2015).

38. Gaspar, P. *et al.* Action myoclonus-renal failure syndrome: diagnostic applications of activity-based probes and lipid analysis. *J. Lipid Res.* **55,** 138–145 (2014).

39. Aerts, J. M. *et al.* Elevated globotriaosylsphingosine is a hallmark of Fabry disease. *Proc. Natl. Acad. Sci.* **105,** 2812–2817 (2008).

40. Mirzaian, M. *et al.* Simultaneous quantitation of sphingoid bases by UPLC-ESI-MS/MS with identical 13C-encoded internal standards. *Clin. Chim. Acta* **466,** 178–184 (2017).

41. Miyatake, T. & Suzuki, K. Additional deficiency of psychosine galactosidase in globoid cell leukodystrophy: an implication to enzyme replacement therapy. *Birth Defects Orig. Artic. Ser.* **9,** 136–140 (1973).

42. Svennerholm, L., Vanier, M. T. & Månsson, J. E. Krabbe disease: a galactosylsphingosine (psychosine) lipidosis. *J. Lipid Res.* **21,** 53–64 (1980).

43. Ferraz, M. J. *et al.* Lyso-glycosphingolipid abnormalities in different murine models of lysosomal storage disorders. *Mol. Genet. Metab.* **117,** 186–193 (2016).

44. Yamaguchi, Y., Sasagasako, N., Goto, I. & Kobayashi, T. The synthetic pathway for glucosylsphingosine in cultured fibroblasts. *J. Biochem.* **116,** 704–710 (1994).

45. Ferraz, M. J. *et al.* Lysosomal glycosphingolipid catabolism by acid ceramidase: formation of glycosphingoid bases during deficiency of glycosidases. *FEBS Lett.* **590,** 716–725 (2016).

46. Lavoie, P., Boutin, M. & Auray-Blais, C. Multiplex analysis of novel urinary lyso-Gb3-related biomarkers for Fabry disease by tandem mass spectrometry. *Anal. Chem.* **85,** 1743–1752 (2013).

47. Ballabio, A. & Gieselmann, V. Lysosomal disorders: from storage to cellular damage. *Biochim. Biophys. Acta* **1793,** 684–696 (2009).

48. Gieselmann, V. Lysosomal storage diseases. *Biochim. Biophys. Acta* **1270,** 103–136 (1995).

49. Cox, T. M. & Cachón-González, M. B. The cellular pathology of lysosomal diseases. *J. Pathol.* **226,** 241–254 (2012).

50. Pastores, G. M. Krabbe disease: an overview. *Int. J. Clin. Pharmacol. Ther.* **47 Suppl 1,** S75-81 (2009).

51. de Fost, M. *et al.* Immunoglobulin and free light chain abnormalities in Gaucher disease type I: data from an adult cohort of 63 patients and review of the literature. *Ann. Hematol.* **87,** 439–49 (2008).

52. Pavlova, E. *et al.* B cell lymphoma and myeloma in murine Gaucher's disease. *J. Pathol.* **231,** 88–97 (2013).

53. Pavlova, E. V *et al.* Inhibition of UDP-glucosylceramide synthase in mice prevents Gaucher disease-associated B-cell malignancy. *J. Pathol.* **235,** 113–124 (2015).

54. Nair, S. *et al.* Clonal Immunoglobulin against Lysolipids in the Origin of Myeloma. *N. Engl. J. Med.* **374,** 555–561 (2016).

55. Rombach, S. M. *et al.* Vascular aspects of Fabry disease in relation to clinical manifestations and elevations in plasma globotriaosylsphingosine. *Hypertension* **60,** 998–1005 (2012).

56. Biegstraaten, M. *et al.* Small fiber neuropathy in Fabry disease. *Mol. Genet. Metab.* **106,** 135–41 (2012).

57. Choi, L. *et al.* The Fabry disease-associated lipid Lyso-Gb3 enhances voltage-gated calcium currents in sensory neurons and causes pain. *Neurosci. Lett.* **594,** 163–8 (2015).

58. Sanchez-Niño, M. D. *et al.* Globotriaosylsphingosine actions on human glomerular podocytes: implications for Fabry nephropathy. *Nephrol. Dial. Transplant* **26,** 1797–1802 (2011).

59. Barbey, F. *et al.* Cardiac and vascular hypertrophy in Fabry disease: evidence for a new mechanism independent of blood pressure and glycosphingolipid deposition. *Arterioscler. Thromb. Vasc. Biol.* **26,** 839–844 (2006).

60. Brakch, N. *et al.* Evidence for a role of sphingosine-1 phosphate in cardiovascular remodelling in Fabry disease. *Eur. Heart J.* **31,** 67–76 (2010).

6

6

61. Mirzaian, M. *et al.* Accurate quantification of sphingosine-1-phosphate in normal and Fabry disease plasma, cells and tissues by LC-MS/MS with 13C-encoded natural S1P as internal standard. *Clin. Chim. Acta* **459,** 36–44 (2016).

62. Rolfs, A. *et al.* Glucosylsphingosine Is a Highly Sensitive and Specific Biomarker for Primary Diagnostic and Follow-Up Monitoring in Gaucher Disease in a Non-Jewish, Caucasian Cohort of Gaucher Disease Patients. *PLoS One* **8,** e79732 (2013).

63. Murugesan, V. *et al.* Glucosylsphingosine is a key biomarker of Gaucher disease. *Am. J. Hematol.* **91,** 1082–1089 (2016).

64. Gold, H. *et al.* Quantification of Globotriaosylsphingosine in Plasma and Urine of Fabry Patients by Stable Isotope Ultraperformance Liquid Chromatography-Tandem Mass Spectrometry. *Clin. Chem.* **59,** 547–556 (2013).

65. Polo, G. *et al.* Diagnosis of sphingolipidoses: a new simultaneous measurement of lysosphingolipids by LC-MS/MS. *Clin. Chem. Lab. Med.* **55,** 403–414 (2017).

66. Schiffmann, R., Fuller, M., Clarke, L. A. & Aerts, J. M. F. G. Is it Fabry disease? *Genet. Med.* **18,** 1181–1185 (2016).

67. Smid, B. E. *et al.* Diagnostic dilemmas in Fabry disease: a case series study on GLA mutations of unknown clinical significance. *Clin. Genet.* **88,** 161–166 (2015).

68. Smid, B. E. *et al.* Plasma globotriaosylsphingosine in relation to phenotypes of Fabry disease. *J. Med. Genet.* **52,** 262–268 (2015).

69. van Dussen, L. *et al.* Effects of switching from a reduced dose imiglucerase to velaglucerase in type 1 Gaucher disease: clinical and biochemical outcomes. *Haematologica* **97,** 1850–1854 (2012).

70. van Breemen, M. J. *et al.* Reduction of elevated plasma globotriaosylsphingosine in patients with classic Fabry disease following enzyme replacement therapy. *Biochim. Biophys. Acta* **1812,** 70–76 (2011).

71. Rombach, S. M. *et al.* Plasma globotriaosylsphingosine: diagnostic value and relation to clinical manifestations of Fabry disease. *Biochim. Biophys. Acta* **1802,** 741–748 (2010).

72. Rombach, S. M. *et al.* Long-term effect of antibodies against infused alpha-galactosidase A in Fabry disease on plasma and urinary (lyso)Gb3 reduction and treatment outcome. *PLoS One* **7,** e47805 (2012).

73. Smid, B. E. *et al.* Biochemical response to substrate reduction therapy versus enzyme replacement therapy in Gaucher disease type 1 patients. *Orphanet J. Rare Dis.* **11,** 28 (2016).

74. Dahl, M. *et al.* Lentiviral gene therapy using cellular promoters cures type 1 Gaucher disease in mice. *Mol. Ther.* **23,** 835–844 (2015).

75. Mistry, P. K. *et al.* Glucocerebrosidase gene-deficient mouse recapitulates Gaucher disease displaying cellular and molecular dysregulation beyond the macrophage. *Proc. Natl. Acad. Sci.* **107,** 19473–19478 (2010).

76. van Weely, S., Brandsma, M., Strijland, a, Tager, J. M. & Aerts, J. M. Demonstration of the existence of a second, non-lysosomal glucocerebrosidase that is not deficient in Gaucher disease. *Biochim. Biophys. Acta* **1181,** 55–62 (1993).

77. Yildiz, Y. *et al.* Mutation of β-glucosidase 2 causes glycolipid storage disease and impaired male fertility. **116,** (2006).

78. Boot, R. G. *et al.* Identification of the non-lysosomal glucosylceramidase as beta-glucosidase 2. *J. Biol. Chem.* **282,** 1305–12 (2007).

79. Koerschen, H. G. *et al.* The non-lysosomal beta-glucosidase GBA2 is a non-integral membrane-associated protein at the ER and Golgi. *J. Biol. Chem.* **288,** 3381–3393 (2012).

80. Charoenwattanasatien, R. *et al.* Bacterial β-Glucosidase Reveals the Structural and Functional Basis of Genetic Defects in Human Glucocerebrosidase 2 (GBA2). *ACS Chem. Biol.* **11,** 1891–900 (2016).

81. Kallemeijn, W. W. *et al.* A Sensitive Gel-based Method Combining Distinct Cyclophellitol-based Probes for the Identification of Acid/Base Residues in Human Retaining -Glucosidases. *J. Biol. Chem.* **289,** 35351–35362 (2014).

82. Overkleeft, H. S. *et al.* Generation of specific deoxynojirimycin-type inhibitors of the non-lysosomal glucosylceramidase. *J. Biol. Chem.* **273,** 26522–7 (1998).

83. Wennekes, T. *et al.* Development of adamantan-1-yl-methoxy-functionalized 1-deoxynojirimycin derivatives as selective inhibitors of glucosylceramide metabolism in man. *J. Org. Chem.* **72,** 1088–97 (2007).

84. Cobucci-Ponzano, B. *et al.* A new archaeal beta-glycosidase from Sulfolobus solfataricus: seeding a novel retaining beta-glycan-specific glycoside hydrolase family along with the human non-lysosomal glucosylceramidase GBA2. *J. Biol. Chem.* **285,** 20691–20703 (2010).

85. Hammer, M. B. *et al.* Mutations in GBA2 cause autosomal-recessive cerebellar ataxia with spasticity. *Am. J. Hum. Genet.* **92,** 245–51 (2013).

86. Martin, E. *et al.* Loss of function of glucocerebrosidase GBA2 is responsible for motor neuron defects in hereditary spastic paraplegia. *Am. J. Hum. Genet.* **92,** 238–44 (2013).

87. Sultana, S. *et al.* Lack of enzyme activity in GBA2 mutants associated with hereditary spastic paraplegia/cerebellar ataxia (SPG46). *Biochem. Biophys. Res. Commun.* **465,** 35–40 (2015).

88. Citterio, A. *et al.* Mutations in CYP2U1, DDHD2 and GBA2 genes are rare causes of complicated forms of hereditary spastic paraparesis. *J. Neurol.* **261,** 373–381 (2014).

89. Votsi, C., Zamba-Papanicolaou, E., Middleton, L. T., Pantzaris, M. & Christodoulou, K. A novel GBA2 gene missense mutation in spastic ataxia. *Ann. Hum. Genet.* **78,** 13–22 (2014).

90. Kancheva, D. *et al.* Novel mutations in genes causing hereditary spastic paraplegia and Charcot-Marie-Tooth neuropathy identified by an optimized protocol for homozygosity mapping based on whole-exome sequencing. *Genet. Med.* **18,** 600–607 (2016).

91. Zancan, I. *et al.* Glucocerebrosidase deficiency in zebrafish affects primary bone ossification through increased oxidative stress and reduced Wnt/β-catenin signaling. *Hum. Mol. Genet.* **24,** 1280–94 (2015).

92. Walden, C. M. *et al.* Accumulation of Glucosylceramide in Murine Testis, Caused by Inhibition of beta-Glucosidase 2: IMPLICATIONS FOR SPERMATOGENESIS. *J. Biol. Chem.* **282,** 32655–32664 (2007).

93. Raju, D. *et al.* Accumulation of Glucosylceramide in the Absence of the Beta-Glucosidase GBA2 Alters Cytoskeletal Dynamics. *PLoS Genet.* **11,** 1–24 (2015).

94. Gonzalez-Carmona, M. A. *et al.* Beta-glucosidase 2 knockout mice with increased glucosylceramide show impaired liver regeneration. *Liver Int.* **32,** 1354–1362 (2012).

95. Aerts, J. M., Hollak, C., Boot, R. & Groener, A. Biochemistry of glycosphingolipid storage disorders: implications for therapeutic intervention. *Philos. Trans. R. Soc. Lond. B. Biol. Sci.* **358,** 905–14 (2003).

96. Mistry, P. K. *et al.* Glucocerebrosidase 2 gene deletion rescues type 1 Gaucher disease. *Proc. Natl. Acad. Sci.* **111,** 4934–4939 (2014).

97. Burke, D. G. *et al.* Increased glucocerebrosidase (GBA) 2 activity in GBA1 deficient mice brains and in Gaucher leucocytes. *J. Inherit. Metab. Dis.* **36,** 869–872 (2013).

98. Marques, A. R. A. *et al.* Reducing GBA2 Activity Ameliorates Neuropathology in Niemann-Pick Type C Mice. *PLoS One* **10,** e0135889 (2015).

99. Schonauer, S. *et al.* Identification of a feedback loop involving β-glucosidase 2 and its product sphingosine sheds light on the molecular mechanisms in Gaucher disease. *J. Biol. Chem.* **292,** 6177–6189 (2017).

100. Salvioli, R. *et al.* Glucosylceramidase mass and subcellular localization are modulated by cholesterol in Niemann-Pick disease type C. *J. Biol. Chem.* **279,** 17674–80 (2004).

101. Besley, G. T. & Moss, S. E. Studies on sphingomyelinase and beta-glucosidase activities in Niemann-Pick disease variants. Phosphodiesterase activities measured with natural and artificial substrates. *Biochim. Biophys. Acta* **752,** 54–64 (1983).

102. Marques, A. R. A. *et al.* Glucosylated cholesterol in mammalian cells and tissues: formation and degradation by multiple cellular β-glucosidases. *J. Lipid Res.* **57,** 451–463 (2016).

103. Kallemeijn, W. W., Witte, M. D., Wennekes, T. & Aerts, J. M. F. G. in *Advances in carbohydrate chemistry and biochemistry* **71,** 297–338 (2014).

104. Hehre, E. J. Glycosyl transfer: a history of the concept's development and view of its major contributions to biochemistry. *Carbohydr. Res.* **331,** 347–68 (2001).

105. Aguilera, B. *et al.* Transglycosidase activity of chitotriosidase: improved enzymatic assay for the human macrophage chitinase. *J. Biol. Chem.* **278,** 40911–6 (2003).

106. Vanderjagt, D. J., Fry, D. E. & Glew, R. H. Human glucocerebrosidase catalyses transglucosylation between glucocerebroside and retinol. *Biochem. J.* 309–15 (1994).

107. Akiyama, H., Kobayashi, S., Hirabayashi, Y. & Murakami-Murofushi, K. Cholesterol glucosylation is catalyzed by transglucosylation reaction of β-glucosidase 1. *Biochem. Biophys. Res. Commun.* **441,** 838–843 (2013).

108. Grille, S., Zaslawski, A., Thiele, S., Plat, J. & Warnecke, D. The functions of steryl glycosides come to those who wait: Recent advances in plants, fungi, bacteria and animals. *Prog. Lipid Res.* **49,** 262–288 (2010).

109. Kunimoto, S., Kobayashi, T., Kobayashi, S. & Murakami-Murofushi, K. Expression of cholesteryl glucoside by heat shock in human fibroblasts. *Cell Stress Chaperones* **5,** 3–7 (2000).

110. Kunimoto, S. *et al.* Cholesteryl Glucoside-induced Protection against Gastric Ulcer. *Cell Struct. Funct.* **28,** 179–186 (2003).

111. Nair, S. *et al.* Type II NKT-TFH cells against Gaucher lipids regulate B-cell immunity and inflammation. *Blood* **125,** 1256–1271 (2015).

112. Salio, M. & Cerundolo, V. NKT-dependent B-cell activation in Gaucher disease. *Blood* **125,** 1200–2 (2015).

113. Liu, J. *et al.* Gaucher disease gene GBA functions in immune regulation. *Proc. Natl. Acad. Sci.* **109,** 10018–10023 (2012).

114. Akiyama, H. *et al.* Novel sterol glucosyltransferase in the animal tissue and cultured cells: evidence that glucosylceramide as glucose donor. *Biochim. Biophys. Acta* **1811,** 314–322 (2011).

115. van Meer, G., Wolthoorn, J. & Degroote, S. The fate and function of glycosphingolipid glucosylceramide. *Philos. Trans. R. Soc. Lond. B. Biol. Sci.* **358,** 869–73 (2003).

116. Rasilo, M. L., Ito, M. & Yamagata, T. Liberation of oligosaccharides from glycosphingolipids on PC12 cell surface with endoglycoceramidase. *Biochem. Biophys. Res. Commun.* **162,** 1093–1099 (1989).

117. Ito, M. & Yamagata, T. Purification and characterization of glycosphingolipid-specific endoglycosidases (endoglycoceramidases) from a mutant strain of Rhodococcus sp. Evidence for three molecular species of endoglycoceramidase with different specificities. *J. Biol. Chem.* **264,** 9510–9519 (1989).

118. Ishibashi, Y. *et al.* A novel endoglycoceramidase hydrolyzes oligogalactosylceramides to produce galactooligosaccharides and ceramides. *J. Biol. Chem.* **282,** 11386–11396 (2007).

119. Basu, M. *et al.* Ceramide glycanase from rat mammary tissues: inhibition by PPMP(D-/L-) and its probable role in signal transduction. *Indian J. Biochem. Biophys.* **34,** 142–149

120. Basu, M. *et al.* Hydrophobic nature of mammalian ceramide glycanases: purified from rabbit and rat mammary tissues. *Acta Biochim. Pol.* **45,** 327–342 (1998).

121. Basu, M., Kelly, P., Girzadas, M., Li, Z. & Basu, S. Properties of animal ceramide glycanases. *Methods Enzymol.* **311,** 287–297 (2000).

122. Basu, M. *et al.* Ceramide glycanase activities in human cancer cells. *Biosci. Rep.* **19,** 449–460 (1999).

123. Witte, M. D. *et al.* Ultrasensitive in situ visualization of active glucocerebrosidase molecules. *Nat. Chem. Biol.* **6,** 907–913 (2010).

124. Kallemeijn, W. W. *et al.* Novel activity-based probes for broad-spectrum profiling of retaining β-exoglucosidases in situ and in vivo. *Angew. Chemie - Int. Ed.* **51,** 12529–12533 (2012).

125. Kallemeijn, W. W. *et al.* Endo-β-Glucosidase Tag Allows Dual Detection of Fusion Proteins by Fluorescent Mechanism-Based Probes and Activity Measurement. *Chembiochem* **17,** 1698–704 (2016).

126. Nietupski, J. B. *et al.* Iminosugar-based inhibitors of glucosylceramide synthase prolong survival but paradoxically increase brain glucosylceramide levels in Niemann-Pick C mice. *Mol. Genet. Metab.* **105,** 621–628 (2012).

127. van den Berg, R. J. B. H. N. *et al.* Synthesis and Evaluation of Hybrid Structures Composed of Two Glucosylceramide Synthase Inhibitors. *ChemMedChem* **10,** 2042–62 (2015).

128. Ashe, K. M. *et al.* Iminosugar-based inhibitors of glucosylceramide synthase increase brain glycosphingolipids and survival in a mouse model of Sandhoff disease. *PLoS One* **6,** e21758 (2011).

6

6

7

β-Xylosidase and transxylosidase activities of human glucocerebrosidase

β-Xylosidase and transxylosidase activities of human glucocerebrosidase

Based on

Mina Mirzaian[1*], Maria J. Ferraz[1*], Daphne E.C. Boer[1], Saskia V. Ousoren[1], Marc Hazeu[1], Jasper Wermink[1], Per Haberkant[1#], Sybrin P. Schroder[3], Karen Ghauharali[2], Edward Blommaart[2], Roelof Ottenhoff[2], Andre R.A. Marques[1], Rianne Meijer[1], Wouter Kallemeijn[1], Rolf G. Boot[1], Herman S. Overkleeft[3], Navraj S. Pannu[4], Johannes M. Aerts[1]

[1]Dept. of Medical Biochemistry, LIC, Leiden University
[2]Dept. of Medical Biochemistry, AMC, Amsterdam
[3]Dept. of Bio-organic Synthesis, LIC, Leiden University
[4]Dept. of Macromolecular Biochemistry, LIC, Leiden University
#Present address; EMBL, Heidelberg
*These authors contributed equally to this work

Manuscript pending submission

Abstract

The lysosomal retaining β-glucosidase, glucocerebrosidase (GBA1), hydrolyzes β-glucosidic substrates and transglucosylates cholesterol to cholesterol-β-glucoside (GlcChol). We here present evidence that the enzyme also cleaves 4-methylumbelliferyl-β-D-xylose (4MU-β-Xyl) in vitro and in vivo. This activity is stimulated by saposin C. In addition, GBA1 is shown to transxylosylate fluorescent 25-NBD-cholesterol and natural cholesterol using 4MU-β-Xyl as donor. The xylosyl-cholesterol (XylChol) formed by GBA1 acts as subsequent acceptor to render di-xylosyl-cholesterol. Exposure of GBA1 to cholesterol and sequentially 4MU-β-Glc and 4MU-β-Xyl results in generation of GlcXylChol. The cytosolic β-glucosidase GBA3 shows in vitro also β-xylosidase and transxylosylase activitiy, in contrast to the membrane-bound cellular β-glucosidase GBA2. Cultured cells also generate xylosylated cholesterols when exposed to 4MU-β-Xyl in their medium, independent of the presence of glucosylceramide synthase.. This synthesis is enhanced by the drug U18666A causing an increase in lysosomal cholesterol. The prior inhibition of GBA1 with conduritol B-epoxide prohibits generation of xylosylated cholesterols by cells. In conclusion, our findings reveal further catalytic versatility of GBA1. The natural occurrence of xylosylated cholesterol as well as other xylosylated lipids warrants future investigation.

Introduction

Xylose mimics glucose except for the lacking pendant CH_2OH group. It is a main building block of the ubiquitous xylan in plants[1]. In animals, xylose is present in O-glycans of proteoglycans as the first saccharide linked to serine or threonine residues. It is added by the protein by UDP-xylose dependent xylosyltransferases, an essential step in the synthesis of the glycosaminoglycans heparan sulfate, keratan sulfate and chondroitin sulfate[2]. The human body synthesizes UDP-xylose is from UDP-glucuronate by UDP-glucuronic acid decarboxylase 1 encoded by the UXS1 gene[3]. Since the studies by Fisher & Kent and Patel & Tappel, degradation of β-xylosides in animals is thought to depend on β-glucosidases[4,5]. We earlier reported that the lysosomal acid β-glucosidase GBA1, aka glucocerebrosidase, can hydrolyze 4-methylumbelliferyl-β-xyloside (4MU-β-Xyl)[6]. Inherited deficiency of GBA1 causes Gaucher disease (GD), a lysosomal disorder characterized by the glucosylceramide (GlcCer) accumulating macrophages in tissues[7,8]. The occurrence of storage of β-D-xylose-containing glycopeptides in GD patients has not been actively investigated. More recently another catalytic activity of GBA1 has been recognized. Through transglucosylation, GBA1 can transfer of glucose from β-glucoside substrates to cholesterol, thus forming β-D-glucosylcholesterol (GlcChol)[9,10]. Glew and colleagues earlier demonstrated that GBA1 can transglucosylate retinol in vitro[11]. Formation of GlcChol by GBA1 also takes place in vivo[10]. In Niemann Pick type C disease (NPC), cholesterol accumulates in lysosomes is due to genetic defects in either NPC1 or NPC2, two proteins mediating the export of the sterol from lysosomes[12]. In NPC, GBA1 actively generates GlcChol[10]. The generation of GlcChol by cells can also be induced by exposure to U18666A, an inhibitor of cholesterol export from lysosomes. The transglucosylation in these cells is prohibited by inhibition of GBA1[10]. Also GBA2, the β-glucosidase inserted in the cytoplasmic leaflet of membranes, shows transglucosylase activity in vitro and in vivo[10,13–15].

We here examined whether GBA1 is also able to generate xylosyl-β-D-cholesterol (XylChol). It is reported that GBA1 indeed xylosylates cholesterol, generating not only XylChol but even di-xylosyl-cholesterol (Xyl$_2$Chol) and traces of tri-xylosyl-cholesterol (Xyl$_3$Chol). The physiological relevance of these findings is discussed.

Results

Cleavage of 4-methylumbelliferyl-β-D-xylose by GBA1.

We first incubated pure recombinant hGBA1 with either 4-methylumbelliferyl β-D-xylose (4MU-β-Xyl) or 4-methylumbelliferyl β-D-glucose (4MU-β-Glc). The enzyme was found to release fluorescent 4MU from both substrates. The activity towards 4MU-β-Xyl was about 50-fold less due to a higher Km and lower Vmax (Table 1). The pH optimum of the activity of GBA1 towards both substrates was found to be similar (Fig 1A). The same held true for the stimulation of activity by taurocholate (fig 1B). The activity towards both substrates was also comparably stimulated by recombinantly produced saposin C (Fig 1C). The kcat/Km of

recombinant GBA1 is about 40-fold higher for 4MU-β-Glc than 4MU-β-Xyl (Table 1). GBA1 uses double displacement for catalysis with E340 as nucleophile and E325 as acid/base[16]. Blocking E340 through permanent linkage of the suicide inhibitor cyclophellitol eliminates activity[17]. The activities of GBA1 towards 4MU-β-Glc and 4MU-β-Xyl substrates were both inhibited by pre-incubation for 90 minutes and subsequent activity assay for 60 minutes. The slightly higher apparent IC_{50} with 4MU-β-Glc (85 nM) than with 4MU-β-Xyl (61 nM) is likely due to greater protection by the β-D-glucose substrate against irreversible inhibition of GBA1. A recently synthesized xylose analogue of cyclophellitol[18] also irreversibly inactivated GBA1, although with lower affinity than cyclophellitol (Table 1). The apparent IC_{50} with 4MU-β-Glc (10.16 μM) was slightly higher than with 4MU-β-Xyl substrate (6.41 μM), presumably again due to better protection by the former substrate against irreversible inhibition of GBA1.
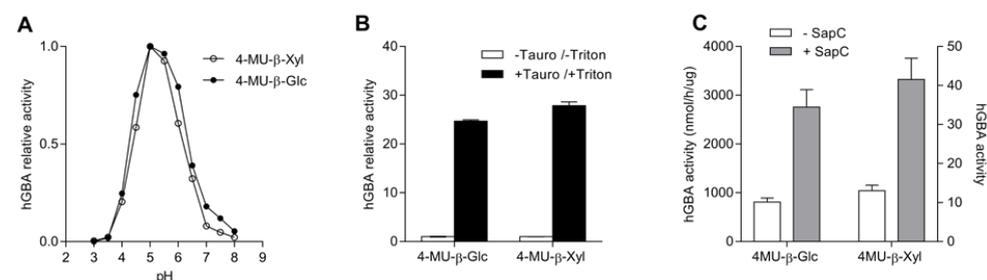
Transxylosylase activity of GBA1.
We next studied the potential transxylosidase activity of recombinant GBA1. Enzyme was incubated for 16 hours with 4MU-β-Glc or 4MU-β-Xyl as donors and fluorescent 25-NBD-cholesterol as acceptor. Products were visualized by HPTLC and fluorescence scanning. Formation of fluorescent sterol metabolites occurred with both donors (fig 2A). With 4MU-β-D-Glc, glucosylated 25-NBD-cholesterol is formed as earlier described[10]. In the case of 4MU-β-Xyl, two novel fluorescent metabolites were detected, presumably mono- and di-xylosylated 25-NBD cholesterol.

Subsequently we used natural cholesterol as acceptor in the same assay and the formed products were analyzed by LC-MS/MS. Formation of XylChol, Xyl_2Chol, and traces of Xyl_3Chol was detected (fig 2B). In sharp contrast, incubation of GBA1 and cholesterol with 4MU-β-Glc only yields GlcChol as product (fig 2C).

Figure 1. Cleavage of 4MU-β-Glc and 4MU-β-Xyl by recombinant hGBA1. A. pH optimum of 4MU release by GBA1 from 4MU-β-Glc (closed circles) and 4MU-β-Xyl (open circles); **B.** Stimulation by 0.2 % (w/v) taurocholate of 4MU release from the substrates 4MU-β-Glc (left) and 4MU-βXyl (right). The measured activity is expressed as 100 % in the absence of taurocholate at pH 5.2, with 0.1 % (v/v) Triton X-100; **C.** Stimulation of 4MU release from the substrates 4MU-β-Glc (left axis) and 4MU-β-Xyl (right axis) by recombinant saposin C at pH 4.5 in the presence of phosphatidylserine.

Figure 2. Transxylosylation and transglucosylation of cholesterol by GBA1. A. HPTLC analysis of fluorescent products formed from 25-NBD-cholesterol, following incubation with GBA1 in the presence of 4MU-β-Glc or 4MU-β-Xyl for 16 h; **B.** LC-MS/MS analysis of products formed during 1 h incubation of GBA1, cholesterol and 4MU-β-Xyl; **C.** LC-MS/MS analysis of products formed during 1 h incubation of GBA1, cholesterol and 4MU-β-Glc.

Table 1. Kinetic parameters hGBA1.

hGBA1	4MU-β-Glc	4MU-β-Xyl
IC50 cyclophellitol (μM)	0.085 ± 0.002	0.061 ± 0.002
IC50 D-xylo-cyclophellitol (μM)	10.16 ± 1.03	6.41 ± 0.47
Km (mM)	0.76 ± 0.06	5.24 ± 1.04
Vmax (nmol/h.mg)	$1.23 \times 10^6 \pm 3.32 \times 10^4$	$1.88 \times 10^5 \pm 2.88 \times 10^4$
Kcat/Km (mM/s)	25.03	0.55

Time dependence of glycosidase and transglycosidase activities of GBA1.

GBA1 and cholesterol were incubated with 4MU-β-Glc or 4MU-β-Xyl for different time periods at 37 ˚C. The release of fluorescent 4MU and formation of glycosylated products was determined. The generated GlcChol was already maximal after 30 min incubation and then declined with time (fig 3A). This indicates that the formed GlcChol is also subject to hydrolysis by GBA1. In sharp contrast, XylChol showed no reduction over time, and Xyl_2Chol was formed after a lag period (fig 3B). Apparently, XylChol is barely hydrolyzed and serves as acceptor for further xylosylation. Even Xyl_2Chol may act as acceptor, rendering Xyl_3Chol (fig 3). Comparison of the release of 4MU with concomitant formation of glycosylated sterol indicates that GBA1 shows considerably higher net transxylosylation than transglucosylation efficiency (fig 3).

We next studied the outcome of the sequential incubation of GBA1 and cholesterol with 4MU-β-Xyl (3h) followed by 4MU-β-Glc (1h). Formation of GlcXylChol (with m/z 698.5 > 369.3) was demonstrable at these conditions, again indicating that XylChol is as excellent acceptor in glycosylation reaction (Supplemental Table 2).
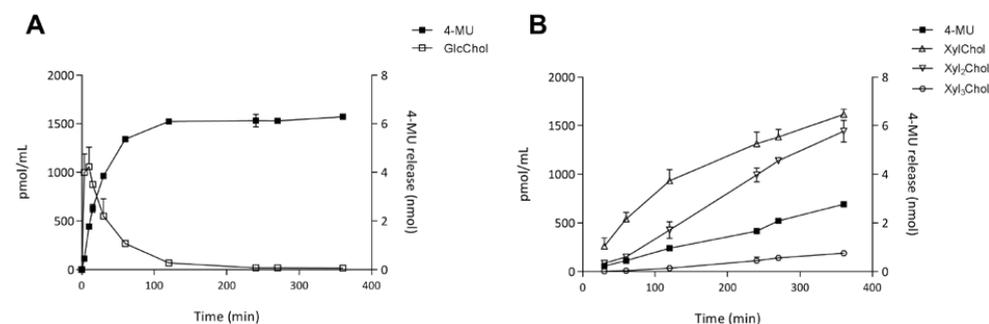

Figure 3. Glycosylation of cholesterol in time. A. Release of 4MU from 4MU-β-Glc and concomitant formation of glucosylated cholesterol; **B.** Release of 4MU from 4MU-β-Xyl and concomitant formation of xylosylated cholesterol. GBA1 was incubated at pH 5.2 in the presence of taurocholate and Triton X-100 with 3.0 mM 4MU-substrates for the indicated times after which released 4MU and formed glycosylated cholesterol were determined.

In vivo formation of xylosylated cholesterol.

Building on the *in vitro* findings, potential transxylosylation by cultured RAW264.7 cells exposed to 3.7 mM 4MU-β-Xyl in the medium was studied. Cells were incubated without or with conduritol β-epoxide (CBE), an irreversible GBA1 inhibitor, either in the absence (fig. 4A) or presence of 10 μM U18666A (fig. 4B) to induce lysosomal accumulation of cholesterol[10]. Formation of XylChol, Xyl_2Chol and Xyl_3Chol was determined by LC-MS/MS (fig.

4A). The levels of xylosylated cholesterols were markedly increased by exposure of cells to U18666A and prohibited by pre-incubation with CBE (fig. 4A and B).

We next examined the possible involvement of UDP-glucose dependent glucosylceramide synthase (GCS)[19,20] in the formation of xylosylated cholesterols. HEK293 cells deficient in GCS produced XylChol on a par to corresponding *wt* cells when exposed to 4MU-β-Xyl and U18666A (fig. 4C and D).
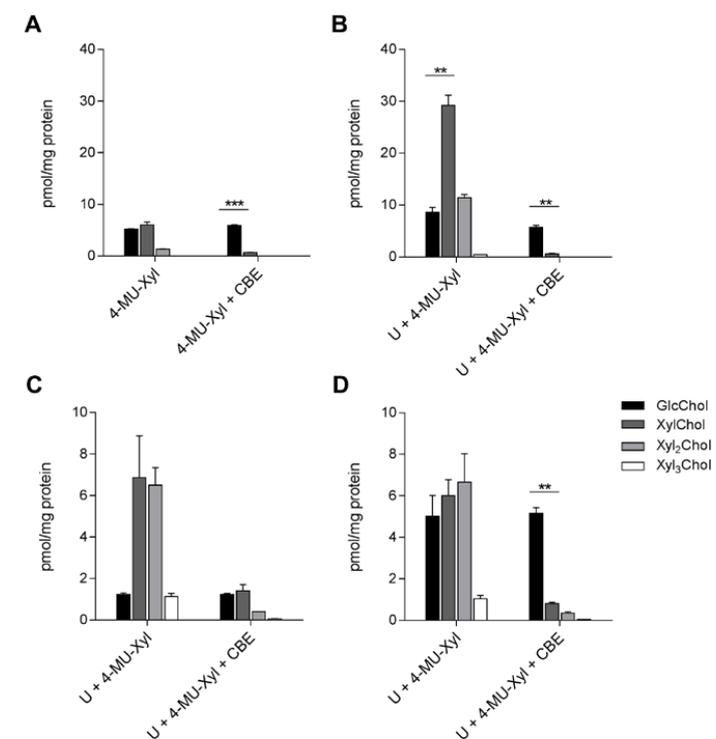
Figure 4. *In vivo* formation of xylosylated cholesterols. A. LC-MS/MS detection of formed xylosylated cholesterols in RAW264.7 cells incubated with 3.7 mM 4MU-β-Xyl for 24 h, with or without CBE; **B.** Idem, in the presence of 10 μM U18666A; **C.** LC-MS/MS detection of formed xylosylated and glucosylated cholesterols in HEK293 exposed to 3.7 mM 4MU-β-Xyl and U18666A for 24 hours in the presence or absence of CBE; **D.** LC-MS/MS detection of formed glycosylated cholesterols in HEK293 cells deficient in GCS as in panel C. Significance of differences in formation of GlcChol and XylChol was determined and is shown in the panels A-D.

Specificity of transxylosylation.

Finally, we investigated the potential transxylosylation by the two other human retaining β-glucosidases, GBA2 and GBA3. We previously noticed that GBA2, but not GBA3, can mediate

transfer of the glucosyl moiety from 4MU-β-D-glucose to cholesterol or ceramide[10]. While this finding was recapitulated (fig. 5), no xylosylation by GBA2 was concomitantly detectable, consistent with its inability to hydrolyze 4MU-β-D-Xyl[21]. However, GBA3, albeit less prominent than GBA1, is able to hydrolyze 4MU-β-Xyl as well as to transxylosylate cholesterol (fig. 5).

Figure 5. Lack of transxylosylation by GBA2. HPTLC analysis of formation of glycosylated 25-NBD-cholesterol by β-glucosidases with 4MU-β-Xyl and 4MU-β-Glc as donor. Enzymes: recombinant hGBA1; lysate of HEK293 cells overexpressing GBA2; lysate of HEK293 cells overexpressing GBA3. Incubation for 16 hours with (+) or without (-) enzyme preparation.
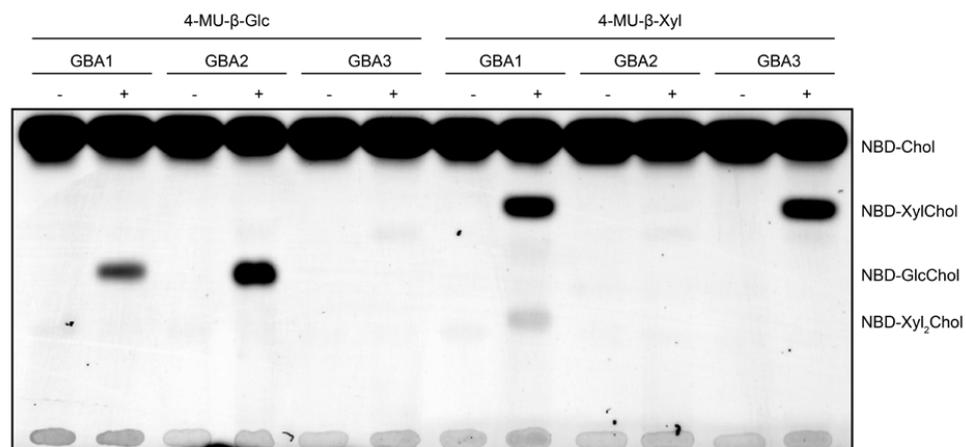
Discussion
Our present investigation reveals further catalytic versatility of the lysosomal glucocerebrosidase GBA1. The enzyme *in vitro* cleaves besides 4MU-β-Glc also 4MU-β-Xyl. Moreover, GBA1 uses both substrates as sugar donors in transglycosylation of cholesterol. Next, GBA1 in cultured cells generates xylosylated cholesterol when exposed to 4MU-β-Xyl. The induction of lysosomal cholesterol accumulation with U18666A increases formation of xylosylated cholesterols, a reaction prohibited by inactivation of GBA1 with the irreversible inhibitor CBE. Both *in vitro* and *in vivo,* GBA1 may even produce di-xylosyl-cholesterol through a repetitive transglucosylation not seen with 4MU-β-Glc as sugar donor[10]. The affinity of GBA1 for 4MU-β-Glc as substrate for cleavage is higher than that for 4MU-β-Xyl. Likewise, XylChol is a poorer substrate for hydrolysis by GBA1 than GlcChol. Following exposure of GBA1 to cholesterol and 4MU-β-Xyl, the concentration of XylChol steadily builds up and it starts to act as acceptor in a second round of transxylosylation, rendering Xyl2Chol. Incubation of GBA1 and cholesterol with a mixture of 4MU-β-Xyl and 4MU-β-Glc leads to

formation of GlcXylChol, further illustrating the suitability of XylChol as acceptor in transglycosylation.

Net formation of XylChol by GBA1 exceeds that of GlcChol, a phenomenon that can be ascribed to the lower rate of hydrolysis of XylChol than GlcChol. At present, it can't be excluded that a xylose covalently bound to the catalytic nucleophile E340 of GBA1 is also somehow transferred more efficiently to cholesterol than a covalently bound glucose. Further insight might be obtained by crystallography employing β-glucose and β-xylose configured cyclophellitol-epoxides covalently bound to E340-GBA1. Of note, Aerts and co-workers earlier reported relative higher transxylosylase than transglucosylase efficiency of a β-D-glucosidase from *Stachybotrys atra*[19], quite comparable to our findings with GBA1.

The physiological relevance of transxylosylation catalyzed by GBA1 is presently unclear. Mass spectrometry suggests the presence of XylChol (m/z 536.5 > 369.3) in liver of Npc1^{-/-} mice (data not shown). Of note, in the same livers accumulation of GlcChol has previously been detected[10]. Definitive confirmation of XylChol in NPC liver by NMR analysis of purified lipid is needed. In this connection, a key question is whether physiological xyloside donors occur. Several β-xylosidic compounds are known to be produced by plants and their uptake via food can a priori not be excluded[20]. β-D-xylosyl moieties are also present in endogenous proteoglycans from which xylosyl-peptides are formed during lysosomal degradation. It is unclear whether these are suitable donors for GBA1-mediated formation of xylosylated sterols. In theory, a UDP-xylose dependent xylosyltransferase may hitherto generate unknown β-xyloside donors to be used in transxylosylation. One such candidate is UGT3A2, a UDP-xylose-utilizing glycosyltransferase reported to glycosylate various hydrophobic structures *in vitro*[22]. Lastly, it should be rigorously investigated whether other lipids besides cholesterol may act as acceptors in transxylosylation by GBA1[10]. We already observed that GBA1 *in vitro* also transxylosylates sphingosine and ceramide (not shown).

Our investigation has further revealed that GBA3, a cytosolic glucosidase implicated in metabolism of xenophobic glycosides[23], also shows xylosidase and transxylosidase activity. In contrast, the β-glucosidase GBA2, recently shown to be a potent transglucosylase[10], has no significant activity towards β-xyloside substrates. Apparently the pendant CH_2OH group in glucoside substrates is crucial in the interaction of GBA2 with substrate. The importance of the presence of the additional CH_2OH group in glucose is also suggested by the much lower affinity of GBA2 for the inhibitor conduritol-B-epoxide as compared to cyclophellitol (with the pendant CH_2OH group).

In conclusion, human GBA1 is more versatile in catalysis as hitherto considered. Investigation of the (patho)physiological relevance of various reactions catalyzed by GBA1 might increase our understanding of the complex symptomatology of Gaucher disease[7,8] and other conditions for which abnormal GBA1 imposes a risk such as multiple myeloma and α-synucleinopathies like Parkinsonism and Lewy-body dementia[24,25].

7

7

Materials and Methods

Materials

25-[N-[(7-nitro-2-1,3-benzoxadiazol-4-yl)methyl]amino]-27-norcholesterol (25-NBD-Cholesterol) and cholesterol were from Avanti Polar Lipids (Alabaster, AL, USA). 4-methylumbelliferyl-β-D-glucose (4MU-β-Glc) and 4-methylumbelliferyl-β-D-xylose (4MU-β-Xyl) were purchased from Glycosynth™ (Winwick Quay Warrington, Cheshire, England). Conduritol β epoxide (D, L-1,2-anhydro-*myo*-inositol; CBE) was from Enzo Life Sciences Inc. (Farmingdale, NY, USA). Cholesterol trafficking inhibitor U18666A, 1-*O*-cholesteryl-β-D-glucose (β-cholesteryl glucose, β-GlcChol) and ammonium formate (LC-MS quality) were from Sigma-Aldrich (St Louis, MO, USA). GBA1 inhibitor cyclophellitol, and the GBA2 inhibitor N-(5-adamantane-1-yl-methoxy-pentyl)-deoxynojirimycin (AMP-DNM) and GBA3 inhibitor α-1-C-nonyl-DIc (anDIX) were synthesized at Leiden Institute of Chemistry (Leiden, The Netherlands)[23,26]. Cerezyme®, a recombinant human GBA1 was obtained from Genzyme (Genzyme Nederland, Naarden, The Netherlands). LC-MS–grade methanol, 2-propanol, water, and HPLC-grade chloroform was purchased from Biosolve. D-xylo-cyclophellitol was synthesized as described previously[18].

Mouse materials

Npc1^{-/-} mice (*Npc1*[nih]) as well as wild-type littermates (*Npc1*^{+/+}), were generated by crossing *Npc1*^{+/-} males and females. The heterozygous BALB/c Nctr-*Npc1*[m1N]/J mice (stock number 003092) were obtained from the Jackson Laboratory (Bar Harbor, USA). Mouse pups were genotyped according to published protocols[27]. Mice (± 3 weeks old) received the rodent AM-II diet (Arie Blok Diervoeders, Woerden, The Netherlands). The mice were housed at the Institute Animal Core Facility in a temperature- and humidity-controlled room with a 12-h light/dark cycle and given free access to food and water *ad libitum*. All animal protocols were approved by the Institutional Animal Welfare Committee of the Academic Medical Centre Amsterdam in the Netherlands (DBC101698). Animals were first anesthetized with a dose of Hypnorm (0.315 mg/mL phenyl citrate and 10 mg/mL fluanisone) and Dormicum (5 mg/mL midazolam) according to their weight. The given dose was 80 μL/10 g bodyweight. Animals were sacrificed by means of cervical dislocation. Organs were collected by surgery, rinsed with PBS, directly snap-frozen in liquid nitrogen and stored at -80 °C. Later, homogenates were made from the frozen material in 25 mM potassium phosphate buffer pH 6.5, supplemented with 0.1 % (v/v) Triton X-100 and protease inhibitors (4 μL of buffer per mg of tissue).

Cloning and expression of cDNAs encoding β-glucosidases GBA2 and GBA3.

Stable GBA2 expressing HEK293T cells were generated as follows. The PCR-amplified human GBA2 (GBA2 acc. nr: NM_020944.2) coding sequence (using the following oligonucleotides: sense. 5'-GGGGACAAGTTTGTACAAAAAAGCAGGCTTAACCACCATGGGGACCCAGGATCCAG-3'and antisense 5'-GGGGACCACTTTGTACAAGAAAGCTGGGTTTCACTCTGGGCTCAGGTTTG-3')

was cloned into pDNOR-221 and sub-cloned in pLenti6.3/TO/V5-DEST using the Gateway system (Invitrogen). Correctness of the construct was verified by sequencing. To produce lentiviral particles HEK293T cells were transfected with pLenti6.3-GBA2 in combination with the envelope and packaging plasmids pMD2G, pRRE and pRSV. Subsequently, culture supernatant containing viral particles was collected and used for infection of HEK293T cells. Selection by blasticidin for several weeks rendered cells stably expressing human GBA2 as determined by activity assays. For stable expression of human GBA3 in HEK293T cells, the PCR-amplified GBA3 (GBA3 acc. Nr: NM_020973.4) coding sequence (using the following oligonucleotides: sense. 5'-GAATTCG CCGCCACCATGGCTTTCCCTGCAGGATTTG-3' and antisense 5'- GCGGCCGCAGATGTG CTTCAAGGCCATTG-3') was cloned in pcDNA3.1/Zeo and transfected into HEK293T cells using FuGENE® 6 Transfection Reagent (Promega Benelux, Leiden, The Netherlands). Zeocin selection for several weeks rendered cells stably expressing human GBA3 as confirmed by activity assays.

In vitro assays with fluorogenic 4-methylumbelliferyl-β-D-glycosides.

Enzymatic activity of GBA1 was measured with 3.7 mM 4MU-β-Glc or 4MU-β-Xyl, dissolved in 150 mM McIlvaine buffer (pH 5.2 supplemented with 0.2 % (w/v) sodium taurocholate, 0.1 % (v/v) Triton X-100) and 0.1 % BSA[28]. The reaction was stopped with NaOH-glycine (pH 10.3), and fluorescence was measured with a fluorimeter LS55 (Perkin-Elmer, Beaconsfield, UK) at λ_{ex} 366 nm and λ_{ex} 445 nm. Enzymatic activity of GBA2 was measured in lysates of cells overexpressing the enzyme using the same conditions as above, but without detergents and at pH 5.8. Enzymatic activity of GBA3 was measured without detergents at pH 7.0[23].

Stimulation of GBA1 activity by the activator protein saposin C, produced recombinantly in *E. coli*[29], was monitored with 3.7 mM 4-MU-β-glucoside as substrate in 150mM McIlvaine buffer pH4.5 (150 mM McIlvaine buffer (pH 4.5) containing 0.1 % (w/v) bovine serum albumin and 0.4 mg/ml phosphatidylserine[30].

In vitro assay of transglycosylase activity with fluorescent 25-NBD-Cholesterol as acceptor.

Lysates of COS-7 cells overexpressing GBA2, and GBA3, and recombinant GBA1 were used to determine transglycosylase activity of every enzyme. The assays were performed as described earlier[10]. First, 40 μL of homogenate of cells overexpressing GBA2, or GBA3 was pre-incubated with 10 μL of 25 μM CBE in water for 20 min (samples containing diluted recombinant GBA1 were pre-incubated in the absence of CBE). To every sample 200 μL of the appropriate buffer containing 100 μM of donor (either 4MU-β-Xyl or 4MU-β-Glc) and 40 μM of acceptor (either 25-NBD-Cholesterol), was added. Transglycosylase activity of GBA2 overexpressing cells was measured in 150 mM McIlvaine buffer pH 5.8 and the assay for recombinant GBA1 was performed in 150 mM McIlvaine buffer pH 5.2 containing 0.1 % BSA, 0.1 % Triton X-100 and 0.2 % sodium taurocholate. For GBA3 the assay contained 100 mM HEPES buffer, pH 7.0. After 16 h of incubation at 37 °C, the reaction was ended by addition of chloroform/methanol (1:1, v/v) and lipids were extracted according to Bligh and Dyer[31]. Afterwards lipids were separated by thin layer chromatography on HPTLC silica gel 60 plates

(Merck, Darmstadt, Germany) using chloroform/methanol (85:15, v/v) as eluent followed by detection of NBD-labelled lipids using a Typhoon Variable Mode Imager (GE Healthcare Bio-Science Corp., Piscataway, NJ, USA)[21].

***In vitro* assay of transglycosylase activity with cholesterol as acceptor.**
Assays with natural cholesterol as acceptor were performed exactly as described in the section above and the subsequent analysis of products was performed by LC-MS/MS as described in the section below. In short, pure recombinant GBA1 (IU) was incubated at 37 ˚C with 32 µM cholesterol and 3.7 mM 4MU-β-Xyl and/or 4MU-β-Glc in 150 mM McIlvaine buffer pH 5.2 containing 0.1 % BSA, 0.1 % Triton X-100 and 0.2 % sodium taurocholate for the indicated time periods. The incubations were stopped by addition of chloroform/methanol (1:1, v/v) and lipids were extracted according to Bligh and Dyer.

Assays with cultured RAW264.7 and HEK293 cells.
Experiments with cultured RAW264.7 and HEK293 cells exposed to 3.7 mM 4MU-β-Xyl or 4MU-β-Glc in the medium, either with or without U18666A (10 µM), inducing lysosomal cholesterol accumulation, were performed as described earlier[10]. Lysosomal GBA1 was irreversibly inhibited by prior incubation of cells with 300 µM conduritol β-epoxide (CBE). Cells were harvested and lipids extracted as earlier described[10]. In HEK293 cells glucosylceramide synthase (GCS)[32] was knocked-down by the CRISPR-Cas method.

Analysis of GlyChol and XylChol by LC-MS/MS.
A Waters Xevo-TQS micro instrument was used in all experiments. The instrument consisted of a UPLC system combined with a tandem quadruple mass spectrometer as mass analyzer. Data were analyzed with Masslynx 4.1 Software (Waters, Milford MA, USA). Tuning conditions for both GlcChol and XylChol's in ES$^+$ (electrospray positive) mode are presented in Supplemental table 1. GlcChol, $^{13}C_6$-GlcChol and XylChol's were separated using a BEH C18 reversed-phase column (2.1 x 50 mm, particle size 1.7 µm; Waters), by applying an isocratic elution of mobile phases, 2-propanol:H$_2$O 90:10 (v/v) containing 10 mM ammonium formate (Eluent A) and methanol containing 10 mM ammonium formate (Eluent B). The column temperature and the temperature of the auto sampler were kept at 23 °C and 10 °C respectively during the run. The flow rate was 0.25 mL/min. Volume of injection was 10 µL.

For the identification of a new compound of interest, the extracted sample was dried and dissolved in 100 µL of Eluent B. The sample was introduced in the mass spectrometer using LC-MS (0 to 5.5 min to the detector). MS parents scan and daughters scan were performed (figure 2). As for GlcChol[10], the most abundant species of XylChol are ammonium adducts, [M+NH$_4$]$^+$ and the product ion 369.3 represents the cholesterol part of the molecule after loss of the xylose moiety. Ammonium adducts of XylChol, Xyl$_2$Chol and Xyl$_3$Chol show the transitions 536.5>369.3, 668.5>369.3 and 800.5>369.3 respectively. The transitions for GlcChol are 566.5>369.3 and for $^{13}C_6$-GlcChol 572.5>369.3.

For Multiple Reaction Monitoring (MRM) the UPLC program was applied during 5.5 minutes consisting of 10 % eluent A and 90 % eluent B. The divert valve of the mass spectrometer was programmed to discard the UPLC effluent before (0 to 0.8 min) and after (4.5 to 5.5 min) the elution of the analytes to prevent system contamination. The retention time of both GlcChol and the internal standard $^{13}C_6$-GlcChol was 1.36 min. XylChol's were generated *in vitro* by incubation of GBA1 with cholesterol. The retention time of XylChol, Xyl$_2$Chol and Xyl$_3$Chol was 1.71 min, 1.49 min and 1.40 min respectively (Supplemental figure 1).

LC-MS/MS quantitation of GlcChol and XylChol's produced *in vitro*.
Following incubation of GBA1 and cholesterol with either 4MU-β-Glc or 4MU-β-Xyl, from 180 µL of sample, to which 12.5 pmol of $^{13}C_6$-GlcChol in methanol was added, lipids were extracted according to the Bligh and Dyer method by addition of methanol, chloroform and water (1:1:0.9, v/v/v). The lower phase was taken to dryness in an Eppendorf concentrator. Isolated lipids were purified by water/butanol extraction (1:1, v/v). The upper phase (butanol phase) was taken to the dryness. The residue is dissolved in 100 µL eluent B, sonicated in bath sonicator and samples were analyzed by LC-MS.

LC-MS/MS quantitation of GlcChol and XylChol's in cultured cells.
Cells were homogenized in water by sonication on ice. The protein concentration was around 1 mg/ml. Prior to extraction, 12.5 pmol of ^{13}C-labelled GlcChol in methanol (used as an internal standard) was added to 100 µL of homogenate. After protein precipitation, the supernatant was further treated as described above.

Protein determination.
Protein was analysed with the Pierce BCA Protein Assay kit (Thermo Scientific). Absorbance was measured in EL808 Ultra Microplate Reader (BIO-TEK Instruments Inc.) at 562 nm.

Statistical Analysis.
Values in figures are presented as a mean ± S.D. Data were analyzed by unpaired Student's t-test. *P* values < 0.05 were considered significant. * *P* < 0.05, ** *P* < 0.01 and *** *P* < 0.001.

References

1. Rennie, E. A. & Scheller, H. V. Xylan biosynthesis. *Curr. Opin. Biotechnol.* **26,** 100–7 (2014).
2. Esko, J. D., Kimata, K. & Lindahl, U. *Proteoglycans and Sulfated Glycosaminoglycans*. *Essentials of Glycobiology* (2009).
3. Moriarity, J. L. *et al.* UDP-glucuronate decarboxylase, a key enzyme in proteoglycan synthesis: cloning, characterization, and localization. *J. Biol. Chem.* **277,** 16968–75 (2002).

7
7

4. Fisher, D. & Kent, P. W. Rat liver beta-xylosidase, a lysosomal membrane enzyme. *Biochem. J.* **115,** 50P–51P (1969).
5. Patel, V. & Tappel, A. L. Identity of beta-glucosidase and beta-xylosidase activities in rat liver lysosomes. *Biochim. Biophys. Acta* **191,** 86–94 (1969).
6. van Weely, S., Brandsma, M., Strijland, a, Tager, J. M. & Aerts, J. M. Demonstration of the existence of a second, non-lysosomal glucocerebrosidase that is not deficient in Gaucher disease. *Biochim. Biophys. Acta* **1181,** 55–62 (1993).
7. Beutler, E. & Grabowski, G. A. in *The Metabolic and Molecular Bases of Inherited Disease. 7th ed. New York, NY: McGraw-Hill;* (ed. McGraw-Hill) 2641–2670 (1995).
8. Ferraz, M. J. *et al.* Gaucher disease and Fabry disease: New markers and insights in pathophysiology for two distinct glycosphingolipidoses. *Biochim. Biophys. Acta - Mol. Cell Biol. Lipids* **1841,** 811–825 (2014).
9. Akiyama, H., Kobayashi, S., Hirabayashi, Y. & Murakami-Murofushi, K. Cholesterol glucosylation is catalyzed by transglucosylation reaction of β-glucosidase 1. *Biochem. Biophys. Res. Commun.* **441,** 838–43 (2013).
10. Marques, A. R. A. *et al.* Glucosylated cholesterol in mammalian cells and tissues: formation and degradation by multiple cellular β-glucosidases. *J. Lipid Res.* **57,** 451–463 (2016).
11. Vanderjagt, D. J., Fry, D. E. & Glew, R. H. Human glucocerebrosidase catalyses transglucosylation between glucocerebroside and retinol. *Biochem. J.* 309–15 (1994).
12. Vanier, M. T. Complex lipid trafficking in Niemann-Pick disease type C. *J. Inherit. Metab. Dis.* **38,** 187–99 (2015).
13. Yildiz, Y. *et al.* Mutation of β-glucosidase 2 causes glycolipid storage disease and impaired male fertility. **116,** (2006).
14. Boot, R. G. *et al.* Identification of the non-lysosomal glucosylceramidase as beta-glucosidase 2. *J. Biol. Chem.* **282,** 1305–12 (2007).
15. Körschen, H. G. *et al.* The non-lysosomal β-glucosidase GBA2 is a non-integral membrane-associated protein at the endoplasmic reticulum (ER) and Golgi. *J. Biol. Chem.* **288,** 3381–93 (2013).
16. Kallemeijn, W. W. *et al.* A Sensitive Gel-based Method Combining Distinct Cyclophellitol-based Probes for the Identification of Acid/Base Residues in Human Retaining -Glucosidases. *J. Biol. Chem.* **289,** 35351–35362 (2014).
17. Witte, M. D. *et al.* Ultrasensitive in situ visualization of active glucocerebrosidase molecules. *Nat. Chem. Biol.* **6,** 907–913 (2010).
18. Schröder, S. P. *et al.* A Divergent Synthesis of l - arabino - and d -xylo -Configured Cyclophellitol Epoxides and Aziridines. *European J. Org. Chem.* **2016,** 4787–4794 (2016).
19. Aerts, G. M., Van Opstal, O. & De Bruyne, C. K. β-d-glucosidase-catalysed transfer of the glycosyl group from aryl β-d-gluco- and β-d-xylo-pyranosides to phenols. *Carbohydr. Res.* **100,** 221–233 (1982).
20. Kay, C. D., Mazza, G., Holub, B. J. & Wang, J. Anthocyanin metabolites in human urine and serum. *Br. J. Nutr.* **91,** 933–42 (2004).
21. van Weely, S., Brandsma, M., Strijland, A., Tager, J. M. & Aerts, J. M. Demonstration of the existence of a second, non-lysosomal glucocerebrosidase that is not deficient in Gaucher disease. *Biochim. Biophys. Acta* **1181,** 55–62 (1993).
22. Mackenzie, P. I. *et al.* Identification of UDP glycosyltransferase 3A1 as a UDP N-acetylglucosaminyltransferase. *J. Biol. Chem.* **283,** 36205–10 (2008).
23. Dekker, N. *et al.* The cytosolic β-glucosidase GBA3 does not influence type 1 Gaucher disease manifestation. *Blood Cells, Mol. Dis.* **46,** 19–26 (2011).
24. Westbroek, W. *et al.* A new glucocerebrosidase-deficient neuronal cell model provides a tool to probe pathophysiology and therapeutics for Gaucher disease. *Dis. Model. Mech.* **9,** 769–78 (2016).
25. Nair, S. *et al.* Clonal Immunoglobulin against Lysolipids in the Origin of Myeloma. *N. Engl. J. Med.* **374,** 555–561 (2016).
26. Overkleeft, H. S. *et al.* Generation of specific deoxynojirimycin-type inhibitors of the non-lysosomal glucosylceramidase. *J. Biol. Chem.* **273,** 26522–7 (1998).
27. Marques, A. R. A. *et al.* Reducing GBA2 Activity Ameliorates Neuropathology in Niemann-Pick Type C Mice. *PLoS One* **10,** e0135889 (2015).
28. Aerts, J. M. *et al.* The occurrence of two immunologically distinguishable beta-glucocerebrosidases in human spleen. *Eur. J. Biochem.* **150,** 565–74 (1985).
29. Ahn, V. E., Leyko, P., Alattia, J.-R., Chen, L. & Privé, G. G. Crystal structures of saposins A and C. *Protein Sci.* **15,** 1849–57 (2006).
30. Aerts, J. M. *et al.* Conditions affecting the activity of glucocerebrosidase purified from spleens of control subjects and patients with type 1 Gaucher disease. *Biochim. Biophys. Acta* **1041,** 55–63 (1990).
31. Bligh, E. G. & Dyer, W. J. A RAPID METHOD OF TOTAL LIPID EXTRACTION AND PURIFICATION. *Can. J. Biochem. Physiol.* **37,** 911–917 (1959).
32. Ichikawa, S., Sakiyama, H., Suzuki, G., Hidari, K. I. & Hirabayashi, Y. Expression cloning of a cDNA for human ceramide glucosyltransferase that catalyzes the first glycosylation step of glycosphingolipid synthesis. *Proc. Natl. Acad. Sci. U. S. A.* **93,** 12654 (1996).

Supplemental data
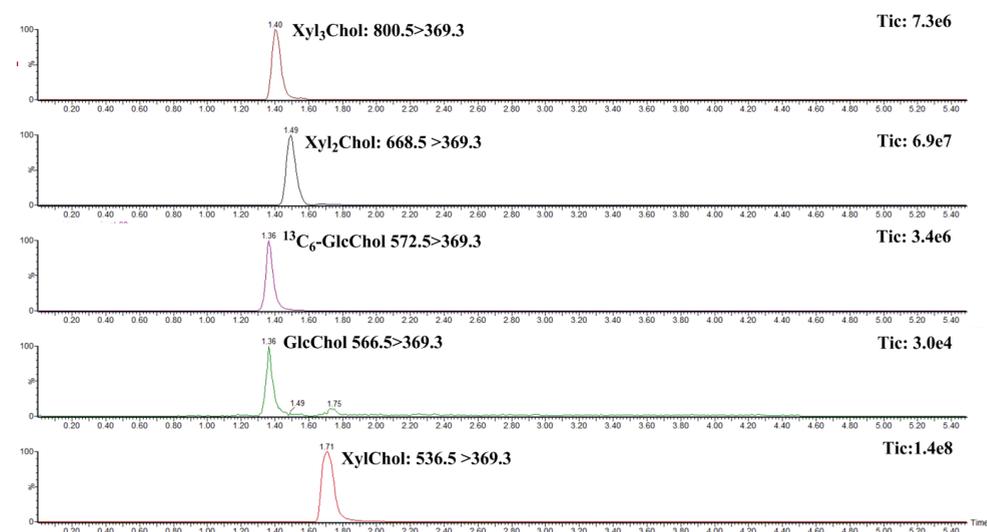
Supplemental Figure 1. Chromatogram of XylChol, Xyl₂Chol, Xyl₃Chol, GlcChol and ¹³C₆-GlcChol.

Supplemental Table 1. MS/MS instrument parameters.

Capillary voltage	**3.50 KV**
Cone voltage	20 V
Source temperature	150 °C
Desolvation temperature	450 °C
Cone gas	50 L/h
Desolvation gas	950 L/h
Collision voltage	15 V
Type	Multiple reaction monitoring
Ion mode	ES$^+$ (electrospray positive)
Dwell time	0.1 s
Interchannel delay	0.005 s
Interscan delay	0.005 s
Transitions:	**RT (min.):**
GlcChol	1.36
$^{13}C_6$-GlcChol	1.36
XylChol	1.71
Xyl$_2$Chol	1.49
tXyl$_3$Chol	1.40
Fit weight	None
Smooth method	Mean
Smooth width	2

Supplemental Table 2. Formation of hybrid GlcXylChol following incubation of GBA1 with 1:1 mixture of 4MU-β-Xyl and 4MU-β-Glc.

MRM transitions	4MU-Xyl (3h) 4MU-Glc (1h)	pmol/mL
536.5 > 369.3	XylChol	631.56
566.5> 369.3	GlcChol	293.20
668.5> 369.3	Xyl2Chol	76.34
698.5> 369.3	XylGlcChol	10.58
800.5> 369.3	Xyl3Chol	3.34
830.5> 369.3	Xyl2GlcChol	0.42

7

Discussion

Discussion

GBA in health and disease.

Glucocerebrosidase (GBA: EC 3.2.1.45) is the lysosomal β-glucosidase degrading glucosylceramide (GlcCer) to ceramide, an essential step in the cellular recycling of glycosphingolipids[1,2]. The enzyme, a 495 AA glycoprotein with 4 N-linked glycans, employs for catalysis a double displacement mechanism with glutamate 340 as nucleophile and glutamate 325 as acid/base residue[3]. GBA (also named GBA1), unlike other soluble acid hydrolases, is not sorted to lysosomes via mannose-6-phosphate receptors, but through binding to the lysosomal integral membrane protein II (LIMP-2)[1] (figure 1). Deficiency of GBA forms the molecular basis of Gaucher disease (GD), a recessively inherited lysosomal storage disorder[2]. GD patients have two mutated GBA alleles encoding mutant forms of GBA. Most of these mutations encode single amino acid substitutions that may impair folding of the enzyme in the endoplasmic reticulum and/or stability and catalytic activity in lysosomes[2]. A significantly reduced GBA activity causes ongoing accumulation of GlcCer in storage deposits inside lysosomes, a phenomenon that particularly occurs in macrophages of GD patients[2]. Most cell types of GD patients manage to limit lysosomal glucosylceramide accumulation through its conversion to glucosylsphingosine, the sphingoid base that may leave lysosomes and even cells[1].

Chronic supplementation of the lysosomes of macrophages with normal (recombinant produced) GBA forms the basis for the registered enzyme replacement therapy (ERT) of GD[4–6]. This treatment, employing enzyme with mannose-terminated N-linked glycans favoring uptake by macrophages, is remarkably effective in non-neuronopathic type 1 GD patients: it results in prominent reversal and prevention of hepatomegaly, splenomegaly and hematological abnormalities and thus markedly improves the quality of life of patients[6]. ERT is now worldwide applied for over 25 years in type 1 GD patients with a non-neuropathic disease course. The long-term efficacy of ERT has meanwhile been thoroughly analyzed[7]. The various recombinant enzyme preparations nowadays used for ERT are relatively expensive and largely determine the cost of the treatment, usually ranging from €100.000 to 300.000 per year for an adult patient[8]. Individualized dosing regimens are increasingly used to reach optimal clinical response at a minimum of costs[5]. Biomarkers, ranging from Gaucher cell-derived proteins (chitotriosidase, CCL18, soluble gp-NMB) to lipids (glucosylsphingosine), are increasingly used to monitor response to ERT and optimize treatment regimens[1,9]. Present ERTs with macrophage-targeted recombinant enzymes unfortunately do not prevent neurological manifestations in the more severely affected (type 2 and 3) GD patients. ERT neither offers full protection against skeletal disease, pulmonary hypertension, gammopathies and related leukemia's and Parkinson's disease[7].

The considerable costs of the present ERTs and moreover the clinical limitations of the treatment motivate ongoing investigations on additional therapies for GD (table 1), including the research described in this thesis that focused on elucidating factors modulating lysosomal GBA (see figure 2). The identification of GBA deficiency as major risk factor for developing α-synucleinopathies has boosted further the research interest in GBA and its therapeutic modulation[10].

Modulating lysosomal GBA.

The initial focus of research described in this thesis originates from the observation in the eighties that exposure of cells to leupeptin, a serine and cysteine protease inhibitor[11], causes an increase in GBA. Compared to other lysosomal hydrolases, GBA survives relatively short in lysosomes due to fast proteolytic degradation. This is even more pronounced for some mutant forms of GBA occurring in GD patients, for example N370S GBA that is present in the vast majority of Caucasian type 1 GD patients and shows slightly abnormal kinetic parameters[11–15]. Like wildtype GBA, the mutant N370S enzyme folds in the endoplasmic reticulum and subsequently ends up in lysosomes (figure 1). However, inside lysosomes N370S GBA undergoes abnormal fast proteolytic degradation, a process that can be inhibited by leupeptin[11]. Thus, pharmacological augmentation of mutant GBA's like the common N370S enzyme through inhibition of their lysosomal proteolytic degradation offers in theory a novel therapeutic avenue to treat specific GD patients (figure 2).

At the start of this thesis research (chapter 1), the old finding that cellular GBA is significantly increased by leupeptin was first re-capitulated. Subsequently, it was established that stabilization of the enzyme can also be induced by E64 (IUPAC name: (1S,2S)-2-(((S)-1-((4-Guanidinobutyl)amino)-4-methyl-1-oxopentan-2-yl)carbamoyl)cyclopropanecarboxylic acid), an irreversible inhibitor of cysteine proteases, but not by AEBSF (IUPAC name: 4-(2-Aminoethyl)benzene sulfonyl fluoride), an inhibitor of serine proteases (data not shown). E64 has been earlier used by Greenbaum et al. as scaffold of an activity based probe (ABP) named DCG-04[16]. This ABP when tagged with a fluorescent BODIPY group (DCG-04 BODIPY) covalently binds to the cathepsins C, S, F, H, K, V, B and L, each proteases with a catalytic mechanism involving a nucleophilic cysteine thiol in a catalytic triad or diad[17]. Labeling of GBA with a specific BODIPY tagged cyclophellitol-epoxide ABP[18] and labeling of proteases with DCG-04 BODIPY in combination with electron microscopy (correlative light and electron microscopy imaging) confirmed co- localization in lysosome structures (DM van Elsland, unpublished data). It was next established that BODIPY DCG04, like leupeptin and E64, stabilizes GBA in cultured cells. Exposure of cultured lymphoblasts from N370S GBA carrying GD patients was found to reduce their glucosylsphingosine content, a sign of functional correction of lysosomal GlcCer metabolism[1,19]. The cathepsins C, S, F, H, K, V, B and L were all candidates to mediate the lysosomal degradation of GBA. It was therefore next investigated which of the cathepsins mediate the breakdown of GBA. For this purpose, specific cathepsins were deleted by shRNA and/or CRISPR-CAS technology (chapter 1). Moreover, in vitro digestion of recombinant GBA by commercially obtained recombinant cathepsins B, F, H, L and S was examined. The combined findings led to the conclusion that not a single cathepsin is entirely responsible for lysosomal degradation of GBA. Apparently there exists redundancy among the examined cysteine cathepsins in degrading GBA, as illustrated by the observed

compensation of each' s absence. In other words, to slow down intra-lysosomal proteolytic turnover of GBA multiple cathepsins will need to be concomitantly inhibited. Such broad inhibition likely results in major impairment of protein turnover in lysosomes in general and a chronic intervention along this line therefore offers no realistic therapy.

Since a therapy based on specific inhibition of the proteolytic degradation of GBA inside lysosomes seems elusive, attention was next focused to the structural stability of the enzyme inside lysosomes (figure 2). Key questions to be addressed in this connection are which factors stabilize the fold of GBA in lysosomes and does re-folding occur? The structural stability of recombinantly produced GBA was first examined (chapter 2). In the experiments use was made of known reversible inhibitors as well as cyclophellitol-based ABPs that covalently bind to the catalytic nucleophile glutamate 340[3]. It was found that occupancy of the catalytic pocket with inhibitors stabilizes the fold of the enzyme. The melting temperature (T_m) of GBA determined by tryptophan fluorescence and circular dichroism is increased by the presence of inhibitors interacting with the catalytic pocket. The effect is smallest for hydrophilic reversible inhibitors like isofagomine, more potent with the semi-reversible 2-deoxy-2-fluoro-β-d-glucopyranosyl-2-deoxy-2-fluoro-β-d-glucopyranosyl-N-phenyltrifluoroacetimidate and highest with irreversible cyclophellitol-based inhibitors tagged with a hydrophobic BODIPY moiety[18]. Similar, GBA proved more resistant against trypsin digestion upon prior incubation with irreversible inhibitors, again particularly with the amphiphilic cyclophellitol-type ABPs. In summary, it is quite apparent that structural stability of GBA is remarkably improved by the occupancy of the catalytic pocket with an amphiphilic inhibitor. Consistent with this conclusion are the observations that an ABP pre-labeled GBA after uptake by cultured macrophages is remarkably protected against proteolytic degradation and the same holds for pre-labeled enzyme following infusion in mice (chapter 2,[20]).

The beneficial outcome of occupancy of the catalytic pocket with inhibitors regarding structural stability of GBA and its resistance against proteolytic breakdown are of great interest. It might be speculated that the physiological substrate glucosylceramide exerts a similar protective effect. In such case, the lack of substrate would promote the degradation of "idle" enzyme. Another implication would be that lysosomes will tend to always contain a small residual amount of glucosylceramide.
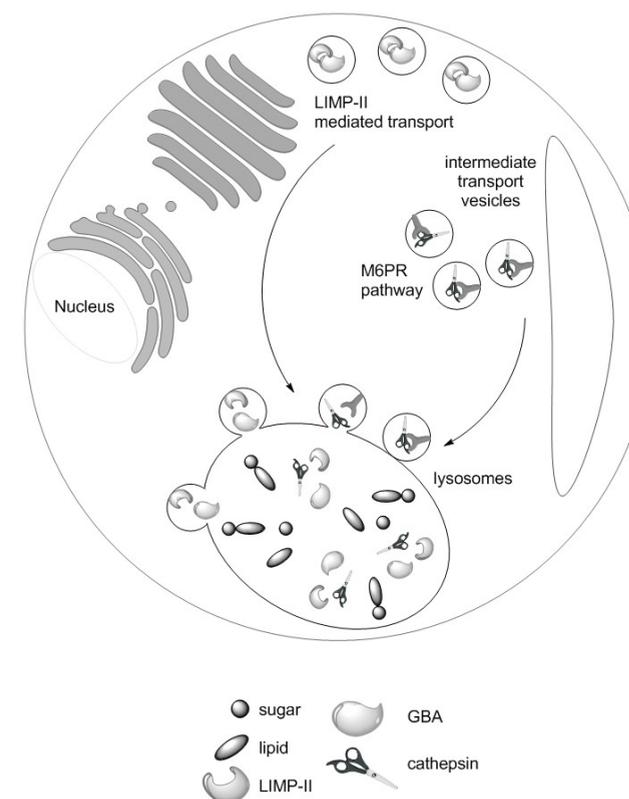

Figure 1. Cellular pathways of GBA via LIMP-2 associated transport and other lysosomal proteins such as cathepsins via M6P-mediated transport. LIMP-II: LIMP-2.

Catalysis by GBA.

The catalytic pocket of GBA, in particular the glycon binding domain, can nowadays be probed with cyclophellitol-type ABPs designed by researchers at the Leiden Institute of Chemistry at Leiden University and Academic Medical Center of the University of Amsterdam[18,21]. In sharp contrast, insight in the aglycon (lipid) binding domain of the enzyme is at present still very limited which seriously impairs full understanding of the actions of the enzyme. The relevance of the lipid moiety binding (aglycon) domain is highlighted by the recent realization that GBA can act as transglycosylase[22]. When exposed to a high concentration of cholesterol, GBA may transfer the glucose from a β-glucoside substrate to the sterol and thus generate glucosyl-β-cholesterol (GlcChol)[22]. The physiological relevance of this reaction is illustrated by the accumulation of GlcChol in patients suffering from Niemann-Pick type C disease (NPC). This lysosomal storage disorder is due to an inherited deficiency in egress of cholesterol from lysosomes and leads to dramatic lysosomal sterol accumulation. U18666A-induced lysosomal cholesterol accumulation also promotes GlcChol generation in cultured cells[22]. More recently it was noted that GBA, *in vitro* as well as in cultured cells, when exposed to β-xyloside

substrates acts as β-xylosidase and transxylosylase generating xylosylated sterols (chapter 4). The physiological relevance of these activities of GBA towards β-xylosides still needs to be established. In particular, it will be of interest to study the natural occurrence of xylosylated sphingolipids and sterols.

The observed formation of GlcChol by GBA suggests that the enzyme has a high affinity binding site for sterols in its catalytic region. To further increase insight in this matter, a new procedure to probe the catalytic pocket of GBA with a lipid substrate was developed (chapter 3). A mimic of glucosylceramide equipped with an internal diazirine and terminal alkyne in its fatty acyl moiety, so-called pacGlcCer, is used for this[23]. Following incubation of GBA with pacGlcCer, the diazirine in the lipid can be UV cross-linked to closely neighboring amine groups of the protein. Hereafter, a fluorophore can be linked to the alkyne by click chemistry allowing the detection of lipid-labeled protein following SDS-polyacrylamide gel electrophoresis. Using this method, it was observed that saturated labeling of enzyme with pacGlcCer already occurs at low lipid concentration, pointing to a high affinity interaction of pacGlcCer with GBA. This is not surprising since pacGlcCer proves to be an excellent substrate for GBA. The binding of pacGlcCer to GBA shows similar pH dependency as the enzymatic activity, again suggesting that the lipid preferentially binds in the catalytic pocket like the natural glucosylceramide substrate. Next it was noted that compounds binding in the glycon binding site of GBA like cyclophellitols prohibit pacGlcCer labeling of the enzyme. This further confirms that pacGlcCer is truly bound in the catalytic pocket. Of interest is the finding that the presence of cholesterol, an acceptor in transglycosylation, prohibits already at low concentration the labeling of GBA with pacGlcCer. Thus, the high affinity cholesterol binding site must be part of the catalytic pocket. In principle, the new method, in conjunction with the ABPs, can be used to probe which compounds interact with high affinity with the catalytic pocket of GBA, both the glycon and aglycon binding domain.

The novel findings presented in Chapters 3 and 4 illustrate that GBA is catalytically far more diverse than hitherto considered. The physiological relevance of the noted transglycosylase and β-xylosidase capacity of GBA warrants further research. In the first place, the impact of Gaucher disease-associated mutations in GBA on various catalytic activities needs to be investigated. Of further interest in this connection is the occurrence of active GBA in the extracellular layer of the skin, the stratum corneum[24]. This membrane layer is very rich in glucosylceramide and cholesterol and it is theoretically conceivable that GBA might locally generate GlcChol. Another consideration worthwhile to explore further is the potential use of β-xylosides as stabilizing chaperones for GBA. In principle, carefully selected β-xylosides might also stabilize GBA in its structure and render protection against proteolytic breakdown. Such β-xylosides are likely relative poor substrates compared to β-glucosides and therefore might act as long-lived stabilizers inside lysosomes.

Proteins influencing GBA inside lysosomes.

The sorting of newly formed GBA to lysosomes has been enigmatic for a long time. It was soon clear that GBA acquires no mannose-6-phosphate moieties in its glycans and therefore is not transported to lysosomes through binding to mannose-6-phosphate specific receptors[1,25]. A major breakthrough was the discovery that the lysosomal integral membrane protein 2 (LIMP-2) following binding of GBA in the ER, transports the enzyme to lysosomes[26,27,28]. Although low pH is reported to promote dissociation of GBA and LIMP-2, it seems likely that interaction of the two proteins still (transiently) occurs in lysosomes[10]. Indeed, the experiments described in Chapter 5 provide evidence that LIMP-2 protects the enzyme against proteolytic degradation in lysosomes. HEK293T cells expressing mannose receptors were found to endocytose well *Cerezyme* (mannose-terminated recombinant human GBA). The half-life of recombinant GBA was considerably shorter in cells lacking LIMP-2 as the result of faster proteolytic degradation. The stabilizing effect of the interaction of GBA with LIMP-2 in lysosomes might be of great importance regarding ERT. It seems conceivable that LIMP-2 becomes "rate limiting" during ERT with high doses of therapeutic enzyme. Administration of very high doses of *Cerezyme* might result in lysosomal enzyme concentrations that exceed the capacity of LIMP-2 to stabilize it. In view of this consideration of the recent finding that a LIMP-2 helix 5-derived peptide is able to activate GBA is highly relevant[29]. Co-administration of a stabilizing LIMP-2 fragment and recombinant enzyme might be considered for ERT. In addition, the LIMP-2 peptide might be able to increase endogenous GBA capacity in those GD patients with residual lysosomal enzyme.

Saposin C (SapC) is another protein known to interact with GBA inside lysosomes[30]. SapC is formed by proteolytic cleavage from the large precursor prosaposin[31,32]. It is an 80 amino acid peptide that binds in nanomolar range to GBA and thus stimulates the enzyme in activity towards natural lipid substrate GlcCer as well as artificial (water-soluble) substrates, β-glucosides and β-xylosides alike (chapter 4)[33–36]. The interaction of SapC with GBA is strongly promoted by the presence of negatively charged phospholipids, in particular the lysosomal phospholipid BMP (bis(monoacylglycero)phosphate)[36,37]. The physiological relevance of the activation of GBA by SapC is illustrated by the finding that deficiency of SapC causes GD-like pathology, including the presence of Gaucher cells and related markers[38–40]. Over the years several hypotheses have been put forward regarding the physiological action of SapC. Initially a role for SapC in facilitating access of lipid substrate to the pocket of GBA was envisioned as its primary mode of action[41]. According to this mechanism, SapC would solubilize GlcCer from membranes allowing its hydrolysis by GBA to take place in an aqueous environment [42,43]. Evidence for a direct interaction of SapC with membranes has indeed been presented. SapC was shown to destabilize membranes and promote fusion[44–46]. Binding of SapC to GBA affects the enzyme as such. Clearly, SapC binding influences the catalytic pocket of GBA, as reflected by increased catalytic activity and changed substrate affinity. It remains unclear whether SapC also promotes structural stability of GBA. SapC has been proposed by Sun *et al*. to protect GBA from proteolytic degradation by facilitating association of GBA with membranes[47]. Moreover, it was speculated that specific mutations in GBA reduce the interaction with SapC and thus cause a decreased stability of the enzyme[47]. In view of these observations, the shortened lysosomal half-life of N370S GBA might partly be caused by diminished stabilization by SapC. The residues 48-122 of GBA appear to be involved in the activation of enzyme by SapC as

established by effects on enzymatic activity[48]. A docking model of GBA-SapC interactions generated by Atrian *et al.* suggests that the SapC binding sites in GBA are the TIM barrel-helixes 6 and 7 and the Ig-like domain[49]. Further studies, in particular co-crystallization of GBA and SapC, are required to precisely establish the interaction between the two proteins. Detailed insight in this matter might offer new clues on factors influencing structural stability of GBA and even find therapeutic application.

The relatively recent realization that defective GBA in GD patients and even carriers constitutes a major risk factor for developing alpha-synucleinopathies such as Parkinson's disease (PD) and Lewy-Body dementia has greatly raised the interest in the interplay between α-synuclein (α-Syn) and GBA[50,51]. The underlying cause for the remarkable association between GBA defects and PD risk is still enigmatic. There are conflicting reports on the relationship between the severity of the mutation in GBA and the risk for developing PD, although recently it has been proposed that in symptomatic GBA-deficient PD patients the severity of cognitive decline is influenced by the severity of the GBA mutation[52–54]. α-Syn abnormalities in GBA-deficient PD patients are not restricted to the brain. In such patients higher plasma oligomeric α-Syn levels were observed compared to controls as well as other PD patients[55]. Michelakakis and co-workers observed increased dimerization of α-Syn in the red blood cell membrane of GD patients[56,57].

Numerous reports on direct and indirect interaction of α-Syn and GBA are published in recent time. A clear picture has still not emerged. In the first place, some of the literature points to a direct inactivation of GBA by α-Syn[51,58]. For example, α-Syn was reported to interact with GBA via its C-terminal region in a pH-dependent way[51]. This complex did not form at neutral pH and N370S GBA presented decreased affinity for α-Syn[51]. In a more recent study membrane-bound α-Syn was shown to interact with GBA and inhibit enzymatic activity in sub-micromolar range both via substrate accessibility and turnover[58]. It was proposed that α-Syn could influence GBA-membrane interaction and/or induce conformational change influencing stability[58,60]. Of interest, it was reported that SapC protects GBA against inhibition by α-Syn[61]. Since SapC and α-Syn both have acidic regions it was suggested that they have overlapping binding sites on GBA[61]. Yap *et al.* recently proposed that α-Syn binding displaces GBA from the membrane by which it perhaps hampers access to substrate and disturbs the active site[60]. On the other hand, GBA significantly changes membrane-bound α-Syn by shifting helical residues away from the bilayer. It was speculated that in this manner lysosomal α-Syn breakdown is regulated[60]. Again, it still needs to be more precisely established how α-Syn binds to GBA and whether this interaction affects the structural stability of the enzyme.
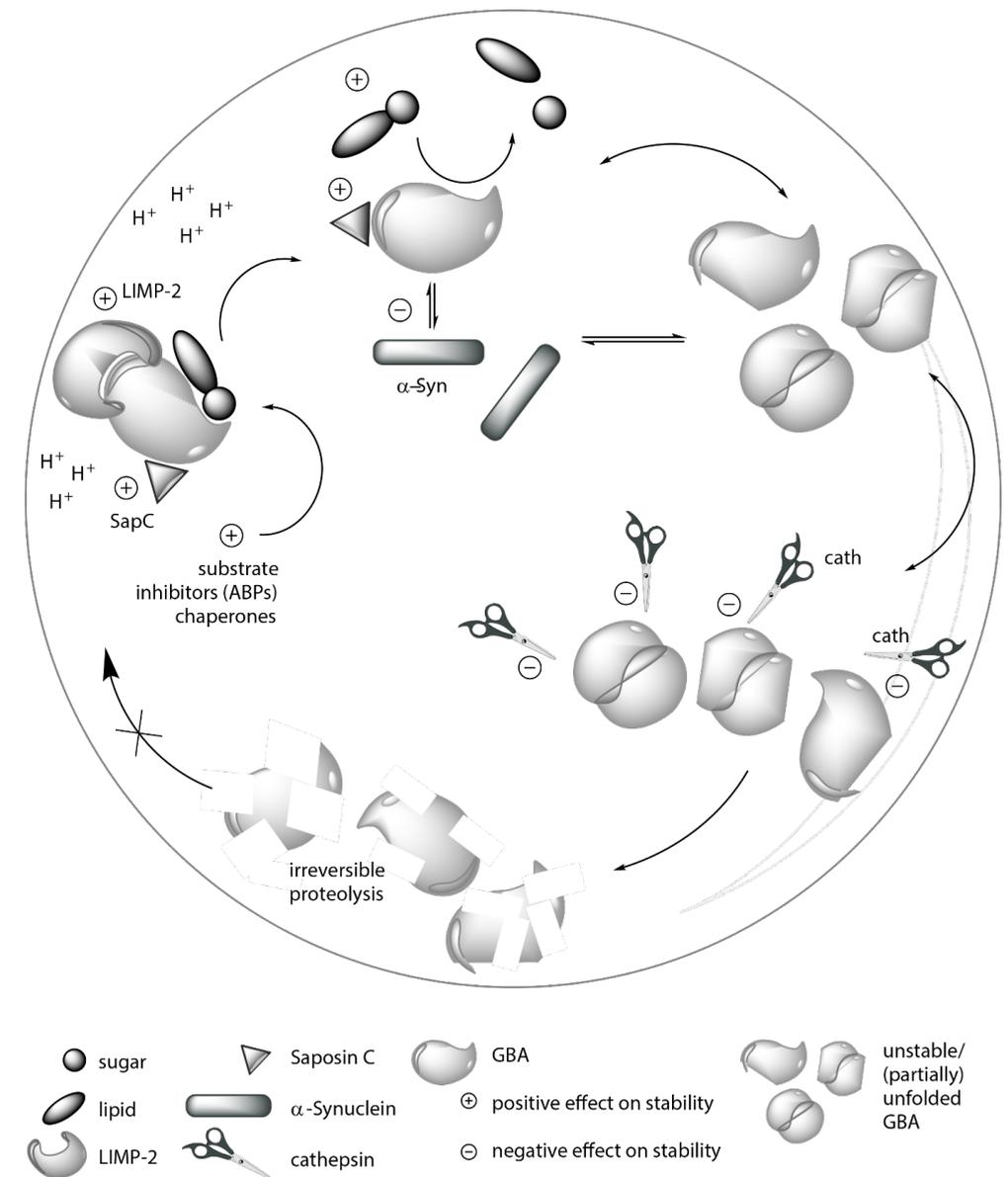
Figure 2. Positive and negative influences on GBA during its (lysosomal) life cycle.

In addition to a direct detrimental binding of GBA and α-Syn, functional deficiency of GBA has been claimed to cause lysosomal α-Syn accumulation and aggregation[50]. GlcCer was demonstrated to directly affect amyloid formation by stabilization of soluble α-Syn oligomeric intermediates[50]. Furthermore, elevated α-Syn was shown by Mazulli *et al.* to impair the intracellular transport of newly formed GBA to lysosomes and thus reduce the capacity of

lysosomes to degrade GlcCer[50]. Such mechanism would create a forward loop, resulting in ongoing α-Syn accumulation.

Importantly, recent studies indicate that augmentation of lysosomal GBA in the CNS of mice by adeno-associated virus-mediated expression of enzyme has positive effects on α-Syn accumulation and aggregation[62,63]. Of interest in this connection is also the recent demonstration that LIMP-2 may ameliorate α-Syn accumulation[64]. Deficiency of LIMP-2 in mice triggers accumulation of soluble as well as insoluble oligomeric α-Syn species in brain, probably as the result of lysosomal GBA deficiency and buildup of GlcCer or related metabolite[64]. The cell permeable LIMP-2 helix 5-derived peptide that promotes GBA capacity in lysosomes was found to diminish α-Syn in cultured cells[29].

Translation of fundamental knowledge to therapy.

As summarized in Table 1, multiple approaches to increase GBA are presently used or envisioned as therapeutic intervention for GD patients and individuals with GBA deficiency developing Parkinson's disease.

The seminal studies by Brady and co-workers identified supplementation of lysosomes of tissue macrophages with GBA as therapy approach for non-neuronopathic type 1 GD[65–67]. Indeed, ERT with macrophage-targeted, mannose-terminal recombinant GBA is proven efficacious for type 1 GD patients. Chronic bi-weekly enzyme infusion corrects and prevents organomegaly and hematological abnormalities in these patients[5]. New developments regarding ERT concern the use of different, more economic and saver production platforms for recombinant enzyme, for example plants[68]. Attention is also focused by pharmaceutical industry to additives increasing stability of therapeutic recombinant enzyme, to generation of fusion proteins able to cross the blood-brain barrier and to production of alternatively targeted recombinant GBAs to be used in combination with the present macrophage-targeted recombinant enzyme preparations.

An effective alternative treatment for type 1 GD is offered by substrate reduction therapy (SRT)[69–71]. This treatment modality makes use of oral administration of inhibitors of glucosylceramide synthase (GCS) and thus attempts to lower the intralysosomal flux of GlcCer. The first agent applied, and registered for 15 years, was N-butyl-deoxynojirimycin (*Miglustat; Zavesca*, Actelion Corp.)[69]. *Miglustat* is no potent and specific inhibitor of GCS, but nevertheless it was found to stabilize disease in mild type 1 GD patients[69]. More recently, *Eliglustat* (N-[(1R,2R)-1-(2,3-dihydro-1,4-benzodioxin-6-yl)-1-hydroxy-3-pyrrolidin-1-ylpropan-2-yl]octanamide; *Cerdelga,* Genzyme Corp.) is also registered as SRT drug for type 1 GD. Clinical and biochemical responses to *Eliglustat* are on a par with high dose ERT[72–74]. Unfortunately, *Eliglustat* is not brain permeable and offers no prevention against neuropathology in severely affected type 2 and 3 GD patients. Moreover, *Eliglustat* is subject to CYP 2D6 metabolism, complicating its application in some patients due to aberrant metabolism of the drug. Considerable room remains for improvement of GCS inhibitors. More potent and brain permeable inhibitors are presently under investigation[75,76].

Lately much of the attention regarding therapeutic agents goes out to small molecule chaperones of GBA which can penetrate the blood-brain barrier and complement ERT. These should assist folding and improve transport of mutant GBAs to lysosomes. A very large number of structures has been proposed as candidate chaperones for GBA, for recent comprehensive reviews on the topic see references[77,78]. A major fraction of the studied chaperones are active-site specific iminosugars, either unmodified such as isofagomine (IFG), or *N*-alkylated such as NN-DNJ and NB-DNJ[77,78]. *N*-(*n*-nonyl)deoxynojirimycin (NN-DNJ) was the first molecule proposed as chaperone for GBA, in particular N370S GBA[79]. *Miglustat* (NB-DNJ) was next proposed to increase lysosomal activity of N370S GBA[80]. The potent competitive inhibitor IFG was also shown to augment mutant GBA activity[81,82]. However, a clinical trial did not substantiate a beneficial action of isofagomine in GD patients and further drug development was aborted by the pharmaceutical company involved (Amicus Corp.)[83]. Other classes are *C*-alkylated iminosugars comprising 1-azasugars, calystegines and DIX, amphiphilic bicyclic sp[2]-iminosugars comprising sp[2]-iminosugars related to the natural reducing alkaloid nojirimycin (NJ), such as 5N,6O-(N0-octyliminomethylidene) nojirimycin (39, NOI-NJ) or its 6-thio (40,6S-NOI-NJ) and 6-amino-6-deoxy (41, 6N-NOI-NJ) analogues, aminocyclitols such as *N*-octyl-β-valienamine (NOV) and aminosugars such as derivatives with the cis-1,2-fused (gluco)pyranose-2-alkylsulfanyl-1,3-oxazoline (PSO) structure[78]. Some of the chaperones presently pursued deserve special mentioning. Compelling evidence has been reported for the use of α-1-C-substituted imino-D-xylitols (DIXs) as GBA chaperones with low cytotoxicity[84]. APP (3-amino-3-hydroxymethylpyrano[3,2-b]pyrrol-2(1H)-one) compounds with differing aglycone moieties offer another potentially useful class of chaperones since they competitively inhibit GBA at neutral pH but this inhibition strongly decreases at acid (lysosomal) pH[85]. A conformationally locked C-glycoside based on the APP scaffold with an incorporated palmitoylamido segment as aglycone moiety was reported to boost N370S/N370S GBA activity with an efficacy comparable to that of Ambroxol (see below)[85].

Lately high throughput screening of large numbers of compounds has been used in the search for new GBA chaperones[86–90]. The traditional screens usually identify GBA chaperones which are concomitant inhibitors of enzyme activity. This impedes clinical application since there is only a small window between desired chaperone function and enzyme inhibition. Therefore, Patnaik *et al.* developed a new high throughput screen with which they identified a series of allosteric compounds that do not or hardly inhibit GBA but can still assist transport to lysosomes[91–94]. Specific pyrazolopyrimidines and salicylic acid derivatives ML198 and ML266 were reported to activate GBA and function as a chaperone and lack inhibitory activity[95]. Another class of selective non-iminosugar chaperones comprises quinazoline derivatives[96]. A new set of selective quinazoline derivatives displaying linear mixed inhibition was shown to stabilize GBA and increase intralysosomal N370S enzyme[97]. Moreover, a novel non-inhibitory small molecule chaperone NCGC607 was recently reported to augment GBA and decrease GlcCer levels in GD macrophages[98]. Additionally, GD iPSC-derived dopaminergic neurons were shown to have higher GBA activity, improved lysosomal translocation of GBA, diminished GlcCer levels and reversed build-up of α-Syn upon NCGC607 treatment[98]. Allosteric

activators of GBA are presently developed: one such compound LTI-291 (Lysosomal Therapeutics Inc; Allergan Corp.) is to be tested in PD with GBA abnormalities[99].

Some existing approved drugs for other disease conditions might also boost GBA. A thermal denaturation assay of 1040 FDA-approved drugs identified Ambroxol (ABX) as GBA interactor[100]. ABX is used for many years to treat airway mucus hypersecretion and hyaline membrane disease in newborns[101–103]. ABX turned out to be a pH-dependent, mixed-type inhibitor of GBA, with maximum inhibition at neutral pH[100,104,105]. The treatment of GD fibroblasts with ABX, including cells homozygous for L444P GBA, significantly augmented GBA and ABX-treated GD lymphoblasts displayed reduced GlcCer accumulation[100,104,105]. Macrophages derived from GD iPS cells showed phenotypic correction upon treatment with ABX, displaying diminished elevation of TNF-α, IL-1β and IL-6[106]. Additionally, ABX was found to reduce oxidative stress in fibroblasts of normal subjects, GD patients and GD carriers with and without PD[107]. Wildtype mice treated for one week with ABX showed increased GBA activity in spleen, heart and cerebellum[108]. Furthermore, wildtype as well as transgenic heterozygous L444P mice and mice overexpressing human α-Syn had significantly increased GBA activity and reduced α-Syn in the brain[109]. A pilot study reported improvement of GD specific parameters in ERT naïve GD patients receiving ABX[110]. Furthermore, ABX treatment of neuronopathic GD patients led to significantly augmented lymphocyte GBA activity and reduced GlcSph levels in cerebrospinal fluid[111]. Neurological manifestations such as myoclonus, seizures and pupillary light reflex dysfunction were stable during the treatment[111]. In a type 3 GD patient ABX treatment ameliorated epileptic attacks[112]. The findings made with ABX treatment of GD patients have led Ishay *et al*. to recommend simultaneous administration of ERT and ABX to carriers of mutant GBA at risk for PD[113].

To develop small compound stabilizers of GBA a distinct approach from the high throughput screening of compound libraries (and subsequent medicinal chemistry) described above might be considered, i.e. is to obtain rational leads from fundamental investigations on GBA. It has been recently recognized that GBA is catalytically more diverse as hitherto assumed (chapter 3, 4). Furthermore, there is increasing evidence that occupancy of the catalytic pocket of GBA favors structural stability of the enzyme (chapter 2). One of the newly identified interactors with GBA is cholesterol. The sterol is able to reach the catalytic pocket as indicated by competition of pacGlcCer labeling of GBA (chapter 3) and it acts as acceptor in transglucosylation (chapter4). Moreover, GlcChol also serves as substrate for GBA (chapter 4). A careful examination of potential chaperone or inhibitory actions of (glycosylated) cholesterol or mimics thereof might be of interest. Particularly intriguing is also the affinity of GBA for β-xylosides that are poorer substrates than corresponding β-glucosides. Again, it seems worthwhile to investigate the impact of β-xylosides on GBA in living cells and organisms.

The knowledge on proteins interacting with GBA in lysosomes might also be translated to (additive) therapy approaches. For example, it is now apparent that LIMP-2 is critical for lysosomal GBA activity and α-Syn clearance[64]. Indeed, it was earlier shown that defects in the SCARB2 gene also constitute an increased risk for developing PD[114]. A cell-penetrating LIMP-2

helix 5-derived peptide has been shown to increase lysosomal GBA and decrease α-Syn levels[29]. Further investigations on therapeutic use of such peptides are warranted. The same holds for potential chaperoning SapC peptides. Recently, SapC was chemically synthesized and found to activate and stabilize GBA and moreover guard it from cathepsin D breakdown[115–117]. Cathepsin D was chosen because the authors previously found positive effects of its inhibitor on GBA activity[47] (in contrast to our results, data not shown). A major challenge with peptide supportive therapy is the limited ability of peptides to cross the blood-brain barrier. Design of cell penetrating peptides able to cross the BBB will be an essential next step for developing a realistic therapeutic agent.

A completely novel therapeutic approach employs pharmacological induction of the heat shock protein, HSP70[118–120]. HSP70 has been shown to protect lysosomes during stress and stabilize acid sphingomyelinase (ASM), an enzyme deficient in Niemann-Pick types A and B[118]. Niemann-Pick type B fibroblasts were found to display corrected lysosomal morphology upon treatment with recombinant HSP70[118]. This finding was extended to fibroblasts of eight different lysosomal storage disorders[120]. It has recently become clear that Arimoclomol potently induces endogenous HSP70[120]. Arimoclomol is presently tested in phase II studies by Orphazyme Corp. as experimental drug to treat Amyotrophic Lateral Sclerosis (ALS). A clinical study for the lysosomal storage disorder NPC is also approved by the FDA. Investigation of the outcome of Arimoclomol-mediated induction of HSP70 in neuronopathic GD will be of great interest.

A true cure for GD would in principle be offered by gene therapy. In the case of type 1 GD, successful bone marrow transplantation has been reported to result in major clinical correction[121–124], indicating that correction of GBA content in blood cells is sufficient for a satisfactory clinical response. The risk associated with allogenic bone marrow transplantation has limited the application. The combination of genetic correction of own hematopoietic cells of GD patients is appealing[125]. Recently very promising results have been obtained in a type GD mouse model with viral vectors allowing macrophage specific expression of GBA[124]. The recent advances with CRISPR/Cas technology should in the future offer possibilities for substituting aberrant genetic information by the correct one in the endogenous GBA alleles of GD patients[126,127].

Table 1. Existing and proposed (theoretical) therapy options for Gaucher disease.

Therapy	Agent	Mode of action
Existing therapies		
ERT	Recombinant GBA1 (Imiglucerase/ Cerezyme)	Enzyme supplementation
	Recombinant GBA1 Taliglucerase alfa (Elelyso)	Plant produced Enzyme supplementation
SRT	GCS inhibitor (Cerdelga/ Eliglustat)	Substrate reduction
Iminosugar chaperone	NB-DNJ (Zavesca)	Chaperone, transport promotion & Substrate reduction
Experimental therapies		
Iminosugar chaperone	NN-DNJ	Chaperone, Folding promotion
	Isofagomine (Plicera)	Chaperone, transport promotion
Chemical chaperones; Small compounds	Ambroxol	Chaperone, transport promotion
	APPs	Chaperone
	ML155, ML156	Chaperone
	ML198, ML266	Chaperone
	Quinazoline derivatives	Chaperone, transport promotion
	NCGC607	Chaperone
Allosteric compound	LTI-291	Activator, transport promotion
Heat Shock Protein response	Arimoclomol	Enzyme stabilization, refolding
Allosteric protein chaperones	LIMP-2 peptide	Transporting chaperone
	sapC (peptide)	Lysosomal chaperone
Gene therapy	DNA construct	cDNA/gene correction
Theoretical therapies		
Chemical chaperones; Small compounds	Cholesterol based compounds	Active site chaperone
	Xylosyl-β-glucsosides	Active site chaperone
Protease inhibition	Cathepsin inhibitor	Lysosomal proteolysis protection

The adaptations to GBA deficiency.

A final topic for discussion forms the relative recent realization that deficiency of GBA leads to adaptations with potential pathological consequences (see also chapter 5 for a review). Primary GBA deficiency occurs in GD patients due to defects in their two GBA alleles. A secondary deficiency of GBA occurs in AMRF (action myoclonus-renal failure syndrome) patients due to defects in the SCARB2 gene encoding LIMP-2[128,129]. Reduced GBA is also noted in patients with Niemann-Pick type C (NPC) disease due to defects in NPC1 or NPC2, proteins mediating the export of cholesterol from lysosomes[130].

One adaptation to lack of GBA in GD patients is the increased formation of gangliosides, likely due to permanent excess of the precursor GlcCer[131–133]. Elevated gangliosides like GM3 seem to promote the noted insulin resistance in GD patients[132]. The same metabolic abnormality occurs frequently in obese individuals in which formation of ceramide and subsequent glycosphingolipids is chronically increased[133,134]. The insulin receptor is present at the cell's plasma membrane in glycosphingolipid-rich rafts and a disturbed environment of gangliosides is thought to cause impaired insulin signaling. This mechanism is substantiated by findings in cell and animal models[135,136]. For example, mice deficient in ganglioside synthesis are protected against diet-induced obesity and the pharmacological reduction of GlcCer synthesis has been shown to increase insulin signaling in adipocytes and in various mouse and rat models of obesity-induced insulin resistance[134]. It has been debated whether excessive glycosphingolipids or elevated ceramide underlies impaired insulin signaling during obesity. A consensus is now reached in which excessive gangliosides are thought to cause insulin insensitivity in adipocyte, whereas excessive ceramide is the primary toxic agent in muscle[137,138]. Likely, the common chronic tissue inflammation during obesity drives the pathology onwards by promoting excessive ceramide synthesis and subsequent formation of glycosphingolipids that on their turn again promote inflammation.

A further adaptation to deficient GBA concerns the cytosol-faced membrane β-glucosidase GBA2[139–141]. The 3D-structure of GBA2 has not been resolved yet, but it is known that the enzyme's catalytic pocket is inserted in the cytosolic membrane leaflet. GBA2 is found to be increased during GBA1 deficiency[141,142], likely a compensation to regulate cellular GlcCer[130]. In mice with a conditional knockout of GBA in white blood cells concomitant absence of GBA2 reduces hepatosplenomegaly, cytopenia and skeletal disease[143]. Likewise, genetic loss of GBA2 as well as pharmacological inhibition of the enzyme is found to ameliorate manifestations of NPC in mice, particularly the loss of motor neurons[130]. These findings point to detrimental consequences of GBA2 over-activity during deficiency of GBA. On the other hand, several patients with defects in the GBA2 gene developing spastic paraplegia and cerebellar ataxia have recently been identified[144–149]. This suggests that a marked reduction of GBA2 activity, at least in some individuals, has negative consequences. Puzzling in this connection is that GBA2 deficiency in mice does not cause any overt pathology except for partially blocked spermatogenesis and that the treatment of GD and NPC patients with *Miglustat,* a nanomolar inhibitor of GBA2, is generally well tolerated[71,150,151]. In view of

this conundrum of conciliating the various findings a closer look to GBA2 is of interest. It has recently been demonstrated that the enzyme acts as a transglucosylase, reversibly transferring glucose from GlcCer to cholesterol to yield ceramide and GlcChol[22]. It can presently not be excluded that other metabolites also participate in these transglucosylation reactions. In view of this, changes in ceramide and glucosylated metabolites might be implicated in the noted beneficial effects of inhibition of GBA2 as well as in the neuropathology shown by GBA2-deficient individuals.

Another key adaptation to GBA deficiency is the active formation of glucosylsphingosine (GlcSph) by de-acylation of GlcCer through lysosomal acid ceramidase[152]. Most cell types of GD and AMRF patients manage to limit GlcCer accumulation through this pathway[153]. Formed GlcSph may leave cells and even the body via bile and urine[152]. As a consequence, plasma GlcSph is several hundred-fold increased in symptomatic GD patients[154]. This abnormality is however not without health risk. It was observed that excessive plasma GlcSph is linked to B-cell lymphoma[155]. Nair et al. recently reported that GlcSph in GD patients acts as auto-antigen that drives B-cell proliferation and increase the risk for associated multiple myeloma, a leukemia with increased incidence in GD patients[156,157]. A similar pathway of acid ceramidase-mediated formation of sphingoid bases from accumulating glycosphingolipid is active in other inherited glycosphingolipidoses[158]. For example, in α-galactosidase A deficient Fabry disease patients the water-soluble base lysoGb3 (globotriaosylsphingosine) is generated from accumulating Gb3 (globotriosylceramide)[159]. Plasma lysoGb3 is markedly elevated and lysoGb3 is present in urine[160]. Excessive lysoGb3 has been demonstrated to be toxic for nociceptive peripheral neurons and podocytes, contributing to the common pain in the extremities and the renal failure of Fabry disease patients[161,162]. Another example forms the neurotoxic galactosylsphingosine in Krabbe disease, the sphingoid base formed from the primary storage lipid galactosylceramide in the galactocerebrosidase-deficient patients[163]. The quantitative detection of glycosphingoid bases in plasma samples by UPLC-ESI-MS/MS using ^{13}C-encoded internal standards has enormously improved diagnosis of GD and Fabry disease patients as well as the monitoring of efficacy of therapeutic intervention[154,160,164] (addendum 2). Another important application for ^{13}C-encoded glycosphingolipids is laid in their use for detailed investigation of in vivo lipid metabolism and the impact of (potential) therapeutic agents[152].

Perspectives

GBA is a truly fascinating enzyme. Fifty years after its discovery by Brady and colleagues[165] and despite subsequent intense research, the enzyme today still poses multiple challenging questions. GBA differs from other lysosomal hydrolases in fundamental aspects. Newly formed GBA is uniquely transported to lysosomes, bound to the integral membrane protein LIMP-2, traversing distinct compartments from the other mannose-6-phosphate receptor bound acid hydrolases[26,166,167]. The evolutionary pressure for this unique sorting is still not elucidated. The (transient) interaction of GBA with LIMP-2 may have physiological implications. LIMP-2 (aka SCARB2) has been proposed to harbor a lipid transport function similar to the related proteins SCARB1 and SCARB3[168]. It is appealing to speculate that a product of GBA is channeled via LIMP-2 from lysosomes to the cytosol. The recent insight that GBA also interacts with cholesterol and can generate GlcChol might be relevant in this connection. It might be hypothesized that the GBA/LIMP-2 complex plays a role in (glucosylated) cholesterol transport from lysosomes. Closer investigation of the impact of cholesterol and its metabolites on GBA and GlcCer metabolism is highly warranted. In view of this, the presence of active GBA in the extracellular layer of skin rich in GlcCer and cholesterol is intriguing[24]. A local role for GBA in the fine-tuning of glucosylated sterols and sphingolipids with impact on skin permeability is a hypothetical possibility that should be further investigated.

This thesis research primarily focused on factors influencing stability and activity of GBA in lysosomes. The interest in this topic has enormously increased after GBA deficiency was implicated in neurodegenerative conditions like Parkinson's disease and Lewy-Body dementia. Increasing the lifespan of GBA molecules by inhibition of a specific cathepsin involved in the enzyme's lysosomal breakdown is appealing. However, the conducted research on this topic did not render a suitable target cathepsin. A more attractive approach to increase lifespan of GBA seems the stabilization of GBA conformation. Own research and literature suggests that there are multiple potential targets for this. Firstly, there are indications that both LIMP-2 and saposin C by binding to GBA inside lysosomes may stabilize the enzyme and increase its hydrolytic activity. The amphiphilic polypeptide α-synuclein seems to interfere with these beneficial interactions and therefore impairs GBA. It can be envisioned that in the near future polypeptides, like LIMP-2 fragments and potentially also saposin C fragments, may be selected to promote stability and activity of GBA inside lysosomes. The induction of specific proteins, like HSP70, able to actively refold proteins inside lysosomes is also offering an exciting new option for augmenting GBA and deserves further investigation. Secondly, it has become clear that small compounds may influence the folding and structural stability GBA in cells. Chemical chaperones directly interacting with the catalytic pocket of GBA receive considerable attention, in particular glyco-mimetics interacting with the glycon binding site of the enzyme. An intrinsic disadvantage of these type of agents is their ability to effectively inhibit enzyme activity when present at too high dose. This offers considerable challenges in their practical use in patients where ideally concomitantly in various tissues and cell types the desired concentrations is reached. A new promising development is the identification of small compounds that allosterically (beyond the catalytic pocket) boost GBA. Stemming from own research the impact of cholesterol and β-xylosides on GBA also deserves further investigation in this light. Finally, the more direct approaches to increase lysosomal GBA such as enzyme replacement therapy and in particular gene therapy remain to hold great therapeutic potential for Gaucher disease as well as Parkinson's disease induced by GBA deficiency.

The recent discovery of unexpected catalytic actions of GBA opens up new exciting research fields. It will be interesting to identify which glucosylated metabolites beyond GlcCer and GlcChol naturally occur in the human body and what the precise role of GBA is in their

metabolism. In this connection, the potential natural occurrence of β-xylosylated metabolites should also be carefully examined. In addition, the possible impact on GBA of food-derived exogenous hydrophobic β-glucosides and β-xylosides as well as sterol-like structures should be taken in mind.

In conclusion, half a century after its discovery GBA still resembles the mythological Sphinx, a multi-faceted creature posing riddles.

References

1. Ferraz, M. J. *et al.* Gaucher disease and Fabry disease: New markers and insights in pathophysiology for two distinct glycosphingolipidoses. *Biochim. Biophys. Acta - Mol. Cell Biol. Lipids* **1841,** 811–825 (2014).
2. E. Beutler, G. A. G. in *C.R. Scriver,W.S. Sly, D. Valle (Eds.), The Metabolic and Molecular Bases of Inherited Disease, 8th ed.* 3635–3668 (McGraw-Hill, New York, 2001).
3. Kallemeijn, W. W. *et al.* A Sensitive Gel-based Method Combining Distinct Cyclophellitol-based Probes for the Identification of Acid/Base Residues in Human Retaining -Glucosidases. *J. Biol. Chem.* **289,** 35351–35362 (2014).
4. Barton, N. W. *et al.* Replacement Therapy for Inherited Enzyme Deficiency — Macrophage-Targeted Glucocerebrosidase for Gaucher's Disease. *N. Engl. J. Med.* **324,** 1464–1470 (1991).
5. de Fost, M. *et al.* Superior effects of high-dose enzyme replacement therapy in type 1 Gaucher disease on bone marrow involvement and chitotriosidase levels: a 2-center retrospective analysis. *Blood* **108,** 830–5 (2006).
6. Pastores, G. M. *et al.* Therapeutic goals in the treatment of Gaucher disease. *Semin. Hematol.* **41,** 4–14 (2004).
7. van Dussen, L., Biegstraaten, M., Dijkgraaf, M. G. & Hollak, C. E. Modelling Gaucher disease progression: long-term enzyme replacement therapy reduces the incidence of splenectomy and bone complications. *Orphanet J. Rare Dis.* **9,** 112 (2014).
8. van Dussen, L., Biegstraaten, M., Hollak, C. E. M. & Dijkgraaf, M. G. W. Cost-effectiveness of enzyme replacement therapy for type 1 Gaucher disease. *Orphanet J. Rare Dis.* **9,** 51 (2014).
9. van Dussen, L. *et al.* Value of plasma chitotriosidase to assess non-neuronopathic Gaucher disease severity and progression in the era of enzyme replacement therapy. *J. Inherit. Metab. Dis.* **37,** 991–1001 (2014).
10. Aflaki, E., Westbroek, W. & Sidransky, E. The Complicated Relationship between Gaucher Disease and Parkinsonism: Insights from a Rare Disease. *Neuron* **93,** 737–746 (2017).
11. Jonsson, L. M. V *et al.* Biosynthesis and maturation of glucocerebrosidase in Gaucher fibroblasts. *Eur. J. Biochem.* **164,** 171–179 (1987).
12. Grace, M. E., Graves, P. N., Smith, F. I. & Grabowski, G. A. Analyses of catalytic activity and inhibitor binding of human acid beta-glucosidase by site-directed mutagenesis. Identification of residues critical to catalysis and evidence for causality of two Ashkenazi Jewish Gaucher disease type 1 mutations. *J. Biol. Chem.* **265,** 6827–35 (1990).
13. Boot, R. G. *et al.* Glucocerebrosidase genotype of Gaucher patients in The Netherlands: limitations in prognostic value. *Hum. Mutat.* **10,** 348–58 (1997).
14. van Weely, S. *et al.* Role of pH in determining the cell-type-specific residual activity of glucocerebrosidase in type 1 Gaucher disease. *J. Clin. Invest.* **91,** 1167–75 (1993).
15. Wei, R. R. *et al.* X-ray and Biochemical Analysis of N370S Mutant Human Acid -Glucosidase. *J. Biol. Chem.* **286,** 299–308 (2011).
16. Greenbaum, D., Medzihradszky, K. F., Burlingame, A. & Bogyo, M. Epoxide electrophiles as activity-dependent cysteine protease profiling and discovery tools. *Chem. Biol.* **7,** 569–581 (2000).
17. Greenbaum, D. *et al.* Chemical approaches for functionally probing the proteome. *Mol. Cell. Proteomics* **1,** 60–8 (2002).
18. Witte, M. D. *et al.* Ultrasensitive in situ visualization of active glucocerebrosidase molecules. *Nat. Chem. Biol.* **6,** 907–913 (2010).
19. Dekker, N. *et al.* Elevated plasma glucosylsphingosine in Gaucher disease: relation to phenotype, storage cell markers, and therapeutic response. *Blood* **118,** e118–e127 (2011).
20. Kallemeijn, W. W. *et al.* Investigations on therapeutic glucocerebrosidases through paired detection with fluorescent activity-based probes. *PLoS One* **12,** e0170268 (2017).
21. Kallemeijn, W. W. *et al.* Novel activity-based probes for broad-spectrum profiling of retaining β-exoglucosidases in situ and in vivo. *Angew. Chemie - Int. Ed.* **51,** 12529–12533 (2012).
22. Marques, A. R. A. *et al.* Glucosylated cholesterol in mammalian cells and tissues: formation and degradation by multiple cellular β-glucosidases. *J. Lipid Res.* **57,** 451–463 (2016).
23. Haberkant, P. & Holthuis, J. C. M. Fat & fabulous: Bifunctional lipids in the spotlight. *Biochim. Biophys. Acta - Mol. Cell Biol. Lipids* **1841,** 1022–1030 (2014).
24. van Smeden, J. *et al.* Intercellular skin barrier lipid composition and organization in Netherton syndrome patients. *J. Invest. Dermatol.* **134,** 1238–45 (2014).
25. Aerts, J. M. *et al.* Glucocerebrosidase, a lysosomal enzyme that does not undergo oligosaccharide phosphorylation. *Biochim. Biophys. Acta* **964,** 303–8 (1988).
26. Reczek, D. *et al.* LIMP-2 Is a Receptor for Lysosomal Mannose-6-Phosphate-Independent Targeting of β-Glucocerebrosidase. *Cell* **131,** 770–783 (2007).
27. Blanz, J. *et al.* Mannose 6-phosphate-independent Lysosomal Sorting of LIMP-2. *Traffic* **16,** 1127–1136 (2015).
28. Zachos, C., Blanz, J., Saftig, P. & Schwake, M. A Critical Histidine Residue Within LIMP-2 Mediates pH Sensitive Binding to Its Ligand β-Glucocerebrosidase. *Traffic* **13,** 1113–1123 (2012).
29. Zunke, F. *et al.* Characterization of the complex formed by β-glucocerebrosidase and the lysosomal integral membrane protein type-2. *Proc. Natl. Acad. Sci.* **113,** 3791–3796 (2016).
30. Kolter, T. & Sandhoff, K. PRINCIPLES OF LYSOSOMAL MEMBRANE DIGESTION: Stimulation of Sphingolipid Degradation by Sphingolipid Activator Proteins and Anionic Lysosomal Lipids. *Annu. Rev. Cell Dev. Biol.* **21,** 81–103 (2005).
31. Morimoto, S. *et al.* Interaction of saposins, acidic lipids, and glucosylceramidase. *J. Biol. Chem.* **265,** 1933–7 (1990).
32. Leonova, T. *et al.* Proteolytic processing patterns of prosaposin in insect and mammalian cells. *J. Biol. Chem.* **271,** 17312–20 (1996).
33. Vaccaro, A. M. *et al.* An endogenous activator protein in human placenta for enzymatic

degradation of glucosylceramide. *Biochim. Biophys. Acta* **836,** 157–66 (1985).

34. Vaccaro, A. M. *et al.* The binding of glucosylceramidase to glucosylceramide is promoted by its activator protein. *FEBS Lett.* **216,** 190–4 (1987).

35. Weiler, S., Kishimoto, Y., O'Brien, J. S., Barranger, J. A. & Tomich, J. M. Identification of the binding and activating sites of the sphingolipid activator protein, saposin C, with glucocerebrosidase. *Protein Sci.* **4,** 756–64 (1995).

36. Qi, X., Leonova, T. & Grabowski, G. A. Functional human saposins expressed in Escherichia coli. Evidence for binding and activation properties of saposins C with acid beta-glucosidase. *J. Biol. Chem.* **269,** 16746–53 (1994).

37. Qi, X. & Grabowski, G. A. Acid beta-glucosidase: intrinsic fluorescence and conformational changes induced by phospholipids and saposin C. *Biochemistry* **37,** 11544–54 (1998).

38. Tylki-Szymańska, A. *et al.* Non-neuronopathic Gaucher disease due to saposin C deficiency. *Clin. Genet.* **72,** 538–542 (2007).

39. Vaccaro, A. M. *et al.* Saposin C mutations in Gaucher disease patients resulting in lysosomal lipid accumulation, saposin C deficiency, but normal prosaposin processing and sorting. *Hum. Mol. Genet.* **19,** 2987–2997 (2010).

40. Motta, M. *et al.* Gaucher disease due to saposin C deficiency is an inherited lysosomal disease caused by rapidly degraded mutant proteins. *Hum. Mol. Genet.* **23,** 5814–26 (2014).

41. Tamargo, R. J., Velayati, A., Goldin, E., Sidransky, E. & Rafael, J; Tamargo, Arash Velayati; Ehud, Goldin; Sidransky, E. The role of saposin C in Gaucher disease. *NIH Public Access* **106,** 257–263 (2012).

42. Wilkening, G., Linke, T. & Sandhoff, K. Lysosomal degradation on vesicular membrane surfaces. Enhanced glucosylceramide degradation by lysosomal anionic lipids and activators. *J. Biol. Chem.* **273,** 30271–8 (1998).

43. Salvioli, R., Tatti, M., Ciaffoni, F. & Vaccaro, A. M. Further studies on the reconstitution of glucosylceramidase activity by Sap C and anionic phospholipids. *FEBS Lett.* **472,** 17–21 (2000).

44. Vaccaro, A. M. *et al.* Saposin C induces pH-dependent destabilization and fusion of phosphatidylserine-containing vesicles. *FEBS Lett.* **349,** 181–6 (1994).

45. Wang, Y., Grabowski, G. A. & Qi, X. Phospholipid vesicle fusion induced by saposin C. *Arch. Biochem. Biophys.* **415,** 43–53 (2003).

46. Qi, X. & Chu, Z. Fusogenic domain and lysines in saposin C. *Arch. Biochem. Biophys.* **424,** 210–218 (2004).

47. Sun, Y., Qi, X. & Grabowski, G. A. Saposin C is required for normal resistance of acid beta-glucosidase to proteolytic degradation. *J. Biol. Chem.* **278,** 31918–23 (2003).

48. Liou, B. *et al.* Analyses of variant acid beta-glucosidases: effects of Gaucher disease mutations. *J. Biol. Chem.* **281,** 4242–53 (2006).

49. Atrian, S. *et al.* An evolutionary and structure-based docking model for glucocerebrosidase-saposin C and glucocerebrosidase-substrate interactions - relevance for Gaucher disease. *Proteins* **70,** 882–91 (2008).

50. Mazzulli, J. R. *et al.* Gaucher disease glucocerebrosidase and α-synuclein form a bidirectional pathogenic loop in synucleinopathies. *Cell* **146,** 37–52 (2011).

51. Yap, T. L. *et al.* ??-Synuclein interacts with glucocerebrosidase providing a molecular link between Parkinson and gaucher diseases. *J. Biol. Chem.* **286,** 28080–28088 (2011).

52. Liu, G. *et al.* Specifically neuropathic Gaucher's mutations accelerate cognitive decline in Parkinson's. *Ann. Neurol.* **80,** 674–685 (2016).

53. Mata, I. F. *et al.* Glucocerebrosidase Gene Mutations. *Arch. Neurol.* **65,** 379–82 (2008).

54. Nichols, W. C. *et al.* Mutations in GBA are associated with familial Parkinson disease susceptibility and age at onset. *Neurology* **72,** 310–316 (2009).

55. Pchelina, S., Emelyanov, A., Baydakova, G., Andoskin, P. & Senkevich, K. Neuroscience Letters Oligomeric _ -synuclein and glucocerebrosidase activity levels in GBA-associated Parkinson's disease. **636,** 70–76 (2017).

56. Argyriou, A. *et al.* Increased dimerization of alpha-synuclein in erythrocytes in Gaucher disease and aging. *Neurosci. Lett.* **528,** 205–209 (2012).

57. Moraitou, M. *et al.* α-Synuclein dimerization in erythrocytes of Gaucher disease patients: correlation with lipid abnormalities and oxidative stress. *Neurosci. Lett.* **613,** 1–5 (2016).

58. Yap, T. L., Velayati, A., Sidransky, E. & Lee, J. C. Membrane-bound α-synuclein interacts with glucocerebrosidase and inhibits enzyme activity. *Mol. Genet. Metab.* **108,** 56–64 (2013).

59. Mak, S. K., McCormack, A. L., Manning-Bog, A. B., Cuervo, A. M. & Di Monte, D. A. Lysosomal degradation of alpha-synuclein in vivo. *J. Biol. Chem.* **285,** 13621–9 (2010).

60. Gruschus, J. M. *et al.* Dissociation of glucocerebrosidase dimer in solution by its co-factor, saposin C. *Biochem. Biophys. Res. Commun.* **457,** 561–6 (2015).

61. Yap, T. L., Gruschus, J. M., Velayati, A., Sidransky, E. & Lee, J. C. Saposin C protects glucocerebrosidase against α-synuclein inhibition. *Biochemistry* **52,** 7161–3 (2013).

62. Sardi, S. P. *et al.* CNS expression of glucocerebrosidase corrects alpha-synuclein pathology and memory in a mouse model of Gaucher-related synucleinopathy. *Proc. Natl. Acad. Sci. U. S. A.* **108,** 12101–6 (2011).

63. Sardi, S. P. *et al.* Augmenting CNS glucocerebrosidase activity as a therapeutic strategy for parkinsonism and other Gaucher-related synucleinopathies. *Proc. Natl. Acad. Sci. U. S. A.* **110,** 3537–42 (2013).

64. Rothaug, M. *et al.* LIMP-2 expression is critical for -glucocerebrosidase activity and -synuclein clearance. *Proc. Natl. Acad. Sci.* **111,** 15573–15578 (2014).

65. Brady, R. O., Pentchev, P. G., Gal, A. E., Hibbert, S. R. & Dekaban, A. S. Replacement Therapy for Inherited Enzyme Deficiency. *N. Engl. J. Med.* **291,** 989–993 (1974).

66. Brady, R. O. Benefits from unearthing 'a biochemical Rosetta Stone'. *J. Biol. Chem.* **285,** 41216–21 (2010).

67. Aerts, J. M. & Cox, T. M. Roscoe O. Brady: Physician whose pioneering discoveries in lipid biochemistry revolutionized treatment and understanding of lysosomal diseases. *Blood Cells, Mol. Dis.* (2017). doi:10.1016/j.bcmd.2016.10.030

68. Grabowski, G. A., Golembo, M. & Shaaltiel, Y. Taliglucerase alfa: An enzyme replacement therapy using plant cell expression technology. *Mol. Genet. Metab.* **112,** 1–8 (2014).

69. Cox, T. *et al.* Novel oral treatment of Gaucher's disease with N-butyldeoxynojirimycin (OGT 918) to decrease substrate biosynthesis. *Lancet* **355,** 1481–1485 (2000).

70. Platt, F. M. *et al.* Inhibition of substrate synthesis as a strategy for glycolipid lysosomal storage disease therapy. *J. Inherit. Metab. Dis.* **24,** 275–90 (2001).

71. Elstein, D. *et al.* Sustained therapeutic effects of oral miglustat (Zavesca, N-butyldeoxynojirimycin, OGT 918) in type I Gaucher disease. *J. Inherit. Metab. Dis.* **27,** 757–766 (2004).

72. Cox, T. M. *et al.* Eliglustat compared with imiglucerase in patients with Gaucher's

disease type 1 stabilised on enzyme replacement therapy: a phase 3, randomised, open-label, non-inferiority trial. *Lancet* **385,** 2355–2362 (2015).

73. Mistry, P. K. *et al.* Effect of Oral Eliglustat on Splenomegaly in Patients With Gaucher Disease Type 1. *JAMA* **313,** 695 (2015).

74. Smid, B. E. *et al.* Biochemical response to substrate reduction therapy versus enzyme replacement therapy in Gaucher disease type 1 patients. *Orphanet J. Rare Dis.* **11,** 28 (2016).

75. Ghisaidoobe, A. T. *et al.* Identification and Development of Biphenyl Substituted Iminosugars as Improved Dual Glucosylceramide Synthase/Neutral Glucosylceramidase Inhibitors. *J. Med. Chem.* **57,** 9096–9104 (2014).

76. Ashe, K. M. *et al.* Efficacy of Enzyme and Substrate Reduction Therapy with a Novel Antagonist of Glucosylceramide Synthase for Fabry Disease. *Mol. Med.* **21,** 389–99 (2015).

77. Benito, J. M., García Fernández, J. M. & Ortiz Mellet, C. Pharmacological chaperone therapy for Gaucher disease: a patent review. *Expert Opin. Ther. Pat.* **21,** 885–903 (2011).

78. Sanchez-Fernandez, E. M., Garcia Fernandez, J. M. & Mellet, C. O. Glycomimetic-based pharmacological chaperones for lysosomal storage disorders: lessons from Gaucher, GM1-gangliosidosis and Fabry diseases. *Chem. Commun.* **52,** 5497–5515 (2016).

79. Sawkar, A. R. *et al.* Chemical chaperones increase the cellular activity of N370S beta - glucosidase: a therapeutic strategy for Gaucher disease. *Proc. Natl. Acad. Sci. U. S. A.* **99,** 15428–33 (2002).

80. Offman, M. N., Krol, M., Silman, I., Sussman, J. L. & Futerman, A. H. Molecular basis of reduced glucosylceramidase activity in the most common Gaucher disease mutant, N370S. *J. Biol. Chem.* **285,** 42105–14 (2010).

81. Chang, H.-H., Asano, N., Ishii, S., Ichikawa, Y. & Fan, J.-Q. Hydrophilic iminosugar active-site-specific chaperones increase residual glucocerebrosidase activity in fibroblasts from Gaucher patients. *FEBS J.* **273,** 4082–92 (2006).

82. Steet, R. A. *et al.* The iminosugar isofagomine increases the activity of N370S mutant acid beta-glucosidase in Gaucher fibroblasts by several mechanisms. *Proc. Natl. Acad. Sci. U. S. A.* **103,** 13813–8 (2006).

83. Amicus Therapeutics Announces Preliminary Results of Phase 2 Study with Plicera(TM) for Gaucher Disease (NASDAQ:FOLD). (2009). Available at: http://ir.amicusrx.com/releasedetail.cfm?releaseid=413437. (Accessed: 9th March 2017)

84. Serra-Vinardell, J. *et al.* Glucocerebrosidase enhancers for selected gaucher disease genotypes by modification of α-1-C-substituted Imino- D -xylitols (DIXs) by click chemistry. *ChemMedChem* **9,** 1744–1754 (2014).

85. Navo, C. D. *et al.* Conformationally-locked C-glycosides: tuning aglycone interactions for optimal chaperone behaviour in Gaucher fibroblasts. *Org. Biomol. Chem.* **14,** 1473–1484 (2016).

86. Díaz, L., Casas, J., Bujons, J., Llebaria, A. & Delgado, A. New Glucocerebrosidase Inhibitors by Exploration of Chemical Diversity of *N* -Substituted Aminocyclitols Using Click Chemistry and in Situ Screening. *J. Med. Chem.* **54,** 2069–2079 (2011).

87. Goddard-Borger, E. D. *et al.* Rapid assembly of a library of lipophilic iminosugars via the thiol-ene reaction yields promising pharmacological chaperones for the treatment of Gaucher disease. *J. Med. Chem.* **55,** 2737–45 (2012).

88. Motabar, O. *et al.* A high throughput glucocerebrosidase assay using the natural substrate glucosylceramide. *Anal. Bioanal. Chem.* **402,** 731–9 (2012).

89. Zheng, W. *et al.* Three classes of glucocerebrosidase inhibitors identified by quantitative high-throughput screening are chaperone leads for Gaucher disease. *Proc. Natl. Acad. Sci. U. S. A.* **104,** 13192–7 (2007).

90. Goldin, E. *et al.* High throughput screening for small molecule therapy for Gaucher disease using patient tissue as the source of mutant glucocerebrosidase. *PLoS One* **7,** e29861 (2012).

91. Patnaik, S. *et al.* Discovery, structure-activity relationship, and biological evaluation of noninhibitory small molecule chaperones of glucocerebrosidase. *J. Med. Chem.* **55,** 5734–48 (2012).

92. Inglese, J. *et al.* Quantitative high-throughput screening: a titration-based approach that efficiently identifies biological activities in large chemical libraries. *Proc. Natl. Acad. Sci. U. S. A.* **103,** 11473–8 (2006).

93. Motabar, O. *et al. Identification of Modulators of the N370S Mutant Form of Glucocerebrosidase as a Potential Therapy for Gaucher Disease - Chemotype 1. Probe Reports from the NIH Molecular Libraries Program* (2010).

94. Motabar, O. *et al. Identification of Modulators of the N370S Mutant Form of Glucocerebrosidase as a Potential Therapy for Gaucher Disease - Chemotype 2. Probe Reports from the NIH Molecular Libraries Program* (2010).

95. Rogers, S. *et al. Discovery, SAR, and Biological Evaluation of Non-inhibitory Chaperones of Glucocerebrosidase*. *Probe Reports from the NIH Molecular Libraries Program* (National Center for Biotechnology Information (US), 2010).

96. Marugan, J. J. *et al.* Evaluation of quinazoline analogues as glucocerebrosidase inhibitors with chaperone activity. *J. Med. Chem.* **54,** 1033–58 (2011).

97. Zheng, J., Chen, L., Schwake, M., Silverman, R. B. & Krainc, D. Design and Synthesis of Potent Quinazolines as Selective β-Glucocerebrosidase Modulators. *J. Med. Chem.* **59,** 8508–20 (2016).

98. Aflaki, E. *et al.* A New Glucocerebrosidase Chaperone Reduces α-Synuclein and Glycolipid Levels in iPSC-Derived Dopaminergic Neurons from Patients with Gaucher Disease and Parkinsonism. *J. Neurosci.* **36,** 7441–52 (2016).

99. Allergan Enters Parkinson's Disease Through Option Arrangement with Lysosomal Therapeutics Inc. (LTI) for its Potential First-In-Class Breakthrough Compounds - Allergan. Available at: https://www.allergan.com/news/news/thomson-reuters/allergan-enters-parkinson-s-disease-through-option. (Accessed: 1st March 2017)

100. Maegawa, G. H. B. *et al.* Identification and Characterization of Ambroxol as an Enzyme Enhancement Agent for Gaucher Disease. *J. Biol. Chem.* **284,** 23502–23516 (2009).

101. Renovanz, V. K. [Results of some clinical-pharmacological studies on ambroxol (NA 872)]. *Arzneimittelforschung.* **25,** 646–52 (1975).

102. Wiessmann, K. J. & Niemeyer, K. [Clinical results in the treatment of chronic obstructive bronchitis with ambroxol in comparison with bromhexine (author's transl)]. *Arzneimittelforschung.* **28,** 918–21 (1978).

103. Wauer, R. R. *et al.* The antenatal use of ambroxol (bromhexine metabolite VIII) to prevent hyaline membrane disease: a controlled double-blind study. *Int. J. Biol. Res. Pregnancy* **3,** 84–91 (1982).

104. Shanmuganathan, M. & Britz-McKibbin, P. Inhibitor screening of pharmacological

chaperones for lysosomal β-glucocerebrosidase by capillary electrophoresis. *Anal. Bioanal. Chem.* **399,** 2843–2853 (2011).

105. Bendikov-Bar, I., Ron, I., Filocamo, M. & Horowitz, M. Characterization of the ERAD process of the L444P mutant glucocerebrosidase variant. *Blood Cells, Mol. Dis.* **46,** 4–10 (2011).

106. Panicker, L. M. *et al.* Gaucher iPSC-derived macrophages produce elevated levels of inflammatory mediators and serve as a new platform for therapeutic development. *Stem Cells* **32,** 1–16 (2014).

107. McNeill, A. *et al.* Ambroxol improves lysosomal biochemistry in glucocerebrosidase mutation-linked Parkinson disease cells. *Brain* **137,** 1481–1495 (2014).

108. Luan, Z. *et al.* The chaperone activity and toxicity of ambroxol on Gaucher cells and normal mice. *Brain Dev.* **35,** 317–322 (2013).

109. Migdalska-Richards, A., Daly, L., Bezard, E. & Schapira, A. H. V. Ambroxol effects in glucocerebrosidase and α-synuclein transgenic mice. *Ann. Neurol.* **80,** 766–775 (2016).

110. Zimran, A., Altarescu, G. & Elstein, D. Pilot study using ambroxol as a pharmacological chaperone in type 1 Gaucher disease. *Blood Cells, Mol. Dis.* **50,** 134–137 (2013).

111. Narita, A. *et al.* Ambroxol chaperone therapy for neuronopathic Gaucher disease: A pilot study. *Ann. Clin. Transl. Neurol.* **3,** 200–215 (2016).

112. Pawlinski, L., Malecki, M. T. & Kiec-Wilk, B. The additive effect on the antiepileptic treatment of ambroxol in type 3 Gaucher patient. The early observation. *Blood Cells, Mol. Dis.* (2016). doi:10.1016/j.bcmd.2016.12.001

113. Ishay, Y. *et al.* Combined beta-glucosylceramide and ambroxol hydrochloride in patients with Gaucher related Parkinson disease: From clinical observations to drug development. *Blood Cells, Mol. Dis.* (2016). doi:10.1016/j.bcmd.2016.10.028

114. Michelakakis, H. *et al.* Evidence of an association between the scavenger receptor class B member 2 gene and Parkinson's disease. *Mov. Disord.* **27,** 400–5 (2012).

115. Yoneshige, A., Muto, M., Watanabe, T., Hojo, H. & Matsuda, J. The effects of chemically synthesized saposin C on glucosylceramide-β-glucosidase. *Clin. Biochem.* **48,** 1177–1180 (2015).

116. Hojo, H. *et al. Synthesis of the sphingolipid activator protein, saposin C, using an azido-protected O-acyl isopeptide as an aggregation-disrupting element. Tetrahedron Letters* **52,** (2011).

117. Hojo, H. *et al.* Chemoenzymatic Synthesis of Hydrophobic Glycoprotein: Synthesis of Saposin C Carrying Complex-Type Carbohydrate. *J. Org. Chem.* **77,** 9437–9446 (2012).

118. Kirkegaard, T. *et al.* Hsp70 stabilizes lysosomes and reverts Niemann-Pick disease-associated lysosomal pathology. *Nature* **463,** 549–53 (2010).

119. Ingemann, L. & Kirkegaard, T. Lysosomal storage diseases and the heat shock response: convergences and therapeutic opportunities. *J. Lipid Res.* **55,** 2198–2210 (2014).

120. Kirkegaard, T. *et al.* Heat shock protein-based therapy as a potential candidate for treating the sphingolipidoses. *Sci. Transl. Med.* **8,** 355ra118 (2016).

121. Young, E., Chatterton, C., Vellodi, A. & Winchester, B. Plasma chitotriosidase activity in Gaucher disease patients who have been treated either by bone marrow transplantation or by enzyme replacement therapy with alglucerase. *J. Inherit. Metab. Dis.* **20,** 595–602 (1997).

122. Enquist, I. B. *et al.* Effective cell and gene therapy in a murine model of Gaucher disease. *Proc. Natl. Acad. Sci. U. S. A.* **103,** 13819–24 (2006).

123. Enquist, I. B. *et al.* Successful low-risk hematopoietic cell therapy in a mouse model of type 1 Gaucher disease. *Stem Cells* **27,** 744–752 (2009).

124. Dahl, M. *et al.* Lentiviral gene therapy using cellular promoters cures type 1 Gaucher disease in mice. *Mol. Ther.* **23,** 835–844 (2015).

125. Correll, P. H. & Karlsson, S. Towards therapy of Gaucher's disease by gene transfer into hematopoietic cells. *Eur. J. Haematol.* **53,** 253–64 (1994).

126. Moreno, A. M. & Mali, P. Therapeutic genome engineering via CRISPR-Cas systems. *Wiley Interdiscip. Rev. Syst. Biol. Med.* e1380 (2017). doi:10.1002/wsbm.1380

127. Fellmann, C., Gowen, B. G., Lin, P.-C., Doudna, J. A. & Corn, J. E. Cornerstones of CRISPR–Cas in drug discovery and therapy. *Nat. Rev. Drug Discov.* **16,** 89–100 (2016).

128. Badhwar, A. *et al.* Action myoclonus-renal failure syndrome: characterization of a unique cerebro-renal disorder. *Brain* **127,** 2173–2182 (2004).

129. Berkovic, S. F. *et al.* Array-Based Gene Discovery with Three Unrelated Subjects Shows SCARB2/LIMP-2 Deficiency Causes Myoclonus Epilepsy and Glomerulosclerosis. *Am. J. Hum. Genet.* **82,** 673–684 (2008).

130. Marques, A. R. A. *et al.* Reducing GBA2 Activity Ameliorates Neuropathology in Niemann-Pick Type C Mice. *PLoS One* **10,** e0135889 (2015).

131. Ghauharali-van der Vlugt, K. *et al.* Prominent increase in plasma ganglioside GM3 is associated with clinical manifestations of type I Gaucher disease. *Clin. Chim. Acta* **389,** 109–113 (2008).

132. Langeveld, M. *et al.* Type I Gaucher Disease, a Glycosphingolipid Storage Disorder, Is Associated with Insulin Resistance. *J. Clin. Endocrinol. Metab.* **93,** 845–851 (2008).

133. Langeveld, M. & Aerts, J. M. F. G. Glycosphingolipids and insulin resistance. *Prog. Lipid Res.* **48,** 196–205 (2009).

134. Aerts, J. M. *et al.* in *Advances in experimental medicine and biology* **721,** 99–119 (2011).

135. Bijl, N. *et al.* Modulation of glycosphingolipid metabolism significantly improves hepatic insulin sensitivity and reverses hepatic steatosis in mice. *Hepatology* **50,** 1431–41 (2009).

136. Langeveld, M. *et al.* Treatment of genetically obese mice with the iminosugar N-(5-adamantane-1-yl-methoxy-pentyl)-deoxynojirimycin reduces body weight by decreasing food intake and increasing fat oxidation. *Metabolism.* **61,** 99–107 (2012).

137. Chavez, J. A. *et al.* A Role for Ceramide, but Not Diacylglycerol, in the Antagonism of Insulin Signal Transduction by Saturated Fatty Acids. *J. Biol. Chem.* **278,** 10297–10303 (2003).

138. Park, M. *et al.* A Role for Ceramides, but Not Sphingomyelins, as Antagonists of Insulin Signaling and Mitochondrial Metabolism in C2C12 Myotubes. *J. Biol. Chem.* **291,** 23978–23988 (2016).

139. van Weely, S., Brandsma, M., Strijland, a, Tager, J. M. & Aerts, J. M. Demonstration of the existence of a second, non-lysosomal glucocerebrosidase that is not deficient in Gaucher disease. *Biochim. Biophys. Acta* **1181,** 55–62 (1993).

140. Boot, R. G. *et al.* Identification of the non-lysosomal glucosylceramidase as beta-glucosidase 2. *J. Biol. Chem.* **282,** 1305–12 (2007).

141. Yildiz, Y. *et al.* Functional and genetic characterization of the non-lysosomal glucosylceramidase 2 as a modifier for Gaucher disease. *Orphanet J. Rare Dis.* **8,** 151 (2013).

142. Burke, D. G. *et al.* Increased glucocerebrosidase (GBA) 2 activity in GBA1 deficient mice brains and in Gaucher leucocytes. *J. Inherit. Metab. Dis.* **36,** 869–872 (2013).

143. Mistry, P. K. *et al.* Glucocerebrosidase 2 gene deletion rescues type 1 Gaucher disease.

Proc. Natl. Acad. Sci. **111,** 4934–4939 (2014).

144. Sultana, S. *et al.* Lack of enzyme activity in GBA2 mutants associated with hereditary spastic paraplegia/cerebellar ataxia (SPG46). *Biochem. Biophys. Res. Commun.* **465,** 35–40 (2015).

145. Hammer, M. B. *et al.* Mutations in GBA2 cause autosomal-recessive cerebellar ataxia with spasticity. *Am. J. Hum. Genet.* **92,** 245–51 (2013).

146. Martin, E. *et al.* Loss of Function of Glucocerebrosidase GBA2 Is Responsible for Motor Neuron Defects in Hereditary Spastic Paraplegia. *Am. J. Hum. Genet.* **92,** 238–244 (2013).

147. Kancheva, D. *et al.* Novel mutations in genes causing hereditary spastic paraplegia and Charcot-Marie-Tooth neuropathy identified by an optimized protocol for homozygosity mapping based on whole-exome sequencing. *Genet. Med.* **18,** 600–607 (2016).

148. Citterio, A. *et al.* Mutations in CYP2U1, DDHD2 and GBA2 genes are rare causes of complicated forms of hereditary spastic paraparesis. *J. Neurol.* **261,** 373–81 (2014).

149. Votsi, C., Zamba-Papanicolaou, E., Middleton, L. T., Pantzaris, M. & Christodoulou, K. A novel GBA2 gene missense mutation in spastic ataxia. *Ann. Hum. Genet.* **78,** 13–22 (2014).

150. Yildiz, Y. *et al.* Mutation of β-glucosidase 2 causes glycolipid storage disease and impaired male fertility. **116,** (2006).

151. Walden, C. M. *et al.* Accumulation of Glucosylceramide in Murine Testis, Caused by Inhibition of beta-Glucosidase 2: IMPLICATIONS FOR SPERMATOGENESIS. *J. Biol. Chem.* **282,** 32655–32664 (2007).

152. Ferraz, M. J. *et al.* Lysosomal glycosphingolipid catabolism by acid ceramidase: formation of glycosphingoid bases during deficiency of glycosidases. *FEBS Lett.* **590,** 716–725 (2016).

153. Gaspar, P. *et al.* Action myoclonus-renal failure syndrome: diagnostic applications of activity-based probes and lipid analysis. *J. Lipid Res.* **55,** 138–145 (2014).

154. Mirzaian, M. *et al.* Mass spectrometric quantification of glucosylsphingosine in plasma and urine of type 1 Gaucher patients using an isotope standard. *Blood Cells, Mol. Dis.* **54,** 307–314 (2015).

155. Pavlova, E. V. *et al.* B cell lymphoma and myeloma in murine Gaucher's disease. *J. Pathol.* **231,** 88–97 (2013).

156. de Fost, M. *et al.* Immunoglobulin and free light chain abnormalities in Gaucher disease type I: data from an adult cohort of 63 patients and review of the literature. *Ann. Hematol.* **87,** 439–49 (2008).

157. Nair, S. *et al.* Type II NKT-TFH cells against Gaucher lipids regulate B-cell immunity and inflammation. *Blood* **125,** 1256–1271 (2015).

158. Ferraz, M. J. *et al.* Lyso-glycosphingolipid abnormalities in different murine models of lysosomal storage disorders. *Mol. Genet. Metab.* **117,** 186–193 (2016).

159. Aerts, J. M. *et al.* Elevated globotriaosylsphingosine is a hallmark of Fabry disease. *Proc. Natl. Acad. Sci. U. S. A.* **105,** 2812–7 (2008).

160. Gold, H. *et al.* Quantification of Globotriaosylsphingosine in Plasma and Urine of Fabry Patients by Stable Isotope Ultraperformance Liquid Chromatography-Tandem Mass Spectrometry. *Clin. Chem.* **59,** 547–556 (2013).

161. Choi, L. *et al.* The Fabry disease-associated lipid Lyso-Gb3 enhances voltage-gated calcium currents in sensory neurons and causes pain. *Neurosci. Lett.* **594,** 163–8 (2015).

162. Sanchez-Niño, M. D. *et al.* Lyso-Gb3 activates Notch1 in human podocytes. *Hum. Mol. Genet.* **24,** 5720–32 (2015).

163. Suzuki, K. Twenty five years of the "psychosine hypothesis": a personal perspective of its history and present status. *Neurochem. Res.* **23,** 251–9 (1998).

164. Mirzaian, M. *et al.* Accurate quantification of sphingosine-1-phosphate in normal and Fabry disease plasma, cells and tissues by LC-MS/MS with 13C-encoded natural S1P as internal standard. *Clin. Chim. Acta* **459,** 36–44 (2016).

165. Brady, R. O., Kanfer, J. N., Bradley, R. M. & Shapiro, D. Demonstration of a deficiency of glucocerebroside-cleaving enzyme in Gaucher's disease. *J. Clin. Invest.* **45,** 1112–1115 (1966).

166. Rijnboutt, S., Aerts, H. M., Geuze, H. J., Tager, J. M. & Strous, G. J. Mannose 6-phosphate-independent membrane association of cathepsin D, glucocerebrosidase, and sphingolipid-activating protein in HepG2 cells. *J. Biol. Chem.* **266,** 4862–8 (1991).

167. Saftig, P. & Klumperman, J. Lysosome biogenesis and lysosomal membrane proteins: trafficking meets function. *Nat. Rev. Mol. Cell Biol.* **10,** 623–635 (2009).

168. Neculai, D. *et al.* Structure of LIMP-2 provides functional insights with implications for SR-BI and CD36. *Nature* **504,** 172–176 (2013).

Addendum

Simultaneous quantitation of sphingoid bases by UPLC-ESI-MS/MS with identical ^{13}C-encoded internal standards

Simultaneous quantitation of sphingoid bases by UPLC-ESI-MS/MS with identical ^{13}C-encoded internal standards

Based on

M. Mirzaian[a], P. Wisse[b], M.J. Ferraz[a], A.R.A. Marques[c], P. Gaspar[d],
S.V. Oussoren[a], K. Kytidou[a], J.D.C. Codée [b], G. van der Marel [b],
H.S. Overkleeft[b], J.M. Aerts[a] *

[a]Dep. Medical Biochemistry, LIC, Leiden University
[b]Dep. Bio-organic Synthesis, LIC, Leiden University
[c]present address: Dep. Biochemistry,
Christian-Albrechts-Universität, Kiel, Germany
[d]present address: NSMGU, Human Genetics Dept,
National Institute of Health Dr Ricardo Jorge, Porto, Portugal

Abstract

Free sphingoid bases (lysosphingolipids) of primary storage sphingolipids are increased in tissues and plasma of several sphingolipidoses. As reported previously by us, sphingoid bases can be accurately quantified using UPLC-ESI-MS/MS, particularly in combination with identical ^{13}C-encoded internal standards. The feasibility of simultaneous quantitation of sphingoid bases in plasma specimens spiked with a mixture of such standards is described here. The sensitivity and linearity of detection is excellent for all examined sphingoid bases (sphingosine, sphinganine, hexosyl-sphingosine (glucosylsphingosine), hexosyl$_2$-sphingosine (lactosylsphingosine), hexosyl$_3$-sphingosine (globtriaosylsphingosine), phosphorylcholine-sphingosine) in the relevant concentration range and the measurements display very acceptable intra- and inter-assay variation (<10 % average). Plasma samples of a series of male and female Gaucher Disease and Fabry Disease patients were analyzed with the multiplex assay. The obtained data compare well to those previously determined for plasma globotriaosylsphingosine and glucosylsphingosine in GD and FD patients. The same approach can also be utilized to measure sphingolipids in the same sample. After extraction of sphingolipids from the same sample these can be converted to sphingoid bases through microwave exposure and next quantified using ^{13}C-encoded internal standards.

Introduction

Previously we reported on marked increases of globotriaosylsphingosine (lysoGb3) in Fabry disease (FD) patients and glucosylsphingosine (GlcSph) in Gaucher disease (GD) patients[1–4]. Similarly, galactosylsphingosine (GalSph) is known to be elevated in Krabbe disease (KD), lysosulfatide in Metachromatic Leukodystrophy (MLD), phosphorylcholine-sphingosine (lysoSM) in Niemann Pick type A/B disease as well as lysoSM and GlcSph in Niemann Pick type C disease (NPC)[5–9]. Quantitation of elevated sphingoid bases has great diagnostic value for all these disorders. In place are validated measurements of lysoGb3 and hexosyl-sphingosine (HexSph, is GlcSph and/or GalSph) by UPLC-ESI-MS/MS with identical [13]C$_5$-encoded standards. The use of identical internal standards in these measurements offers compensation for losses during extraction, ionization efficiency and mass spectrometric performance.

No correction for the sample matrix, such as ion suppression and in some cases ion enhancement, is necessary. [13]C$_5$-encoded lysoGb3, GlcSph, sphingosine (Spho) and sphinganine (Spha) have been synthesized by us[2,10]. We now developed and validated a convenient method for simultaneous UPLC-ESI-MS/MS quantitation of plasma sphinganine, sphingosine, GlcSph, LacSph (lactosylsphingosine), lysoGb3 and lysoSM using isotope-encoded standards and C17-lysoSM. The sample preparation requires just 50 µL of plasma and implies lipid extraction according to modified Bligh and Dyer with acidic buffer. Excellent sensitivity, high accuracy and good reproducibility are obtained with the described method. We additionally show that from the same sample sphingolipids (ceramide, hexosyl-ceramide, hexosyl$_2$-ceramide, and hexosyl$_3$-ceramide) can be quantified with the same method. For this, sphingolipids are extracted, deacylated by microwave exposure and the obtained sphingoid bases are quantified with corresponding standards.

Results

Assay validation

Calibration curves.
A linear response was obtained over the entire concentration range (M&M), R^2 for each sphingoid bases exceeded 0.995 (data not shown).

Intra- and inter-assay validation.
Different concentrations of non-labeled C18 bases (M&M) were added to control plasma from a healthy subject. Samples were separately extracted six times to examine the intra-assay variation. To examine inter-assay variation the same plasma specimens were extracted and measured six times on subsequent days. Figure 1 shows the inter- and intra-assay variations for the individual sphingoid bases. The intra- and inter-assay variation was on average 4.58 % and 9.83 %, respectively (ranges 1.34-14.54 % and 1.28-19.28 %, respectively), (see also table 1 in supplemental information). The limit of detection (LOD) for GlcSph, LacSph, lysoGb3 and lysoSM was 0.05 nmol/L, and for sphingosine and sphinganine 0.08 nmol/L. The LOQ for

GlcSph, LacSph, lysoGb3 and lysoSM was 0.15 nmol/L, and for sphingosine and sphinganine 0.45 nmol/L.

Effect of different storage conditions and stability of sphingoid bases.
Plasma samples, identical to the ones described above, were stored for 1 wk at -20˚ C, 4˚ C and RT. As presented in figure 2, no significant differences in levels of various bases when stored at different conditions were observed. The levels of bases were similar to those in the directly used same plasma sample (figure 1 and table 2 in supplemental information), indicating acceptable stability. Excellent stability of the sphingoid bases lysoGb3 and GlcSph was previously noted by us and others[3,11].
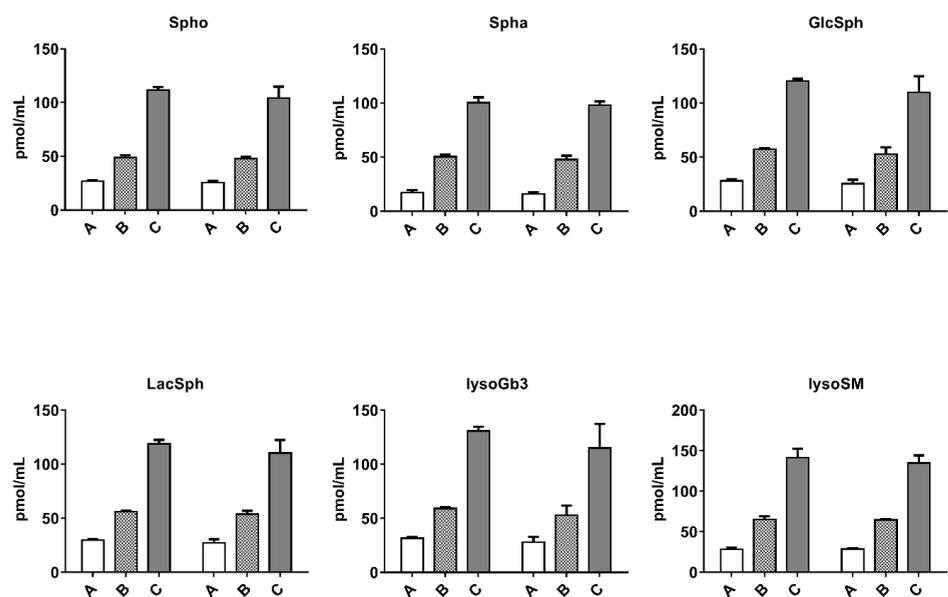

Figure 1. Intra-assay and inter-assay validation. Left bars represent intra-assay and right bars represent inter-assay validation. A, B and C are different concentrations of spike of equal amounts of lyso-glycosphingolipids in control plasma, 20, 50 and 100 pmol/mL respectively.

UPLC-ESI-MS/MS quantitation of sphingoid bases in female and male control, GD and FD plasma specimens.
We then simultaneously quantified sphingoid bases in plasma specimens of control subjects (males n=21, females n=21) by a single extraction, in plasma of GD patients (males n=10, females n=10) in duplicate and in plasma of FD patients (males n=10, females n=10) in duplicate (see figure 3). Significant elevations of Hex_3Sph (=lysoGb3) in male FD patients and to a more modest extent in female FD patients were detected, exactly as noted before[1,12].

Notably, plasma lysoGb3 tended to be increased in male and female GD patients, again described previously[12]. As expected, plasma HexSph (=GlcSph) was found to be clearly increased in all GD patients[3]. Plasma sphingosine in GD patients was higher than in gender matched controls or FD patients, except for FD females. Plasma sphinganine levels were comparable in the case of controls and LSD patients, except for FD males showing a significantly lower level. Notably, plasma lysoSM and presumed LacSph were significantly elevated in GD patients. The plasma Hex_2Sph was significantly elevated in GD males and females. A much smaller, but significant, elevation was noted for FD males and females. The plasma Hex_2Sph (at least in GD patients) therefore appears to be mostly LacSph and not the indistuinguishable Gal_2-Sph; Gal_2-Cer and its base are expected to be increased in FD since they are both substrates of the deficient α-galactosidase A in FD.
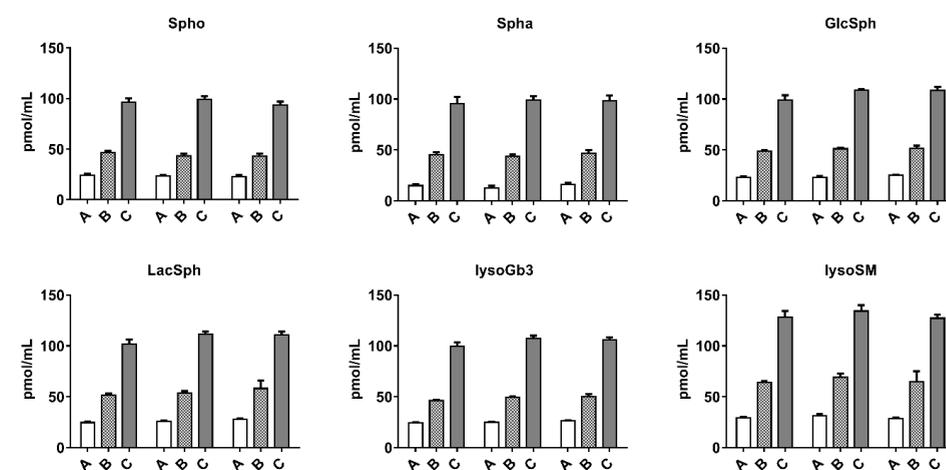

Figure 2. Sphingoid bases in plasma stored for 1 week at different conditions. From left to right bars, samples kept in freezer (-20°C), fridge (4°C) and room temperature. A, B and C are different concentrations of spiked equal amounts of lyso-GSLs in control plasma, 20, 50 and 100 pmol/mL respectively. Presented data were calculated with correction for the appropriate blanks.

Effect of contraceptives in females.
We studied the influence of the oral use of contraceptives (OC) by females on their plasma sphingoid bases. Significantly lower levels of plasma GlcSph were detected in OC females (see figure 4). This difference could not be ascribed to an age difference (see supplemental information figure 2).
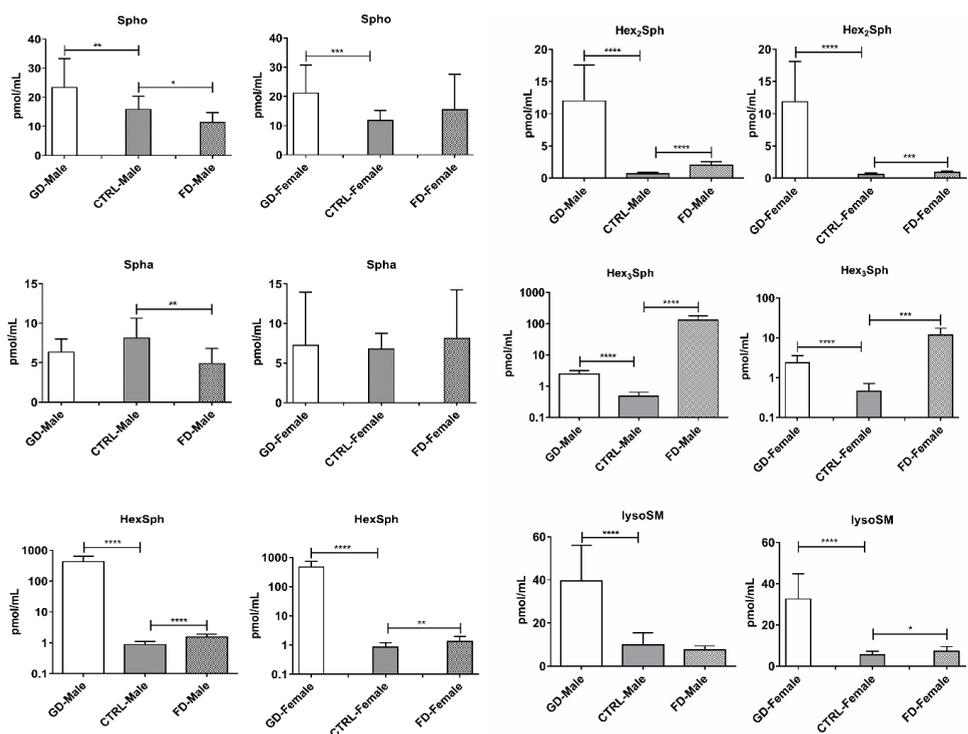
Figure 3. Levels of various sphingoid bases in plasma specimens of male and female control subjects, symptomatic GD and FD patients. Sphingoid bases were simultaneously quantified as described in Materials and Methods. To assist comparison the levels of sphingoid bases in control plasma are depicted as the central bar. Significance of differences: * $P < 0.05$, ** $P < 0.01$, *** $P < 0.001$ and **** $P < 0.0001$.

Concomitant determination of neutral (glyco)sphingolipids in same plasma sample following their deacylation to sphingoid bases.

We next investigated whether the described analysis of sphingoid bases can be used to develop a convenient procedure for accurate quantitation of sphingolipids in the same sample. It is possible to separate sphingolipids and sphingoid bases during extraction, the bases partitioning in the upper water phase and sphingolipids in the lower chloroform phase. Sphingolipids can then be microwave-assisted deacylated[13,14] and the resulting sphingoid bases can subsequently be analyzed precisely as the sphingoid bases collected from the upper phase of the extraction. Like this, parallel data could be generated for sphingolipid and sphingoid bases in the same sample.

To study the feasibility of this approach, we first spiked C18-Cer, C18-GlcCer, C18-LacCer and C18-Gb3 into normal plasma. Also C17-dhCer was added to be used as alternative internal standard. Following the procedure precisely as defined in M&M, the recoveries of all spiked lipids were high, either when using $^{13}C_5$ lyso-GSL as internal standard or C17-dhCer as

internal standard to calculate absolute amounts of lipid (see table 1). The linearity of detection was high for Cer, dhCer, GlcCer, LacCer and Gb3, exceeding in all cases 0.96 (see table 3 supplemental information).
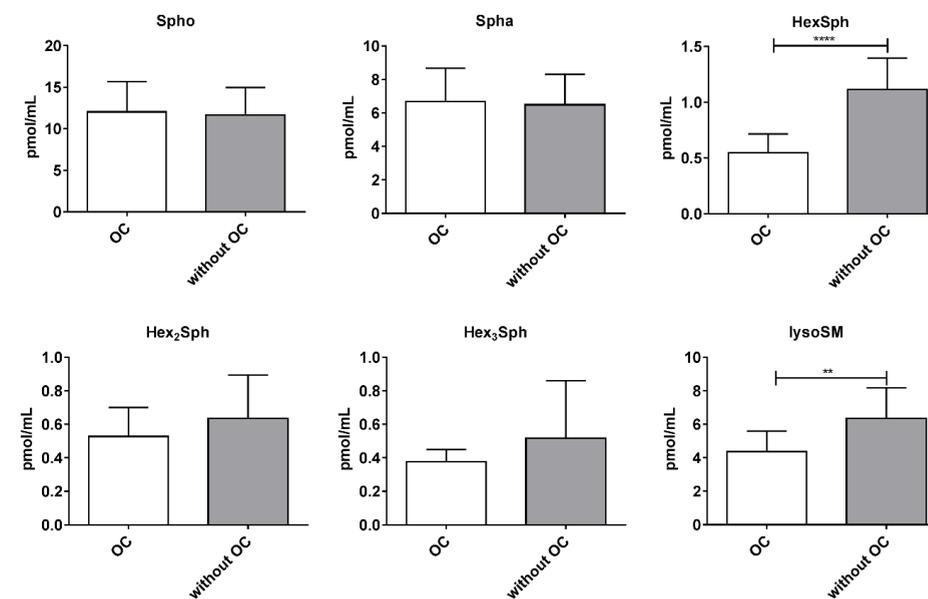

Figure 4. Levels of various sphingoid bases in plasma specimens of female using oral contraceptives (OC) or not. Sphingoid bases were simultaneously quantified as described in Materials and Methods. To assist comparison the levels sphingoid bases in control plasma are depicted as the central bar. Significance of differences: ** $P < 0.01$ and **** $P < 0.0001$.

Table 1. Recovery of spiked sphingolipids lipids.

%	C18-Cer	C18-GlcCer	C18-LacCer	C18-Gb3
$^{13}C_5$ lyso-GSL	96.9	84.9	98.8	92.9
C17-dhcer	108.7	99.2	110.7	104.5

Subsequently, we determined the concentrations of endogenous sphingolipids (Cer, dhCer, HexCer, Hex$_2$Cer and Hex$_3$Cer) in plasma using $^{13}C_5$- sphingoid bases as standards in a variety of plasma samples, see table 2. Quite similar data were acquired with C17-dhCer as internal standard (see supplemental information table 4 and figure 3 supplemental information).

Table 2. Quantitation of plasma (glyco)sphingolipids (Cer, dhCer, HexCer, Hex$_2$Cer and Hex$_3$Cer).

Plasma sample ^{13}C$_5$ lyso-GSLs (IS)		Cer nmol/mL	dhCer nmol/mL	HexCer nmol/mL	Hex$_2$Cer nmol/mL	Hex$_3$Cer nmol/mL
CTRL Male	Mean	5.30	0.57	3.28	1.86	0.63
	SD	0.26	0.04	0.59	0.51	0.32
FD Male 1	Mean	3.18	0.33	2.54	1.71	2.77
	SD	0.14	0.00	0.24	0.15	0.11
FD Male 2	Mean	4.13	0.48	3.51	1.87	0.93
	SD	0.16	0.02	0.43	0.24	0.14
GD Male 1	Mean	2.61	0.42	7.47	1.69	0.50
	SD	0.13	0.01	1.46	0.21	0.04
GD Male 2	Mean	2.59	0.40	8.96	1.77	0.44
	SD	0.05	0.01	1.60	0.33	0.08
CTRL Female	Mean	4.78	0.69	3.82	1.73	0.66
	SD	0.84	0.02	0.43	0.26	0.12
FD Female 1	Mean	4.30	0.50	4.01	2.49	0.94
	SD	0.01	0.00	0.22	0.11	0.03
FD Female 2	Mean	6.28	0.92	4.87	2.13	0.77
	SD	0.21	0.02	0.31	0.36	0.09
GD Female 1	Mean	4.99	0.63	13.61	2.53	0.85
	SD	0.02	0.06	0.18	0.19	0.21
GD Female 2	Mean	2.99	0.51	6.45	1.27	0.36
	SD	0.26	0.00	0.74	0.29	0.08

Discussion

We here show the feasibility of simultaneous quantitation of the sphingoid bases sphinganine, sphingosine, HexSph (GlcSph), Hex$_2$Sph (LacSph), Hex$_3$Sph (lysoGb3) and lysoSM in plasma specimens by UPLC-ESI-MS/MS and identical ^{13}C$_5$-encoded internal standards, with the exception of LacSph and lysoSM. For LacSph no isotope-encoded standard was available. In the case of ^{13}C$_5$-lysoSM there was background in plasma and superior quantitation was obtained with C17-lysoSM as standard. The sensitivity and linearity of detection is excellent for all examined sphingoid bases in the relevant concentration range and the measurements display very acceptable intra- and inter-assay variation. Plasma samples of a series of male and female GD and FD patients were analyzed with this multiplex method. The acquired data compare well to those prior determined for plasma lysoGb3 and GlcSph in GD and FD patients[2,3,12]. Very recently Polo and colleagues described a method for concurrent measurements of HexSph, lysoGb3, lysoSM and lysoSM-509[11]. Their procedure employs the same equipment as our study, but differs in the used extraction method and the use of a single internal standard (GlcSph from plant source). Polo et al. report rather similar accuracy,

linearity of detection and inter- and intra-assay variation as stated here. They verified the value of their procedure by analysis of plasma from 194 control subjects, 16 FD patients, 10 GD patients, 3 KD patients and 11 NPC patients. The stated values for lysoGb3 and GlcSph in control subjects, GD and FD patients differ somewhat from ours[11]. For instance, in control plasma the median value for lysoGb3 was 0.29 nmol/L and for HexSph 2.09 nmol/L. In our study, in male control plasma the median value for lysoGb3 (Hex$_3$Sph) was 0.47 nmol/L and for HexSph 0.87 nmol/L; in female control plasma these were 0.45 nmol/L and 0.84 nmol/L, respectively. Hence, we quantified higher amounts of lysoGb3 but smaller ones for HexSph. These differences might be because of differences in the used internal standards. Theoretically, the use of a non-identical internal standard is less attractive because of possibly needed corrections for sample matrix effects such as ion suppression and in some cases ion enhancement.

Our investigation confirms the occurrence of modestly increased levels of other sphingoid bases (LacSph, lysoGb3 and lysoSM) in plasma of symptomatic GD patients. The levels of lysoGb3 in GD females actually overlap with those in female FD patients. We previously pointed out that caution is needed when interpreting modest elevations in plasma lysoGb3 as confirmative for (atypical) FD[12,15]. The non-specific modest increases in lysoGb3, LacSph and lysoSM in plasma of GD patients are presumably caused by activation of acid ceramidase in lysosomes of lipid-laden macrophages (Gaucher cells) resulting in deacylation of various sphingolipids[12]. Another interesting discovery made in the study is the noted lowering effect of oral contraceptives on plasma GlcSph level. It has been prior reported that OC use is associated with decrease of plasma GlcCer[16]. This glycosphingolipid serves as a cofactor for activated protein C (APC), an anti-coagulant. Diminished GlcCer has consequently been proposed to endorse the raised risk of venous thrombosis in females using OCs[16]. It has previously been described that estradiol reduces GlcCer by inhibiting its synthesis, while testosterone has contrary effects[17].

Since it is possible to separate sphingolipids and sphingoid bases by differential extraction and the obtained sphingolipids can next be de-acylated, either microwave-assisted or by enzymatic digestion with ceramide N-deacylase[13,14,18,19], we looked into the possibility to develop a method for convenient simultaneous quantitation of sphingolipids and sphingoid bases in the same plasma sample. We applied microwave exposure for the de-acylation of extracted sphingolipids. We concluded from the extremely poor recovery of spiked sphingomyelin standard that this procedure cannot be used for this sphingolipid. Nevertheless, for the other (glyco)sphingolipids tested (Cer, GlcCer, LacCer and Gb3) the recovery was excellent and quantitation was linear. Clearly, no data are obtained on the fatty acyl composition of the sphingolipids with this method, but the offered absolute quantitation of sphingolipids is likely superior to that reached by shot gun lipidomics or other methods based on scanning for isoforms of a sphingolipid.

To conclude, sensitive simultaneous quantitation of (glyco)sphingoid bases is feasible with LC-MS/MS using ^{13}C-encoded internal standards requiring a small amount of plasma. Potentially an extended method can be developed to also determine absolute amounts of

specific (glyco)sphingolipids after their deacylation and quantitation of the corresponding bases.

Materials and Methods

Chemicals and reagents

LC-MS–grade methanol, 2-propanol, water, formic acid and HPLC-grade chloroform were purchased from Biosolve (Valkenswaard, The Netherlands). LC-MS grade ammonium formate and sodium hydroxide were from Sigma-Aldrich Chemie GmbH (St Louis, USA), butanol and hydrochloric acid were from Merck Millipore (Billerica, USA). C18-lysoSM and C18-lysoGb3 were from Avanti (Albaster, USA). $^{13}C_5$-sphinganine, $^{13}C_5$-sphingosine, $^{13}C_5$-GlcSph and $^{13}C_5$-lysoGb3 were synthesized at the Department of Bio-organic Synthesis of the Leiden Institute of Chemistry, Leiden University[10]. The label was incorporated in C5, 6, 7, 8, and 9 of the sphingosine backbone (see fig 5). C18-sphingosine, C18-sphinganine, C18-GlcSph, C18-lactosylsphingosine and C17-lysoSM were obtained from Avanti. C17-dihydroceramide (C17-dhCer) was synthesized in house (see scheme 1); C17-sphinganine, C18-ceramide (Cer), C18-glucosylceramide (GlcCer) and Lactosylceramide (LacCer) were purchased from Avanti and C18-globotriaosylceramide (Gb3) from Matreya (State College, USA).
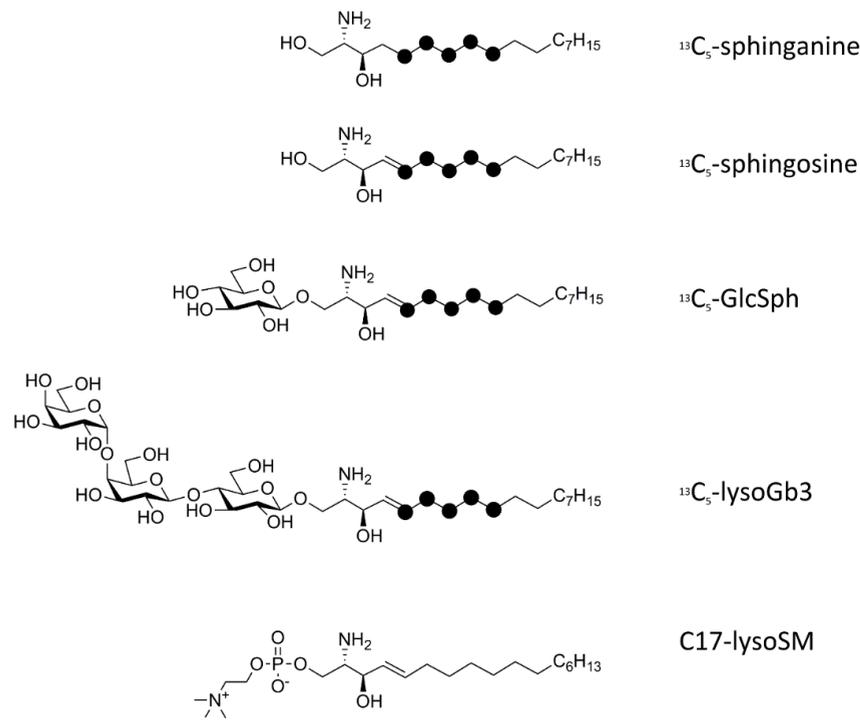

$^{13}C_5$-sphinganine

$^{13}C_5$-sphingosine

$^{13}C_5$-GlcSph

$^{13}C_5$-lysoGb3

C17-lysoSM

Figure 5. Structures of internal standards.

Synthesis of C17-dihydroceramide

The synthesis of C17-dhCer started with acetylation of commercial C17-sphinganine. C17-sphinganine (5 mg, 0.016 mmol, 1 eq) was dissolved in tetrahydrofuran (THF) (0.2 mL) and sat. aq. NaOAc (0.2 mL), was added. Palmitoyl chloride (6.6 µL, 0.022 mmol, 1.3 eq) was added and the reaction mixture was stirred vigorously at room temperature for 3 hours. The mixture was diluted with THF (5 mL) and washed with water (5 mL). The water layer was extracted with THF (3x 5 mL) and the combined organics were dried (MgSO4), filtered and concentrated *in vacuo*. The C17-dhCer was purified by silica column chromatography (chloroform to 5% MeOH in chloroform) giving a white solid (6 mg, 0.011 mmol, 72%). R_f = 0.5 (5% MeOH in chloroform), ^{1}H NMR (400 MHz, CDCl3) δ 6.36 (d, 1 H, *J* = 7.6 Hz), 4.01 (d, 1 H, *J* = 11.3 Hz), 3.83 (m, 1 H), 3.80-3.72 (m, 2 H), 2.90-2.50 (bs, 2 H), 2.23 (t, 2 H, *J* = 7.4 Hz), 1.68-1.59 (m, 4 H), 1.59-1.45 (m, 2 H), 1.38-1.19 (m, 44 H), 0.88 (t, 6 H, *J* = 7.2 Hz); ^{13}C NMR (101 MHz, CDCl3) δ 173.6, 74.4, 62.7, 54.2, 37.1, 34.7, 32.10, 29.86 x4, 29.84 x3, 29.82 x3, 29.79x 2, 29.75 x3, 29.72, 29.71, 29.67, 29.66, 29.52, 29.51, 29.48, 22.84, 14.2.
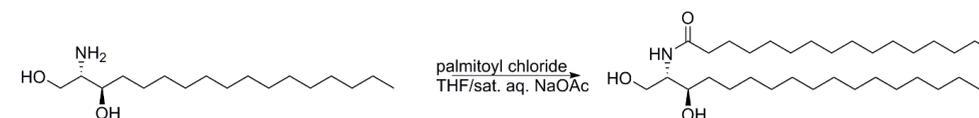
Scheme 1. C17-dihydroceramide (C17-dhCer) synthesis.

Samples

All plasma samples were prepared from EDTA-anticoagulated blood by centrifugation and stored at −20 °C until analysis. Approval had been obtained from the institutional ethics committee and informed consent according to the Declaration of Helsinki.

Internal standard mixture

An internal standard mixture (ISM) of isotope-labeled and C17-lysoSM standards was made in methanol containing an equal concentration of each internal standard with the concentration of 0.1 pmol/µL (0.1 µM). To 50 µL of plasma sample 25 µL of ISM was added as spike. This is 50 nmol/L plasma.

Assay validation

Calibration curves for C18-sphingosine, C18-sphinganine, C18-lysoGb3, C18-LacSph, C18-GlcSph and C18-lysoSM were constructed in plasma of healthy controls: 0-1-2-5-10-20-50-100-200-500-1000 nmol/L. As internal standard ISM (25 µL of 0.1 pmol/µL) was used. Plasma was spiked with equal amounts of C18 sphingoid bases. Equimolar amounts of C18-sphingosine, C18-sphinganine, C18-lysoGb3, C18- LacSph, C18-GlcSph and C18-lysoSM were added to plasma.

Intra and inter-assay variation

For the determination of intra-assay variation control plasma was spiked with three different concentrations of all C18 bases (A: added 20 pmol/mL, B: added 50 pmol/mL and C: added 100 pmol/mL) and extracted in 6-fold, one without internal standards and five with internal standards. The same control plasma specimen without any spike was also extracted in 6-fold one without internal standards and five with internal standards. Extraction and measurement of samples was repeated on a following day to determine inter-assay variation.

Limit of detection (LOD) and Limit of quantitation (LOQ)

The LOD is defined as signal-to-noise ratio of 3 (peak to peak). The LOQ is defined as signal-to-noise ratio of 10 (peak to peak).

Stability assessment

Samples were tested under three different conditions: freezer (-20°C), fridge (4°C) and room temperature. After preparation of plasma samples, the samples were stored in different conditions for one week. The samples were extracted and measured on the same day. For each condition, three differently spiked plasma controls (A, B and C) were extracted in 6-fold, one without internal standards and five with internal standards. Same control plasma without any spike was also extracted in 6-fold, one without internal standards and five with internal standards.

Studied plasma specimens of healthy volunteers (CTRLs), GD and FD patients

Plasma lyso-sphingolipids were measured for male (n=21) and female CTRLs (n=21), GD (n=10 each gender) and FD patients (n=10 each gender). Of the female CTRLs 10 were using oral contraceptives, and 11 were not.

Lipid extraction

Sphingoid bases were extracted from plasma by a modified Bligh and Dyer extraction[20] using acidic buffer (100 mM ammonium formate buffer pH 3.1). Plasma (50 µL) was pipetted into a 1.5 mL Eppendorf tube with a screw cap. Next 25 µL of ISM was added. To this, 350 µL methanol (or 325 µL methanol + 25 µL ISM) and 175 µL chloroform were added and stirred. The sample was subsequently incubated for 10 min at room temperature and stirred occasionally, then centrifuged for 10 min at 15,700 ×g to precipitate protein. The supernatant was transferred to a clean tube, 175 µL chloroform and 265 µL buffer were added. After stirring the sample for 1 min, the tube was centrifuged for 5 min at 15,700 ×g. The upper phase was transferred to a clean tube (extract A). To the lower phase (chloroform phase) 350 µL methanol and 315 µL buffer were added and stirred for 1 min. The sample was then centrifuged for 5 min at 15,700 ×g and the upper phase was removed and pooled with extract A. This was dried at 45 ˚C in an Eppendorf Concentrator Plus. The residue was further extracted with 500 µL butanol and 500 µL H_2O stirred for 1 min and centrifuged for 5 min at 15,700 ×g. The upper phase (butanol phase) was transferred to a clean tube and taken to dryness in Eppendorf Concentrator Plus at 45 ˚C. The residue was dissolved in 100 µL methanol, stirred and sonicated in a bath for 30 seconds and centrifuged for 5 min at 15,700 ×g. Finally, 10 µL of the solution was applied to the UPLC-MS.

Table 3. LC parameters.

UPLC				
Column	Acquity BEH C18 column, 2.1 × 50 mm with 1.7 µm			
Column temperature	23 ˚C			
Wash	MeOH: H_2O (50:50)			
Mobile phase A	H_2O, 1 mM ammonium formate, 0.5 % Formic acid			
Mobile phase B	MeOH, 1 mM ammonium formate, 0.5 % Formic acid			
Gradient				
Time (min)	Flow (mL/min)	% A	% B	Curve
Initial	0.25	100	0	Initial
2.5	0.25	0	100	6
5.05	0.25	0	100	6
6.00	0.25	100	0	6
6.50	0.25	100	0	6

Table 4. MS/MS parameters.

MS/MS parameters					
Mass spectrometer	Xevo-TQS-Micro (Waters)				
Ionization mode	ESI[+]				
Capillary voltage	3.50 kV				
Source temperature	150 ˚C				
Desolvation temperature	450 ˚C				
Cone gas flow	50 L/h				
Desolvation gas flow	950 L/h				
Dwell time	0.05 s				
MS Inter-Scan	0.005 s				
Inter-channel delay	0.005 s				
Compound	**Parent (m/z)**	**Daughter (m/z)**	**Cone voltage (V)**	**Collision energy (V)**	**Retention time (min)**
Sphingosine	300.3	282.3	20	15	3.39
Sphinganine	302.3	284.3	20	15	3.42
$^{13}C_5$-sphingosine (IS)	305.3	287.3	20	15	3.37
$^{13}C_5$-sphinganine (IS)	307.3	289.3	20	15	3.42
C17-lysoSM (IS)	451.4	184.4	20	25	3.24
lysoSM	465.4	184.4	20	25	3.31
GlcSph	462.3	282.3	30	20	3.33
$^{13}C_5$-GlcSph (IS)	467.3	287.3	30	20	3.33
LacSph	624.4	282.3	43	30	3.28
lysoGb3	786.4	282.3	55	40	3.29
$^{13}C_5$-lysoGb3 (IS)	791.4	287.4	55	40	3.27

LC-MS/MS

Measurements were performed by reverse-phase liquid chromatography with a Waters UPLC-Xevo-TQS micro and a BEH C18 column, 2.1 × 50 mm with 1.7 µm particle size (Waters, USA) using the following eluents: eluent A was 1 mM ammonium formate and 0.5 % formic acid in water. Eluent B was 1 mM ammonium formate and 0.5 % formic acid in methanol. A mobile-phase gradient was used during a 6.50 min run: 0.00 min 0% B; 2.50 min 100% B; 5.05 min 100% B; 6.00 min 0% B; 6.50 min 0% B. The flow rate was 0.25 mL/min. The eluent was diverted to waste between 0.00 and 2.00 min to keep the source free of contaminants; data were collected between 2.00 and 5.05 min, and after 5.05 min the eluent was again diverted to waste. Mass spectrometry detection in positive mode using an electrospray ionization (ESI) source was performed with a Xevo TQS micro instrument. Data were analyzed with Masslynx 4.1 Software (Waters Corporation; Milford MA). All LC and MS/MS parameters are presented in Table 3 and Table 4.

In figure 6 chromatograms of various sphingoid bases and the $^{13}C_5$ isotope analogues are displayed. Of note, the chromatography used is not able to separate GlcSph and GalSph. Therefore these (HexSph) lipids in biological samples will not be separately quantified. Similarly, the chromatography not necessarily separates Glu-Gal-Sph (LacSph) from Gal-Gal-Sph (Gal$_2$-Sph). Again, these (Hex$_2$Sph) lipids are *a priori* not separately quantified. Though lysoSM and GlcSph are not separated by the chromatography, their separate quantitation is feasible by their distinct parent and daughter *m/z* values (see table above).
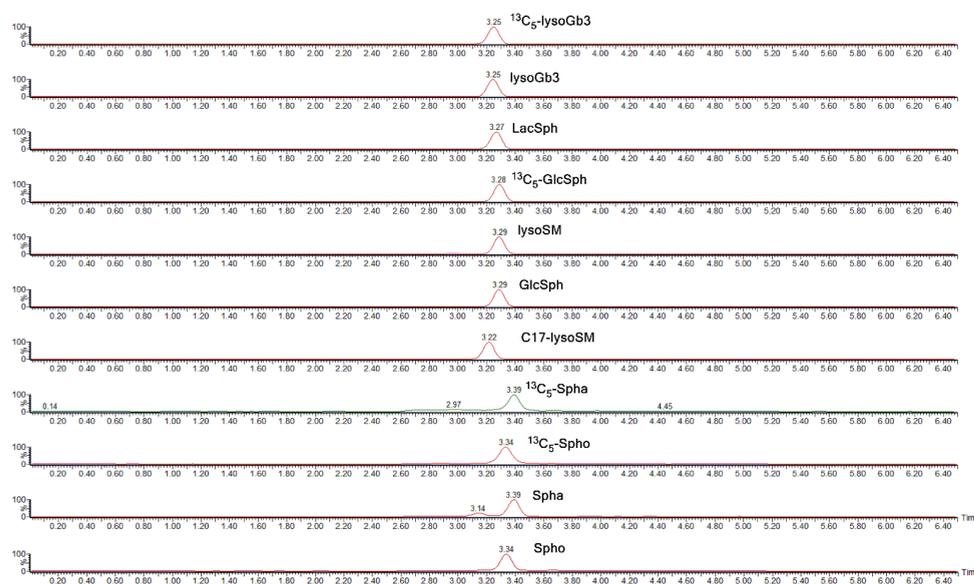

Figure 6. Chromatogram of lyso(glyco)sphingolipids and their internal standards.

Determination of neutral (glyco)sphingolipids (NGSL) in the same sample

Plasma was subjected to the modified Bligh and Dyer extraction precisely as designated above. In some experiments, 50 µL of C17-dhCer (20 µM) was added to the sample to establish efficiency of deacylation, generate calibration curves and for comparison with the use of ^{13}C-encoded lyso-lipids as internal standards. The lower phase of the extraction procedure was transferred to a Pyrex tube, dried at 45 ˚C under the gentle stream of nitrogen gas. The residue was dissolved in 500 µL of methanolic NaOH (0.1 M) by stirring. After putting the screw cap tightly on the tube, the sample was placed in the microwave for 1 hour for deacylation[13]. The sample was cooled down and stirred well. Subsequently, 200 µL of deacylated sample was transferred to a 1.5 mL Eppendorf tube with a screw cap and 20 µL of methanolic HCl (1 M) was added to neutralize the sample. 80 µL of $^{13}C_5$ lyso-GSL ISM (5 pmol/µL of each standard) was added to the sample. The sample was dried in an Eppendorf concentrator Plus at 45 ˚C. Then the samples were handled precisely as designated above via butanol extraction and 10 µL of the solution was applied to the UPLC-MS. All plasma samples were extracted in duplicate. Pooled plasma of normal males (two sets of 4 individuals), pooled plasma of 4 healthy females using a contraceptive and that of 4 females not using a contraceptive was analyzed. Moreover, plasma of 2 male GD patients, 2 female GD patients, 2 male FD patients and 2 female FD patients were analyzed (see supplemental information figure 1).

Calibration curves of NGSL in normal control plasma were constructed as follows. Normal plasma was spiked with a mixture of C18-Cer, C18-GlcCer, C18-LacCer, C18-Gb3 (1pmol/µL). The concentrations of each NGSL were 0-0.2-0.4-1-2-5-10-20 nmol/mL plasma. NGSL and C17-dhCer were added before acidic extraction. Deacylation of C17-dhCer to C17-Spha was monitored by detection of m/z 288.3 > 270.3 (cone (v) 20, Collision(v) 15). The mixture of $^{13}C_5$ lyso-GSL ISM was added after the microwave step.

Statistical Analysis

Values in figures are presented as mean ± S.D. Data were analyzed by unpaired Student's t-test using GraphPad Prism. *P* values < 0.05 were considered significant. * *P* < 0.05, ** *P* < 0.01, *** *P* < 0.001 and **** *P* < 0.0001.

References

1. Aerts, J. M. *et al.* Elevated globotriaosylsphingosine is a hallmark of Fabry disease. *Proc. Natl. Acad. Sci.* **105,** 2812–2817 (2008).
2. Gold, H. *et al.* Quantification of Globotriaosylsphingosine in Plasma and Urine of Fabry Patients by Stable Isotope Ultraperformance Liquid Chromatography-Tandem Mass Spectrometry. *Clin. Chem.* **59,** 547–556 (2013).

3. Mirzaian, M. *et al.* Mass spectrometric quantification of glucosylsphingosine in plasma and urine of type 1 Gaucher patients using an isotope standard. *Blood Cells, Mol. Dis.* **54,** 307–314 (2015).

4. Ferraz, M. J. *et al.* Gaucher disease and Fabry disease: New markers and insights in pathophysiology for two distinct glycosphingolipidoses. *Biochim. Biophys. Acta - Mol. Cell Biol. Lipids* **1841,** 811–825 (2014).

5. Igisu, H. & Suzuki, K. Analysis of galactosylsphingosine (psychosine) in the brain. *J. Lipid Res.* **25,** 1000–6 (1984).

6. Chuang, W.-L. *et al.* Determination of psychosine concentration in dried blood spots from newborns that were identified via newborn screening to be at risk for Krabbe disease. *Clin. Chim. Acta.* **419,** 73–6 (2013).

7. Chuang, W.-L. *et al.* Lyso-sphingomyelin is elevated in dried blood spots of Niemann-Pick B patients. *Mol. Genet. Metab.* **111,** 209–11 (2014).

8. Vanier, M. T. *et al.* Diagnostic tests for Niemann-Pick disease type C (NP-C): A critical review. *Mol. Genet. Metab.* **118,** 244–54 (2016).

9. Welford, R. W. D. *et al.* Plasma lysosphingomyelin demonstrates great potential as a diagnostic biomarker for Niemann-Pick disease type C in a retrospective study. *PLoS One* **9,** e114669 (2014).

10. Wisse, P. *et al.* Synthesis of a Panel of Carbon-13-Labelled (Glyco)Sphingolipids. *European J. Org. Chem.* **2015,** 2661–2677 (2015).

11. Polo, G. *et al.* Diagnosis of sphingolipidoses: a new simultaneous measurement of lysosphingolipids by LC-MS/MS. *Clin. Chem. Lab. Med.* **55,** 403–414 (2017).

12. Ferraz, M. J. *et al.* Lysosomal glycosphingolipid catabolism by acid ceramidase: formation of glycosphingoid bases during deficiency of glycosidases. *FEBS Lett.* **590,** 716–25 (2016).

13. Groener, J. E. M. *et al.* HPLC for simultaneous quantification of total ceramide, glucosylceramide, and ceramide trihexoside concentrations in plasma. *Clin. Chem.* **53,** 742–7 (2007).

14. Taketomi, T., Hara, A., Uemura, K., Kurahashi, H. & Sugiyama, E. A microwave-mediated saponification of galactosylceramide and galactosylceramide I3-sulfate and identification of their lyso-compounds by delayed extraction matrix-assisted laser desorption ionization time-of-flight mass spectrometry. *Biochem. Biophys. Res. Commun.* **224,** 462–7 (1996).

15. Schiffmann, R., Fuller, M., Clarke, L. A. & Aerts, J. M. F. G. Is it Fabry disease? *Genet. Med.* **18,** 1181–1185 (2016).

16. Deguchi, H., Bouma, B. N., Middeldorp, S., Lee, Y. M. & Griffin, J. H. Decreased plasma sensitivity to activated protein C by oral contraceptives is associated with decreases in plasma glucosylceramide. *J. Thromb. Haemost.* **3,** 935–8 (2005).

17. Shukla, A., Shukla, G. S. & Radin, N. S. Control of kidney size by sex hormones: possible involvement of glucosylceramide. *Am. J. Physiol.* **262,** F24-9 (1992).

18. Wing, D. R. *et al.* High-performance liquid chromatography analysis of ganglioside carbohydrates at the picomole level after ceramide glycanase digestion and fluorescent labeling with 2-aminobenzamide. *Anal. Biochem.* **298,** 207–17 (2001).

19. Zama, K. *et al.* Simultaneous quantification of glucosylceramide and galactosylceramide by normal-phase HPLC using O-phtalaldehyde derivatives prepared with sphingolipid ceramide N-deacylase. *Glycobiology* **19,** 767–75 (2009).

20. Bligh, E. G. & Dyer, W. J. A RAPID METHOD OF TOTAL LIPID EXTRACTION AND PURIFICATION. *Can. J. Biochem. Physiol.* **37,** 911–917 (1959).

Supplemental Data

Supplementary Table 1. Intra-assay and inter-assay variation in pmol/mL (n=5).

| Compound	Assay	Mean A	SD	CV%	Mean B	SD	CV%	Mean C	SD	CV%
Sphingosine	Intra	26.76	1.14	4.26	48.89	2.14	4.38	111.65	2.86	2.56
	Inter	25.41	1.92	7.56	47.82	1.51	3.16	104.05	10.75	10.33
Sphinganine	Intra	17.13	2.49	14.54	50.38	2.18	4.33	100.53	4.90	4.87
	Inter	16.02	1.57	9.80	47.86	3.55	7.42	98.07	3.47	3.54
GlcSph	Intra	28.15	1.54	5.47	57.32	0.77	1.34	120.5	2.10	1.74
	Inter	25.54	3.69	14.45	52.92	6.22	11.75	109.82	15.11	13.76
lysoSM	Intra	28.02	2.01	7.17	65.30	3.94	6.03	141.52	11.09	7.84
	Inter	28.70	0.95	3.31	64.71	0.83	1.28	134.84	9.45	7.01
LacSph	Intra	29.59	1.09	3.68	56.01	1.13	2.02	118.86	3.76	3.16
	Inter	27.14	3.46	12.75	53.77	3.17	5.90	110.34	12.05	10.92
lysoGb3	Intra	31.55	1.21	3.84	59.17	1.22	2.10	130.78	4.08	3.12
	Inter	28.08	4.91	17.49	52.77	9.05	17.15	115.09	22.19	19.28
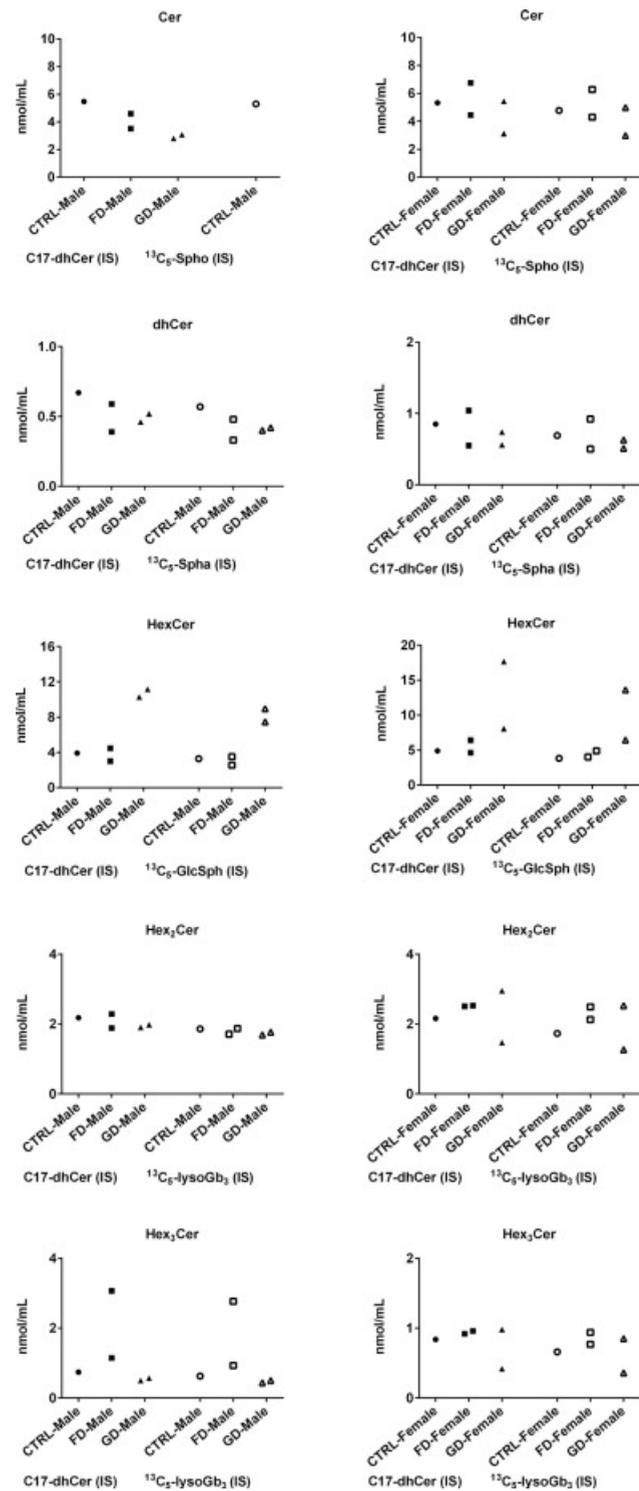
Figure S1. Plasma NGSLs.
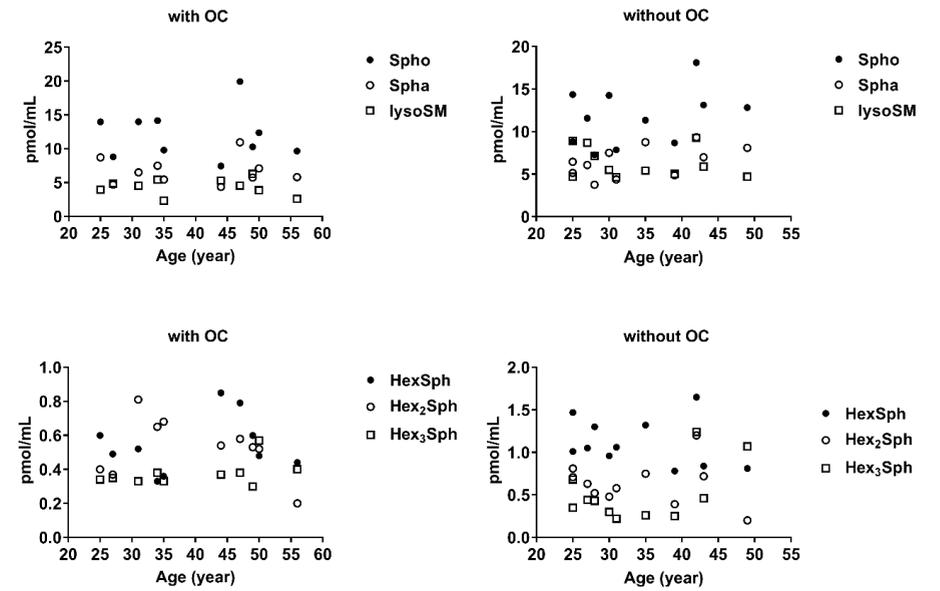
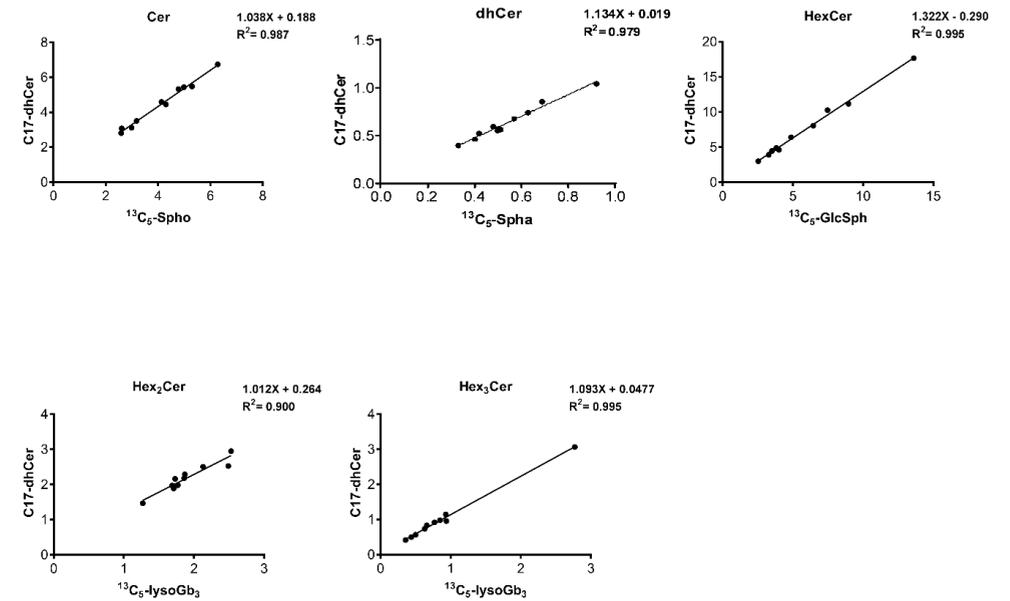Figure S2. Plasma sphingoid bases female with OC versus without OC.

Figure S3. Comparison concentration (in nmol/mL) of NGSLs in human plasma calculated with both internal standards, $^{13}C_5$ lyso-GSLs versus C17-dhCer as the internal standards.

Supplementary Table 2. Stability test in pmol/mL (n=5).

Compound	Assay	Mean A	SD	Mean B	SD	Mean C	SD
Sphingosine	-20°C	24.05	1.51	46.75	1.58	96.45	3.68
	4°C	23.55	0.90	43.47	2.03	99.34	2.83
	RT	22.95	1.56	43.01	2.44	93.52	3.56
Sphinganine	-20°C	14.91	1.13	45.35	2.36	95.62	6.64
	4°C	12.81	1.92	43.61	1.93	99.08	3.80
	RT	16.18	1.80	46.95	2.96	98.13	5.27
GlcSph	-20°C	22.93	0.93	48.53	1.43	99.13	4.67
	4°C	23.23	1.07	51.17	0.96	108.69	0.84
	RT	25.25	0.49	51.64	2.72	108.44	3.56
lysoSM	-20°C	29.37	0.94	64.12	1.29	128.15	6.30
	4°C	31.36	1.80	69.27	3.57	134.19	5.93
	RT	28.38	0.90	64.93	10.24	127.22	3.52
LacSph	-20°C	24.70	0.94	51.53	1.57	101.82	4.40
	4°C	25.98	0.42	53.57	2.06	111.44	2.76
	RT	28.04	0.53	58.24	7.83	110.85	3.33
lysoGb3	-20°C	24.61	0.35	46.37	0.41	99.40	4.14
	4°C	24.75	0.82	49.48	0.75	107.4	2.63
	RT	26.23	0.75	49.97	2.58	105.64	2.85

Supplementary Table 3. NGSLs linearity of detection.

R^2 of calibration line	C17-dhCer as IS	$^{13}C_5$ lyso-GSL as IS
Cer	0.993	0.998
GlcCer	0.962	0.977
LacCer	0.970	0.976
Gb3	0.991	0.995

Supplementary Table 4. Concentration of NGSLs in human plasma.

Gender		C17-dhCer (IS)					$^{13}C_5$ lyso-GSLs (IS)				
		Cer nmol/mL	dhCer nmol/mL	HexCer nmol/mL	Hex$_2$Cer nmol/mL	Hex$_3$Cer nmol/mL	Cer nmol/mL	dhCer nmol/mL	HexCer nmol/mL	Hex$_2$Cer nmol/mL	Hex$_3$Cer nmol/mL
CTRL Male	Mean	5.48	0.67	3.92	2.18	0.74	5.30	0.57	3.28	1.86	0.63
	SD	0.37	0.02	0.67	0.50	0.34	0.26	0.04	0.59	0.51	0.32
FD Male 1	Mean	3.51	0.39	3.00	1.89	3.07	3.18	0.33	2.54	1.71	2.77
	SD	0.15	0.01	0.29	0.26	0.27	0.14	0.00	0.24	0.15	0.11
FD Male 2	Mean	4.60	0.59	4.47	2.29	1.15	4.13	0.48	3.51	1.87	0.93
	SD	0.16	0.02	0.58	0.29	0.15	0.16	0.02	0.43	0.24	0.14
GD Male 1	Mean	3.08	0.52	10.28	1.91	0.57	2.61	0.42	7.47	1.69	0.50
	SD	0.09	0.01	2.07	0.38	0.09	0.13	0.01	1.46	0.21	0.04
GD Male 2	Mean	2.81	0.46	11.17	1.98	0.50	2.59	0.40	8.96	1.77	0.44
	SD	0.07	0.01	1.02	0.29	0.06	0.05	0.01	1.60	0.33	0.08
CTRL Female	Mean	5.33	0.85	4.89	2.16	0.84	4.78	0.69	3.82	1.73	0.66
	SD	1.07	0.03	0.78	0.39	0.15	0.84	0.02	0.43	0.26	0.12
FD Female 1	Mean	4.45	0.55	4.62	2.53	0.96	4.30	0.50	4.01	2.49	0.94
	SD	0.11	0.00	0.21	0.12	0.02	0.01	0.00	0.22	0.11	0.03
FD Female 2	Mean	6.75	1.04	6.41	2.51	0.92	6.28	0.92	4.87	2.13	0.77
	SD	0.41	0.02	0.30	0.20	0.02	0.21	0.02	0.31	0.36	0.09
GD Female 1	Mean	5.44	0.74	17.67	2.95	0.98	4.99	0.63	13.61	2.53	0.85
	SD	0.46	0.03	1.37	0.23	0.09	0.02	0.06	0.18	0.19	0.21
GD Female 2	Mean	3.12	0.56	8.06	1.47	0.42	2.99	0.51	6.45	1.27	0.36
	SD	0.13	0.02	1.01	0.33	0.09	0.26	0.00	0.74	0.29	0.08

Summary

Summary

This thesis describes biochemical investigations of glucocerebrosidase (GBA), the lysosomal β-glucosidase that is deficient in Gaucher disease (GD). Central in the performed research was the examination of factors influencing the intralysosomal stability and half-life of GBA. The investigations made use of new chemical biology tools such as activity based probes (ABPs) and photo-activatable and clickable (PAC) lipids.

Chapter 1 concerns the lysosomal cathepsins involved in proteolytic breakdown of GBA. More detailed knowledge on the responsible enzymes might open a novel avenue for therapy through boosting lysosomal GBA levels by inhibition of a specific protease. Earlier work had revealed that GBA is degraded in lysosomes by cysteine cathepsins, as indicated by the protective effect of leupeptin, a broad-specific protease inhibitor.

The conducted investigation showed that also E64d and the derived activity-based probe DCG-04, protect lysosomal GBA in normal and GD patient fibroblasts and lymphoblasts against proteolytic degradation, as revealed by enzymatic activity assays and labelling of active GBA with activity-based probes. Exposure of cultured GD lymphoblasts to E64d led to a reduction of glucosylsphingosine, the base formed from accumulating GlcCer, indicating a functional correction in GBA capacity. The candidate proteases involved in lysosomal GBA breakdown were narrowed down to cathepsins B, F and L. However, individual reduction of these cathepsins by shRNA or CRISPR-Cas technology was insufficient to significantly reduce the turnover of GBA in cultured cells. Apparently, multiple cysteine cathepsins are able to degrade GBA in lysosomes and need to be concomitantly inhibited to augment lysosomal GBA. Such approach is considered unattractive as therapy given the expected side effects.

Chapter 2 describes the effect of the occupancy of the catalytic pocket of GBA regarding its structural stability *in vitro* and *in vivo*. Glycomimetics are presently designed as chemical chaperones to promote folding and stabilization of GBA in GD patients, but evidence for *in vivo* efficacy of this approach is scarce.

The performed study made use of amphiphilic cyclophellitol-derived activity-based probes (ABPs) that irreversibly bind to the catalytic nucleophile E340. The potent reversible inhibitor isofagomine, a former therapeutic candidate chaperone for GBA, was used for comparison. Cyclophellitol ABPs increased very markedly stability of recombinant GBA *in vitro* as shown by thermodynamic measurements and relative resistance to tryptic digestion. The stabilizing effect of isofagomine on structural stability of pure GBA was less potent. Stabilization by the cell permeable ABP of GBA in cultured normal and Gaucher disease patient cells was reflected by the clear increase in enzyme. GBA in liver of wild-type mice infused with ABP was also found to be stabilized. In conclusion, occupancy of the pocket of GBA by amphiphilic ABPs markedly stabilizes the enzyme. This finding supports the concept of reversible chaperones of GBA as therapeutic agents for Gaucher disease.

Chapter 3 addresses the investigation of GBA with chemical biology tools: pacGlcCer and fluorescent β-glucose configured cyclophellitols binding to the catalytic nucleophile residue E340 in mechanism-based manner. Structure-function relationships in GBA have so far been studied with conventional enzymology and crystallography and relatively little knowledge exists on the aglycon binding moiety of GBA.

The presented study describes that the photo-activatable (diazirine functionalized) and clickable (alkyne containing) pacGlcCer binds with high affinity to the catalytic pocket of active GBA, following the pH optimum of enzymatic activity. GBA hydrolyzes pacGlcCer, further substantiating its ability to enter the catalytic pocket. The binding of pacGlcCer to GBA is completely competed by the reversible inhibitor AMP-DNM as well as the irreversible inhibitors conduritol β-epoxide, cyclophellitol and derived ABP with a fluorophore tag. The labeling of GBA by pacGlcCer is also competed by the substrates glucosylsphingosine, GlcChol and 4-methylumbelliferyl-β-glucose. Cholesterol, an acceptor in the transglucosylation reaction of GBA, also potently inhibits the binding of pacGlcCer, but not that of ABP. The findings indicate specific labeling of GBA by pacGlcCer via its catalytic pocket. It is envisioned that pacGlcCer and ABP labeling of GBA can be used in screens identifying interacting small compounds. To conclude, the available tools offer novel possibilities to probe the glycon- and aglycon-binding sites of the catalytic pocket of GBA.

Chapter 4 reports on the interaction of the lysosomal membrane protein LIMP-2 with GBA. GD is caused by mutations in GBA itself, whereas Action Myoclonus Renal Failure (AMRF) is due to mutations in LIMP-2 that governs transport of newly formed GBA to lysosomes. The deficiency in LIMP-2 results in faulty secretion of GBA in most cell types. Intriguingly, AMRF patients do not develop the characteristic glucosylceramide (GlcCer)-laden macrophages (Gaucher cell) that are a hallmark of GD. Macrophage-targeted GBA with terminal mannose residues in its N-glycans is successfully used in enzyme replacement therapy (ERT) of GD, but for AMRF no treatment is presently available.

The conducted investigation examined the supplementation of LIMP-2 deficient cells with therapeutic mannose-terminated GBA. Studies were conducted with normal and AMRF fibroblasts as well as normal LIMP-2 deficient HEK293 cells transduced with mannose receptor. In LIMP-2 deficient cells, the endocytosed enzyme was found to be abnormally fast degraded in lysosomes. This suggests that transient interactions of GBA with LIMP-2 in the lysosome stabilize the conformation of the enzyme and slow down its proteolytic breakdown. It furthermore implies that the LIMP-2 in lysosomes determines the efficacy of supplementing the organelles with GBA by ERT. In conclusion, the study revealed that LIMP-2 fulfils a dual purpose in the life cycle of GBA, as transporter and as intralysosomal chaperone.

Chapter 5 concerns the fundamentally different clinical manifestation of GD and AMRF, two inherited diseases in which GBA is reduced. In GD, GBA is mutated, whereas in AMRF the normal enzyme is faulty secreted instead of transported to lysosomes. The cellular and biochemical basis for the different symptomatology of GD and AMRF was examined employing a LIMP-2 deficient mouse model.

The study first addressed the possibility that LIMP-2 deficiency not only affects GBA but also other lysosomal proteins. No abnormalities in lysosomal matrix proteins, except GBA, were observed for lysosomes isolated from liver of LIMP-2-deficient mice. Next, LIMP-2-deficient mice were examined regarding residual GBA and lipid abnormalities in various tissues. A variable deficiency of GBA along tissues of LIMP-2 deficient mice was observed, both by enzymatic activity assays and labelling of active enzyme with an activity-based probe. A high residual GBA was detected in leukocytes of LIMP-2 deficient mice, explaining the absence of macrophage-related symptoms in AMRF patients. Evidence was obtained for endocytotic re-uptake of GBA by white blood cells contrary to fibroblasts. Lipid analysis showed that GlcCer is hardly increased in tissues of LIMP-2 deficient mice and that its levels poorly correlate with residual GBA. In contrast, glucosylsphingosine and glucosylated cholesterol are increased and their levels in tissues negatively correlate with GBA levels. Glucosylsphingosine and glucosylated cholesterol were also found to be increased in isolated lysosomes of LIMP2-deficient liver. To conclude, LIMP-2 deficiency results in cell-type specific reduction of GBA and adaptive changes in glycosphingolipid metabolism.

Chapter 6 reviews the evidence for metabolic adaptations in two glycosphingolipidoses, GD and Fabry disease (FD) caused by defects in GBA degrading GlcCer and alpha-galactosidase A (GLA) degrading globotriaosylceramide (Gb3), respectively. The accumulation of the primary storage lipids in cells and tissues of GD and FD patients tends to level with age, suggesting the induction of metabolic adaptations. An important adaptation in GD as well as FD is the active de-acylation of accumulating GSLs in lysosomes by the action of the enzyme acid ceramidase. Thus, the lysosomal lipid storage is limited through formation of glucosylsphingosine (GlcSph) in GD and globotriaosylsphingosine (lysoGb3) in FD. Excessive GlcSph and lysoGb3 are considered to be toxic and contribute to specific symptoms such as multiple myeloma in GD patients and neuronopathic pain and renal failure in FD patients. Another adaptation in metabolism in GD takes place beyond the lysosome, involving the enzyme GBA2 located in the cytoplasmic leaflet of membranes of the ER and Golgi apparatus. GBA2 allows extra-lysosomal degradation of GlcCer and concomitantly generates ceramide (Cer) and glucosylated cholesterol. Specific targeting of the toxicity caused by metabolic adaptations in GD and FD as therapy approach is discussed.

Chapter 7 deals with the catalytic versatility of GBA, a β-glucosidase that until recently was considered to solely cleave GlcCer to Cer and glucose in lysosomes. Special attention is paid to transglycosylation catalyzed by GBA and its specificity for the glycon moiety of substrate.

GBA is known to hydrolyze β-glucosidic substrates and more recently to also transglucosylate cholesterol to cholesterol-β-glucoside (GlcChol). The described study focused on the ability of GBA to metabolize β-xylosides. It is firstly shown that GBA also cleaves 4-methylumbelliferyl-β-D-xylose (4MU-β-Xyl) *in vitro*, being stimulated in this activity by the activator protein saposin C. Next, GBA is shown to *in vitro* transxylosylate cholesterol using 4MU-β-Xyl as sugar donor. Formed xylosyl-cholesterol (XylChol) acts as subsequent acceptor

to render di-xylosyl-cholesterol. Sequential exposure of GBA and cholesterol to 4MU-β-Xyl and 4MU-β-Glc results in formation of GlcXylChol. Similar to GBA, the cytosolic β-glucosidase GBA3 shows *in vitro* β-xylosidase and transxylosylase activity, in contrast to the membrane-bound GBA2 that lacks activity towards β-xylosides. Cultured cells also generate xylosylated cholesterols when exposed to 4MU-β-Xyl in their medium. This synthetic reaction is enhanced by the drug U18666A causing an increase in lysosomal cholesterol. Prior inactivation of GBA in cells with conduritol B-epoxide prohibits formation of xylosylated cholesterols. In conclusion, further catalytic versatility of GBA is revealed: the enzyme may act as β-glucosidase, β-xylosidase, transglucosylase and transxylosylase. The physiological relevance of the noted ability of GBA to metabolize β-xylosides is presently unclear and warrants further examination.

The **Discussion** reviews the present insights into GBA in health and disease. In this connection, the molecular basis and clinical manifestation of Gaucher disease and Action Myoclonus Renal Failure syndrome are discussed, including the metabolic adaptations to GBA deficiency.

Particular attention is paid to the lysosomal structural stability of GBA and associated resistance against proteolytic degradation by cysteine cathepsins. Literature findings and novel own results on this topic are discussed. New technology to study GBA by labeling with GlcCer and cyclophellitol derived probes is introduced and the application is described. Unresolved research questions on GBA and related disease conditions are identified. As future research objective the translation of fundamental knowledge on GBA to effective therapy of neuronopathic Gaucher disease and other disease conditions caused by enzyme reduction are discussed.

The **Addendum** describes a newly developed multiplex assay for simultaneous quantitation of (lyso)-glycosphingolipid bases in plasma samples by use of UPLC-ESI-MS/MS with identical ^{13}C-encoded internal standards. Glycosphingolipids in the same plasma sample can also be quantified following microwave-assisted de-acylation to glycosphingoid bases.

Appendices

Dutch Summary
List of Publications
Curriculum Vitae
Acknowledgements

Samenvatting

Dit proefschrift beschrijft biochemisch onderzoek aan β-glucocerebrosidase (GBA), de lysosomale β-glucosidase die deficiënt is in de ziekte van Gaucher. Factoren die de intralysosomale stabiliteit en half waarde tijd van GBA beïnvloeden vormen een centraal thema in dit proefschrift. De uitgevoerde studies zijn ontworpen om meer inzicht te verkrijgen in de omzetting van GBA moleculen in lysosomen. Deel van het onderzoek maakt gebruik van nieuw ontwikkeld chemisch biologisch gereedschap zoals activiteit gebaseerde probes (ABPs) en foto activeerbare en klik bare (PAC) lipiden.

Hoofdstuk 1 beschrijft de rol van lysosomale cathepsines in de afbraak van GBA. Meer gedetailleerde kennis over cathepsines in de ziekte van Gaucher is relevant omdat het inzicht kan bieden in de omzetting van GBA in pathologische condities en een nieuwe gelegenheid kan bieden voor therapie, waarin remming van specifieke cathepsines lysosomale GBA niveaus kan verhogen door vermindering van de intralysosomale omzetting. Het is bekend dat het enzym in lysosomen wordt afgebroken door cathepsines, zoals aangetoond door het stabiliserende effect van leupeptine.

Het uitgevoerde onderzoek toonde aan dat ook E64d en de daarvan afgeleide ABP DCG-04, lysosomaal GBA beschermen tegen proteolytische afbraak in normale en Gaucher patiënt fibroblasten en lymfoblasten, zoals aangetoond met behulp van enzymatische activiteitsassays en labeling van actief GBA met ABPs. Blootstelling van gekweekte Gaucher lymfoblasten aan E64d leidde tot een vermindering van glucosylsfingosine (de base gevormd van stapelend GlcCer), wat een functionele correctie van GBA capaciteit aantoont. De kandidaat proteases betrokken in lysosomale GBA afbraak waren terug gebracht tot cathepsines B, F en L. Echter, individuele vermindering van deze cathepsines door shRNA of CRISPR-Cas technologie was onvoldoende om significant de GBA omzetting in gekweekte cellen te verlagen. Blijkbaar zijn meerdere cathepsines in staat om GBA af te breken in lysosomen en moeten deze tegelijkertijd worden geremd om lysosomaal GBA te verhogen. Een dergelijke benadering is niet aantrekkelijk als therapie vanwege de te verwachten nevenwerkingen.

Hoofdstuk 2 behandelt de consequenties van bezetting van de katalytische holte van GBA op zijn structurele stabiliteit in vitro en in vivo. Glycomimetica worden tegenwoordig ontworpen als chemische chaperonnes om de vouwing en stabilisatie van GBA in Gaucher patiënten te promoten, maar bewijs voor *in vivo* efficiëntie van deze benadering is schaars.

De uitgevoerde studie maakte gebruik van amfifiele cyclophellitol-afgeleide ABPs die irreversibel aan de katalytische nucleofiel E340 binden. De potente reversibele remmer isofagomine, een voormalig kandidaat therapeutische chaperonne voor GBA, werd gebruikt ter vergelijking. Cyclophellitol ABPs verhoogden zeer aanzienlijk de stabiliteit van recombinant GBA *in vitro*, zoals aangetoond met thermodynamische metingen en relatieve

resistentie tegen tryptische digestie. Het stabiliserende effect van isofagomine op structurele stabiliteit van puur GBA was minder sterk. Stabilisatie van GBA door cel doordringbare ABP in gekweekte normale en Gaucher patiënt cellen was weerspiegeld door de duidelijke toename in enzym. GBA in lever van wild type muizen geïnfundeerd met ABP was ook gestabiliseerd. Concluderend, bezetting van de holte van GBA door amfifiele ABPs stabiliseert het enzym aanzienlijk. Deze bevinding ondersteunt het concept van reversibele chaperonnes van GBA als therapeutische middelen voor Gaucher.

Hoofdstuk 3 richt zich op de studie van GBA met chemisch biologische tools: pacGlcCer en fluorescente β-glucose geconfigureerde cyclophellitols die de katalytische E340 residu binden op mechanisme gebaseerde wijze. Structuur-functie relaties in GBA zijn tot dusver bestudeerd met conventionele enzymologie en kristallografie en relatief weinig kennis bestaat over de aglycon bindende eenheid in GBA.

De gepresenteerde studie beschrijft dat de foto-activeerbare (diazirine gefunctionaliseerde) en klikbare (alkyne bevattende) pacGlcCer met hoge affiniteit bindt aan de katalytische holte van actief GBA, het pH optimum van enzymatische activiteit volgend. GBA hydrolyseert pacGlcCer, wat verder de mogelijkheid tot het ingaan van de katalytische holte bevestigt. De binding van pacGlcCer aan GBA is compleet gecompeteerd door de reversibele remmer AMP-DNM en de irreversibele remmers conditurol β-epoxide, cyclophellitol en de afgeleide ABP met fluorofoor label. De labeling van GBA door pacGlcCer wordt ook gecompeteerd door de substraten glucosylsphingosine, GlcCer en 4-methylumbelliferyl-β-glucose. Cholesterol, een acceptor in de transglucosylatie reactie van GBA, remt ook sterk de binding van pacGlcCer, maar niet die van ABP. De bevindingen geven aan dat specifieke labeling van GBA door pacGlcCer via zijn katalytische holte mogelijk is. Het kan worden voorgesteld dat pacGlcCer en ABP labeling van GBA gebruikt kunnen worden in screens om kleine interacterende stoffen te identificeren. Concluderend bieden de beschikbare tools nieuwe mogelijkheden om de glycon- en aglycon-bindingsplekken van de katalytische holte van GBA te proben.

Hoofdstuk 4 rapporteert de interactie van het lysosomale membraan eiwit LIMP-2 met GBA. De ziekte van Gaucher wordt veroorzaakt door mutaties in GBA zelf, terwijl Actie Myoclonus Renaal Falen (AMRF) komt door mutaties in LIMP-2, het eiwit dat transport van nieuw gevormd GBA naar lysosomen verzorgt. De deficiëntie in LIMP-2 resulteert in verkeerde secretie van GBA in de meeste celtypes. Intrigerend genoeg, ontwikkelen AMRF patiënten niet de karakteristieke glucosylceramide (GlcCer) geladen macrofagen (Gaucher cellen), die een kenmerk zijn van de ziekte van Gaucher. Macrofaag gerichte GBA met terminale mannose residuen in zijn N-glucanen wordt succesvol gebruikt in enzym vervangingstherapie (ERT) van Gaucher, maar voor AMRF is op dit moment geen behandeling beschikbaar.

Het uitgevoerde onderzoek bestudeerde de suppletie van LIMP-2 deficiënte cellen met therapeutisch mannose getermineerde GBA. Studies werden uitgevoerd met zowel

normale en AMRF fibroblasten, als met LIMP-2 deficiënte HEK293 cellen getransduceerd met mannose receptor. In LIMP-2 deficiënte cellen wordt het geëndocyteerde enzym abnormaal snel afgebroken in lysosomen. Dit suggereert dat kortstondige interacties van GBA met LIMP-2 in het lysosoom de conformatie van het enzym stabiliseren en de proteolytische afbraak vertragen. Het geeft verder aan dat LIMP-2 in lysosomen de efficiënte bepaalt van suppletie van deze organellen met ERT. Samenvattend heeft de studie onthuld dat LIMP-2 een duale rol vervult in de levenscyclus van GBA, zowel als transporteur en als intralysosomale chaperonne.

Hoofdstuk 5 betreft de fundamenteel verschillende klinische manifestatie van Gaucher en AMRF, twee geërfde ziektes waarin GBA verminderd is. In Gaucher is GBA gemuteerd, terwijl in AMRF het normale enzym onjuist uitgescheiden wordt, in plaats van naar lysosomen te worden getransporteerd. De cellulaire en chemische basis voor de verschillende symptomatologie van Gaucher en AMRF werd onderzocht met behulp van een LIMP-2 deficiënt muis model.

De studie richtte zich eerst op de mogelijkheid dat LIMP-2 deficiëntie niet alleen GBA beïnvloedt, maar ook andere lysosomale eiwitten. Geen abnormaliteiten werden gevonden in lysosomale matrix eiwitten in lysosomen geïsoleerd uit lever van LIMP-2 deficiënte muizen, behalve in GBA. Vervolgens werden LIMP-2 deficiënte muizen onderzocht wat betreft rest GBA en lipide abnormaliteiten in verschillende weefsels. Een variabele deficiëntie van GBA tussen weefsels werd opgemerkt, zowel met behulp van enzymatische activiteitsassays als met labeling van actief enzym met ABP. Een hoge rest GBA werd gedetecteerd in leukocyten van LIMP-2 deficiënte muizen, de afwezigheid van macrofaag gerelateerde symptomen in AMRF patiënten verklarend. Bewijs werd verkregen voor endocytotische heropname van GBA door witte bloedcellen, in tegenstelling tot fibroblasten. Lipide analyse toonde aan dat GlcCer nauwelijks verhoogd is in weefsels van LIMP-2 deficiënte muizen en dat de niveaus slecht correleren met rest GBA. In tegenstelling, glucosylsphingosine en geglucosyleerd cholesterol zijn verhoogd en hun niveaus in weefsel correleren negatief met GBA niveaus. Glucosylsphingosine en geglucosyleerd cholesterol waren ook toegenomen in geïsoleerde lysosomen van LIMP-2 deficiënte lever. Concluderend, resulteert LIMP-2 deficiëntie in celtype specifieke vermindering van GBA en adaptieve veranderingen in glycosfingolipide metabolisme.

Hoofdstuk 6 bespreekt het bewijs voor metabole adaptaties in twee glycosfingolipidoses, de ziekte van Gaucher en Fabry, veroorzaakt door defecten in respectievelijk GBA dat GlcCer afbreekt en α-galactosidase A (GLA) dat globotriaosylceramide (Gb3) afbreekt. De opeenhoping van de primaire stapelingslipiden in cellen en weefsels van Gaucher en Fabry patienten neigt te nivelleren met toename van leeftijd, suggererend dat er metabole adaptaties worden geïnduceerd. Een belangrijke adaptatie in zowel Gaucher als Fabry is de actieve de-acetylatie van stapelende glycosfingolipiden in lysosomen door de actie van het enzym zure ceramidase. Dus, de

lysosomale lipiden opslag wordt gelimiteerd door vorming van glucosylsfingosine in Gaucher en globotriaosylsphingosine (lysoGb3) in Fabry. Excessieve GlcSph en lysoGb3 worden gezien als toxisch en dragen bij aan specifieke symptomen zoals multipele myelome in Gaucher patiënten en neuronopathische pijn en nierfalen in Fabry. Een andere aanpassing in metabolisme van Gaucher vindt plaats buiten het lysosoom en betrekt het enzym GBA2 dat gelokaliseerd is in het cytoplasmische blad van membranen van het ER en Golgi apparaat. GBA2 maakt degradatie van GlcCer buiten lysosomen mogelijk en genereert daarmee ceramide en geglucosyleerd cholesterol. Therapeutische benadering specifiek gericht op de toxiciteit veroorzaakt door metabole adaptaties in Gaucher en Fabry wordt besproken.

Hoofdstuk 7 gaat over de katalytische veelzijdigheid van GBA, een β-glucosidase waarvan tot recent gedacht werd dat deze alleen GlcCer tot ceramide en glucose knipt in lysosomen. Speciale aandacht wordt besteed aan transglucosylatie gekatalyseerd door GBA en zijn specificiteit voor de glycon eenheid van een substraat.

GBA staat erom bekend β-glucoside substraten te hydrolyseren en meer recentelijk ook cholesterol te transglucosyleren naar cholesterol-β-glucoside (GlcChol). De beschreven studie richtte zich op de mogelijkheid van GBA om β-xylosides te metaboliseren. Er wordt eerst aangetoond dat GBA ook 4-methylumbelliferyl-β-D-xylose (4MU-β-Xyl) in vitro knipt, gestimuleerd in deze activiteit door activator eiwit saposine C. Vervolgens wordt aangetoond dat GBA in vitro cholesterol transxylosyleerd, gebruikmakend van 4MU-β-Xyl als suiker donor. Gevormd xylosyl-cholesterol (XylChol) dient vervolgens als acceptor om di-xylosyl-cholesterol te verkrijgen. Sequentiële blootstelling van GBA en cholesterol aan 4MU-β-Xyl and 4MU-β-Glc resulteert in vorming van GlcXylChol. Gelijk aan GBA, toont de cytosolische β-glucosidase GBA3 in vitro β-xylosidase en transxylosylase activiteit, in tegenstelling tot GBA2 dat activiteit tegen β-xylosides mist. Gekweekte cellen genereren ook gexylosyleerde cholesterol wanneer blootgesteld aan 4MU-β-Xyl in hun medium. Deze synthetische reactie wordt versterkt door de stof U18666A, die een toename van lysosomaal cholesterol veroorzaakt. Voorafgaande inactivatie van GBA in cellen met condiurol β-epoxide voorkomt vorming van gexylosyleerde cholesterol. Samenvattend, is verdere katalytische veelzijdigheid van GBA onthuld: het enzym kan optreden als β-glucosidase, β-xylosidase, transglucosylase en transxylosylase. De fysiologische relevantie van het vermaarde vermogen van GBA om β-xylosides te metaboliseren is momenteel onduidelijk en waarborgt verder onderzoek.

De Discussie bespreekt de huidige inzichten in GBA in gezondheid en ziekte. In dit verband worden de moleculaire basis en klinische manifestatie van Gaucher en AMRF syndroom besproken, inclusief de metabolische adaptaties aan GBA deficiëntie.

Bijzondere aandacht wordt besteed aan de lysosomale structurele stabiliteit van GBA en geassocieerde resistentie tegen proteolytische degradatie door cysteïne cathepsines. Bevindingen uit literatuur en nieuwe eigen resultaten over dit onderwerp worden besproken. Nieuwe technologie om GBA te bestuderen met labeling door GlcCer en cyclophellitol afgeleide probes wordt geïntroduceerd en de applicatie wordt beschreven.

Onopgeloste onderzoeksvragen over GBA en gerelateerde ziekteomstandigheden worden geïdentificeerd. Als toekomstige onderzoeksdoelstelling wordt de translatie van fundamentele kennis over GBA voor effectieve therapie van neuronopathische Gaucher en andere ziekteomstandigheden veroorzaakt door enzym vermindering besproken.

Het *Addendum* beschrijft een nieuw ontwikkelde multiplex assay voor gelijktijdige kwantificatie van (lyso)-glycosfingolipide basen in plasma monsters door middel van UPLC-ESI-MS/MS met identieke ^{13}C-gecodeerde interne standaarden. Glycosfingolipiden in hetzelfde plasma monster kunnen ook worden gekwantificeerd na magnetron-geassisteerde de-acetylatie tot glycosfingoide basen.

List of Publications

1. Mirzaian M, Wisse P, Ferraz MJ, Marques AR, Gaspar P, Oussoren SV, Kytidou K, Codée JD, van der Marel G, Overkleeft HS, Aerts JM. *Simultaneous quantitation of sphingoid bases by UPLC-ESI-MS/MS with identical (13)C-encoded internal standards.* Clin Chim Acta. 2017 Mar;466:178-184. doi: 10.1016/j.cca.2017.01.014. Epub 2017 Jan 13. PubMed PMID: 28089753.

2. van Weeghel M, Ofman R, Argmann CA, Ruiter JP, Claessen N, Oussoren SV, Wanders RJ, Aten J, Houten SM. *Identification and characterization of Eci3, a murine kidney-specific Δ3,Δ2-enoyl-CoA isomerase.* FASEB J. 2014 Mar;28(3):1365-74. doi: 10.1096/fj.13-240416. Epub 2013 Dec 16. PubMed PMID: 24344334.

3. Saskia V. Oussoren, S. Hoogendoorn, M. Verdoes, S. Scheij, M. Verhoek, M. Artola, R.G. Boot, H.S. Overkleeft, J.M.F.G. Aerts. *Augmentation of lysosomal glucocerebrosidase by the inhibition of its lysosomal proteolysis.* Manuscript in preparation.

4. Wouter W. Kallemeijn*, Fredj Ben Bdira*, Saskia V. Oussoren, Saskia Scheij, Boris Bleijlevens, Cindy P. A. A. van Roomen, Roelof Ottenhoff, Marielle J. F. M. van Kooten, Marthe T. C. Walvoort, Martin D. Witte, Rolf G. Boot, Marcellus Ubbink, Herman S. Overkleeft, Johannes M. F. G. Aerts. *Stabilization of glucocerebrosidase by active-site occupancy.* Manuscript submitted.

5. Saskia V. Oussoren, Jasper Wermink, Jianbing Jang, Herman S. Overkleeft, Johannes M. Aerts, Per Haberkant. *Chemical probing of the catalytic pocket of glucocerebrosidase with photoactivatable glucosylceramide and activity-based probes.* Manuscript in preparation.

6. Paulo Gaspar, Saskia V. Oussoren, Saskia Scheij, Marri Verhoek, Rolf Boot, Hermen S. Overkleeft, Jan Aten, Johannes M. Aerts. *Intralysosomal stabilization of glucocerebrosidase by LIMP-2: potential implications for efficacy of ERT.* Manuscript in preparation.

7. Paulo Gaspar, Maria J. Ferraz, Markus Damme, André R. A. Marques, Saskia V. Oussoren, GertJan Kramer, Mina Mirzaian, Marion Gijbels, Roelof Ottenhoff, Cindy van Roomen, Wilma E. Donker-Koopman, Michael Schwake, Saskia Heybrock, Kondababu Kurakula, Maria Carmo Macário, Clara Sá Miranda, Paul Saftig, Johannes M. Aerts. *Lipid abnormalities in LIMP-2 deficient mice.* Manuscript pending submission.

8. Johannes M. Aerts, Maria J. Ferraz, Mina Mirzaian, Saskia V. Oussoren, Kassiani Kytidou, Ethan Kuo, Lindsey Lelieveld, Marc Hazeu, Daphne Boer, Paulo Gaspar, Daniela Herrera Moro, Tanit L. Gabriel, Wouter W. Kallemeijn, Patrick Wisse, Herman S. Overkleeft, Marco van Eijk, Rolf G. Boot, André R. A. Marques. *Metabolic adaptations to defective lysosomal glycosphingolipid degradation.* Manuscript pending submission.

9. Mina Mirzaian*, Maria J. Ferraz*, Daphne E.C. Boer, <u>Saskia V. Ousoren</u>, Marc Hazeu, Jasper Wermink, Per Haberkant, Sybrin P. Schroder, Karen Ghauharali, Edward Blommaart, Roelof Ottenhoff, Andre R.A. Marques, Rianne Meijer, Wouter Kallemeijn, Rolf G. Boot, Herman S. Overkleeft, Navraj S. Pannu, Johannes M. Aerts. *β-Xylosidase and transxylosidase activities of human glucocerebrosidase.* Manuscript pending submission.

Curriculum Vitae

Saskia Oussoren was born on October 8th in Koog aan de Zaan, The Netherlands. After graduating from St. Michaël College high school in Zaandam in 2007, she started her Bachelor of Science studies at the University of Amsterdam with Neurobiology, Nutrition and Anatomy and Developmental Biology as elective courses. The thesis of her research stay at the Laboratory of Genetic Metabolic Diseases in the Academical Medical Center (AMC) in Amsterdam was titled "A localization study of Δ3, Δ2-enoyl-CoA isomer-ases". In 2010 she completed her Bachelor degree.

She next also performed her Master of Science studies at the University of Amsterdam and followed the courses Molecular biology of the cell, Medical Molecular Systems Biology, Endocrinology and Medical Bio-Chemistry. During her Master studies she performed a research project in the OLVG hospital in Amsterdam, her report was titled "Disseminated intravascular coagulation (DIC) in critically ill patients. Functional analysis of changes in Microparti-cle-induced clot formation in vitro of DIC patients". A second research stay was fulfilled at the Department of Medical Biochemistry in the AMC in Amsterdam, her report being titled "The role of GBA2 at the cellular level". She wrote her Master thesis on the topic "Nod-like receptors link innate immunity to the metabolic syndrome".

In 2012 she obtained her Master degree and started as a PhD candidate at the Department of Medical Biochemistry in the AMC. Saskia performed her research under the supervision of prof. dr. Hans Aerts, dr. Rolf Boot and, at the beginning, dr. Marco van Eijk. After 2.5 years, she continued her research in the newly created department of Medical Biochemistry at the Leiden Institute of Chemistry (Leiden University, The Netherlands), led by prof. dr. Hans Aerts. During her research, she investigated the role of lysosomal proteases in the breakdown of the lysosomal β-glucocerebrosidase and used chemical probing with photo activatable and clickable lipids and activity based probes to study the glycon and aglycon pockets of the same enzyme. She presented her work at several (inter)national conferences, including the 19th Workshop European Study Group on Lysosomal Disorders (ESGLD) in 2013 (Graz, Austria), the FEBS Advanced Lecture Course 360 Degrees Lysosome in 2014 (Kusadasi, Turkey), the ACM/MDL meetings of 2013 and 2014 (Lunteren, The Netherlands) and the ESGLD meeting in 2015 (Pozzuoli, Italy). Furthermore, her abstract titled "Lysosomal cathepsins and glucocerebrosidase in Gaucher disease" was selected for oral presentation at the European Working Group on Gaucher Disease (EWGGD) meeting in Israel in 2014.

Acknowledgements